

Department of Applied Geology

**Sediment dynamics of a temperate water carbonate system of the
Midwestern Australian coast**

Sira Tecchiato

**This thesis is presented for the Degree of
Doctor of Philosophy**

of

Curtin University

July 2014

Declaration

To the best of my knowledge and belief this thesis contains no material previously published by any other person except where due acknowledgment has been made.

This thesis contains no material which has been accepted for the award of any other degree or diploma in any university.

Signature:

Date:

ABSTRACT

An understanding of the processes regulating sediment transport, accumulation, and erosion requires an appropriate mapping of coastal geomorphology, seabed sediments, and benthic habitat distribution to allow management issues to be identified, understood, and addressed. Seabed geomorphology encompasses the shape and hardness of the seabed and is strongly connected to sediment dynamics, which drive sediment transport and regulate the characteristics of soft sediment bodies, especially in shallow littoral sandy environments. Sediment input from temperate water seagrass communities is commonly recognised as a sediment source for the overall sediment budget of the southern and western Australian coastal embayments, and the sediment deriving from biogenic production is redistributed along shore, supplying the beaches and contributing to coastal stability. Geomorphology, sediments, and habitat data provide an environmental understanding of coastal systems; however, they need to be linked to hydrodynamic data to quantitatively assess sediment transport and fully understand the coastal processes regulating the coast and nearshore.

The coastal zone off Geraldton in temperate mid-western Australia is the site of an important port set within two shallow (<30 m) wave-dominated embayments, colonised by seagrass and macroalgal communities. Coastal erosion occurs along the town beaches, similarly to the maritime infrastructure and human use of other coastal sites in Western Australia. The system is complex, with biogenic sediment input, as well as dune and river-derived sediments, coastal erosion, nourishment activities, sand bypassing, natural and artificial sediment sinks, and significant infrastructure, including a dredged shipping channel which is necessary to provide access to port facilities. The lack of previous sediment budget studies in the region required an integrated analysis of hydrodynamics, geomorphology, sediments, and habitat data to model and map the environmental setting of the study area, which is similar to the surrounding region. This data was also used to define the seaward extent of the littoral sediment transport system, and to build a quantitative sediment budget model which is closely related to the identification of sediment transport pathways. The concepts behind the sediment budget model building process also promoted understanding of the relationship between sediment dynamics and coastal stability and assets.

Multibeam echo sounder data was used to map shallow water geomorphological features and the spatial distribution of benthic habitats, with the support of sediment samples and underwater imagery for ground truthing the acoustic data. Topographic features characterising the coastal platform comprise either unconsolidated sediment accumulations (rippled sand flats, underwater sand dunes, nearshore beach zone, sand bars and sheets), low sea-level cemented shoreline features (shallow limestone reefs), or flat or low-sloping

areas with a shallow sandy cover. The identification of sand bar and sheet systems was particularly important in indicating areas of sediment storage. The distribution of these soft sediment bodies appeared to be regulated by wave-induced sediment transport combined with the influence of pre-existing seabed topography. In general, the geology and geomorphology of the coastal platform derives from karstification of pre-existing Pleistocene limestone surfaces, including reef systems. Shallow limestone reefs are the remains of these paleo-reef systems, and are usually considered biodiversity hotspots for fisheries management. The physical substrate, including limestone ridges, has often been regarded as a control for benthic habitat development, and considerations of this kind have been made in this study. Whilst seagrasses are common on sheltered hardgrounds, blanketed by fine sand, macroalgae are found on high-energy limestone reefs. Exposure to wave energy, seabed geomorphology, and sediment characteristics are closely related to the distribution of benthic habitats and sand substrates, highlighting the value of an integrated analysis of these parameters.

The capability of the multibeam echo sounder backscatter data to discriminate between seagrass meadows, macroalgal communities, and sandy substrates was evaluated in this study. The acoustic response from hard substrates and uncolonised sediment substrates has been deeply investigated, and by rule of thumb high backscatter intensity is associated with hardgrounds and is proportional to sediment grain size and surface roughness for unvegetated substrates. However, the high backscatter intensity recorded for seagrass and macroalgal communities remains poorly understood. The new data analysed in this study has shown that the combined analysis of seafloor geomorphology and biota type is likely to better explain the acoustic response from the seabed, as seagrass and macroalgae at Geraldton colonise hardgrounds with shallow consolidated sediment cover and show similar relative backscatter strengths. Also, the low-density mixed seagrass and macroalgal communities are common on hardgrounds and show similar acoustic parameters to dense seagrasses and macroalgae, indicating that the biota density is not driving the acoustic response from these habitats.

The sediment facies of the south-western Australian inner-shelf are described in the literature as a thin sediment blanket composed of quartz grainstone, lithoclastic grainstone, and skeletal grainstone. At Geraldton, sediment facies were found to have a varying amount of modern and relict sediment components, with a remarkable trend of increasing relict grains moving offshore and modern fraction dominance in the nearshore. To distinguish between modern and relict sediment fractions was a primary objective of the analysis; consequently, grain size, carbonate content, sediment thickness, x-ray diffraction analyses, and microscopic characterisation of sediment petrology were carried out on over 100

sediment samples collected along the coast and in the shallow (5 to 20m deep) offshore areas. This data provided important clues on sediment composition and provenance. Modern carbonate sedimentation is linked to seagrass and macroalgal communities colonising the shallow coastal platform <10 m deep, which provide habitats for molluscs, red algae, benthic foraminifera, bryozoans, etc. to secrete their carbonate skeletons and contribute in sediment production, together with non-carbonate secreting organisms such as sponges. Fine-carbonate sand derives from, and is a proxy for, seagrass meadows, which are mostly located within a narrow belt <2 km from shore. Sediment grain size increases moving offshore where macroalgal communities are more common and sediment production diminishes. The reconstruction of the modern depositional environments of the Geraldton embayments provides a useful analogue for the interpretation of high-energy carbonate-dominated palaeoenvironments, and shows that wave energy, sediment types, and local geomorphology are important proxies for carbonate facies distribution.

The nature of the data available for this study (i.e. hydrodynamic modelling, coastal topography, sediments, bathymetry, offshore sediment thickness, and habitat data) led to a detailed understanding of cross-shore and alongshore sediment dynamics on the basis of geomorphological and sedimentological evidence. In the study area, the boundary between wave-worked and non-wave-worked sediment was evident from the sediment size and grain faunal community structure. Bathymetry and seabed bedform measurements also provided useful data for the understanding of the cross-shore sediment transport system. Theoretical calculations of depth of closure were then compared to the environmental data to overcome the lack of previously published studies of sediment dynamics for similar environments of the Western Australian coast. This model is particularly useful for application in a wider region of Western Australia, as the 4 km wide, 10 m deep coastal platform, bordered by shallow shore-parallel limestone reefs that shelters the coast, is common along most of the Western Australian coast. This coastal platform influences cross-shore sediment transport processes by inducing wave breaking offshore and reducing wave heights reaching the coast.

A sediment budget is a tally of sediment gains and losses, or sources and sinks, and longshore sediment transport modelling was carried out to gain quantitative data on sediment transport volumes which were compared to the environmental data to reconstruct sediment transport pathways. Whilst the southern embayment supplies sediment to the northern sediment cells, the main sediment sinks are artificial and are located in the northern embayment where beach erosion is more significant, indicating that coastal infrastructure modifies the local sediment dynamics. The Geraldton dredged channel and Port basin in the northern embayment are in need of ongoing maintenance dredging operations, and sand bypassing activities are also required to stabilise eroding beaches located further north.

However, the volume transported from the southern to the northern Geraldton embayment is substantially higher than the sediment trapped by the Port infrastructure, indicating that sediment transported through the water column is an important component of the coastal sediment budget and is not interacting with the Port infrastructure. This information should be taken into account for future planning of coastal infrastructure which could obstruct the transport of suspended sediment. Moreover, this information also indicates that not all the sediment transported from the Geraldton southern embayment is supplying the beaches of the northern embayment. Coastal erosion appeared to be mainly driven by the interaction of coastal configuration and infrastructure with the cross-shore and longshore sediment transport pathways.

This study provides important information for managing the Geraldton coast as well as regional Western Australia by providing vital background data on sediment dynamics and coastal evolution, considering that little data exists on sediment budgets along the coast of Western Australia. Most of the Western Australian coast, including the Geraldton embayments, is microtidal and dominated by persistent high Southern Ocean swell, which was responsible for transporting carbonate sediment from the shelf to the coast soon after the Holocene sea-level transgression building large dune systems. Southgate dune at Geraldton has been identified as a source of sediment for the Geraldton southern embayment and contributes to beach stability. Seagrass meadows are highly productive benthic habitats of the South and Western Australian coastal areas and contribute to stabilisation of the offshore seabed substrates. The protection of this system should be ensured by environmental managers to preserve coastal stability.

The high-latitude swell waves, associated with wind waves close to shore, drive a northward-oriented sediment transport along the entire coast of Western Australia. Sandy salients, tombolos, barriers, banks, etc. are common features and experience sediment erosion on the southward facing side and deposition on the northern side, as a result of the northward-oriented sediment transport and persistent southerly winds and waves. Evidence of these processes occurring at Geraldton was found in this project in the area surrounding the Point Moore tombolo and indicate that sediment is transported to the north of these features. Infrastructure located on the downdrift side of this sediment transport system is regularly infilled by sediment, such as the Geraldton dredged channel and Port basin, which are in need of ongoing maintenance dredging operations, and sand bypassing activities are also required to stabilise eroding beaches located further north. Future planning of coastal infrastructure such as dredged channels, which are common features of the Western Australian coast, should take into account this sediment transport pathway, so that potential coastal erosion and subsequent remediation costs can be minimised.

ACKNOWLEDGEMENTS

I come from a coastal town and I believe that my natural bond with the beach and the ocean has played a central part in orientating my career towards the understanding and protection of these environments. For me and many other people who find a sense of place to the coast, the ocean and the beach environments represent an important part of self-identity.

I would like to thank my supervisor Professor Lindsay Collins for his guidance and patience. I learnt a lot from him, not only from a scientific prospective. He also supported my application and grant of the Curtin International Postgraduate Research Scholarship (CIPRS) and gave me the chance to work on this project.

I would also like to thank my co-supervisor Dr Iain Parnum from the Centre of Marine Science and Technology (CMST) for his support and assistance. I learnt a lot from his inspiring ideas.

The Western Australian Department of Transport is the main project sponsor and I am grateful for their support, especially the Coastal Management Unit and technical staff operating the hydrographic survey vessel and multibeam data collection and bathymetry processing. The Geraldton Port Authority and City of Geraldton-Greenough are also acknowledged for data provision. The Northern Agricultural Catchment Council is also acknowledged for participation in the project.

Thanks also to: Ian Eliot, Matt Eliot, Tanya Stul and Bob Gozzard (from Damara Pty Ltd and Geological Survey of Western Australia) for data sharing, project revision and supportive comments on the project results; Prof Enzo Pranzini from the University of Florence for useful discussions of the research results; Dr Michael Collins for project revision; Dr Alessandro Bosman from the University of Rome “Sapienza” for his guidance with any kind of marine geology issues; Dr Roman Pevzner from the Department of Geophysics for assistance with seismic data processing; Mr Andrew Zulberti and Dr Sebastian Morillo from GHD Pty Ltd for assistance with sediment transport modelling; Michela Soldati from Med Ingegneria for reviewing the sediment transport model; Anderson Chagas from Petrobras for assistance with mapping techniques; Mr David Mitchell from the University of Sydney for assistance with the collection of seismic data. The staff members of the Department of Applied Geology who have assisted me in the course of my study are also acknowledged, especially Ms Annette Labrooy for administrative support and Dr Robert Madden for technical support. A special thanks goes to Ms Alex Stevens, for her continuous support of my sanity and of my research project. Many thanks to the following project volunteers: Claudio Del Deo, Kieran Sheehan, Antonio Tecchiato, Federico Altobelli, Valentina Segreto,

Andrea Michelotti for assistance during the fieldwork; Yue Xu for assistance in the grain size analysis, Dong Hairou for assistance with the sediment carbonate content measurements; Andrea Terrazzino for assistance with figure preparation; Giada Bufarale and Giovanni De Vita for assistance in seismic data collection and analysis.

I would like to thank my parents Danilo Tecchiato and Concetta Verardo for their continuous support in the course of this project and life in general. Thanks for teaching me to do my best and to believe in me.

Thanks to my brothers Antonio and Vanni Tecchiato for listening to my complaints and being my playmates throughout life.

I would also like to thank my grandmother Maria Tucciarelli in Tecchiato for teaching me to be strong and self-confident.

Finally, I would like to express my deepest gratitude to my husband Claudio Del Deo for his wonderful and continuous support and for the sacrifices he made to allow me to achieve this goal.

“The future is not preordained destiny but unknown potential awaiting exploitation.”

“Il futuro non e' preordinato; e' solo un grumo di potenzialita' che noi dobbiamo far
sviluppare.”

Francesco Alberoni

For Indi and Francesco,
and all children
from whom we borrow this amazing Coast

TABLE OF CONTENTS

ABSTRACT.....	ii
ACKNOWLEDGEMENTS.....	vi
Chapter 1	12
1.1 INTRODUCTION	12
1.1.2 The need for a coastal study at Geraldton	13
1.2 AIMS OF THE STUDY	14
1.2.1 Outline of the thesis.....	15
1.3 THE STUDY AREA	16
1.3.1 Beach characteristics, coastal evolution and sand bypassing activities	18
1.3.2 Climate and wind regimes	22
1.3.3 Coastal processes.....	23
1.3.3.1 Currents.....	24
1.3.3.2 Waves.....	26
1.3.4 Mobile sand dunes	29
1.3.5 Rivers	31
1.3.6 Geological setting.....	36
1.3.6.1 Regolith-landform systems	38
1.4 METHODS	42
1.4.1 Shallow seismic data.....	46
1.4.2 Multibeam echo sounder data	47
1.4.2.1 Underwater morphology mapping.....	48
1.4.3 Towed video data.....	49
1.4.3.1 Standard definition transects	50
1.4.3.3.2 High definition transects	52
1.4.4 Sediment data.....	53
1.4.5 Longshore sediment transport model.....	56
Chapter 2	57
2.1 INTRODUCTION	57
2.2 UNDERWATER GEOMORPHOLOGY	59
2.3 SEABED MOBILITY.....	67
2.4 BENTHIC COVER AND PHYSICAL SUBSTRATES.....	71
2.4.1 Geomorphological parameters and sediments as a surrogate for benthic habitat distribution	79
2.5 ACOUSTIC HABITAT MAPPING	82
2.5.1 Relationship between benthic habitats and backscatter intensity.....	85
2.5.1.1 Relationship between geomorphic features and backscatter intensity	89
2.5.2 Habitat map production	90
2.5.2.1 Methods.....	91
2.5.2.1.1 Supervised and unsupervised classification algorithms	91
2.5.2.1.2 Image segmentation.....	92
2.5.2.1.3 Accuracy assessment.....	94
2.5.2.2 Results.....	94
2.5.2.2.1 Results of the application of supervised and unsupervised classification algorithms ...	94
2.5.2.2.2 Results of the application of image segmentation techniques.....	97

2.6 BENTHIC HABITAT DISTRIBUTION AND SIGNIFICANCE FOR SEDIMENT DYNAMICS	99
Chapter 3	102
3.1 REGIONAL CONTEXT.....	102
3.2 SEDIMENT GRAINSIZE DISTRIBUTION.....	104
3.2.1 Underwater sediments	104
3.2.2 Coastal sediments.....	110
3.3 CARBONATE CONTENT OF SEDIMENTS	112
3.3.1 Underwater sediments	112
3.3.2 Coastal sediments.....	114
3.4 SEDIMENT COMPONENTS: PETROLOGICAL AND X-RAY DIFFRACTION ANALYSES.....	116
3.5 SEDIMENT FACIES	121
3.6 OFFSHORE SEDIMENT THICKNESS	126
3.7 CARBONATE SEDIMENT PRODUCTION AND ACCUMULATION RATES	129
Chapter 4	132
4.1 INTRODUCTION	132
4.2 CROSS-SHORE SEDIMENT TRANSPORT.....	135
4.2.1 Sediments.....	137
4.2.2 Nearshore geomorphology	140
4.2.3 Bedforms	141
4.2.4 Depth of closure	142
4.3 CONCEPTUAL SEDIMENT BUDGET MODEL.....	143
4.3.1 Sediment sources	143
4.3.2 Sediment storage.....	146
4.3.3 Longshore sediment transport pathways	154
4.3.4 Conceptual sediment budget model	160
4.4 SEDIMENT CELLS	163
4.4.1 Methodologies for identifying sediment cell boundaries.....	163
4.4.2 Sediment cells.....	164
4.5 LONGSHORE SEDIMENT TRANSPORT MODELING	168
4.6 SEDIMENT BUDGET MODEL	172
Chapter 5	176
5.1 SHALLOW WATER GEOMORPHOLOGY, HABITATS, AND SEDIMENT DISTRIBUTION OF A TEMPERATE WATER LITTORAL ENVIRONMENT	176
5.1.1 Seabed geomorphology	176
5.1.2 The macroalgal and seagrass carbonate factories: depositional environments and habitat characteristics.....	177
5.2 ABILITY OF THE MULTIBEAM ECHO-SOUNDER BACKSCATTER DATA TO DISCRIMINATE BETWEEN SANDY SUBSTRATES, SEAGRASS MEADOWS, AND MACROALGAL COMMUNITIES	179

5.3 INVESTIGATION OF LITTORAL SEDIMENT DYNAMICS: RESULTS OF AN INTEGRATED ANALYSIS	180
5.3.1 Cross-shore sediment transport.....	180
5.3.2 Relationship between coastal geomorphology, sediment characteristics and longshore sediment transport	182
5.4 ASSESSMENT OF THE GERALDTON COASTAL EVOLUTION USING SEDIMENT BUDGET COMPUTATIONS: IMPLICATIONS FOR COASTAL MANAGEMENT	184
5.5 SUMMARY OF OUTCOMES.....	186
References	189
<i>APPENDIX 1 – Tecchiato et al. (2013). Application of multi-beam echo sounder data to studies of sediment dynamics: an example from Geraldton, Midwestern Australia. International Congress on Natural Sciences and Engineering; Taipei, Taiwan, January 2013.....</i>	197
<i>APPENDIX 2 – Tecchiato et al. (2011). Using multibeam echo-sounder to map sediments and seagrass cover in shallow coastal areas. Proceedings of the Fourth International Conference on Underwater Acoustic Measurements: Technologies and Results. Kos Island, Greece, June 2011.....</i>	205
<i>APPENDIX 3 – Reports, Publications and Presentations.....</i>	213

LIST OF FIGURES

Figure 1: Study area and location map of the city of Geraldton. Refer to this map for visual location of the localities named throughout the thesis.	17
Figure 2: Cardno Pty Ltd modelling of mean summer currents (from Cardno, 2012b). The direction of predominant water current flow is frequently northward throughout Champion Bay.....	25
Figure 3: Cardno Pty Ltd modelling of mean winter currents (from Cardno, 2012b). The direction of predominant water current flow is frequently south-westward out of Champion Bay.....	25
Figure 4: Swell wave heights and directions at Geraldton (Geraldton Outer Channel AWAC data, courtesy of the Department of Transport). Swell wave heights range predominantly between 1 and 1.5 m.	27
Figure 5: Sea wave heights and directions at Geraldton (Geraldton Outer Channel AWAC data, courtesy of the Department of Transport). Sea wave heights are mostly in the range of 0.5–1 m.	27
Figure 6: Cardno Pty Ltd modelling of mean summer wave directions and heights (Cardno, 2012b). Wave heights are in the range of 0.5–1.5 m along the Geraldton coastline.....	28
Figure 7: Cardno Pty Ltd modelling of mean winter wave directions and heights (Cardno, 2012b). Wave heights are in the range of 0.5–1.5 m along the Geraldton coastline, locally increasing to 2 m in winter.	29
Figure 8: Historical evolution of the Southgate dune system boundaries (from Stevens & Collins, 2011). The background layer is an aerial photograph from 1956. Note the potential for spillover of sediments from the north west dune margin to supply the littoral transport system.....	31
Figure 9: View of the Greenough River mouth and adjacent coastal bay to the north on the 2nd March 2011 (view to the south west). Dark waters in the background are turbid as a result of the flooding event that occurred at the end of February 2011.	33
Figure 10: Chapman River mouth on the 2nd March, 2011 (view to the north). This photo shows a limited sediment exchange between river and ocean occurring only at high tide. The sand bar that commonly blocks the river mouth is also visible.....	35
Figure 11: Chapman River mouth on the 27th August, 2011 (view to the north). This photo shows a continuous water flow. The sand bar that commonly blocks the river mouth is not present.	35
Figure 12: Detail of the Sheet SH/50-1 “Geraldton” of the 1:250,000 geological series, compiled by the Geological Survey of Western Australia.....	37
Figure 13: Location of the land systems classified by Langford (2001, GSWA data) recurring in the study area from the Greenough River to the Buller River. Materials from the Quindalup and Spearwood systems are the most likely to be eroded and transported to the ocean by the local rivers.	41
Figure 14: Locations of the data collected during the November–December 2009 (sediment samples and seismic limes) and the May 2010 surveys (sediment samples).	44
Figure 15: Locations of the data collected during the November–December 2010 surveys (multibeam, underwater imagery and one offshore sediment sample), and March 2011 coastal sampling following river flooding events. The multibeam data is indicated by the raster of bathymetry for which the depth range is shown on the right hand side of this figure.	45
Figure 16: Digital Elevation Models (DEMs) of bathymetry resulting from the November–December 2010 multibeam survey at Geraldton. The data extent is ~35 km ² and focused on the Geraldton coastal platform, mainly covering the areas close to the shoreline to ~10 m depth (purple to lighter blue colours); however, off Point Moore the data reached ~25 m depth. Of note, the dredged channel and Port basins indicated by the darker blue colours are 12 to 15 m deep. The location of figure 17 is also indicated.	61
Figure 17: W-E profile of the Geraldton coastal platform (see figure 16 for location) derived from the multibeam bathymetry.....	62
Figure 18: Underwater morphology features mapped at Geraldton as visible on the high resolution DEMS of multibeam bathymetry: A) sand sheet adjacent to an area of low relief substrate; B) sand bars with rippled sand in the bars through; C) offshore boundary of the nearshore beach	

zone, adjacent to a rippled sandy area which evolves into underwater sand dunes further offshore; D) shallow limestone reef system surrounded by an area of low relief substrate. 63

Figure 19: Underwater morphology map at Drummond Cove based on DEMs of bathymetry. The GIS polygons are overlaid on the aerial photography. The blue tones of the colouring scale indicate the artificial elements (i.e. aquaculture zone, dredged channel, dredged port basin, and shipwrecks); yellow to red colours indicate sediment deposition or transport (i.e. nearshore zone, rippled sand flat, sand bars and sheets, and underwater sand dunes); the shallow limestone reefs and low relief substrate polygons indicate areas where no sand is depositing, and were coloured green and grey respectively. 64

Figure 20: Underwater morphology map at Geraldton based on DEMs of bathymetry. The GIS polygons are overlaid on the aerial photography. The blue tones of the colouring scale indicate the artificial elements (i.e. aquaculture zone, dredged channel, dredged port basin, and shipwrecks); yellow to red colours indicate sediment deposition or transport (i.e. nearshore zone, rippled sand flat, sand bars and sheets, and underwater sand dunes); the shallow limestone reefs and low relief substrate polygons indicate areas where no sand is depositing, and were coloured green and grey respectively. 65

Figure 21: Underwater morphology map at Tarcoola Beach based on DEMs of bathymetry. The GIS polygons are overlaid on the aerial photography. The blue tones of the colouring scale indicate the artificial elements (i.e. aquaculture zone, dredged channel, dredged port basin, and shipwrecks); yellow to red colours indicate sediment deposition or transport (i.e. nearshore zone, rippled sand flat, sand bars and sheets, and underwater sand dunes); the shallow limestone reefs and low relief substrate polygons indicate areas where no sand is depositing, and were coloured green and grey respectively. 66

Figure 22: Locations of figures 23 and 24. 67

Figure 23: S-N profile of sand ripples off the Batavia Coast Marina. 67

Figure 24: SW to NE profile of the underwater sand dunes mapped to the east of Separation Point. 67

Figure 25: Seabed mobility map of the Geraldton coastal system. The GIS polygons are overlaid on the aerial photography. The nearshore zone indicates the seaward limit of sediment exchange between the beach system and the offshore based on bathymetry data. Sediment is transported towards the deposition areas, which represent sediment sinks. Sediment transport as bedload is visible on the bathymetry data within the zones mapped as equilibrium/potential transport areas. Finally, stable areas show no evidence of sediment deposition/erosion or bedload transport. ... 70

Figure 26: Habitat distribution across depth at Geraldton. Both seagrass meadows and macroalgae communities are patchy, showing a gradual density decrease while transiting to sand-dominated substrates. 72

Figure 27: A) location map of the Greenough area (from the Greenough River mouth to Separation Point); B) mean percent cover of seagrass, algae and sand in the Greenough area. The red-bordered segments represent seagrasses: AG = *Amphibolis griffithii*; AA = *Amphibolis antarctica*, PSP = *Posidonia* sp. and HSP = *Halophila* sp. 73

Figure 28: Mean percent cover of seagrass, algae and sand (\pm Standard Error) at *Amphibolis antarctica*-dominated sites in the Greenough area (from the Greenough River mouth to Separation Point). The red-bordered bars represent seagrasses: AG = *Amphibolis griffithii*; AA = *Amphibolis antarctica*; PSP = *Posidonia* sp.; and Coloniser = *Syringodium isoetifolium* + *Halophila decipiensis* + *Halophila* sp. 73

Figure 29: Mean percent cover of seagrass, algae and sand (\pm Standard Error) at *Amphibolis griffithii*-dominated sites in the Greenough area (from the Greenough River mouth to Separation Point). The red-bordered bars represent seagrasses: AG = *Amphibolis griffithii*; AA = *Amphibolis antarctica*; PSP = *Posidonia* sp.; and Coloniser = *Syringodium isoetifolium* + *Halophila decipiensis* + *Halophila* sp. 74

Figure 30: A) location map of the Separation Point area (from Separation Point to Point Moore); B) mean benthic percent cover in the Separation Point area. 75

Figure 31: A) location map of the area between Point Moore and the Chapman River mouth; B) mean percent cover of seagrass, algae, and sand in the area between Point Moore and the Chapman River mouth. The red-bordered segments represent seagrasses: AG = *Amphibolis griffithii*; AA = *Amphibolis antarctica*; PSP = *Posidonia* sp.; HSP = *Halophila* sp.; and HD = *Halophila decipiensis*. 76

Figure 32: Mean percent cover of seagrass, algae and sand (\pm Standard Error) at *Posidonia* sp.-dominated sites, only found in the Point Moore to Chapman river area, more specifically between Pages beach and the dredged channel basin. The red-bordered bars represent seagrasses: AG = *Amphibolis griffithii*; AA = *Amphibolis antarctica*; PSP = *Posidonia* sp.; and Coloniser = *Syringodium isoetifolium* + *Halophila decipiensis* + *Halophila* sp. 76

Figure 33: Mean percent cover of seagrass, algae, and sand (\pm Standard Error) at *Amphibolis griffithii*-dominated sites in the area between Point Moore and the Chapman River mouth. The red-bordered bars represent seagrasses: AG = *Amphibolis griffithii*; AA = *Amphibolis antarctica*; PSP = *Posidonia* sp.; and Coloniser = *Syringodium isoetifolium* + *Halophila decipiensis* + *Halophila* sp. 77

Figure 34: Mean percent cover of seagrass, algae, and sand (\pm Standard Error) at *Amphibolis antarctica*-dominated sites in the area between Point Moore and the Chapman River mouth. The red-bordered bars represent seagrasses: AG = *Amphibolis griffithii*; AA = *Amphibolis antarctica*; PSP = *Posidonia* sp.; and Coloniser = *Syringodium isoetifolium* + *Halophila decipiensis* + *Halophila* sp. 77

Figure 35: A) Location map of the area to the north of the Chapman River mouth; B) mean percent cover of seagrass, algae, sand and pavement in the area to the north of the Chapman River mouth. The red-bordered segments represent seagrasses: AG = *Amphibolis griffithii*; AA = *Amphibolis antarctica*; and ASP = *Amphibolis* sp. 78

Figure 36: Mean percent cover of seagrass, algae and sand (\pm Standard Error) at *Amphibolis griffithii*-dominated sites in the area to the north of the Chapman River mouth. The red-bordered bars represent seagrasses: AG = *Amphibolis griffithii*; AA = *Amphibolis antarctica*; PSP = *Posidonia* sp.; and Coloniser = *Syringodium isoetifolium* + *Halophila decipiensis* + *Halophila* sp. 78

Figure 37: Mean percent cover of seagrass, algae and sand (\pm Standard Error) at *Amphibolis antarctica*-dominated sites in the area to the north of the Chapman River mouth. The red-bordered bars represent seagrasses: AG = *Amphibolis griffithii*; AA = *Amphibolis antarctica*; PSP = *Posidonia* sp.; and Coloniser = *Syringodium isoetifolium* + *Halophila decipiensis* + *Halophila* sp. 79

Figure 38: Count of broad scale geomorphic features associated with seagrass meadows (seagrass >69%), as resulting from a combination of GIS mapping of underwater geomorphology using multibeam bathymetry models and identification of benthic habitats through underwater photography data. 80

Figure 39: Percentage of fine carbonate sands at seagrass-dominated sites (seagrass >69%). Seagrasses were often found where fine sand >70% of the bulk of the sample (right-hand side of the plot). The minor mode of this bimodal plot (left-hand side) indicates that a minor percentage of seagrass meadows was found on coarser sediment substrates. 81

Figure 40: Count of broad scale geomorphic features associated with macroalgal communities (macroalgae >69%), as a result from a combination of GIS mapping of underwater geomorphology using multibeam bathymetry models and identification of benthic habitats through underwater photography data. 82

Figure 41: Photos of representative habitat types used for the acoustic habitat mapping practices. . 84

Figure 42: Probability density distribution of the mean relative backscatter strength values associated with the main habitat categories investigated in this study. This figure outlines the similarity of the acoustic response of seagrass meadows, macroalgal communities and mixed low density macroalgal and seagrass communities. 86

Figure 43: Angular response curves of the main seabed types found in the study area. 86

Figure 44: Mean backscatter intensity versus slope of the oblique incidence angles of the angular response curves for the seabed classes indicated in table 8 (top figure). The bottom figure shows a plot of the residuals. 87

Figure 45: Probability density distribution of the mean backscatter intensity values associated with the underwater geomorphic features mapped on the multibeam bathymetry models. Refer to the main body of the text for an explanation of this figure. 90

Figure 46: 5 m spaced raster grid of angle-independent backscatter levels resulting from the 2010 multibeam survey at Geraldton (data extent = ~35 km² to ~10 m depth, reaching ~25 m depth in some locations) overlain on the aerial photography. Backscatter intensity values are relative only. Higher values are associated to dense vegetation, lower values to sandy substrates, and intermediate values to sparse vegetation..... 93

Figure 47: Benthic habitat map resulting from the supervised classification of a 5 m spaced raster of angle-independent backscatter levels. Seagrass percentage of cover and mean benthic cover resulting from the analysis of the quantitative video transects are overlain on the classified acoustic map. 96

Figure 48: Polygons of acoustically similar regions of the seabed obtained from image segmentation with ground truth data overlain on it (left) and habitat map resulting from the association of ground data to the polygons using GIS techniques (right). Note the reduced data extent of the habitat map (right) due to limited availability of ground truth data. 98

Figure 49: Probability density distribution of the angle-independent backscatter levels extracted within the polygons deriving from image segmentation (left-hand side of figure 48) for the main habitat categories investigated in this study. This figure outlines the similarity of the acoustic response of densely and sparsely vegetated substrates. 99

Figure 50: The western continental margin of Australia, showing regional oceanography and biotic zones (southern Australia warm temperate and northern Australia tropical provinces; from Collins, 2010)..... 103

Figure 51: Sediment grainsize map of gravel and mud at Geraldton. The blue raster indicates <1% of mud. 106

Figure 52: Sediment grainsize map of coarse and very coarse sands at Geraldton. Blue tones indicate low %, yellow tones intermediate %, and red tones high % of coarse sand..... 107

Figure 53: Sediment grainsize map of medium sand at Geraldton. Blue tones indicate low %, yellow tones intermediate %, and red tones high % of medium sand..... 108

Figure 54: Sediment grainsize map of fine and very fine sands at Geraldton. Blue tones indicate low %, yellow tones intermediate %, and red tones high % of fine and very fine sand..... 109

Figure 55: Sediment grainsize along the Geraldton beaches; a comparison of the results of spring (2009 and 2010) and autumn (2010) sediment deposition. Note: older to newer datasets from left to right at repeated sites..... 111

Figure 56: Sediment carbonate content map at Geraldton. Blue tones indicate low %, grey tones intermediate %, and red tones high % of carbonate sediment..... 113

Figure 57: Sediment carbonate content along the Geraldton beaches; a comparison of the results of spring (2009 and 2010) and autumn (2010) sediment deposition. Note: older to newer datasets from left to right at repeated sites. 115

Figure 58: Sediment composition based on visual estimation of the percentages of modern bioclasts, reworked grains and relict bioclasts. Note poor discrimination of sediment types in this plot.... 118

Figure 59: Sediment composition resulting from the microscopic observation of sediment samples. Sediment composition was not undertaken to a species level but was assessed through visual estimation of the percentages of modern bioclasts, reworked grains and relict bioclasts..... 120

Figure 60: Mineralogical composition of selected sediment samples derived from the XRD analysis. Amorphous material includes silica from sponges, and other non-crystalline materials. Of note is the dominance of High Mg Calcite and the similarity in the abundances of Aragonite and Low Mg Calcite. This seems to indicate that sediment mineralogy is not changing significantly from modern to relict grains, and there is no apparent inversion of Aragonite and High Mg Calcite to

Low Mg calcite.....	121
Figure 61: Sediment facies map at Geraldton. Sediment facies were determined by considering percentage of fine, medium, and coarse sands, percentage of modern skeletal grains, and sediment carbonate content. The distribution of fine-medium quartzose and modern skeletal sand south of Geraldton is an artefact of data interpolation, and these areas are likely to be part of the surrounding fine modern skeletal sand and medium-coarse modern and relict skeletal sand polygons.....	124
Figure 62: Microscope photos of loose grains of the following sediment facies: A) Fine modern skeletal sand; B) Medium-coarse modern and relict skeletal sand; C) Coarse quartzose and relict skeletal sand; D) Cross-shore transect showing the distribution of sediment facies across depth at Geraldton; E) Line plots of sediment grainsize across depth showing percentage of fine, medium, and coarse sands; F) Line plots across depth showing carbonate content (%CaCO ₃), percentage of modern skeletal grains, and percentage of relict carbonate grains (intraclasts + relict skeletal grains). Whilst this profile represents an average sediment distribution across depth throughout the study area, off the Chapman River mouth the “fine-medium quartzose and modern skeletal sand” sediment facies dominates the coastal platform (refer to the main body of the text for further explanations).....	124
Figure 63: Fossil composition of the modern skeletal grain sediment fractions for A) Fine modern skeletal sand and B) Medium-coarse modern and relict skeletal sand.....	125
Figure 64: Microscope photos of the two most common sediment facies found at Geraldton: fine modern skeletal sand (A, B and C) and medium-coarse modern and relict skeletal sand (D, E and F). A, C, D & E – 10x enlargement on high power; B & F – 40x enlargement.	125
Figure 65: Isopach map of sediment thickness based on seismic data at Geraldton. Commonly sediment thickness is 1 m (orange contour), but it increases to 2 m (pink contour) where sediment accumulation occurs.	128
Figure 66: Example of the unconformities indicating the sediment rock interface (green) found at the northern extreme of the study area, off the Drummond Cove coast. For locations of seismic lines see figure 14.....	129
Figure 67: Sediment wedge overlying the sediment base reflector (green) off the Southgate dune system. For locations of seismic lines see figure 14.....	129
Figure 68: Quaternary eustatic sea level curve after Chappell et al. (1996). The study area was emerged until the Holocene transgression started ~20 Ka ago.	131
Figure 69: Sketch showing the limits of the nearshore zone and the position of the depth of closure, coincident with the d_c limit depth of Hallermeier (1981) and indicating a depth where “intense bed activity is caused by extreme near-breaking waves and breaker-related currents” (source: Schwartz, 2006).....	136
Figure 70: An idealised cross-section of a wave-dominated beach system outlining the nearshore zone, which extends out to wave base, where waves shoal to build a concave-upward slope (source: Short and Woodroffe, 2009).....	137
Figure 71: A) Interpolated % fine sand at Geraldton. The seaward limit of the nearshore based on sediment data is approximately coincident with the extent of >65% fine sand-dominated sediment class. B) Sediment facies at Geraldton. The distribution of fine-medium quartzose and modern skeletal sand south of Geraldton is an artefact of data interpolation, and these areas are likely to be part of the surrounding fine modern skeletal sand and medium-coarse modern and relict skeletal sand polygons.	139
Figure 72: Correspondence between Chapman River input of sediment identified through low carbonate content (a) and higher sediment thickness found at the same locations on the Geraldton coastal platform (b). On the carbonate content map (a), blue tones indicate low %, grey tones intermediate %, and red tones high % of carbonate sediment. On the isopach map of sediment thickness (b), the average sediment thickness of 1 m is indicated by the orange contour, and areas of sediment accumulation (2 m thickness) are shown by the pink contour.	145

Figure 73: Correspondence between the Southgate dune inputs of sediment found through morphology and habitat mapping and a higher sediment thickness on the isopach map. The circled area on the isopach map (A) shows 2 m of sediment thickness, with the surrounding areas at ~1 m. An offshore limestone ridge is also evident and is likely to limit the exchange of sediment supplied by Southgate dune with the offshore. A sand bar and a few sand sheets are visible at the same location on the bathymetry data (B), with the sand dominance confirmed by the low backscatter values (C) and the results of underwater imagery analyses..... **146**

Figure 74: Comparison of multibeam bathymetry data from 2002–2003 and 2010 within the port basin and dredged channel areas (provided by the Western Australian Department of Transport).... **148**

Figure 75: Comparison of multibeam bathymetry data from 2002–2003 and 2010 within the port basin and dredged channel areas (provided by the Western Australian Department of Transport). Blue tones indicate areas deeper in 2010 than in 2003, yellow tones indicate areas of no bathymetry change, and red tones indicate areas shallower in 2010 than in 2003. Consequently sediment accumulation occurs in the areas in the red zones. **149**

Figure 76: Comparison of multibeam bathymetry data from 2002–2003 and 2010 within the port basin and dredged channel areas (provided by the Western Australian Department of Transport). Blue tones indicate areas deeper in 2010 than in 2003, yellow tones indicate areas of no bathymetry change, and red tones indicate areas shallower in 2010 than in 2003. Consequently sediment accumulation occurs in the areas in the red zones. **150**

Figure 77: Location of figures 78 and 79. **151**

Figure 78: W-E bathymetric profile of the dredged channel (location on figure 73). The dotted area indicates the sediment cover. **151**

Figure 79: SSW-NNE bathymetric profile of the dredged channel (location on figure 73). The dotted area indicates the sediment cover. **151**

Figure 80: Detail of a modified version of the seabed mobility map discussed in Chapter 2 to allow the location of shallow limestone reefs to be visualised (yellow polygons). The map outlines the sediment deposition areas (green polygons) developed in between the limestone reef to the north of Point Moore, which are natural sediment sinks for the coastal system. The dredged channel and Port basins are indicated by the grey polygons where sediment deposition does not occur; however, the green polygons falling within their basins indicate areas of sediment deposition. The Batavia Coast Marina also includes a green polygon and it was recognised as an artificial sediment sink for the coastal system. **152**

Figure 81: Detail of the seabed mobility map discussed in Chapter 2 outlining the sediment deposition areas (yellow polygons) off the Chapman River mouth. These are natural sediment sinks for the coastal system. **153**

Figure 82: Cross-shore profiles extracted from multibeam bathymetry and coastal topographic surveys. Vertical and horizontal scales are in meters. The profiles are used to identify patterns of sediment transport alongshore and cross-shore. Refer to the main body of text for further explanation. **156**

Figure 83: Shoreline change rate deviations along the Geraldton coastline from 1942 to 2010 (data developed as part of Tecchiato et al., 2012). The horizontal axis shows the distance between the locations indicated on the top of the graphs and outlined in figure 1..... **157**

Figure 84: Migration of the area surrounding Point Moore at Geraldton over ~70 years from 1942 to 2010. Note the northward and westward movement of the coastlines in the area, with stability reached from 1988..... **158**

Figure 85: The asymmetry of the beach north and south of the island breakwater, located north of the Batavia Coast Marina, is a qualitative indicator of prevalent northward littoral transport. The image is an enlargement from the July 2007 aerial photograph. **159**

Figure 86: The conceptual sediment budget model is summarised in this figure, using the seabed mobility map discussed in Chapter 2 as a background layer. Swell waves come from SW and the wind component in the Champion Bay area is mainly from S-SW. There are two sediment sources: Southgate dunes and Chapman River (GIS layer courtesy of GSWA). In situ sediment

production linked to seagrass meadows and macroalgal communities is also considered a sediment source but could not be indicated on the map as it is accounted as part of the longshore sediment supply. The sediment deposition areas are accurately located on this map and include the dredged channel, the Geraldton port, and the Batavia Coast Marina basins. Black arrows indicate sediment transport pathways. 162

Figure 87: Sediment cells of the Geraldton coastal system (see the text for a detailed explanation of sediment pathways). The identified sediment cell boundaries and their characteristics are also indicated: blue and light blue lines are fixed permeable boundaries and define major cells; green and red lines indicate free permeable limits and delineate sub-cells. The coastline evolution pattern is summarised in this figure, with accreting, eroding, and stable areas. The black arrows indicate transport pathways, and areas of sediment deposition within the littoral sediment cells are also indicated. Of note is that sediment nourishment is ongoing within Cell 4 and provides occasional sediment input within Cell 2. 167

Figure 88: Results of the longshore sediment transport modelling by LITDRIFT, indicating the volume of sediment transiting across the investigated profiles in cubic meters (m^3). Positive values indicate northward-oriented sediment transport and were recorded for most of the investigated locations. Negative values indicate southward-oriented sediment transport and were only measured at one profile south of Point Moore. 171

Figure 89: Quantitative sediment budget model of the Geraldton embayments. A) The black arrows indicate sediment transport pathways, the red arrows locations of sediment nourishment, and the green arrow the beach where sediment is mined. The balance of each sediment cell is indicated next to the cell name ($10^6 m^3/year$), as well as the amount of sediment supplied (Q_{source} and P), sinking (Q_{sink}), and artificially removed from the beach (R). B) This conceptual map shows location of sediment sources and sediment sinks identified on the basis of sediment, bathymetry, habitat, and seismic data. The approximate location of the offshore reefs sheltering the coast is also visible on the map, as well as the main swell and wind waves direction. 175

Figure 90: Shore normal sketch illustrating the nature of shallow water carbonate sediment production in the studied shallow water warm-temperate marine embayments. Both the macroalgal and seagrass carbonate factories are producing similar, but somewhat different, carbonate sediments with higher production rates for seagrass meadows. The arrows indicate sediment transport directions. A lack of mixing of the particles deriving from these benthic communities occurs in the study area, with fine sands dominating the seagrass sites and medium-coarse sands occurring where macroalgal communities are prevalent. The figure also summarises the substrate-related partitioning of these communities with macroalgae located on the high-energy shallow limestone reef systems at the seaward edge of the coastal platform and seagrasses rooted in the troughs of flat or low sloping hardgrounds with sediment veneers at sheltered locations close to shore. Mixed seagrass and macroalgal communities are also common at Geraldton and colonize sediment veneer over rocky substrates, similarly to seagrass meadows. 179

Figure 91: Shore normal sketch illustrating the cross-shore distribution of sediments, benthic habitats, and geomorphological features. The calculated depth of closure is also indicated, to allow a linkage with the environmental parameters to be made. Distance from shore is given on the horizontal axis. 182

LIST OF TABLES

Table 1: Characteristics of the Geraldton beaches and linkage to infrastructure and nourishment activities (modified from Tecchiato et al.; 2012). For beach locations see figure 1.....	21
Table 2: Summary of the bypassing activities undertaken at Geraldton (from Tecchiato et al.; 2012). Sediment is bypassed downdrift from west to east and north of the Port of Geraldton.....	22
Table 3: Wave sources and characteristics along the Western Australian coast (Short, 2006).....	24
Table 4: Stream discharge volume for the Greenough River measured at Karlanew peak (http://www.water.wa.gov.au/idelve/rms/index.jsp).....	32
Table 5: Stream discharge volume for the Chapman River measured at Utakarra (http://www.water.wa.gov.au/idelve/rms/index.jsp).....	34
Table 6: Biota classification definitions used for classifying the standard definition video transects. .	51
Table 7: Substrate classification definitions used for classifying the standard definition video transects.....	52
Table 8: Habitat classes used to classify the multibeam backscatter data. Refer to figure 41 for the habitat photos.	85
Table 9: Summary of the acoustic properties for the seabed classes analysed in this study.	89
Table 10: Error matrix for the benthic habitat map resulting from the supervised classification of angle-independent backscatter levels shown in figure 47. The bottom line summarises the classification accuracy for each habitat.	95
Table 11: Error matrix derived from a reinterpretation of Table 10, showing the mapping accuracy increase which could be achieved by restricting the habitat categories to sand and vegetation only.....	95
Table 12: Error matrix for the benthic habitat map shown on the right hand side of figure 48. The bottom line summarises the classification accuracy for each habitat.	99
Table 13: Summary of the main characteristics of the Geraldton sediment facies.	126
Table 14: Offshore geomorphology and beach characteristics throughout the study area.	141
Table 15: Summary of the volume of sediment input into a sediment cell or transported out of a sediment cell, as simulated by the longshore sediment transport modelling.	172

Chapter 1

INTRODUCTION

1.1 INTRODUCTION

Human activity and the coast have a strong link, as more than one third of the world's population lives in coastal areas and 80% of Australians live within 100 km from the coast (Cox et al., 2004; Harvey and Caton, 2010). Ports and harbours have traditionally facilitated international commercial activities and made cultural exchange between world civilizations possible. Today, the coast (especially sandy beaches and warm weather) attracts tourists and offers recreational activities, such as swimming, fishing, surfing, and boating. Globally, the fishing industry and fisheries products provide direct employment for 38 million people, and in general people are dependent on the ocean and coast for their survival and wellbeing (UNEP, 2006). The coastal strip also fulfils a natural sheltering function for communities as coastal ecosystems support shoreline stabilization from hurricanes, flooding, cyclones and other beach losses due to seasonal and climate change (UNEP, 2006; DCC, 2009). The sense of place which an individual experiences, a contribution to personal wellbeing, may be affected by the condition of local coastal ecosystems as people tend to identify with aspects of the physical environment which have generated a sense of attachment (Cox et al., 2004; DCC, 2009). Personal wellbeing, commercial activities, and environmental and estate values make the natural link between humans and the beach, and promote the need for efficient environmental management which may well ensure coastal conservation and access, especially where the major drivers of change, degradation, or loss of coastal and marine ecosystems have been demonstrated to be mainly anthropogenic (UNEP, 2006). The Australian Department of Climate Change has identified the need for a unified national approach towards coastal management issues, which is to be developed on the basis of the best science and to be updated periodically as new science becomes available (DCC, 2009).

This research has developed scientific information for managing a section of the Australian coast and may provide a template for future studies of this kind at a local as well as a regional level. The study focuses on the sediment dynamics of a section of the mid-western Australian coast, providing valuable information for understanding ongoing dredging and sand bypassing activities. Such operations are common in Western Australia and consequently this study may support the understanding of processes at locations with similar infrastructure and environmental settings across the state. The research also studies the temperate water marine habitats contributing to sediment production and accumulation,

outlining the important role of seagrass and macroalgal communities for Western Australian coastal areas. It provides new data on the linkage between coastal geomorphology, habitats, and sediments, which are beneficial to coastal management and conservation. The aim of this section is to put the research into context and outline the significance of the study. This chapter also describes the objectives and introduces the thesis structure (section 1.2). Background information is included to introduce the environmental setting and coastal development characterising the study area (section 1.3). The chapter concludes with the methods used for the analyses (section 1.4).

1.1.2 The need for a coastal study at Geraldton

This study was conducted for the Western Australian Department of Transport (DoT) and is part of the Coastal Vulnerability and Risk Assessment Program, which is a partnership between the Northern Agricultural Catchments Council with the City of Geraldton-Greenough, Geraldton Port Authority, Department of Planning and Department of Transport. The scope of the Program is to ensure future planning projects take into account the impact of various environmental factors on the coast and inshore waters between the Greenough River mouth to the south and the Buller River mouth to the north (figure 1). To achieve these aims, the overall program includes a series of projects which focus on different topics relevant to the assessment of coastal vulnerability.

Geraldton is an expanding urban and industrial complex, which serves an important port facility of the state of Western Australia. The significant coastal infrastructure and the coastal erosion phenomenon that is impacting the town beaches make Geraldton a “hot spot” for local environmental attention, but similar situations are reported elsewhere in the state including localised sites where maritime transport is vital for sustaining the international commercial activities of Western Australia. This study of the coastal system may provide a template for similar future studies across the state and a basis for future analysis in areas where planning and management are required by local and regional coastal and marine agencies. In particular, the project was intended to provide a greater understanding of the Geraldton coastal system in terms of geomorphic settings, sediments and habitat distribution and their linkage to sediment production, transport, and storage. Understanding the sources and transport pathways of sediment is essential to understanding the long-term implications of climate change for coastal erosion and recession. This study has provided vital information to inform the City of Geraldton in determining long-term management of the Geraldton coastline and promote the development of planning and adaptation measures.

1.2 AIMS OF THE STUDY

The main objective of this research project was the development of a quantitative sediment budget model for the Geraldton embayments, which has provided useful information to assist local government agencies in long-term management of the Geraldton coastline despite the limitations due to data availability. Previous studies developed on the basis of sediment transport models were available for the most impacted section of the study area; however, there was an emerging need to understand in detail the coastal environment and the processes driving the shallow sediment transport.

The formulation of a quantitative sediment budget model and the environmental characterization of the study area have required the following objectives to be achieved:

- Underwater geomorphology mapping. Multibeam bathymetry data provided high resolution data for mapping geomorphological features at Geraldton to overcome the lack of information at a local and regional level.
- Acoustic habitat mapping. Multibeam backscatter data and underwater imagery was used to map the benthic habitats at Geraldton.
- Mapping of sediment facies. Sediment data were analysed for grainsize, carbonate content, mineralogical composition, and petrological composition.
- Mapping of sediment geometry. Seismic data were used to assess sediment availability (i.e. the amount of sediment covering the rocky coastal platform).
- Identification of the seaward limit of the littoral sediment transport system. A combination of sediments, geomorphology, and hydrodynamic data was analysed to assess the depth of closure at Geraldton.
- Identification of sediment sources. Sediment data provided useful insights on sediment provenance.
- Identification of sediment “sinks”. Sediment thickness, bathymetry, and habitat data allowed sediment accumulation areas to be identified; these are basically accumulation areas distinguished by limited sediment reworking and/or transport to different locations.
- Identification of sediment transport pathways. An integrated analysis of all data available for this project was required to accurately identify sediment transport pathways.
- Definition of sediment cells. An integrated analysis of sediment, bathymetry, hydrodynamic, and aerial photography data was necessary to identify littoral sediment cells.

- Simulation of a sediment transport model. Bathymetry, habitat, and hydrodynamic data were entered in dedicated modelling software to obtain quantitative measurements of longshore sediment transport from one littoral cell to another.
- Formulation of a quantitative sediment budget model. Calculation of the balance of sediment accumulating or exiting the identified sediment cells was required.

The nature of the data used allowed this research to generate an appropriate environmental background for sediment dynamics analysis at a local and regional level. The data available (i.e. aerial photography, sediments, underwater videography, bathymetry, sediment thickness, and habitat data) led to a detailed mapping of underwater geomorphology, sediments and habitat distribution providing spatially extensive information on littoral sediment dynamics along with a significant sedimentological understanding of the coastal system, in terms of sediment production, transport, and storage. The available data allowed the identification of sediment cells to be achieved by considering not only the local hydrodynamic conditions but also the geomorphology, sediments and habitat distribution of the whole study area. This is in contrast to many sediment budget studies which often base the delimitation of sediment cells mainly on hydrodynamic information and have a more limited understanding of the overall environmental characteristics of the systems. Finally, the understanding of the Geraldton coastal system achieved here overcame the lack of previous similar studies along the Western Australian coastline and built a background for understanding the seaward limits of the littoral sediment transport system and the geomorphological features and marine ecosystems influencing local and regional sediment dynamics.

One of the objectives of the analysis of multibeam data was the evaluation of their capability to distinguish different seabed types using bathymetry, backscatter intensity, and angular response data. The use of multibeam echo sounder data for seabed mobility investigation of coastal temperate water environments was also tested. These analyses have provided new data for the mapping of temperate water habitats using acoustic data, which will support future understanding of the acoustic response from these benthic biota and substrates.

1.2.1 Outline of the thesis

This thesis is divided into five chapters, beginning with an introductory chapter which describes the project scope and methodologies, the general context of the work, and the environmental setting of the study area. Chapters 2, 3, and 4 begin with an introductory section which describes the general knowledge (worldwide and regionally) of the topics

discussed in the relative chapter. These sections provide useful information on the context of the analyses and link the study to similar projects carried out elsewhere in the world.

Chapter 2 describes the underwater geomorphology and habitat investigations carried out in this research, as well as the main outcomes of the application of multibeam backscatter data to seabed characterization. The relationship between the spatial distribution of benthic habitats, geomorphic features and sediment grainsize are also explained in this chapter.

Chapter 3 explains the sediment characteristics (i.e. grainsize, carbonate content, mineralogy and petrology) of the Geraldton coastal system, and compares the current carbonate production to the surrounding Western and South Australian temperate-water coastal sedimentation. Chapter 3 presents the sediment geometry in the nearshore areas, and evaluates the sediment production rate at Geraldton, comparing it to other situations previously documented for seagrass and macroalgal systems of Australia.

Chapter 4 combines the information presented in Chapters 2 and 3 to determine the seaward limits of the littoral sediment transport system, and presents the results of the longshore sediment transport modelling developed for the study area. The entire dataset analysed in this project is subsequently used to identify littoral sediment cells and develop a sediment budget model.

Finally, Chapter 5 concludes and summarises the main outcomes of this research project, comparing the study to similar projects conducted elsewhere with attention to the benefits provided by this project to local management and as a reference for future studies of a similar nature.

1.3 THE STUDY AREA

The study area encompasses the city and port of Geraldton, approximately 400 km north of Perth, Western Australia. Shoreline salients, cusped forelands and tombolos are common coastal sedimentary landforms of the Western Australian coast, and along the central west coast are developed in correspondence to semi-continuous Pleistocene limestone reef systems located up to 15 km from the shore (Sanderson and Eliot, 1996). The interaction between local sediment transport and offshore limestone reefs at Geraldton has resulted in the formation of the Point Moore tombolo which separates the coast into two main embayments, both analysed in this study. In more detail, the project studied the section of coast between the Greenough and Buller Rivers down to the 30 m bathymetric contour (figure 1).

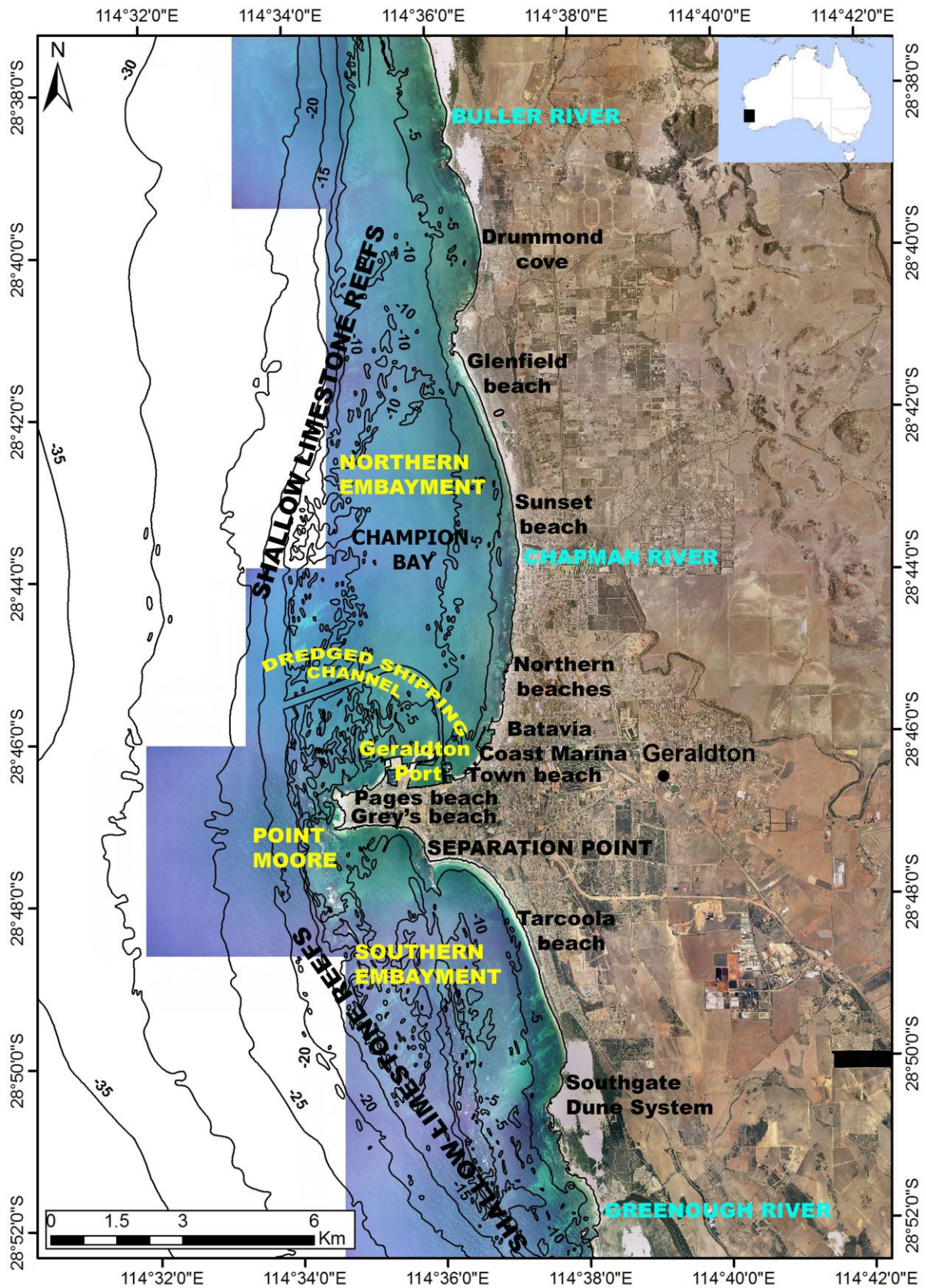


Figure 1: Study area and location map of the city of Geraldton. Refer to this map for visual location of the localities named throughout the thesis.

Geraldton is a coastal town with approximately 30,000 inhabitants which provides important services for regional mining, fishing, wheat, sheep, and tourism industries. The Port of Geraldton is central infrastructure for the receipt and transport of regional products of agricultural, farming, and mining activities, as the port handles iron ores, grains, fuels, metals, mineral sands, talc, garnet, and fertilisers. Establishment of the Port of Geraldton in the northern embayment began in the 1850s and the extension of the port groynes continued until the 1990s. A port access channel was originally dredged in the 1960-70s, and in 2003 both the harbour and channel basins were deepened to allow for larger ship loadings and reached their current configuration. Additional coastal development exists along the coast, such as the Batavia Coast Marina to the north of the Port of Geraldton, which was built in the 1980s and extended in the 1990s, with the current groyne configuration of port and marina structures reached in the early 2000s. These infrastructure components influence local sediment transport in different ways, and this will be discussed throughout the dissertation. In particular, the dredged channel and port basins trap sediment and require maintenance dredging activities. Moreover, sand bypassing is frequently undertaken to maintain the shoreline of the town beaches to a stable position. A description of the beach characteristics in the study area with linkage to sediment nourishment activities is reported in section 1.3.1, and is important as it provides useful clues to the main direction of littoral sediment transport.

The wind climate is responsible for much of the coastal dune activity along the Geraldton coast with the strong sea breezes, in particular, contributing to the littoral sediment transport (section 1.3.2). Wave and current characteristics are fundamental in determining the coastal processes and, together with the local winds, drive the dominantly northward-oriented sediment transport (section 1.3.3). The onshore coastal geomorphological settings are introduced in section 1.3.4 and include an important coastal dune systems developed south of Geraldton. A description of the small river channels and streams in the area is included (section 1.3.5) for completeness, as it provides basic data for evaluating sediment sources in the studied coastal system. The geological setting of the study area is described in section 1.3.6, and provides vital information for understanding the littoral sediment composition and coastal geomorphology.

1.3.1 Beach characteristics, coastal evolution and sand bypassing activities

The Australian coast south of the 26th parallel is exposed to persistent Southern Ocean swell, with a mean significant wave height (H_s) of 3 m and tides of less than 2 m. All these areas are wave-dominated and are characterised by wave-dominated beaches associated

with fine carbonate sands and the beaches of the study region are part of this category (Short, 2006b). The coastline of the study area shows an abundance of Quaternary carbonate-rich barriers and backing dunes, paralleled by largely submerged Pleistocene calcarenite barriers, which form near-continuous limestone reefs in the nearshore. Beaches are usually “swash-aligned”, meaning they are aligned parallel to the crest of the dominant wave and these nearshore reefs tend to alter the direction and amount of energy which reaches the shore due to refraction and shoaling of the approaching waves. This reduced wave intensity generally results in numerous reflective beaches (constituting approximately 80% of the beaches of the central-west coast of Australia).

North and south of Point Moore (Figure 1), the beaches show different characteristics in terms of morphology, extent, and evolution pattern. Table 1 summarises the beach and onshore development and the net shoreline movement for the period 2001–2010. Most of the coastal infrastructure (especially groynes and breakwaters) was developed in the area in the period 1967–2000, whilst the dredged channel and Port basin were deepened in 2002–2003; consequently, some of the shoreline change recorded in the last decade may reflect the effect of offshore bathymetry increase due to the dredging operations. The historical shoreline change information presented here was developed for the study area as summarised in Tecchiato et al (2012), and was based on aerial photography data from the past 70 years. The shoreline rate of change was assessed using the widely accepted DSAS extension (Digital Shoreline Analysis System) for ArcGIS developed by the U.S. Geological Survey (Thieler et al., 2009), which is based on the vegetation line - a shoreline proxy commonly accepted for determining longer term trends in shoreline position (Stul, 2005).

The beaches of the Geraldton southern embayment (figure 1) are relatively wide (~30 m) and mainly stable or accreting (North Tarcoola Beach), with low erosion rates at locations where coastal development was undertaken on the adjacent sand dunes (Southgate and South Tarcoola Beach).

The most significant shoreline rate of change has been noted for the beaches around Point Moore. Grey's beach, on the south side of Point Moore, is narrow (20 m) and shows significant erosion, with part of the adjacent road collapsing into the upper beach zone. Point Moore and Pages Beach appear to be the widest beaches and are showing an accretion pattern, with shelter from waves provided by the offshore reef system. Sand is naturally accumulating at Pages Beach and is mined for nourishing the Northern Beaches with an average sand volume of 12,500 m³ per year. Pages Beach, on the north side of Point Moore, has shown very significant accretion, mainly as a consequence of the port infrastructure and

rock groynes to the west of the port, facilitating the accumulation of sand transported there by nearshore currents.

Town Beach is wide and has a well-developed sediment wedge in the nearshore, but is an artificial beach, currently subject to nourishment activities and has been stabilised by the placement of groynes in the 2000s.

Overall, the shoreline between the Batavia Coast Marina and the Chapman River is composed of narrow beaches (so called Northern Beaches, ~17 m wide) and has remained relatively stable with some minor (averaging $\pm 0.15\text{m/year}$ over the last 70 years) accretion and erosion noted. Repetitive nourishment activities are ongoing in this area from 1991 at an average rate of $12,500\text{ m}^3$ per year; however, the sediment seems to be transported northwards and lost offshore, as evidenced by rock exposure along the coastline. Table 2 summarises the sediment bypassing activities around the Port of Geraldton on the basis of data extracted from various technical reports (MRA, 2001; Bailey, 2005) and a datasheet provided by the Geraldton Port Authority. However, as often reported in sediment budget studies, a complete record of sand bypassing activities has not yet been obtained. The Geraldton Port Authority deposited between $\sim 4,000$ and $\sim 20,000\text{ m}^3$ of sand per year on the beaches north of the Batavia Coast Marina and in 2009, 2010, and 2011 the nourishment included Town Beach as well. Sources of sand were Explosive (east of Pages beach), Pages and Point Moore beaches. A major sand placement was undertaken by Thiess Pty Ltd in September 2004 and consisted of $89,000\text{ m}^3$ of sand derived from the excavation works associated with the development of the Southern Transport Corridor. This material was placed on the beach north of the Batavia Coast Marina and, according to a monitoring program that followed nourishment activities, the sand was transported northwards.

Sunset Beach is very narrow (14 m) and records the highest erosion rates at Geraldton, with the adjacent dunes clearly showing an erosive profile and characterised by significant urban development. Sunset Beach shows an average erosion of approximately 0.5 metres a year from 1942 to 2001 with an almost tripling of the average rate of erosion in the most recent decade to 1.45 metres a year, with up to 3.12 metres of erosion noted ~ 1.8 km north of the Chapman River in the mobile dune. Based on aerial photo analysis of images taken before 1969 the area was accreting; the coastal retreat from 1969 onwards appears to coincide with vegetation loss on the dunes (Tecchiato et al., 2012).

The shoreline from Glenfield to Drummond Cove is mostly stable and is not very wide. The Drummond Cove stretch of the coast has retreated steadily over the past 70 years with the rate slowing in the last 10 years. On the southern side, Glenfield Beach shows little accretion

Table 1: Characteristics of the Geraldton beaches and linkage to infrastructure and nourishment activities (modified from Tecchiato et al.; 2012). For beach locations see figure 1.

Beach	Beach typology (Short, 2006b)	Width (m)	Height (m)	Net shoreline movement 2001-2010	Nourishment/ Infrastructure
Southgate	PERCHED	28	NA	Eroding to Stable	Tracks on dune system
South Tarcoola Beach	REFLECTIVE	22	NA	Eroding, up to 1.2 m, per year, average 0.74m	Development on sandunes
North Tarcoola Beach	DISSIPATIVE	37	NA	Stable to accreting	NA
Grey's Beach	REFLECTIVE	20	+1.4	Eroding – up to 1.8m per year, average ~1m	NA
Point Moore	DISSIPATIVE	84	+1.5	Accreting	NA
Pages Beach	REFLECTIVE	50	+0.80	Accreting – up to 4m per year	Sand mined here
Town Beach	REFLECTIVE	33	+2.4	Accreting - note significant infrastructure	Nourished/groynes
Northern Beaches opposite Mark St	PERCHED	16	+1.3	Stable (eroding/accreting less than 1m per year)	Nourished/north of island breakwater
Northern Beaches opposite Hosken St	REFLECTIVE	26	+1.4	Stable (eroding/accreting less than 1m per year)	Nourished
Northern Beaches opposite Morris St	REFLECTIVE	12	+2	Stable (eroding/accreting less than 1m per year)	Nourished
Chapman River mouth	REFLECTIVE	17	+2.2	Stable	NA
Sunset Beach	REFLECTIVE	14	+1.9	Eroding – Up to 3.12m per year, average ~1.45m	Development on sandunes
Drummond Cove North	REFLECTIVE	17	+1.8	Mostly stable. Some areas eroding on average 0.35m per year	NA

Table 2: Summary of the bypassing activities undertaken at Geraldton (from Tecchiato et al.; 2012). Sediment is bypassed downdrift from west to east and north of the Port of Geraldton.

Year	Volume (m ³)	Extraction location	Placement location
1991	20,000	NA	Northern Beaches
1992	19,000	NA	Northern Beaches
2000	4,000	NA	Northern Beaches
2001	4,000	NA	Northern Beaches
2003	11,940	Pages Beach, Explosive Beach	Northern Beaches
2004	10,140	Pages Beach	Northern Beaches
2004	89,000	Southern Transport Corridor	North of Batavia Coast Marina
2006	14,328	Pages Beach	North of Batavia Coast Marina
2007	13,070	Pages Beach	Northern Beaches
2008	16,882	Pages Beach	Northern Beaches
2009	13,540	Pages Beach	North of Batavia Coast Marina, Town Beach
2010	20,025	Pages Beach	Northern Beaches, North of Batavia Coast Marina, Town Beach
2011	13,955	Pages Beach	Northern Beaches, Town Beach

in the past ten 10 years, and considering the low anthropogenic influence in this area this data seems to indicate that the coast at Drummond Cove is retreating naturally. The limestone reef system developed close to shore and the cusped foreland in between Glenfield Beach and Drummond Cove are likely to facilitate sediment deposition on the southern leeward side of the cusped foreland (off Glenfield), limiting sediment transport to the north (towards Drummond Cove).

1.3.2 Climate and wind regimes

Geraldton experiences a Mediterranean-type climate, characterised by warm to hot, dry and windy summers and short and mild, wet winters (BoM, 2011). In the winter months, the temperature averages 20°C with most of the yearly rainfall in this period due to cold fronts from Antarctica moving up and hitting the coast. In the summer months, Geraldton averages 32°C with some days over 40°C; high pressure systems in the Great Australia Bight send warm easterly winds to Geraldton and a west coast trough is formed. The city experiences seasonal extremes in weather, from hot summer days, characterised by north-easterly winds

from the interior of the state, to cold, wet, windy winter days as cold fronts from the Southern Ocean move through the region (BoM, 2011).

Geraldton is one of the windiest cities on the west coast of Australia, with a predominance of moderate to strong winds throughout much of the year (BoM, 2011). The wind climate at Geraldton is highly seasonal with two principal wind regimes: SSW during summer and NE during winter. During warmer months the wind climate at Geraldton is strongly dominated by the effects of the land-sea interface and by the position of the sub-tropical ridge, which generates winds with an easterly component overnight and offshore land breezes in the morning, while sea breezes from the south to southwest dominate the afternoon. Summer sea breezes are frequently quite fresh and often reach 25 knots (46 km/h) or more near the coast (BoM, 2011). Winter tends to be the period of most variability in wind direction due to the latitude and mobility of the sub-tropical ridge, and a weak land-sea temperature contrast (BoM, 2011). It also tends to be the season with the lightest winds; however, cold fronts can occasionally bring strong winds and gales to the area (BoM, 2011). In the November-March period, the winds experience diurnal as well as periodic changes to wind strength and direction (BoM, 2011). On rare occasions, and more likely in late summer or early autumn, a tropical cyclone can be “captured” by a stronger southern front; in this case the cyclone will move rapidly southwards with associated extreme winds (GEMS, 2001). Favourable onshore wind regimes exist at Geraldton and interact with the nature, form, and dimensions of coastal dunes to reflect the character and volume of sand available on nearby beaches, which in turn influences the nearshore sediment budget (Orme, 1988).

1.3.3 Coastal processes

The Western Australian littoral sediment transport is regulated by the wave climate which derives from a combination of sea and swell waves originating from six possible sources summarised in table 3; however, monsoonal winds and tropical cyclones do not influence the study area directly. Swell waves derive from the mid-latitude cyclones which act constantly during the year south of the southern Australian coast. The swell period is 10–14 sec. and wave height is moderate to high (2–3 m) and is higher along the southern Australian coast, decreasing toward the equator (Short, 2006b). Swell waves are rarely less than 0.5 m high (<10%) and their main direction is from southwest (60%) and west (20%) (Short, 2006b). Short and Woodroffe (2009) indicated an average swell of 2 m along parts of the Western Australian coast, including Geraldton. The sea waves are generated from the sea breeze that flows onshore around the entire coast of WA and are strongest during the summer months (Short, 2006b). Short and Woodroffe (2009) indicated that wind waves can often

dominate the wave climate. The combination of prevailing southerly waves and, at times, strong southerly winds drives a northward sediment transportation system that operates for a large region of Western Australia, extending from Geographe Bay all the way north to Shark Bay (Short and Woodroffe, 2009), and including the study area.

The DoT funded a study by Cardno Pty Ltd to model the local hydrodynamics at Geraldton and these data are presented and acknowledged in sections 1.3.3.1 and 1.3.3.2.

Table 3: Wave sources and characteristics along the Western Australian coast (Short, 2006).

Source	Location	Direction	Season	Characteristics
Mid latitude cyclones	latitude 40–60° S	S-SW	year-round	moderate-high SSW swell
High pressure	latitude 30° S	W	winter max. in south	westerly seasonal swell
Sea breeze	along entire coast	S-SW in the south W-NW in the north	summer max.	short, low seas
Trade winds	central-northwest coast	E-SE	year-round, winter max.	short, seas to 3 m
Monsoonal winds	Kimberley region	W-NW	summer	short, seas to 2 m
Tropical cyclones	northwest coast	W	summer	high seas to several metres

1.3.3.1 Currents

The dominant factors considered to influence the water circulation at Geraldton are local winds, and of minor influence is the small tidal range of ~ 0.7 m. There are two principal seasons with respect to the wind-driven circulation:

1. Summer (October-March): the direction of predominant water current flow is frequently northward throughout Champion Bay (figure 2);
2. Winter (April-September): the direction of predominant water current flow is frequently south-westward out of Champion Bay and past Point Moore (figure 3), with a northwards-oriented current throughout Champion Bay, deviating to the west north of the Chapman River mouth.

The Cardno (2012a and 2012b) data indicates that eddies are established near Point Moore and particularly to its south, influencing interactions with both the changing coastal configuration and the discontinuous offshore limestone ridges. The summer and winter eddy patterns are broadly similar.

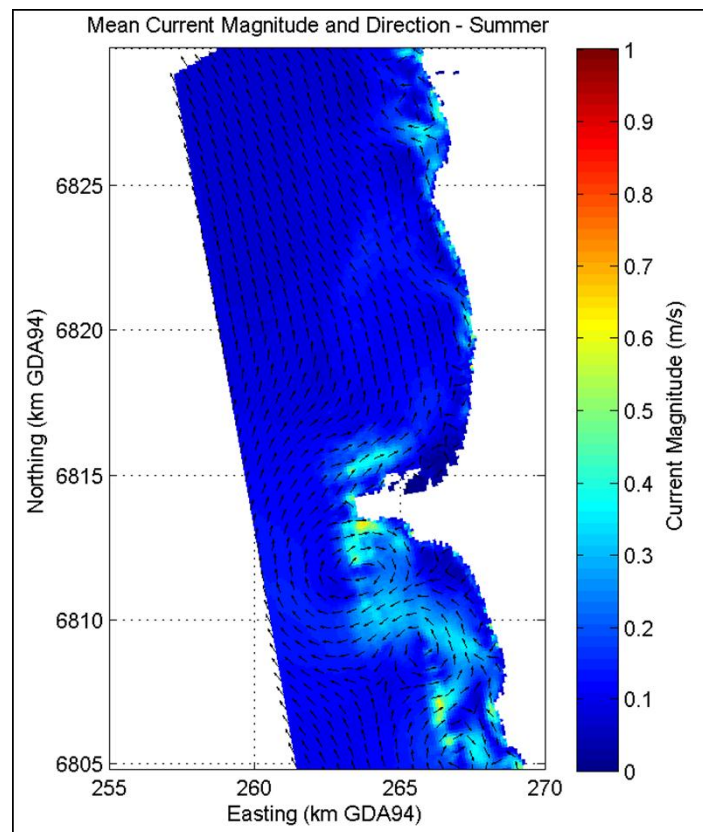


Figure 2: Cardno Pty Ltd modelling of mean summer currents (from Cardno, 2012b). The direction of predominant water current flow is frequently northward throughout Champion Bay.

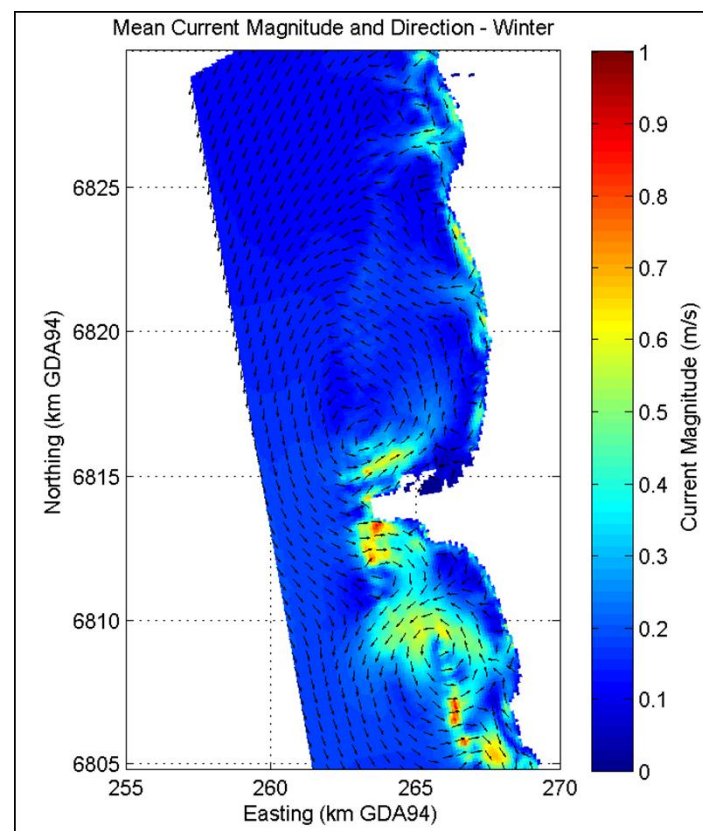


Figure 3: Cardno Pty Ltd modelling of mean winter currents (from Cardno, 2012b). The direction of predominant water current flow is frequently south-westward out of Champion Bay.

1.3.3.2 Waves

The wave climate at Geraldton consists of sea and swell waves. Of note is that the Geraldton summer climate has strong (20–35 knots) SSW winds which produce sea breeze waves in the late morning to afternoon.

As shown by the Acoustic Wave and Current (AWAC) data recorded at the Geraldton Outer Channel, swell wave heights range predominantly between 1–1.5 m (~30%), occasionally lowering to 0.5–1m (~20%) or increasing to 2 m (~20%). Swell waves are rarely less than 0.5 m (<10%) or more than 2 m high (<10%) and their main direction is from WSW (Figure 4).

According to the AWAC data recorded at the Geraldton Outer Channel, the main sea wave direction at Geraldton is from SW (~50%), with occasional WSW and SSW waves (figure 5). Sea wave heights are mostly in the range of 0.5–1m, with occasional increase to 1.5 m (figure 5).

The predominant wave directions at Geraldton range from W to SW, but during storm events in winter the wave direction can range from W to NW as commonly recorded for coastal Western Australia.

The wave climate is moderated within Champion Bay by the protection of the offshore reefs (URS, 2001, Cardno, 2012a) with lower wave height in the area between the Geraldton Port and the Northern Beaches and higher wave height corresponding to the offshore reefs (figures 6 and 7). In the south, the southern part of Tarcoola beach is also sheltered by an offshore limestone ridge. Wave heights are in the range 0.5–1.5m along the Geraldton coastline, locally increasing to 2 m during the winter months (figures 6 and7). Higher wave heights along the shore occur locally at Sunset Beach and Drummond Cove (figures 6 and7). Fluctuations in local wave height are most likely caused by shoaling, sheltering, and refraction effects associated with the discontinuous limestone ridges offshore.

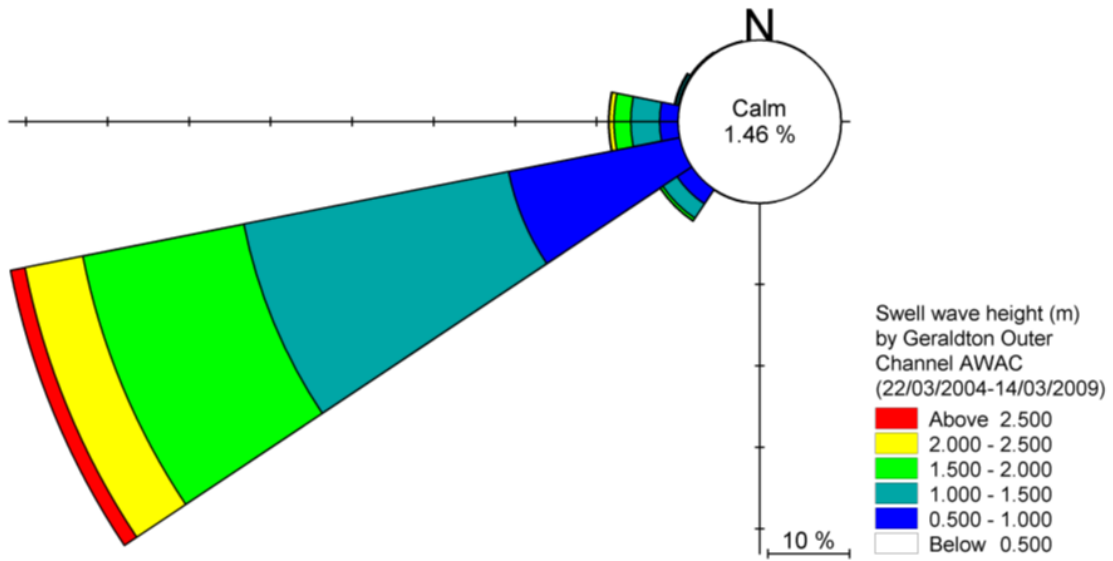


Figure 4: Swell wave heights and directions at Geraldton (Geraldton Outer Channel AWAC data, courtesy of the Department of Transport). Swell wave heights range predominantly between 1 and 1.5 m.

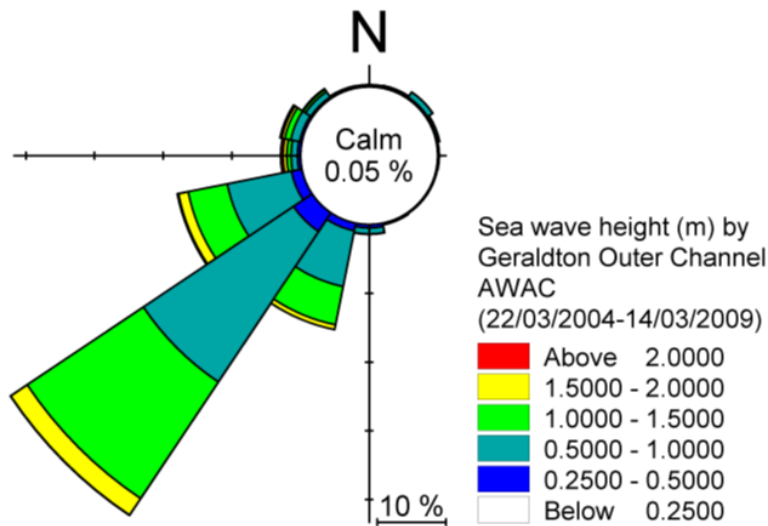


Figure 5: Sea wave heights and directions at Geraldton (Geraldton Outer Channel AWAC data, courtesy of the Department of Transport). Sea wave heights are mostly in the range of 0.5–1 m.

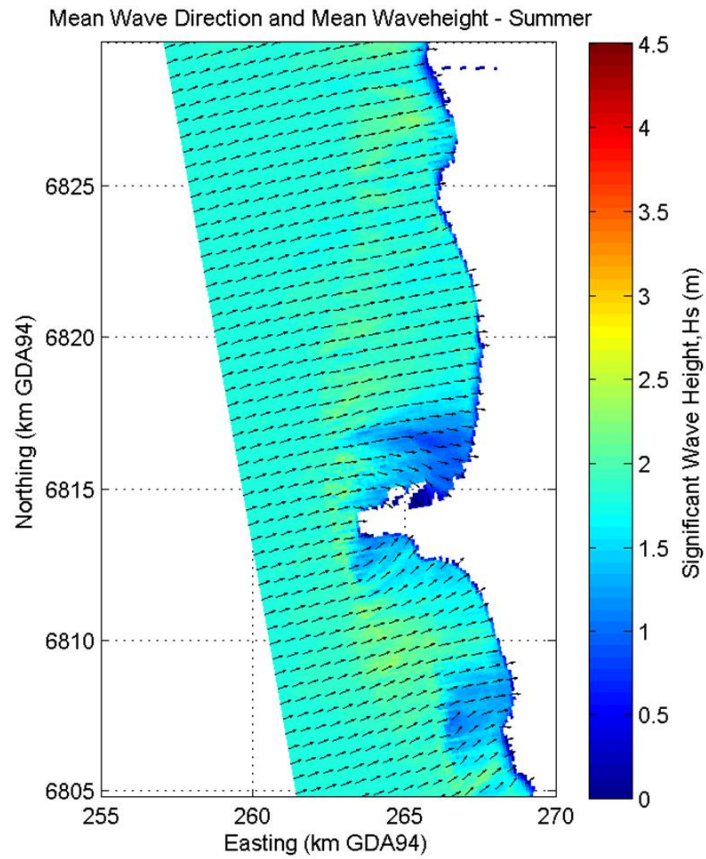


Figure 6: Cardno Pty Ltd modelling of mean summer wave directions and heights (Cardno, 2012b). Wave heights are in the range of 0.5–1.5 m along the Geraldton coastline.

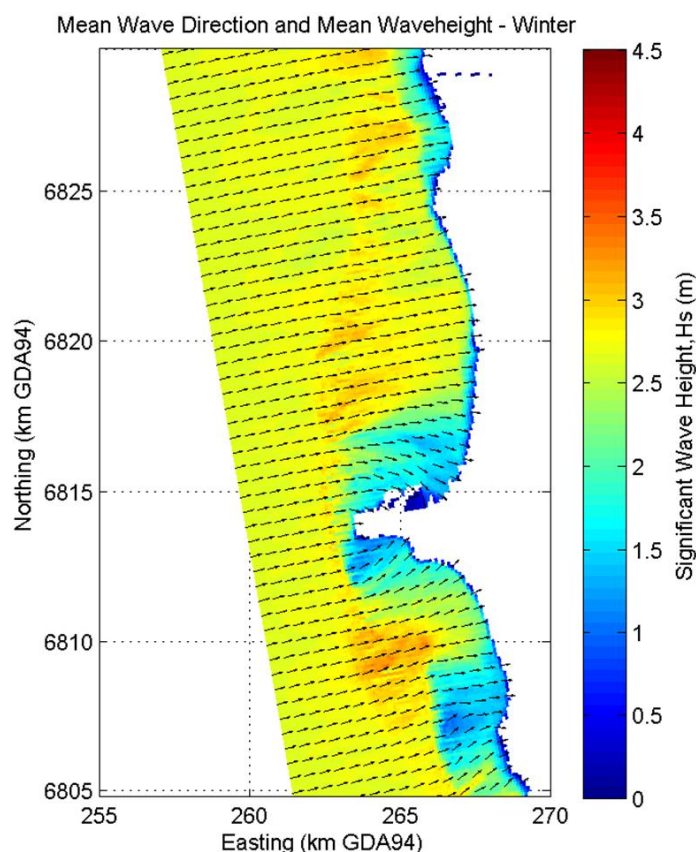


Figure 7: Cardno Pty Ltd modelling of mean winter wave directions and heights (Cardno, 2012b). Wave heights are in the range of 0.5–1.5 m along the Geraldton coastline, locally increasing to 2 m in winter.

1.3.4 Mobile sand dunes

Aeolian dunes composed of Holocene sediments are interspersed with Pleistocene Tamala Limestone and as stated in Stevens and Collins (2011, p.673), “the mobile dunes are blanket-like deposits of Holocene sediment overlying the Tamala Limestone”.

The main dune system of the study area, Southgate, is situated at the southern extreme of the studied area. There is also a smaller dune system north of the Chapman River mouth, at the northern extreme of Sunset Beach which has been previously described as a highly mobile system; however, there is no evidence of sediment supply to the ocean from these dunes, nor has there been enough investigation done into the current erosion phenomenon which is affecting the adjacent Sunset Beach.

The Southgate dune system extends from Cape Burney to the southern extreme of Tarcoola Beach. These parabolic dunes include large blowouts (Langford, 2001) and have at least 6 m of sand exposed above the land surface, below the advancing dune front. The largest active dunes extend 3.5 km north to south and the system covers an area of 300 ha (Short,

2006a). This feature has been classified as a high mobile dune (Short, 2006a), supported by the lack of vegetation covering the dune and the erosive activity currently occurring within this system. It was also noted in the field during summer that the dune is significantly influenced by the wind, partly transporting sand northward and seaward.

The Southgate mobile dune system appears to be a source of sand for the sediment budget of the area. A recent GIS-based coastal assessment mapping project by Stevens and Collins (2011) identified the boundaries of the Southgate dune system in 1982, 2001, and 2006 (figure 8). This study shows that the dune system is moving northwards and oceanwards, which was also outlined by Short (2006a). A decrease in the dune area of $\sim 0.77 \text{ km}^2$ due to revegetation of the southeast and southwest edges of the dune was noted between 1982 and 2001, but no significant change was seen between 2001 and 2006 (Tecchiato et al., 2012). Using this areal measurement and considering sediment thickness, an annual sediment supply of $38,500 \text{ m}^3/\text{year}$ can be estimated. The City of Geraldton – Greenough Town Planning Scheme No.1A Amendment 4 of 2009 compiled by the Environmental Protection Authority (EPA, 2009) state that two estimates of the contribution are available: $10,000 \text{ m}^3/\text{year}$ is the most recent estimate included in the Environmental Review prepared by an environmental consultant as part of a development project; earlier estimates (1990) by the Department of Planning and Infrastructure (DPI) put the sediment contribution at $34,000 \text{ m}^3/\text{yr}$, which is similar to the estimate based on vegetation cover change outlined in this study. Both DPI and the environmental consultants' estimates were based on aerial photogrammetry. The analysis of seismic, bathymetric, and habitat mapping data carried out in this study identified an area of sand accumulation off Southgate dune, which also confirms active sediment supply to the ocean (Chapter 4).

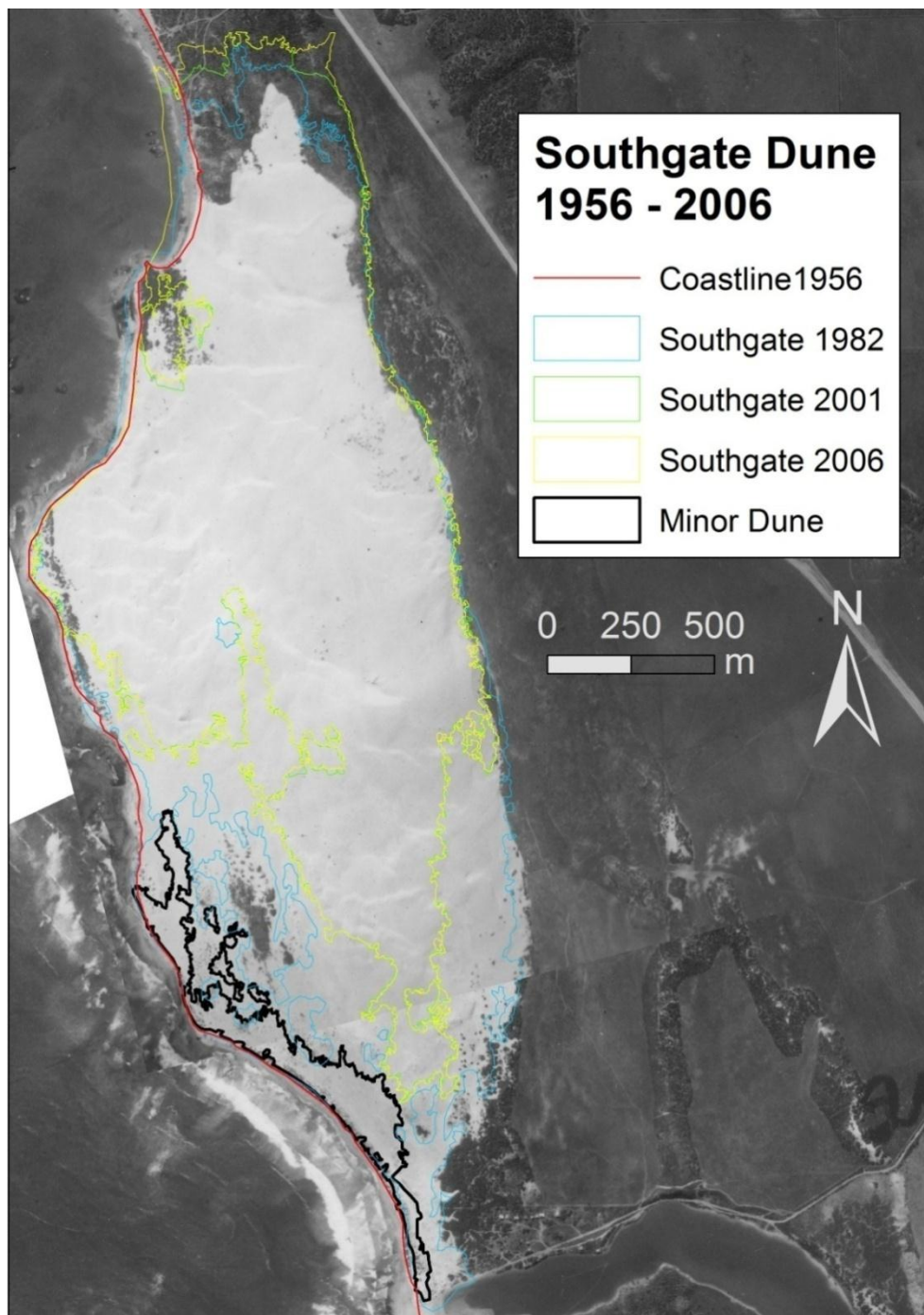


Figure 8: Historical evolution of the Southgate dune system boundaries (from Stevens & Collins, 2011). The background layer is an aerial photograph from 1956. Note the potential for spillover of sediments from the north west dune margin to supply the littoral transport system.

1.3.5 Rivers

The rivers in the study area are, from south to north, the Greenough River, the Chapman River, and the Buller River (figure 1). A review of the available literature has led to the conclusion that only occasional flooding events supply the coastal system with significant

amounts of river-derived sediment; observations from aerial photographs ranging from 1956 to 2007 confirm this finding.

Short (2006a) states that the Greenough River mouth is blocked during the dry summer months and the mouth bar only breaks during winter rains. Department of Water data (<http://www.water.wa.gov.au/idelve/rms/index.jsp>) indicates a mean annual flow volume of 19,710 megalitres. An eleven year record of stream discharge volumes is shown in table 4, and records four flood events above the average volume. The Greenough River mouth was seen to be open on an aerial photo from 2006, forming a channel 50–90 m wide. A flooding event also occurred at the end of February 2011 and sediment sampling carried out at the river mouth as part of this study has shown that the river is mainly transporting mud suspended in the water column and cobbles as bedload. Whilst the metamorphic rock cobbles deposit close to shore, the mud remains suspended in the water column and is transported further offshore. High turbidity was visible at the river mouth and in the adjacent coastal embayment (figure 9).

Table 4: Stream discharge volume for the Greenough River measured at Karlanew peak (<http://www.water.wa.gov.au/idelve/rms/index.jsp>).

YEAR	ANNUAL TOTAL (megalitres per year)	Flooding above average (=19,710 megalitres)
1999	82,180	Yes
2000	36,140	Yes
2001	5,599	No
2002	1,860	No
2003	5,718	No
2004	2,756	No
2005	4,591	No
2006	98,080	Yes
2007	2,078	No
2008	65,560	Yes
2009	7,991	No
2010	NA	NA
2011	NA	NA



Figure 9: View of the Greenough River mouth and adjacent coastal bay to the north on the 2nd March 2011 (view to the south west). Dark waters in the background are turbid as a result of the flooding event that occurred at the end of February 2011.

The Buller River is only ~10 km long and is usually a dry stream (Short, 2006a). In a number of aerial photos ranging from 1956 to 2007 the river mouth was closed.

The Chapman River mouth is usually blocked and is approximately 100 m wide. A report by WorleyParsons (2010) states that the Chapman River mouth is likely to open every year between May and August providing between 3,000 and 16,000 m³/year of sand and an average of 13,000 m³/year of sediment are likely to be lost during flooding events. 10,600 m³/year is considered the average sediment input to the coastal system. Department of Water data (<http://www.water.wa.gov.au/idelve/rms/index.jsp>) indicates a mean annual flow volume of 16,790 megalitres. An eleven year record of stream discharge volumes is shown in table 5, and records one flood event above the average volume. The Chapman River mouth was a small channel on the 2004 and 2007 aerial photos and proof of the river flooding in 1999 was also found in Langford (2001). The City of Geraldton--Greenough provided photos showing a significant flooding event of the 1930s. A survey of the Chapman River mouth on March 2, 2011 (following the Greenough River flooding) demonstrated a limited sediment exchange between river and ocean, and the flood did not appear significant and only occurred at high tide (figure 10). The grainsize analysis has shown that the beach sediment was predominantly composed of medium sand (>55%) and the percentage of carbonate analysis has shown that ~50% of this sand are carbonate constituents, with the remaining grains consisting of quartz and garnet (see Chapter 3 for more information). Garnet grains are common at the Chapman River mouth and have a high visibility due to their pink colour. However, non-carbonate gravel and pebble-sized grains were found on the beaches to the north (Sunset Beach) and south (Northern Beaches) of the Chapman River

mouth (see section 3.3.2 for more information). Figure 11 shows the Chapman River mouth open on the 27th of August 2011 and exchanging sediment with the ocean. This suggests that occasional sediment input can occur during the winter months, but also that a more detailed record of the river activities is required to better assess the river discharge events to the ocean.

Data provided by the City of Geraldton–Greenough and Main Roads on the bridges built on the Greenough, Chapman, and Buller Rivers show that most of the infrastructure is more than twenty years old and is located far enough from the shore to not influence the sediment transport to the ocean. Moreover, observation of the aerial photography available for this study did not show any significant sediment accumulation correspondent to bridge locations or any other infrastructure.

Table 5: Stream discharge volume for the Chapman River measured at Utakarra (<http://www.water.wa.gov.au/idelve/rms/index.jsp>).

YEAR	ANNUAL TOTAL (megalitres per year)	Flooding above average (=16,790 megalitres)
1999	75,440	Yes
2000	11,010	No
2001	5,891	No
2002	2,586	No
2003	6,653	No
2004	3,125	No
2005	4,201	No
2006	125.7	No
2007	30	No
2008	5,013	No
2009	11,860	No
2010	524	No
2011	10,150	No



Figure 10: Chapman River mouth on the 2nd March, 2011 (view to the north). This photo shows a limited sediment exchange between river and ocean occurring only at high tide. The sand bar that commonly blocks the river mouth is also visible.



Figure 11: Chapman River mouth on the 27th August, 2011 (view to the north). This photo shows a continuous water flow. The sand bar that commonly blocks the river mouth is not present.

The rivers of the study area are not considered to play a significant role in the coastal sediment budget, but part of the sediment presently deposited on the coastal platform consists of river-derived sediment. More information is available in Chapter 4 and section 1.3.6 describes the lithologies which the rivers flow through. It is expected that part of the soils constituting the land systems described below are transported into the ocean by the Greenough, Chapman, and Buller Rivers. In summary, quartz, some carbonate and garnet

grains are the materials most likely to be transported by the local rivers to the ocean due to their abundance within the hinterland of the study area. In particular, the Chapman River is the most likely to erode quartz and garnet rich rocks, as well as the Buller River which is characterized by a smaller discharge volume.

1.3.6 Geological setting

The western margin of Australia is an important passive margin at supercontinent scale, as its initial outline commenced with the detachment of the Australian plate from the East Gondwanaland province of Pangea in the Late Jurassic and progressively developed as a rifted margin opening from north to south (Kendrick et al., 1991; Veevers et al., 1991). The relative tectonic stability of the Western Australian margin with its long history of stability relative to changing sea level and climate have been extensively remarked upon as favourable for studies of coastline evolution and coastal sequences (Kendrick et al., 1991; Johnson et al., 1995). The Geraldton area is also considered tectonically stable with only one major geological structure documented in the literature, namely the Geraldton Fault (figures 12 and 13) with a downthrow to the west of about 160 m (Langford, 2001).

As shown in figure 12, the most ancient outcropping formation consists of the Northampton Complex, a Mesoproterozoic metamorphic complex, consisting of a group of high grade metamorphosed sedimentary rocks (granulite, granite, and migmatite) cut by granitic and gabbroic intrusions (Playford et al., 1970; Langford, 2001). Whilst Permian and Cretaceous rocks outcrop further inland from the study area, the Triassic Kockatea Shale and a few Jurassic sequences such as the Cattamarra Coal Measures, and the Cadda and Yarragadee Formations occur closer to shore. Kockatea Shale is composed of fossiliferous sandstone and shale and lies unconformably above the Northampton Complex (Playford et al., 1970). There are only a few exposures of Kockatea Shale at Geraldton (Langford, 2001). Cattamarra Coal Measures rest unconformably on the Triassic Kockatea Shale, and is the only outcropping Triassic sequence at Geraldton (Langford, 2001). The Cadda and Yarragadee Formations, conformably overlying the Triassic Kockatea Shale, were only identified in drill holes (Langford, 2001). These Jurassic sequences are mainly composed of sandstone and siltstone with a marine limestone component in the Cadda Formation (Langford, 2001). Langford (2001, p.6) states that "Jurassic strata underlie most of the land area of Geraldton (figure 13), and can be divided into two broad areas; east and west of the Geraldton Fault. To the west of the fault there is no exposure of Jurassic rocks, and the subcrop comprises the Yarragadee Formation".

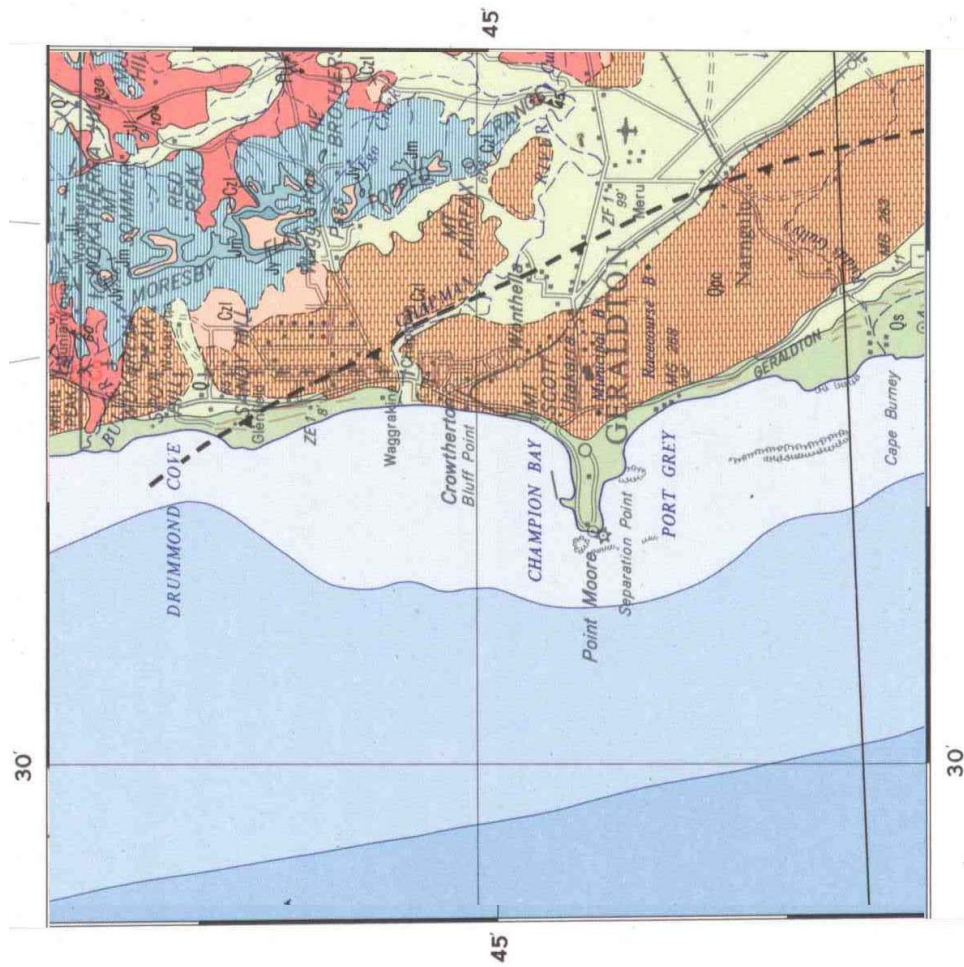
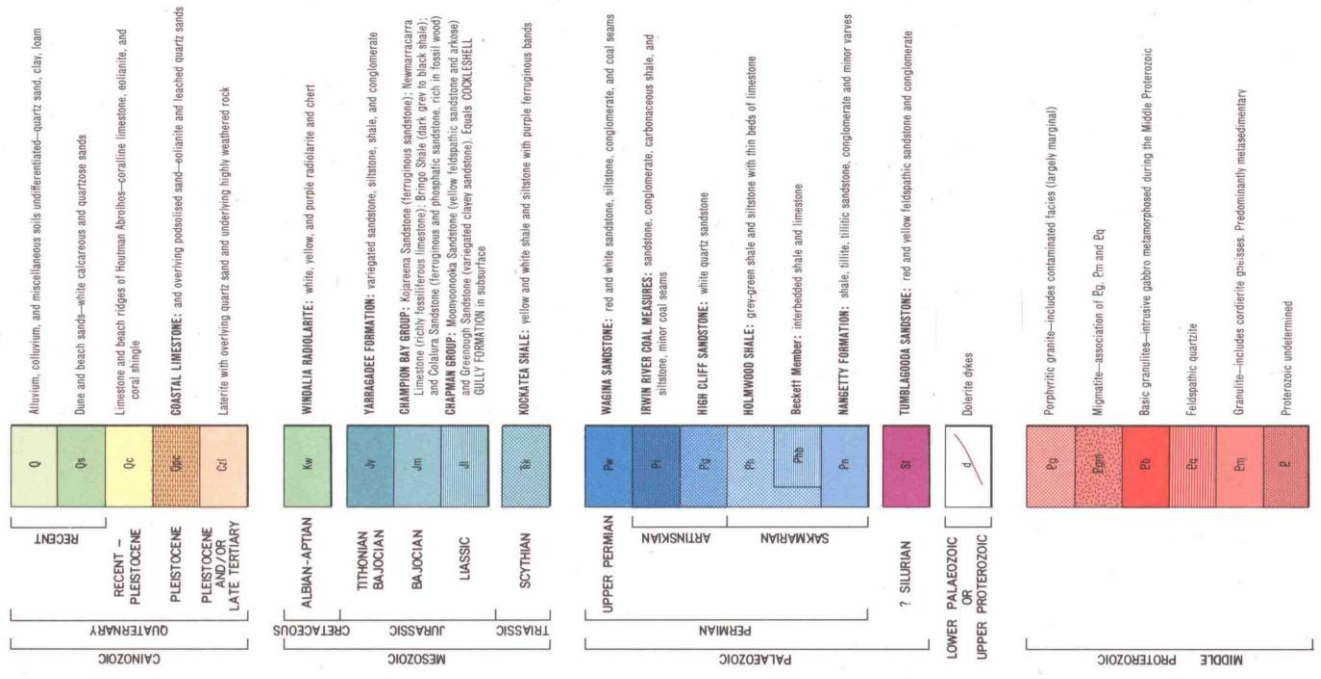


Figure 12: Detail of the Sheet SH/50-1 “Geraldton” of the 1:250,000 geological series, compiled by the Geological Survey of Western Australia.

Cainozoic material in the study area includes colluvial, coastal, eolian, fluvial and marine deposits, which is commonly in the form of a sediment veneer approximately a metre thick but can be up to 75 m thick in large dunes and depositional basins (Langford, 2001). Of note is the Middle Pleistocene Tamala Limestone, a coarse to medium-grained calcarenite deposited in coastal dune and beach-nearshore environments (Kendrick et al., 1991), with an open coast facies dominated by the gastropod *Turbo* and its operculae which occurs at Cape Burney. The Tamala Limestone formed as a series of dunes and associated minor marine deposits that also form several lines of offshore islands and reefs (Kendrick et al., 1991; Langford, 2001; Ryan, 2008). Weathering of the formerly uniform calcareous dune sands has produced a calcrete cap and overlying residual quartz sand on calcarenite (Langford, 2001). The combined thickness of these deflated transgressive barrier, parabolic, and longitudinal dunes is up to 80 m thick, although the residual sand probably rarely exceeds 20 m in thickness (Langford, 2001). Erosion of the dunes occurred during the Last Interglacial ca. 125,000 years ago at a sea-level highstand of about 5 m (Kendrick et al., 1991; Langford, 2001; Ryan, 2008).

The youngest deposits within the study area are eolian dunes of the Safety Bay Sand which are dominantly Holocene in age, with part of the dune sets pre-dating the 2–3 m Holocene sea level high at ~5000 years before present (Langford, 2001).

1.3.6.1 Regolith-landform systems

Langford (2001) classified and mapped a number of land systems, based on aerial photography and landsat imagery interpreted through field observations and soil type information (see figure 13 for their locations). Land systems have been used in Australia to define areas with recurring patterns of topography, soil, and vegetation (Langford, 2001). The description of these systems is considered relevant for this study, due to the ability of local rivers to erode the systems they flow through and transport this material to the ocean. Most likely these materials are derived from the Quindalup and Spearwood systems described below; however, the remaining land systems occurring in the study area have been included for completeness and are described (from Langford, 2001) following the geological order of older to younger formation.

- Northampton System. The dominant material is a thin colluvial soil containing abundant rock debris. The underlying metamorphic rocks are typically fresh to highly weathered, and are also exposed in stream beds throughout the area. As summarised in the previous section, the main rock types in the complex are granulite

and granite, and there are also outcrops of fine-grained gabbro dykes, and both quartz and pegmatite veins. The Northampton System is characterised by a dendritic drainage pattern extending to several narrow channels leading to the ocean. These channels include the Oakabella Creek, Oakajee River, and Buller River.

- Moresby System. A cemented gravelly surface is typically exposed on summit surfaces of the plateau with quartz sand sometimes developed on hillcrests, and weathered bedrock possibly exposed on the scarp slope below the cemented surface. Scree slopes are composed of boulder sized to gravelly colluvium. Weathered rock debris, gravel, and boulders dominate on the proximal slopes. On the more distal slopes, the colluvium grades to gravelly silty sand, sometimes hardened and mottled. These deposits rest on weathered bedrock that ranges from a residual soil of mottled sandy clay to highly-weathered silty sandstone. Narrow, seasonally-active channels on the colluvial sideslopes and footslopes contain small amounts of fluviially deposited silty sandy clay. There are several narrow drainage channels feeding the Chapman River. These channels are all seasonal, with little or no water present in the dry season.
- Spearwood System. This system is dominated by two types of rock materials. The dominant exposed material is calcareous dune sand, which has weathered to form yellow and red residual quartz sand. This lies above a strong and thin calcrete surface coating the underlying Tamala Limestone - the dominant composition of the system at depth. Small waterlogged or swampy areas fill the depressions between the dunes, which contain the same residual quartz sand as on the adjacent hills. The footslopes of the westerly-facing scarp adjacent to the Greenough Flats are composed of calcareous colluvium. The sandy soils are free draining, and there are no mappable channels or streams. There are major drainage channels that cut the Spearwood System and are part of the Northampton System and of the Greenough Alluvium System.
- Greenough System Formed by fluvial deposition of silty sandy clay from the Chapman River, this system occurs on terraced flood plains and in valleys between the adjacent escarpments. The alluvium in the terraces is typically silty sand, gravelly in parts, with grey clay horizons. Incised channels in the terraces expose up to 10 m of silty sand and silty sandy clay. The stream channels are dominantly erosional, with some rock exposures and with a little sandy silt deposited in the stream bed. The rocks in the streams derive from both the Northampton Complex granulite and overlying Jurassic rocks. The Chapman River could erode and transport these materials.

- Greenough Alluvium System. Formed by fluvial deposits from the Greenough and Chapman Rivers, this system is dominated by silty sandy clay, often firm to stiff, with minor sand and gravel. There are also interbedded clayey units, pockets of clay, and limestone clasts up to cobble size may be present. Sections observed in terraces and stream banks show up to 12 m of interbedded alluvial and eolian deposits, and drillholes have intersected at least 40 m of alluvium overlying bedrock. There are also small swamps underlain by waterlogged organic soil and the river bed and banks include exposures of Tamala Limestone and Jurassic sedimentary rocks. The Chapman River may erode materials of the Greenough Alluvium System during flooding events (figure 13) when the bar closing the river mouth opens and releases fluvial sediments into the ocean. The Greenough River is also a drainage channel of this system.
- Quindalup System. The dominant material is eolian sand composed of comminuted marine shell debris and quartz grains, with a minor component of garnet and other heavy minerals. The eolian sands are largely unconsolidated to weakly cemented, well-sorted, calcareous medium sand. Carbonate clasts are subrounded, smooth, flat to elongated shell fragments, and the quartz is subrounded and glassy. Many of the sands contain minor amounts of subrounded pink garnet. The source of these clasts is both reworked marine shell and fluvial quartz sand. Calcium carbonate content varies considerably, ranging from 38 to 95%. The beach sands are coarser grained than the adjacent eolian deposits and also include beach rock. This system forms the coastal sand dunes and river bars within the study area, and likely interacts with the sediment transported to the ocean through eolian processes and river-flooding events.

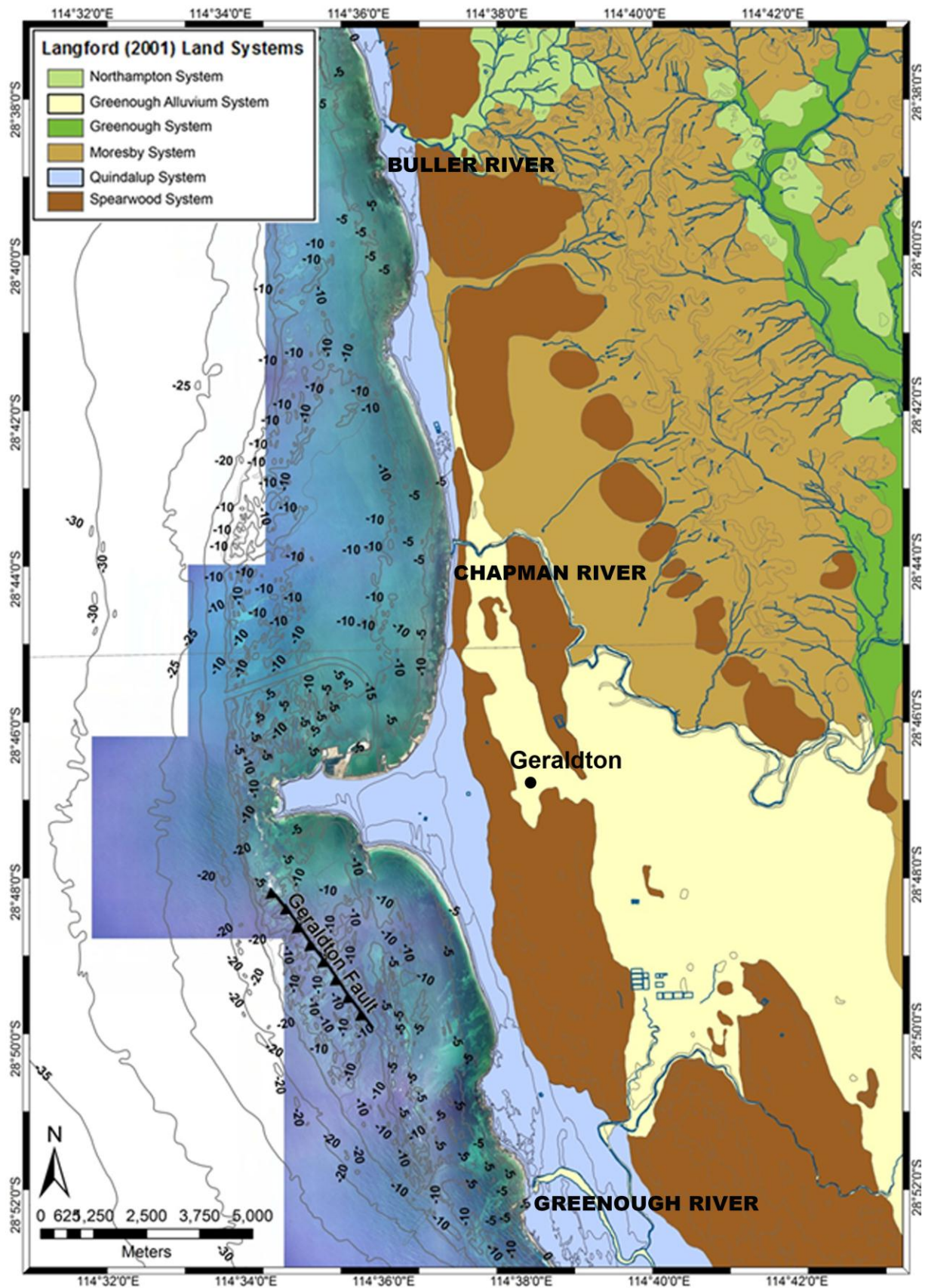


Figure 13: Location of the land systems classified by Langford (2001, GSWA data) recurring in the study area from the Greenough River to the Buller River. Materials from the Quindalup and Spearwood systems are the most likely to be eroded and transported to the ocean by the local rivers.

1.4 METHODS

Both acoustic and ground truth data was collected in the offshore areas investigated in this project, such as seismic, multibeam echo-sounder, sediment and underwater imagery data (figures 14 and 15).

Shallow seismic data was collected in November 2009 and was analysed with the aim of generating an isopach map of sediment thickness, which has assisted in quantifying the amount of sediment participating in the sediment budget and helped in identifying the sediment transport pattern on the coastal platform and in the deeper areas further offshore. Higher sediment thickness areas were also identified as sediment accumulation areas, considered “sinks” in terms of sediment budget. Section 1.4.1 describes the seismic data and analysis.

A multibeam echo sounder survey was carried out in November 2010 using a Western Australian Department of Transport hydrographic vessel. The survey area covered the embayments north and south of the city of Geraldton, between 2 and 30 m depth. Both the bathymetry and backscatter data were fully analysed in this project following the methodologies described in section 1.4.2. These analyses allowed a detailed seabed and habitat mapping to be achieved, providing clues on the location of sediment production and storage areas. The relationships between natural features and backscatter intensity were also assessed and various acoustic habitat mapping methodologies were tested, as described in Chapter 2.

A towed video survey followed the multibeam echo sounder survey in December 2010 and was used to ground truth the acoustic data and map the habitat distribution. The high resolution video transects were 200 m long and their locations replicated the sediment sample positions. A lower definition videography survey was also used to assess the habitat variability across depth and supported the visualisation of the patchy nature of the habitat distribution at Geraldton. Section 1.4.3 describes the underwater imagery data and analysis.

Sediment samples were collected in November 2009 to ~30 m depth along a ~1x1 km spaced grid, and provided vital information for this study. Section 1.4.4 describes sediment data and analysis. Sediment grainsize helped in distinguishing an important spatial relationship between different sediment types and the high carbonate content revealed the mostly biogenic nature of the shallow water sediments, providing important clues on sediment sources. Coastal surveys and sediment sampling were carried out in the spring and autumn seasons of the project time frame (November 2009 and 2010; May 2010) and correspondently to a significant flooding event (February 2011). This data helped in

understanding both the nature of the sediment supplied to the beaches from the deeper offshore areas and the redistribution along the coast of the sediment occasionally supplied to the coastal system by the small river channels of the studied area.

A longshore sediment transport modelling became necessary to quantitatively formulate the sediment budget model. The model is based on wave data provided by the Department of Transport that engaged Cardno Pty Ltd to model the local hydrodynamic at Geraldton (section 1.3). Multibeam bathymetry, beach topography, sediment, and habitat data were also part of the input information for the model. Limited topographic profiling was carried out in the area at the onshore locations corresponding to the positioning of the LITDRIFT cross shore profiles discussed in Chapter 4.

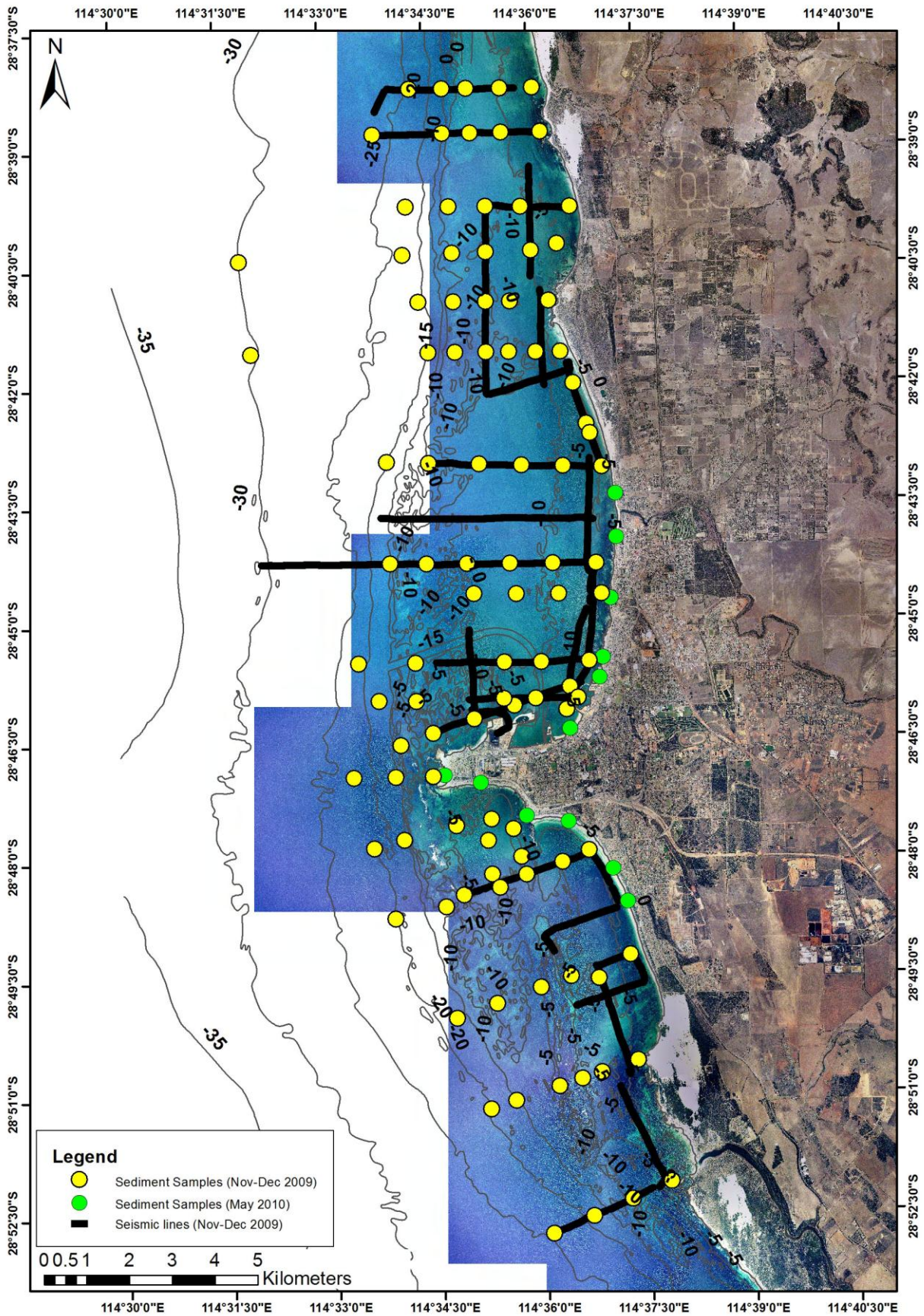


Figure 14: Locations of the data collected during the November–December 2009 (sediment samples and seismic lines) and the May 2010 surveys (sediment samples).

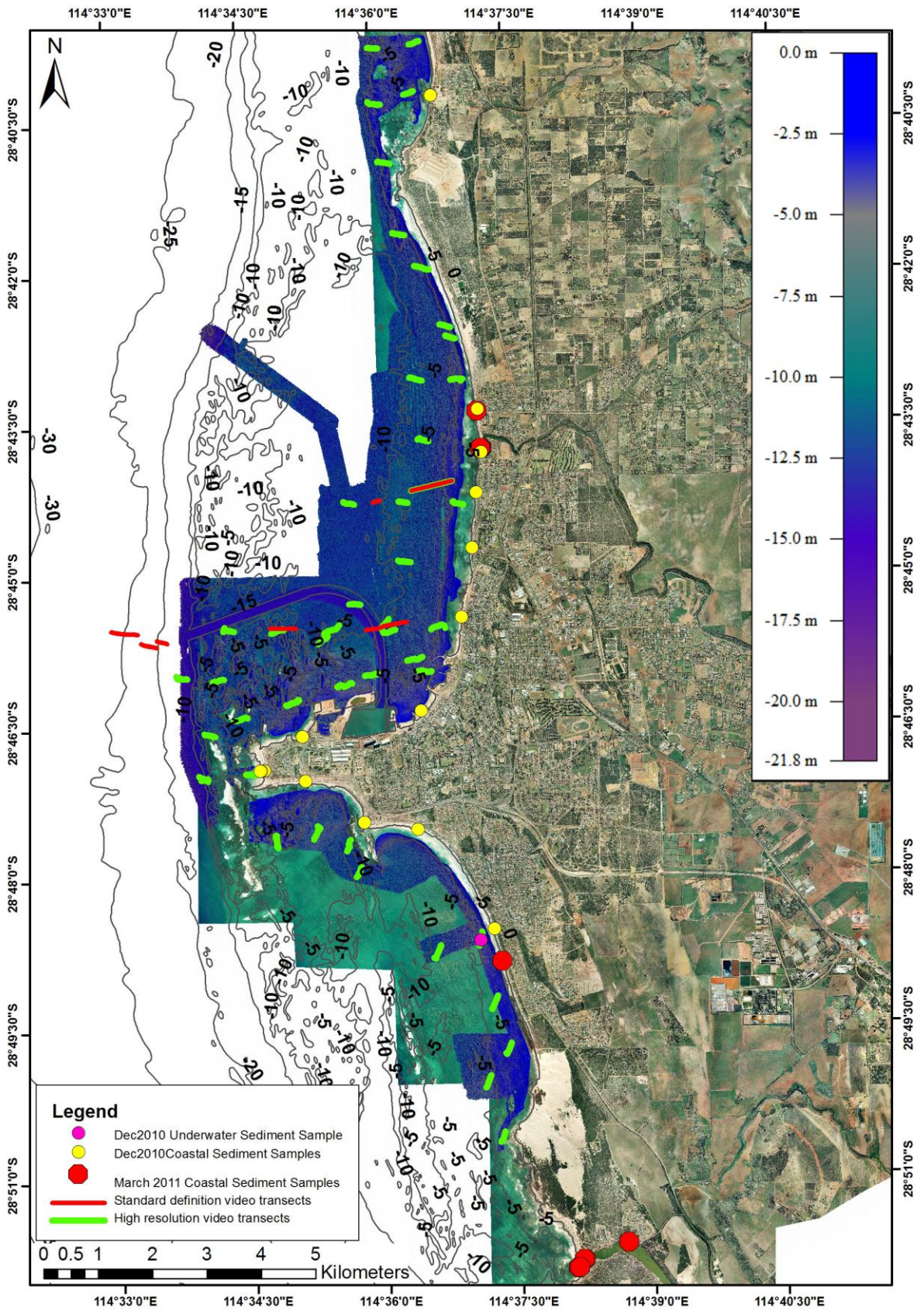


Figure 15: Locations of the data collected during the November–December 2010 surveys (multibeam, underwater imagery and one offshore sediment sample), and March 2011 coastal sampling following river flooding events. The multibeam data is indicated by the raster of bathymetry for which the depth range is shown on the right hand side of this figure.

1.4.1 Shallow seismic data

The seismic lines have a total length of approximately 94 km and extend throughout the study area (figure 14). The bathymetric range of the data is 3.2–30.5 m; however, only four lines are deeper than 20 m. Most of the data is located between Point Moore and Glenfield Beach (61.6%), whereas only a minor portion covers the areas south of Point Moore (20%) and north of Glenfield Beach (18.4%).

The data was logged as *.lin files using the Dr.Geo software interface on the survey vessel, with associated positioning in the Geodetic WGS84 coordinate system. The raw data was converted to *.seggy files using the Dr.Geo software interface. The navigation information associated with the *.segys was also converted to the Geocentric UTM WGS84 coordinate system using the RadExpro Plus Advanced software, which works contemporaneously with the MatLAB software. The following basic filters were applied to the seismic data using RadExpro Plus Advanced: DC removal, bandpass filtering, and amplitude correction. Preliminary processed *.seggy files, with the indicated basic filters applied, were produced with RadExpro Plus Advanced and imported in a Kingdom project specifically developed for the Geraldton data. Preliminary observation of the data indicated that removal of the swell effect was needed since it modified the original layer's shape to a wavy pattern. Removal of the swell effect was performed by applying a static correction through the following procedure. The reflector representing the seafloor was digitized on the *.segys using the Kingdom software interface. The digitized bottom reflectors were exported as xyz files and the difference between the seafloor position detected on the seismic data and the 2009 bathymetry collected by DoT was computed using the MatLAB software interface. This value was used to correct the seismic data for the swell and tide effects, which were previously corrected on the processed multibeam bathymetry data (Mullally, J. pers. comm.). A deconvolution filter was also applied to the bathymetric corrected data using RadExpro Plus Advanced, to provide accurate data visualization.

The main objective of the seismic data analysis was the identification of the sediment–rock interface. This was based exclusively on geometric criteria as recent well data was not available; however, an old drilling campaign provided data for the interpretation of the seismic lines surrounding the port and channel infrastructure (Chapter 3).

The most useful way to visualise the results of the analysis was determined to consist of data interpolation to develop an isopach map of sediment thickness (Chapter 3). Some artefacts, due to interpolation, may be affecting the isopach map, especially at depths greater than 15 m and off the northern sector of Tarcoola Beach; however, a comparison of

the seismic results with sediments, bathymetry, and habitat data has confirmed the reliability of the sediment thickness values.

Finally, it has been noted that complex bathymetry characterises the area north of Point Moore and south and west of the dredged channel. According to the bathymetry and habitat data, it is possible that a higher sediment thickness than that indicated in the seismic data occurs locally at these locations. However, the general trend is an increasing sediment thickness from west to east and from south to north, i.e. toward the dredged channel.

1.4.2 Multibeam echo sounder data

The 2009 data location duplicates the seismic lines (figure 14) and entirely covers the dredged channel and port basins. This data has provided support for seismic data processing and analysis, but was not sufficient for a complete overview of the study region.

A survey of ~35 km² within the shallowest part of the study region was carried out in November-December 2010 (figure 15) and focused on the Geraldton coastal platform, mainly covering the areas close to the shoreline to ~10 m depth; however, off Point Moore the data reached ~25 m depth.

The multibeam data collected through the QUINSy software interface was filtered in real time, as the data was acquired, for signal spikes through a manually selected acquisition range based on seafloor bathymetry. The dynamic correction for boat pitch, roll, and heave were also applied in real time in the field. A further refinement of spikes removal was carried out at the Department of Transport processing centre in Fremantle, using the QLOUD software interface. The data processed this way was provided to Curtin University as xyz tables set to the MGA94 Zone50 coordinate system. The bathymetry xyz tables provided by DoT were interpolated to generate 0.25 to 0.5 m grid spaced Digital Elevation Models (DEMs) to provide a base map for the morphological interpretation of bathymetry data.

The multibeam backscatter data were processed using the Centre for Marine Science and Technology's (CMST) multibeam sonar processing toolbox, which was developed in MatLAB (Parnum, 2007). The CMST processing toolbox calculates the backscatter energy from the snippet signals and reduces these values to the width of the transmitted pulse, and removes the time variable gain applied by the multibeam system. The surface scattering coefficients are calculated by correcting the backscatter energy for the actual spreading and absorption loss for each beam and normalised for the footprint insonification area. The across-track beam pattern for Reson Seabat 8101 is known to not be uniform (Foote et al., 2003) and this

has not been measured or corrected for the multibeam system used in this study, so the backscatter data are in relative units. To produce a map of angle-independent backscatter levels the angular response was corrected by removing the mean angular response from a sliding window of 30 consecutive pings of data, then restoring values to the mean backscatter at 30° (Parnum, 2007). The data processed this way produced xyz (z = mean backscatter strength) tables and 5 m grid-spaced rasters set to the WGS84 Zone50S coordinate system. Backscatter angular response curves were constructed for each ground truth station using a search radius of 50 m. From these angular response curves the mean backscatter and mean slope were calculated for near-vertical (0°–15°) and oblique incidence (20°–60°) angles. As significant work was carried out on this data and the methodologies used were based on the relationships between seabed geomorphology, benthic habitats, and multibeam backscatter data, the methods used for acoustic habitat mapping practices are described together with the results in Chapter 2 so that it is easier to understand the outcomes of the analyses.

1.4.2.1 Underwater morphology mapping

The DEMs of multibeam bathymetry were imported into a GIS project, specifically developed for the Geraldton data, and set to the MGA94 Zone50 coordinate system.

Polygon shapefiles were created with the coordinate system set to the MGA94 Zone 50; the shapefiles were manually digitised on the DEMs at a fixed scale of 1:2,000, which was found to be the most convenient working scale considering data resolution and morphological feature dimensions. During the mapping operations, the multibeam backscatter data was also compared to the bathymetry to correlate the two datasets (i.e. the “sand bars and sheets” layer was mapped as part of sandy substrates, represented by the lower backscatter values as described in Chapter 2). The mapped features have natural and artificial origins; the natural elements are: sand bars and sheets, shallow limestone reefs, nearshore beach zone, rippled sand flat, low relief substrate, and underwater sand dunes. The artificial features mapped are: the dredged channel, the dredged port basin, aquaculture zone, and shipwrecks found in Champion Bay. The polygon shapefiles were then merged into one ESRI shapefile called “UnderwaterMorphology” and referenced to the MGA94 Zone50 coordinate system, with the artificial and natural elements described by the “name” attribute. The criteria used for mapping the natural features at Geraldton are listed below and the completed maps are shown in Chapter 2:

- sand bars and sheets are sand accumulation areas visible as smooth substrates on the bathymetry data, also with sand presence confirmed by the acoustic habitat classification;
- shallow limestone reefs are higher slope gradient and relatively elevated areas compared to the surrounding sea bottom, generally ridge or pinnacle shaped;
- nearshore zone has a sandy substrate continuous with the onshore beach morphology and was mapped when visible, sand presence confirmed by the acoustic habitat classification;
- rippled sand flats are small scale ripples (wavelength <1m) (Ashley, 1990) visible on either flat substrate or on the top of reef and bar systems.
- underwater sand dunes with wavelength = 1–10 m (Ashley, 1990);
- low relief substrate is a flat or low sloping substrate characterised by a rugose bathymetric appearance.

1.4.3 Towed video data

A towed video survey was carried out in December 2010 using a high resolution camera for still imagery to ground truth the multibeam backscatter and 2009 sediment data. A total of 45 transects, ~200 m long, were surveyed within the study area between ~3 and 17.5 m depth (figure 15), mostly coincident with sediment sampling locations. Only 6 transects covered areas where sediment sampling was not carried out in 2009, and were placed at strategic locations in terms of sediment dynamics.

A total of 6 E-W video transects were also recorded, using a lower resolution camera, to quickly assess the habitat variability across depth contours (figure 15) in the central part of Champion Bay. These videos are 500 m long and provide shallow (~5 m) to deep water habitat data (~30 m depth).

Whilst the standard definition videography was used to provide a depth-consistent habitat overview of the Champion Bay embayment to 30 m depth, the high definition imagery provided a quantitative habitat classification throughout the study area at depths shallower than 15 m.

At the processing centre in Perth, the GPS positions of each image were plotted into GIS software and repositioned along the survey track if location errors were present.

1.4.3.1 Standard definition transects

The video footage was analysed in real time in the field by a marine scientist trained and experienced in video analysis and habitat classification. A custom designed Visual Basic software program was used which allows the user to assign biota and substrate attributes to GPS position in a spreadsheet while the video was recorded. The habitats were classified based on an adapted classification (tables 6 and 7) from a national intertidal and subtidal benthic habitat classification scheme (Mount et al., 2007). This classification scheme uses a hierarchical decision process to define benthic habitats. Qualitative estimates of the cover of the different biota and substrate types are made using density classes listed in tables 6 and 7. Substrate type and particle sizes were based on the Wentworth grade scale of particle sizes; particles greater than 64 mm (cobble) are defined as consolidated (reef) substrate and particles smaller than 64 mm (pebble) are defined as unconsolidated (sand) substrate. For poor quality video footage where the substrate type was difficult to see, the substrate type was classified based on the surrounding substrate or what was likely to occur. The presence of specific biota types in each biota class was recorded, with the level of taxonomic detail being limited by the quality of the video footage, which is dependent on the environmental conditions (e.g. water visibility and sea state) and the speed at which the towed video is collected. For this survey, the video was analysed to seagrass genera and macroalgae morphological lifeform level. However, some macroalgae lifeforms could be identified to genus level (i.e. *Ecklonia* and some *Sargassum* and *Caulerpa* species).

Table 6: Biota classification definitions used for classifying the standard definition video transects.

Community Classes	Taxonomic Classes (examples)	Decision rules / examples
Encrusting / turfing algae	Microphytobenthos (MPB) Crustose coralline algae (CCA) Turfing algae Filamentous algae	Only recorded for presence/absence (no density classes) Encrusting algae Hair-like algae <20 mm Hair-like algae >20 mm
Small Algae	>5% recorded as present Red, brown, green Membrane, thin sheets Foliaceous, bushy Lobed, flattened and rounded	Macro algae 20 mm–20 cm Membrane-like (e.g. <i>Lobophora</i> spp. , <i>Padina</i> spp.) Foliaceous; branching (e.g. <i>Gfali</i> = <i>Caulerpa</i> spp.) Lobed; branching (e.g. BLOBE = <i>Dictyopteris</i> spp.)
Large Algae	>5% recorded as present Red, brown, green Flat Branching	Macro algae >20 cm e.g. <i>Ecklonia</i> , <i>Durvillia</i> e.g. <i>Fucoid</i> , <i>Sargassum</i> , <i>Cystophora</i> Separated into genus or species e.g. <i>Halophila</i>, <i>Halodule</i>, <i>Posidonia</i>, <i>Zostera</i>, <i>Amphibolis</i>
Seagrass	>1% recorded as present	Morphological groups defined in English <i>et al.</i> 1997; further classified to genera
Hard Coral	>5% recorded as present Branching Digitate Tabular Encrusting Foliose Massive Submassive	At least 20 branching (e.g. <i>Seriatopora hystrix</i>) No 20 branching (e.g. <i>Acropora digitifera</i>) Horizontal flattened plates (e.g. <i>Acropora hyacinthus</i>) Major portion attached to substrate as a laminar plate (e.g. <i>Porites vaughani</i>) Coral attached at one or more points, leaf-like appearance e.g. <i>Turbinaria</i> spp.) Solid boulder or mound (e.g. <i>Favites</i> spp.) Tends to small columns, knobs or wedges
Soft Coral (BPP)	>5% recorded as present	Photosynthetic soft corals (e.g. <i>Alcyoniidae</i> spp. (BPP))
Filter Feeders (non-BPP)	>5% recorded as present Soft Coral (non-BPP) Sponges Ascidians Hydroids Bryzoan Anemone Polychaete	Ahermatypic animals (not defined as BPP) Non-photosynthetic soft corals (e.g. Gorgonian fans, <i>Alcyoniidae</i> (non-BPP)) Dendronepthia spp.) Can note morphological groups Stalked, encrusting, solitary Foliose, stalked Tube, solitary
Cover Classes	Cover Values	Decision rules
Biota cover >80%	90	no substrate visible.
Biota cover 60-80%	70	some substrate is visible.
Biota cover 40-60%	50	substrate is clearly visible but biota dominates the image frame.
Biota cover 20-40%	30	substrate dominates most of the image frame.
Biota cover 10-20%	15	substrate dominates most of the image frame.
Biota cover 5-10%	7.5	substrate dominates most of the image frame.
Biota cover 1-5%	3	trace densities
Biota cover 0-1%	0	no significant macro-biota

Table 7: Substrate classification definitions used for classifying the standard definition video transects.

Substrate Type	Particle sizes are defined using the geological 'Wentworth Scale'
Consolidated (Reef) substrate	Any substrate predominantly made up of particles of cobble size (>64 mm diameter) or larger.
Unconsolidated (Sand) substrate	Any substrate predominantly made up of particles of pebble size (<64 mm diameter) or smaller.
Reef	
Biotic reef	Biota covers >1% of reef
Abiotic reef	Biota covers <1% of reef
Reef Particle Size	
Rock (unbroken)	Unbroken rock substrate
Boulder	Particles >256 mm
Cobble	Particles 64-256 mm
Reef Profile	
High Profile	>4 m rise over 2 m; a hard or solid substrate with slopes greater than 70 degrees
Medium Profile	1-4 m rise over 2 m; a hard or solid substrate with slopes between 30 and 70 degrees
Low Profile	A hard or solid substrate with slopes between 2 and 30 degrees.
Flat	<1 m over 2 m; a hard or solid substrate with slopes of less than 5 degrees
Sand	
Bioturbation	low, medium, high levels of activity
Sand Particle Size	
Pebble	Particles 4-64 mm
Gravel	Particles 2-4 mm; used to describe large grains of sediment; biogenic particles such as shells and coral rubble
Sand	Particles 63 um-2 mm
Mud	Particles <63 um
Sand Profile	
Flat	No profile (undulations <1cm)
Ripples	Sediment with undulations 1-10 cm high
Ripples	Sediment with undulations 10-50 cm high
Ripples	Sediment with undulations 50-100 cm high
Waves	Sediment with undulations 1-5 m high
Dunes	Sediment with undulations >5 m high
Substrate composition	Reef 100%, 1-24%, 25-49%, 50%, 51-74%, 75-99%, Sand 100%

1.4.3.3.2 High definition transects

Underwater photography was used to assess the relative abundance of benthic percent cover through visual comparison with a photo guide specifically developed for seagrass-dominated habitats (Short et al., 2002). Seagrass and macroalgae were the main biota identified in the study area. Seagrass species included *Amphibolis griffithii* (AG), *Amphibolis antarctica* (AA), *Syringodium isoetifolium*, *Posidonia sp.* (PSP), *Halophila decipiensis* (HD) and *Halophila sp* (HSP). Macroalgae were distinguished as coralline algae and brown algae where possible. Mainly sandy substrates were found throughout the study area; hardrock pavement and rubble were occasionally visible.

The mean benthic cover and standard errors were calculated for each transect and after an initial statistical observation of the video analysis results, representative habitat classes were selected from this data and used to ground truth the multibeam backscatter map. These classes are discussed in Chapter 2.

1.4.4 Sediment data

A total of 104 underwater sediment samples were collected between 4.3 and 30.2 m depth within a sampling area 26.8 km long north-south and 10.1 km wide east-west during the November–December 2009 fieldwork (figure 14). Implementation of the 2009 underwater sediment sampling grid was attempted by Curtin University in 2010, but only one sample could be collected off Tarcoola Beach (figure 15). The location of the sediment samples is depth-consistent, follows the seismic line spatial distribution, and provides ground truth information for validating the acoustic data, adding value to the multibeam backscatter data. Fourteen samples were collected using a Van-Veen Grab; the remaining samples were collected using a pipe dredge and consequently have a poorer positioning accuracy due to the boat drifting to allow sediment dredging on the seafloor.

Underwater and coastal sediment sample positions were recorded using a hand-held GARMIN eTrex H Global Positioning System (GPS), which has an accuracy of <10 m. The pipe dredge sampling operations involved approximately 10 m of boat drifting. Consequently, the actual pipe dredge sample positioning on the seafloor has an accuracy of ≈20 m. The coordinate system used was UTM WGS84 Zone50S.

A total of 9 surficial sediment samples were collected along the Geraldton beaches in November 2009. The Department of Transport provided 12 additional surficial coastal samples collected in May 2010. The location of these coastal samples is shown in figure 14. Sixteen additional surficial sediment samples were collected along the Geraldton beaches in December 2010 to obtain a second spring dataset (figure 15). The Chapman and Greenough River mouths, as well as Sunset and Tarcoola Beaches, were also sampled in March 2011, corresponding with flooding events (figure 15). This data has allowed identification of the river material being transported to the ocean and redistributed along the coast.

Sediment grainsize analysis and calcium carbonate content measurements were completed for the collected samples. Due to the relative similarity of the carbonate content measurements, 36 selected samples were also analysed using mineralogical x-ray diffraction (XRD) and microscopic petrologic identification of the sediment grains. In the laboratory, sediments were initially washed with distilled water to remove salts and then dried in a circulation oven. The next step involved splitting the sediment samples by the cone and quartering method, to provide representative splits of the bulk sample. The procedures followed for the laboratory analysis are described below.

Granulometry. Dried samples were sieved using a mechanical sieve shaker with -1 to 4 ϕ sieve units at 0.5 ϕ intervals based on the Udden-Wentworth grainsize scale. The GRADISTAT package (Blott and Pye, 2001) was used in the calculation of grainsize statistics, textural parameters, and descriptive terminology, allowing both tabular and graphical output into Microsoft Excel and input into ArcGIS. The classification by Folk (1954) was used to describe the sample textural groups. The best way to visualise the analysis results was found to be via their interpolation to develop maps of sediment grainsize (Chapter 3). The results of the analysis of coastal sediment samples is also visualised through maps of sediment grainsize, differentiated on the basis of the sampling season (Chapter 3).

Calcium Carbonate (CaCO₃) Content. Dried samples were ground to a powder of fine sand/silt size. The carbonate content of a sample is determined by reacting the sample with acid in a sealed “bomb” and measuring the pressure of CO₂ evolved. A known volume of 32% hydrochloric acid (HCl) is added to 1.00 g of the powdered sample whilst sealed in the carbonate bomb. The pressure produced by the acid/sediment powder reaction is measured with a 160 kPa gauge. The bomb is calibrated using 1.00 g, 0.50 g and 0.25 g of CaCO₃ powder to represent the equivalent of 100%, 50%, and 25% CaCO₃ content in a sample. A calibration curve can then be constructed on a graph of P vs % CaCO₃ and the pressure measured for each sample is plotted on this graph to obtain the % CaCO₃ of a specific sample. The best way to visualise the analysis was found to be by interpolating the results to develop a map of sediment carbonate content (Chapter 3). The results of the analysis of coastal sediment samples are also visualised through maps of sediment carbonate content differentiated on the basis of the sampling season (Chapter 3).

X-ray Diffraction (XRD). The mineral phase composition and abundance of various carbonate minerals were determined by studying the x-ray diffraction patterns of selected sediment samples. Dried samples were powdered to 5–10 μ m and a fixed amount of a known standard (Fluorite) was added to 3 g of the powdered sample. The sample and standard mixture was placed in a cavity mount holder, taking care not to put any form of pressure on the sample when filling the cavity to ensure sample randomness. XRD patterns were collected on a D8 Advance diffractometer (Bruker AXS, Germany) with a Cu K α source. The data was collected using a Lynx-eye position sensitive detector with a nominal 2 θ step size of 0.015°, a count time of 0.5 s per step, and a 2 θ range of 5°–100°. Approximately 1 g of dried micronised powder was pressed into a plastic sample holder using the “pack and tap” method. This method was used in order to minimise preferred orientation effects. The position and area of the major non-overlapping peak associated with each mineral were measured using TOPAS v4.2 (Bruker-AXS). The peak area data was

used to calculate the mineral abundance in the sample through the reference-intensity-ratio (RIR) using the added Fluorite as the internal standard. The average accuracy of this analysis is $\pm 5\%$, but there were errors up to $\pm 17\%$ which limited the reliability of this data (Chapter 3). Aragonite, High Mg Calcite and Low Mg Calcite are common minerals of the bioclastic sediment fraction, while quartz is typical of reworked river-derived sediments. The amorphous component of the mineralogical composition is a combination of sediment minerals which could not be identified. High Mg Calcite and Low Mg Calcite have overlapping diffraction peaks and the calculations of their abundances using the widely-accepted peak area method have retained the largest errors in the data. In general, mineral phases with relatively low concentrations and heavily overlapped peaks are likely to retain high uncertainties when measuring their concentrations.

Petrology. Dried samples were prepared for microscopic characterisation as grain mounts, which are permanent mounts of sand sized sediment on a microscopic glass slide (Mazzullo and Graham, 1988). The sediment composition was assessed through visual estimation of the percentages of modern bioclasts (i.e. calcareous red algae, foraminifera, bryozoans, molluscs, sponge spicules, etc.), reworked grains (i.e. quartz, feldspar, and intraclasts) and relict bioclasts. These three grain types were found to be the main sediment constituents. The comparison charts of Folk et al. (1970) were used as references for percentage estimations of grain types. The best way to visualize the data was found to be a triangular diagram with modern, reworked, and relict grains as end-members (Chapter 3).

Sediment facies. Sediment petrology partly helped in distinguishing the sediment facies occurring in the study area and in determining the amount of modern and relict sediment constituting the different sediment facies; however, the statistical results of the petrological analysis were not sufficient to clearly separate the sediment facies occurring at Geraldton as the sediment grain size played a strong part in the spatial segregation of coastal sands. The interpolated maps of sediment grain size (including fine, medium and coarse sands), together with the interpolated maps of carbonate content and percentage of modern skeletal grains were used as input layers for an Iso Cluster unsupervised classification operation using ArcMap 10™. The Iso Cluster algorithm was able to measure natural clustering of properties in the five-dimensional feature space of the input data and produced a new raster layer which showed four meaningful thematic information classes (Chapter 3). Similar methods for classifying and mapping sediment facies within Australian coastal areas have been previously adopted by Ryan et al. (2007a).

1.4.5 Longshore sediment transport model

The LITDRIFT numerical modelling software developed by DHI (DHI, 2010) was used to simulate the wave-driven annual longshore sediment transport of the Geraldton embayments. LITDRIFT uses sediment, bathymetry and seabed roughness data, together with wave, wind and current data to determine the longshore current, longshore sediment transport and annual drift.

The summer and winter wave climate timeseries provided by Cardno Pty Ltd were extended to match a one-year time span to allow calculations of the average sediment volumes transported by the littoral drift on an annual basis. Cardno Pty Ltd provided timeseries data at various locations along the 5 and 10 m bathymetric contours and the closest to each of the 13 cross shore profiles examined in the simulation was used to provide wave climate data for each of the modelled profiles. These profiles were oriented perpendicularly to the shoreline and extended to the interpreted depth of closure for the study area between 5 and 10 m depth (Chapter 4).

The sediment transport calculations were carried out by the LITDRIFT software at regularly 10 m spaced points along the profiles; each of the points contained the following information: bathymetry/elevations, sediment grainsize and sorting, seabed roughness, and sediment fall velocity. The bathymetry and elevation information were based on multibeam bathymetry and beach profile data. Sediment grainsize and sorting were extracted from the sediment maps developed as part of this project. Sediment fall velocity was estimated using the formulae by Jiménez and Madsen (2003). Seabed roughness was estimated on the basis of the habitat maps formulated in this study, assigning higher values to seagrass beds, intermediate values to sparsely vegetated substrate, and lower values to sandy substrates, with further differentiation on the basis of the sediment grainsize. Wind data was not available and consequently wind-induced currents were not taken into account in the simulation; however, great uncertainty exists on the estimate of the magnitude of these currents. In terms of a cross-shore wave transformation model, the irregular Battjes-Janses description was used, and for directional wave spreading a 0.5 value was applied. The sediment was not considered graded and no ripples were included in the simulation. Some variations of these modelling settings were applied as an initial testing of the parameters and little differences were noted in the modelling results when changing the above-mentioned user-specified options.

In the LITDRIFT software, the sediment transport calculation in the points along the profile is interpolated and integrated across the profile, assuming that transport varies linearly.

Chapter 2

UNDERWATER GEOMORPHOLOGY AND BENTHIC HABITATS: using multibeam data for seabed characterisation

2.1 INTRODUCTION

Seabed geomorphology encompasses the shape and hardness of the seabed and provides a fundamental control on sediment dynamics, which drive sediment transport and regulate the characteristics of soft sediment bodies especially in shallow littoral sandy environments. The integration of sediment erosion, transport, and depositional processes with pre-existing topography shapes the seabed morphology (Velegrakis et al., 2007); hence the geomorphology of the study area was analysed at high detail through multibeam bathymetry data. Hard and soft substrate features were identified (section 2.2) and particular consideration was given to their significance in terms of sediment transport pathways and seabed mobility (section 2.3). Unvegetated sediment bodies (banks, bars, and sheets) are areas of sediment accumulation. Bedforms are indicators of seabed mobility, and can provide clues on sediment transport direction. Shallow reef systems influence sediment transport pathways by constituting a topographic barrier to sediment movement.

The geomorphology of the Australian coastline and continental shelf is strongly influenced by the sea-level fluctuations of the last 1.8 million years (Ryan, 2008), and some of the morphological features found in this investigation are remains of these processes (section 2.2). Linear topographic ridges of Pleistocene limestone have been widely reported through the western Australian shelf (Johnson et al., 1995; Ryan, 2008) and partition it into varying physical energy, biota, and sediment supply. Moreover, the physical substrate including limestone ridges has often been ascertained as a surrogate for habitat development, and considerations of this kind have been made in this study (section 2.4.1). Previous studies of the south Australian coast (James and Bone, 2011) have partitioned warm-temperate macroalgal and seagrass communities on the basis of the substrate types: macroalgae colonize the lithified substrates and seagrasses occupy adjacent sandy substrates. In contrast, in the Mediterranean Sea, seagrasses can be associated with sedimentary substrates and hardgrounds with the plant rooted in the troughs (De Falco et al., 2010).

Important clues to sediment dynamics are provided by the understanding of underwater geomorphology and characterisation of seabed substrates (Cooper and Pontee, 2006; Velegrakis et al., 2007); for example, sediment accumulation areas indicate locations to

where the sediment is being transported by littoral currents, and consist of mobile unvegetated sediment bodies. The novel aspect of this study was the introduction of multi-beam echo sounder data, providing high resolution bathymetry and backscatter data which were used for seabed characterization. Previous sediment budget studies used sidescan sonars to investigate the seafloor geomorphology (Cooper and Pethick, 2005; Rosati, 2005) but sidescan does not provide co-located bathymetry and backscatter, which are beneficial to seabed mobility studies (Velegrakis et al., 2007). The mapping of the seabed morphological features has allowed the detailed identification of the location of sediment accumulation areas and sediment transport pathways to be completed (section 2.3). An initial understanding of the relationships between seabed mobility, sediment transport pathways, benthic habitats, and underwater geomorphology, developed as part of this study, was also described in Tecchiato et al. (2013) (appendix 1).

Geraldton is characterised by temperate water sedimentation and the coastal platform is colonized by seagrass and macroalgae communities, which supply carbonate sediment to the coastal systems (Short, 2010). The sediment input from these communities is commonly recognised as a sediment source for the overall sediment budget of the southern and western Australian coastal embayments (Short, 2006b; Short, 2010). Waves are attenuated by greater friction across seagrass meadows, which have the capacity to reduce water flow and therefore increase sediment deposition (Fonseca, 1989; Verduin and Backhaus, 2000; Madsen et al., 2001; van Keulen and Borowitzka, 2002; Carruthers et al., 2007). Therefore, seagrass meadows and macroalgal communities must be taken into account when undertaking seabed mobility studies. Hence, the distribution of these habitats was mapped as part of this study using a combination of underwater videography and multibeam backscatter data (sections 2.4 and 2.6).

One of the objectives of the analysis of multibeam data completed in this project was the evaluation of the capability to distinguish different seabed types using bathymetry, backscatter intensity, and angular response data (section 2.5). It is well known that acoustic backscatter can be used to infer seafloor physical and biological properties (or benthic habitats), such as by exploiting the backscatter versus incidence angle curves (Hughes Clarke et al., 1997; Parnum, 2007). For instance, backscatter strength has been found to be directly proportional to sediment grainsize and surface roughness for unvegetated substrates (Hughes Clarke et al., 1997; Goff et al., 2004; Ferrini and Flood, 2006; Parnum, 2007; Fonseca et al., 2009). High backscatter intensity has been previously recorded for rocks, coral reef, gravel-dominated substrates, and marine vegetation (Parnum, 2007). High backscatter levels are to be expected from hard grounds and gravel-dominated substrates, as they have a large surface roughness and high acoustic impedance (Parnum, 2007).

Acoustic scattering from seagrass and macroalgae is poorly understood compared to rock and sediments (De Falco et al., 2010). Possible reasons for high backscatter levels from marine flora compared to surrounding uncolonised seafloor areas include: gas bubbles, foliage, and dense root structure (Parnum, 2007; Wilson and Dunton, 2009; De Falco et al. 2010). As part of this study, new acoustic backscatter data was collected from seagrass and macroalgae benthic habitats and an initial understanding of the relationships between these benthic habitats and their acoustic properties was presented in Tecchiato et al. (2011) (appendix 2), and the final results of the analysis are summarised in section 2.5.

The results of this chapter and Chapter 3 were brought together in Tecchiato et al. (submitted; see appendix 3).

2.2 UNDERWATER GEOMORPHOLOGY

Being a shallow coastal region of mid-western Australia, the study area is part of a stable passive continental margin (section 1.3.6) of a ~50 km wide continental shelf (Collins, 1988). A coastal platform was identified at Geraldton, consisting of a rather flat 10 m deep surface extending from the shoreline to a maximum of ~4 km offshore within Champion Bay. The offshore edge of this coastal platform is bordered by a ridge system followed by a major drop to seaward which reaches approximately 30 m depth at ~8 km from the shoreline (figures 16 and 17). The Geraldton coastal platform has a variable width within the study area and is ~4 km wide within Champion Bay and south of Point Moore off Tarcoola Beach (figures 16 and 17), but it is narrower off the Greenough River mouth, to the south of the Southgate dune system, and at Drummond Cove with a ~1.25 km and ~2 km width respectively. The pinnacles observed in figure 17 at about 20–25 m depth, ~6 km distant from the shoreline, are coincident with the rock-disposal area resulting from the earliest dredging activities carried out in the area.

The GIS mapping of underwater geomorphology compiled in this study, on the basis of high resolution multibeam bathymetry data (see Chapter 1 for the mapping methodologies), identified natural and artificial features mostly developed on the coastal platform <10 m deep. The natural elements are: sand bars and sheets, shallow limestone reefs, nearshore beach zone, rippled sand flat, low relief substrate, and underwater sand dunes. Pictures of these elements were extracted from the DEMs of multibeam bathymetry and are presented in figure 18. The artificial features mapped include the dredged channel, aquaculture zone, and a few shipwrecks found in Champion Bay. Of the above, in terms of morphology and surface area, the dredged channel basin created the largest anthropogenic seabed

alteration as the seafloor was deepened by 5 m within it and its extension is >5 km. The overall distribution of the natural geomorphic features visible in figures 19 to 21 is outlined below. Bedform classification methods are those adopted by Ashley (1990).

Sand bars and sheets: these are sandy bodies showing higher elevation compared to the surrounding substrates due to sediment accumulation. The difference in elevation to the surrounding seabottom is up to 1 m for sand bars, but lower relief was found for sand sheets. The shape of sand bars is often adjusted by adjacent limestone reefs, but dome shaped bars were mapped where reefs did not occur. The sand sheets have variable shapes, but are often WSW–ENE aligned off the Chapman River mouth. These features are common off Southgate dune and the Chapman River, but also in between the Point Moore reef system, to the east toward the dredged channel and partly developed within it, together with the port and marina basins. These features indicate areas of sediment accumulation and are areas where the sediment cover is mobile and does not contribute to stabilizing the seabed.

Shallow limestone reefs: these are generally developed at ~10 m depth along the edge of the coastal platform but are also present in close proximity to the beaches, especially along the Northern Beaches. Well-developed systems were mapped south and north of Point Moore, at Separation Point and Drummond Cove. Sediment accumulation around those reefs is common, with sand bars and sheets and the nearshore beach zone developed next to these features at Point Moore and Separation Point, respectively. Shallow limestone reefs influence sediment transport and deposition by obstructing the sediment flow and creating topographic barriers which support sediment accumulation in the surrounding areas. During glacial lowstand periods, the present western Australian continental shelf was completely exposed down to the current shelf edge at ~-125m (Collins, 1988). Karstification of pre-existing Pleistocene limestone surfaces, including ancient reef systems, took place and influences the current coastal topography. Paleo-reef systems might form the shallow limestone reef systems identified in this study as supported by previous literature (Johnson et al., 1995; Langford, 2001).

Nearshore zone: this was mapped off the northern part of Tarcoola Beach, at Separation Point and off Glenfield Beach and Drummond Cove between ~3.5 and 6.5 m depth. The offshore limit of the nearshore zone specifies the offshore extension of the beach and sediments of the longshore transport system to a depth at which the sediment is rarely moved and reworked by wave energy except during major storms. In other words, it defines the “nearshore”, which is a zone of active bedload sediment transport and is widely recognised as a concave-upward bottom (see Chapter 4 for further discussion about this).

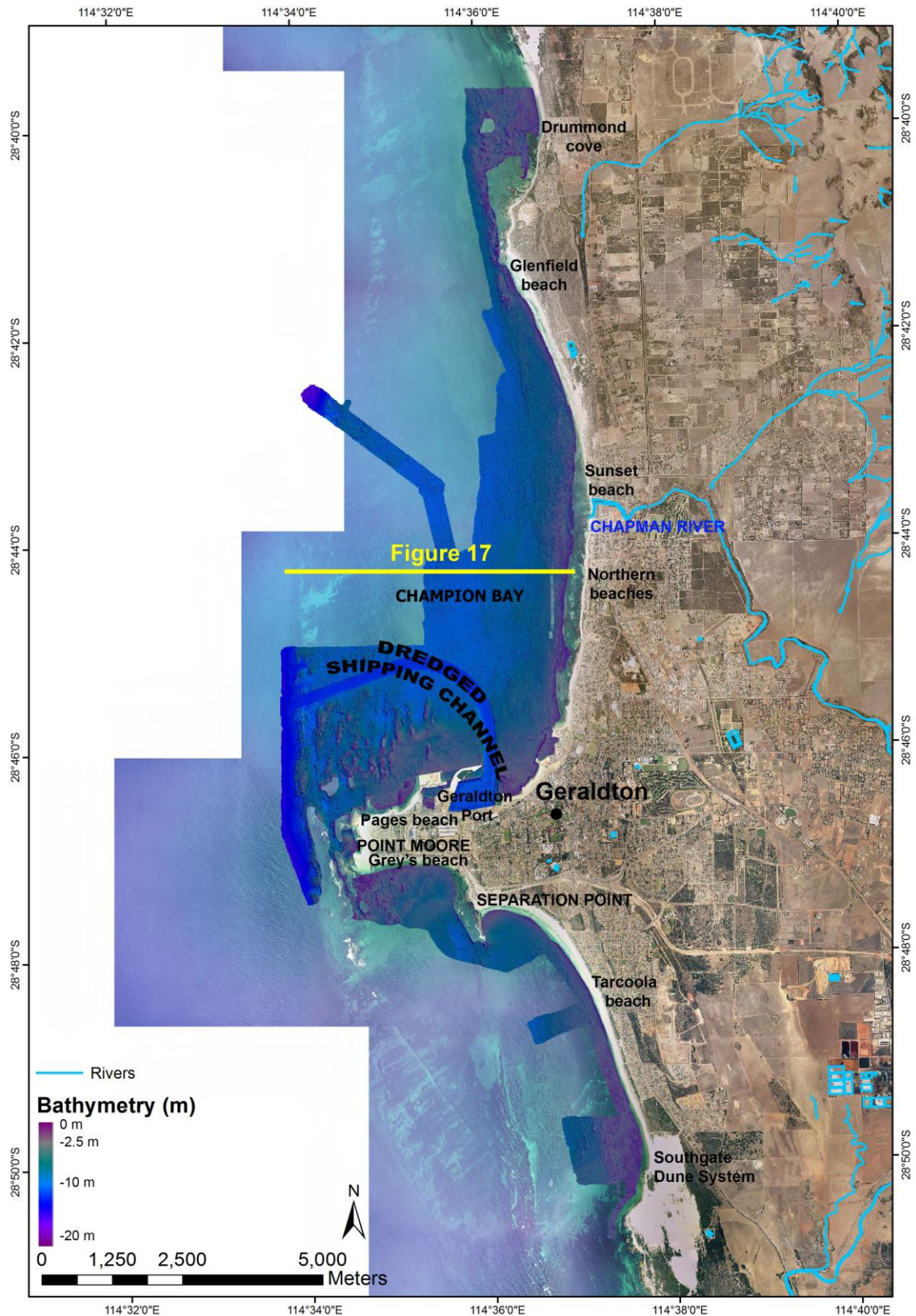


Figure 16: Digital Elevation Models (DEMs) of bathymetry resulting from the November–December 2010 multibeam survey at Geraldton. The data extent is $\sim 35 \text{ km}^2$ and focused on the Geraldton coastal platform, mainly covering the areas close to the shoreline to $\sim 10 \text{ m}$ depth (purple to lighter blue colours); however, off Point Moore the data reached $\sim 25 \text{ m}$ depth. Of note, the dredged channel and Port basins indicated by the darker blue colours are 12 to 15 m deep. The location of figure 17 is also indicated.

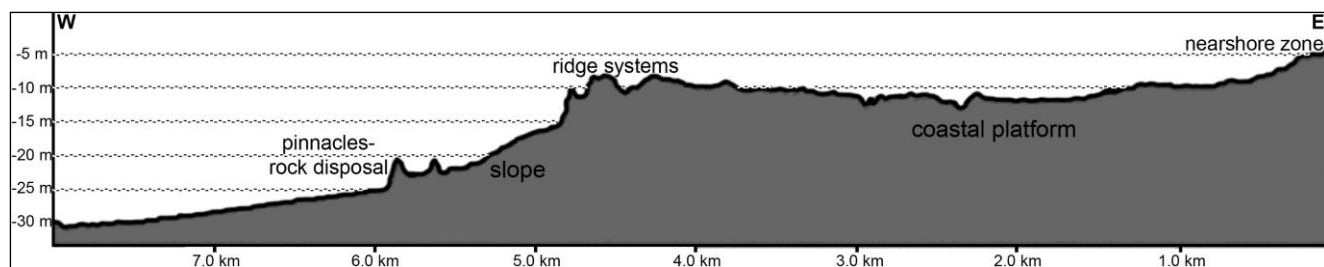


Figure 17: W-E profile of the Geraldton coastal platform (see figure 16 for location) derived from the multibeam bathymetry.

concept). Discontinuously along the shoreline, the nearshore concave surface was observed mostly at a distance of ~400m offshore and at ~5 m depth in the northern Geraldton embayment; however, a depth range between 3.5 and 6.5 m and a distance between ~170 and ~400 m offshore was observed in the southern Geraldton embayment

Rippled sand flats: these are sandy areas where the waves act on the seabed generating symmetric ripples (wavelength <1 m; cf. Ashley, 1990). The only location where asymmetrical ripples were mapped as part of this feature/GIS layer is off the Batavia Coast Marina, indicating a northward oriented bottom current (figures 22 and 23). These ripples are simple 2D bedforms with parallel, slightly undulated or straight crested morphologies and are mostly swash aligned. Rippled sand flats are indicative of sediment movement on the sea bottom, and because they were found to ~10 m depth throughout the study area, they indicate that the wave action influences the whole coastal platform at Geraldton which is ~10m deep.

Underwater sand dunes: dunes are larger scale ripples (wavelength = 1–10 m; cf. Ashley, 1990) than those of the rippled sand flats, generated by a stronger bottom current than the ripple-related current. Dunes represent a higher sediment volume than that available where rippled sand flats are present. They were mapped to the east of Separation Point on a low relief substrate and are asymmetric to the north-east, showing a prevalent sediment transport direction toward the shore (figures 22 and 24). Underwater sand dunes were asymmetric, and mostly composed of 3D bedforms with linguoid morphology and often superimposed smaller scale ripples.

Low relief substrate: flat or low sloping substrate is widespread throughout the study area at all depths showing no evidence of sediment deposition/erosion.

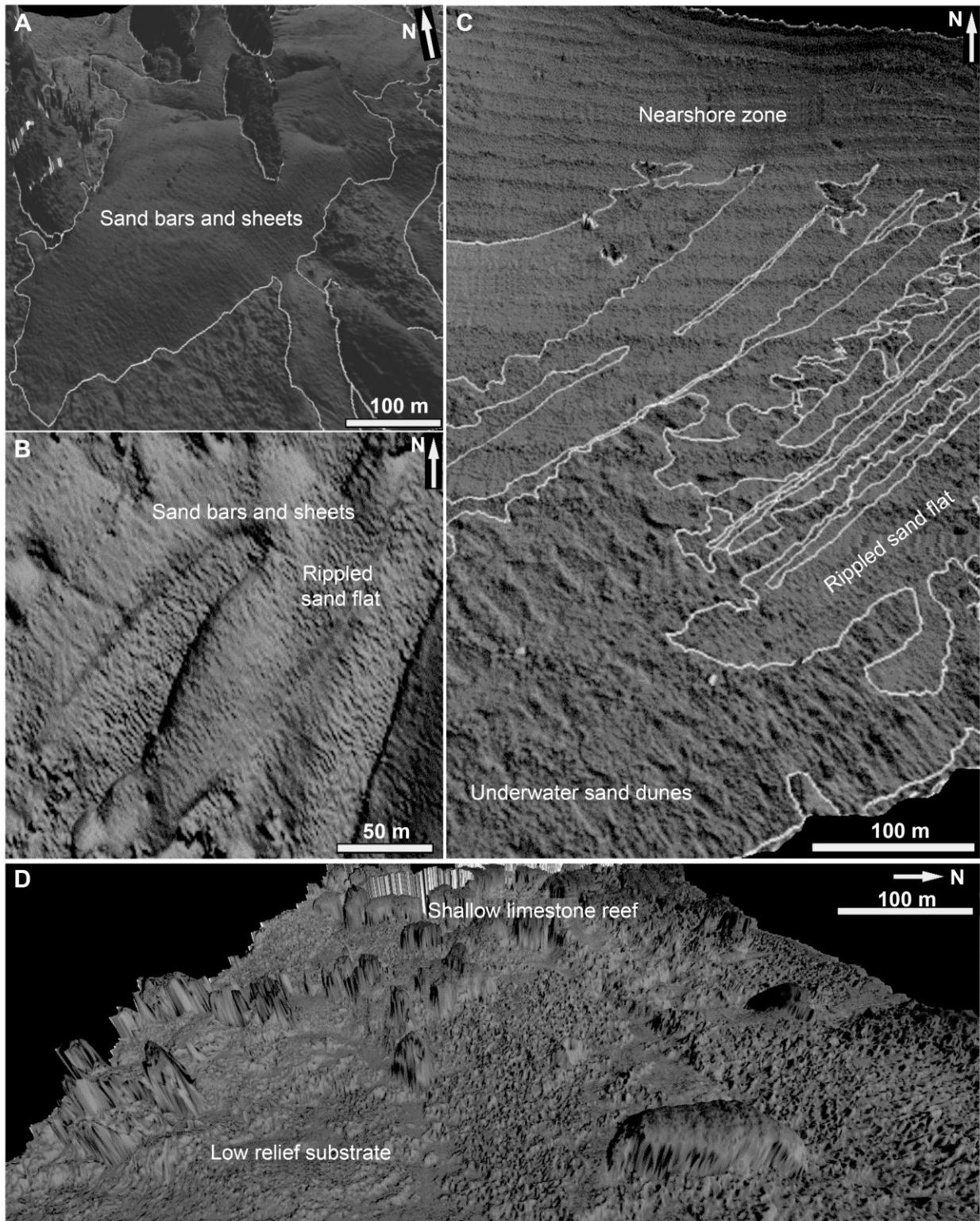


Figure 18: Underwater morphology features mapped at Geraldton as visible on the high resolution DEMS of multibeam bathymetry: A) sand sheet adjacent to an area of low relief substrate; B) sand bars with rippled sand in the bars through; C) offshore boundary of the nearshore beach zone, adjacent to a rippled sandy area which evolves into underwater sand dunes further offshore; D) shallow limestone reef system surrounded by an area of low relief substrate.

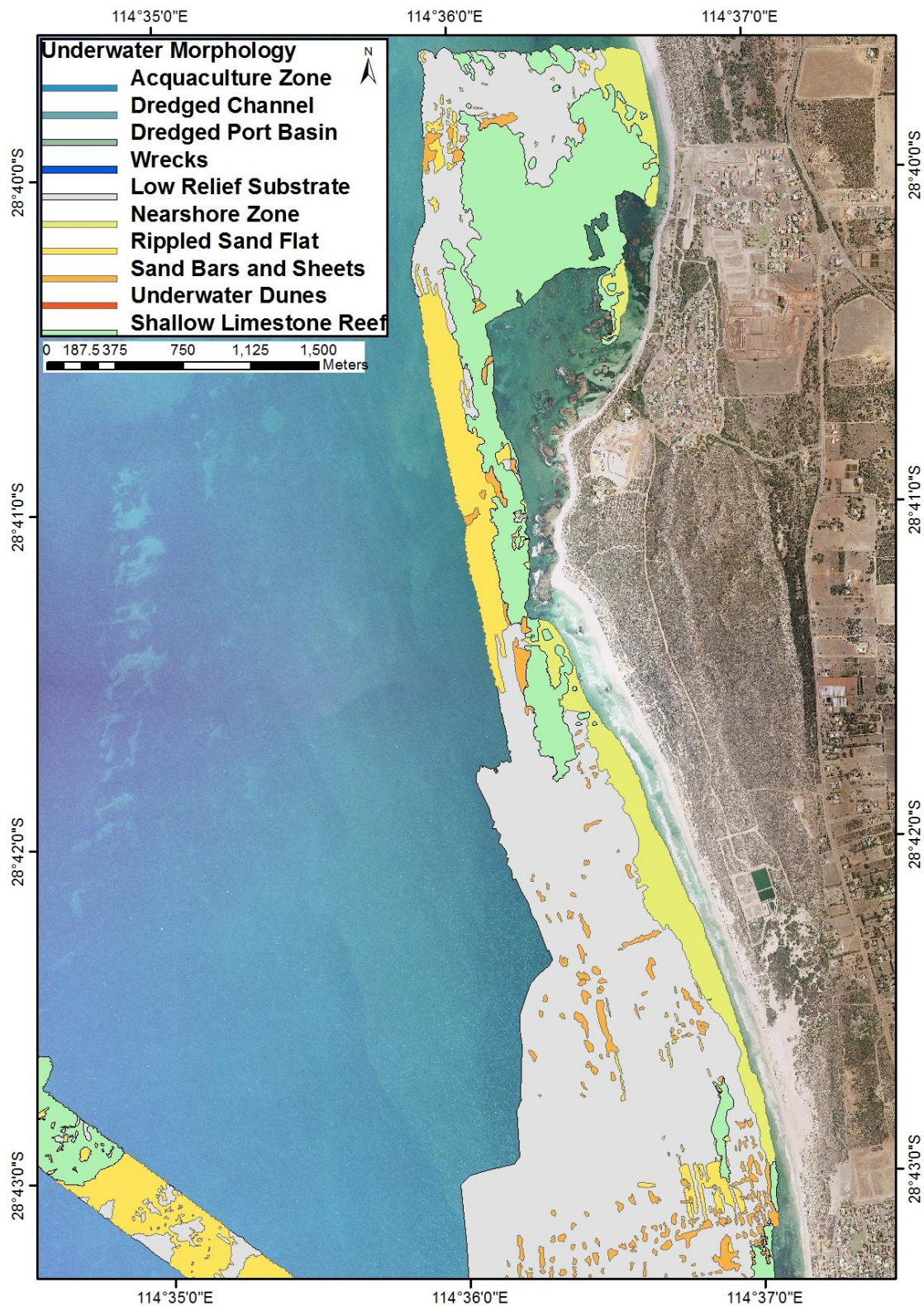


Figure 19: Underwater morphology map at Drummond Cove based on DEMs of bathymetry. The GIS polygons are overlaid on the aerial photography. The blue tones of the colouring scale indicate the artificial elements (i.e. aquaculture zone, dredged channel, dredged port basin, and shipwrecks); yellow to red colours indicate sediment deposition or transport (i.e. nearshore zone, rippled sand flat, sand bars and sheets, and underwater sand dunes); the shallow limestone reefs and low relief substrate polygons indicate areas where no sand is depositing, and were coloured green and grey respectively.

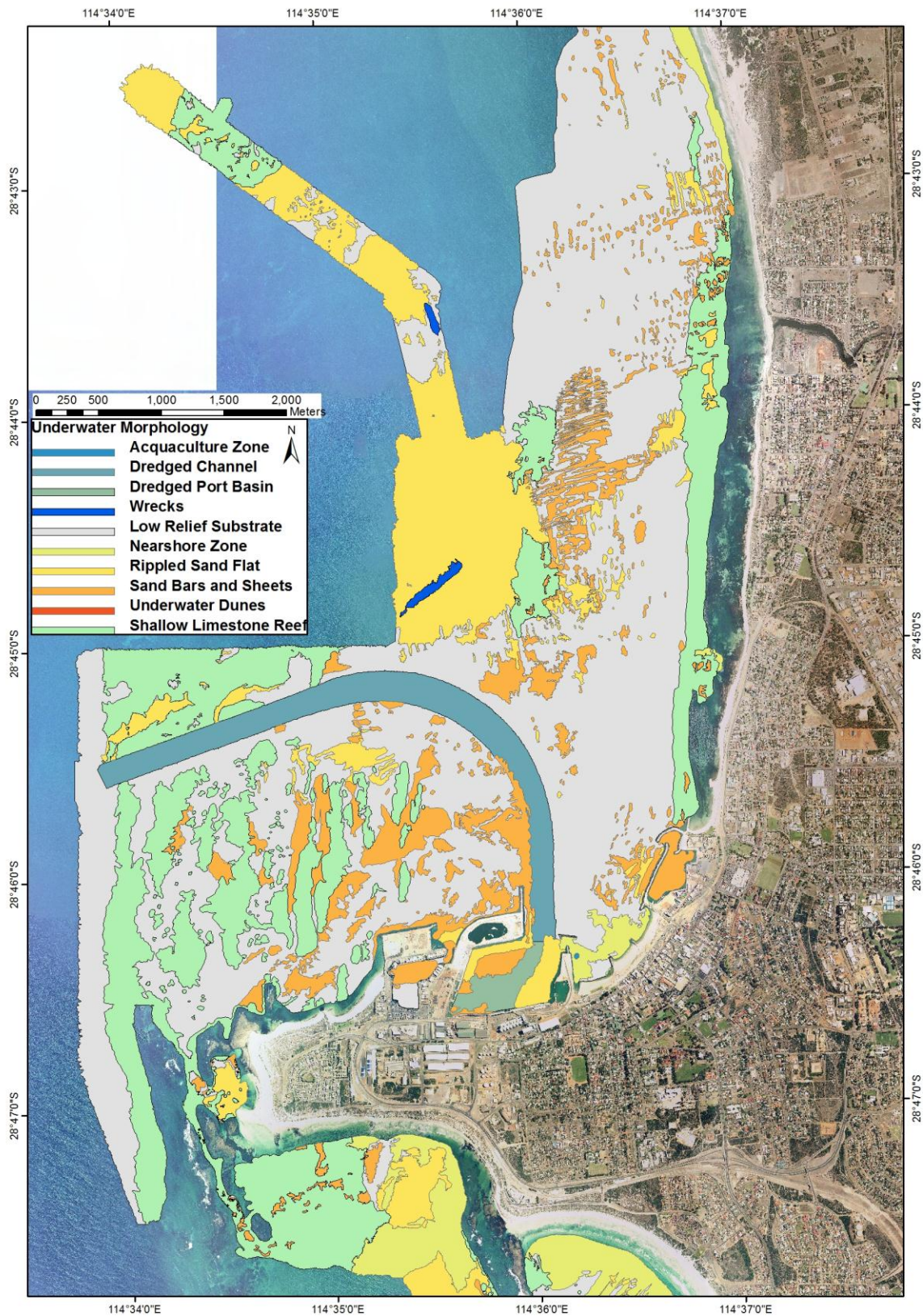


Figure 20: Underwater morphology map at Geraldton based on DEMs of bathymetry. The GIS polygons are overlaid on the aerial photography. The blue tones of the colouring scale indicate the artificial elements (i.e. aquaculture zone, dredged channel, dredged port basin, and shipwrecks); yellow to red colours indicate sediment deposition or transport (i.e. nearshore zone, rippled sand flat, sand bars and sheets, and underwater sand dunes); the shallow limestone reefs and low relief substrate polygons indicate areas where no sand is depositing, and were coloured green and grey respectively.

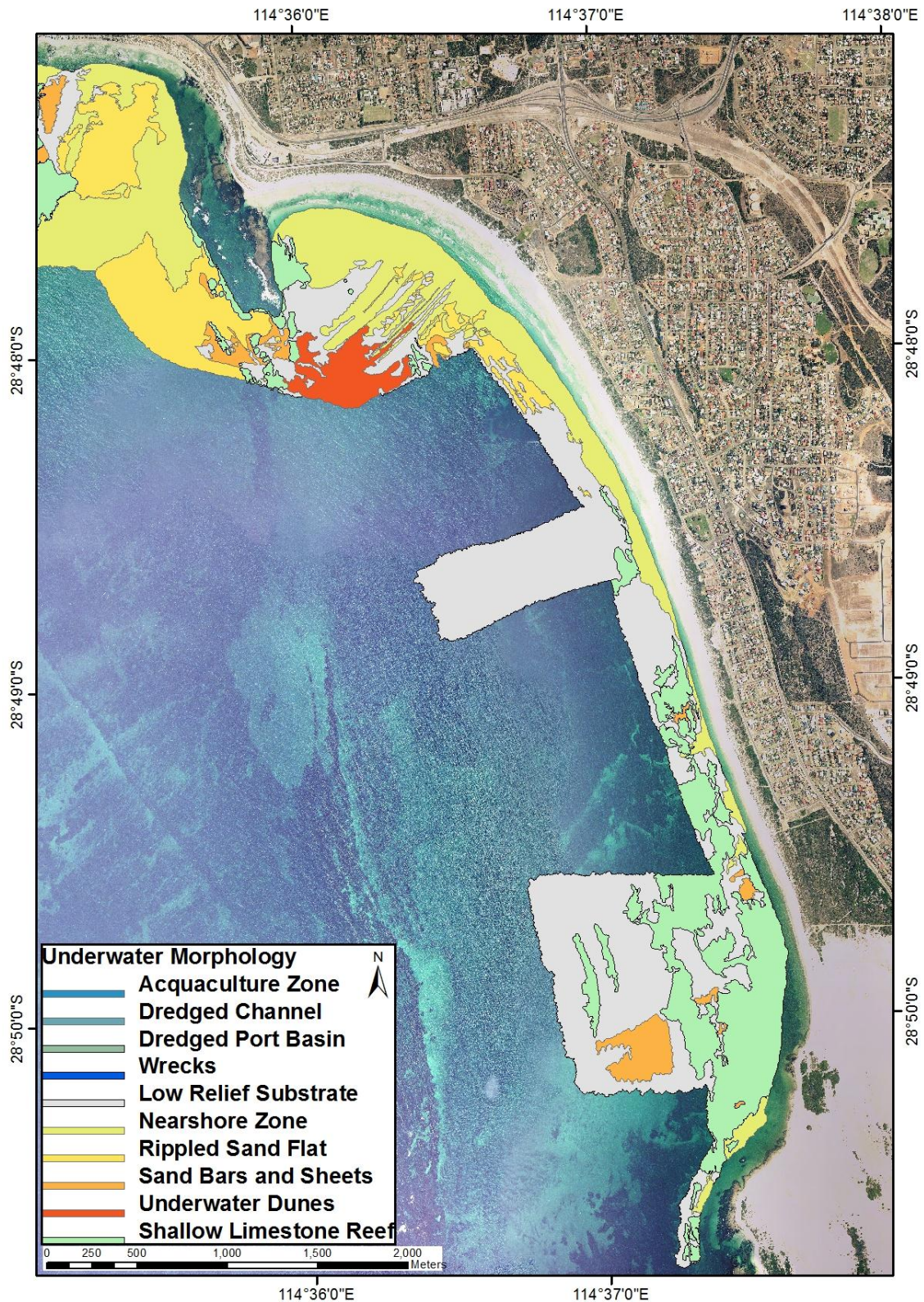


Figure 21: Underwater morphology map at Tarcoola Beach based on DEMs of bathymetry. The GIS polygons are overlaid on the aerial photography. The blue tones of the colouring scale indicate the artificial elements (i.e. aquaculture zone, dredged channel, dredged port basin, and shipwrecks); yellow to red colours indicate sediment deposition or transport (i.e. nearshore zone, rippled sand flat, sand bars and sheets, and underwater sand dunes); the shallow limestone reefs and low relief substrate polygons indicate areas where no sand is depositing, and were coloured green and grey respectively.

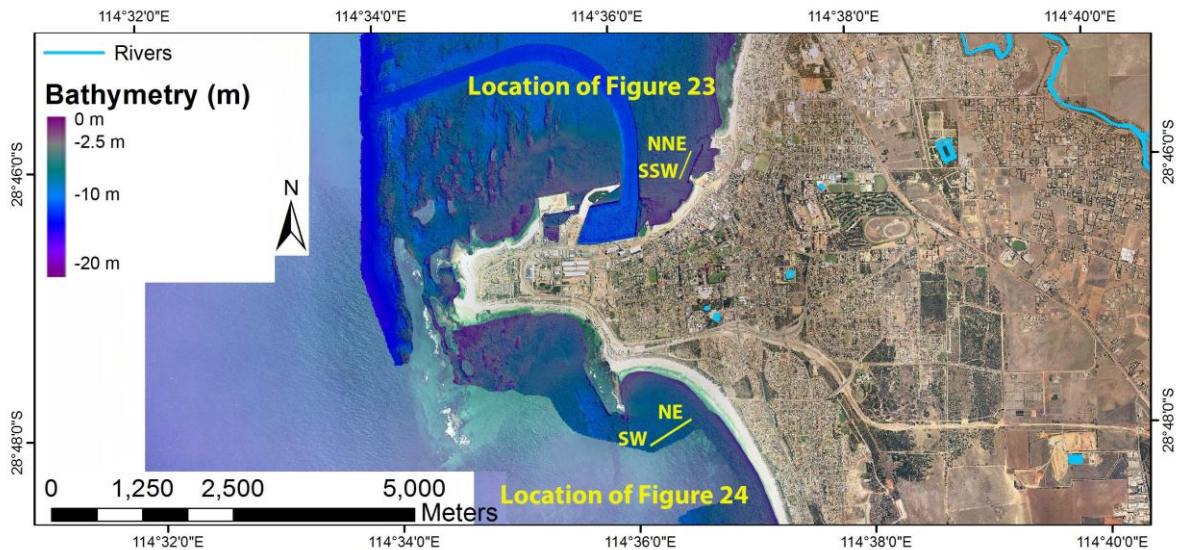


Figure 22: Locations of figures 23 and 24.

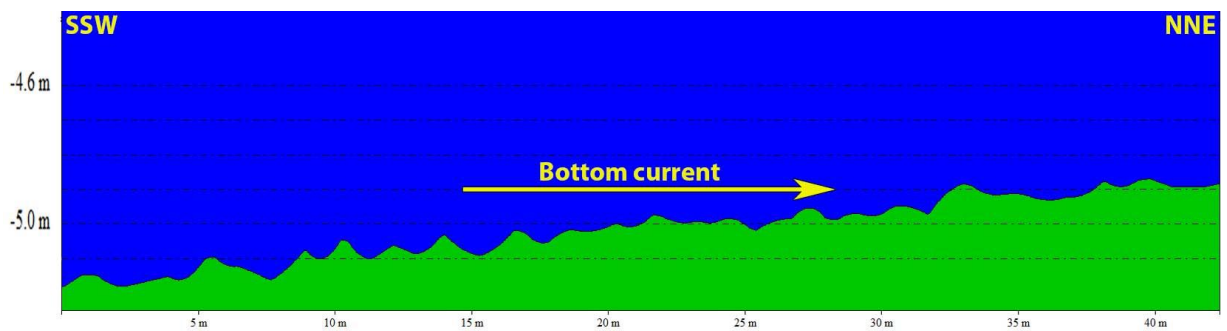


Figure 23: S-N profile of sand ripples off the Batavia Coast Marina.

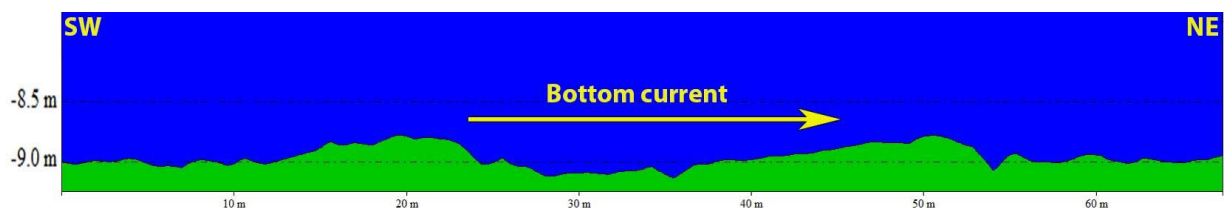


Figure 24: SW to NE profile of the underwater sand dunes mapped to the east of Separation Point.

It should be noted that some of the features described are dynamic in nature and likely to respond to seasonal and other cyclic changes in hydrodynamic conditions; for example, between fair-weather and storm-dominated seasons. Such information is not available to a reconnaissance study such as the present project, which nevertheless provides a useful overview of substrate dynamics and is representative of the data collection season (November–December 2010).

2.3 SEABED MOBILITY

The characterization of underwater geomorphology and habitats undertaken in this study has provided important information to spatially locate areas of sediment deposition (i.e.

sediment sinks) and areas where no evidence of sediment deposition/erosion was found on the basis of environmental data (i.e. stable areas).

Seabed mobility was assessed throughout the study area on the basis of the underwater morphology and habitat mapping. The GIS polygons used for the underwater morphology mapping were merged into more extensive polygons indicating the seabed mobility of the Geraldton coastal system (figure 25). The merged GIS layers were simplified through dedicated ArcGIS 10 applications, which reduce the number of vertices of the single polygons and group smaller shapes into more spatially extensive shapes. The resulting GIS layers have the following sedimentological significance:

- Nearshore zone was mapped as part of the morphology mapping, with the sand dominance confirmed by the habitat mapping. Its seaward boundary defines the limit of an area of active sediment exchange between onshore and offshore. In other words, it defines the “nearshore”, which is a zone of active bedload sediment transport and is widely recognised as a concave-upward bottom (see Chapter 4 for further discussion about this concept). Limestone ridges are also common in close proximity to the beaches and were mapped on the multibeam bathymetry at locations where the nearshore concave surface was not visible. Consequently, this feature is very discontinuous along the Geraldton shoreline and has a limited extent on the seabed mobility map (5% of the mapped area). The seaward extent of the nearshore zone reaches a maximum of 400 m, indicating that a narrow zone of sediment exchange and active bedload transport interact with the beach systems. Further discussion about this concept is presented in Chapter 4.
- Deposition areas indicate locations to where the sediment is being transported by littoral currents, and consist of mobile unvegetated sediment bodies which represent sediment sinks in terms of the coastal sediment budget. These areas were mapped as “sand bars and sheets” in terms of underwater geomorphology and the sandy substrate dominance was confirmed by the habitat mapping. Deposition areas are a relatively common substrate type (14% of the mapped area) and include part of the dredged channel, but also the Port and Batavia Coast Marina basins. Near Point Moore deposition areas are nested between shallow limestone reefs which are bathymetric salient that facilitate sediment accumulation.
- Equilibrium/potential transport areas are areas of active sediment exchange within the coastal platform. The “rippled sand flat” and “underwater sand dunes” polygons

were merged together to generate this layer which extents for 14% of the total mapped area. Evidence of bedload sediment transport were found at these locations on the basis of bathymetry data.

- Stable areas are zones of the coastal platform where no evidence of sediment erosion/deposition or bedload sediment transport was found. The “shallow limestone reefs” and “low relief substrate polygons” were merged together to generate this layer. The “dredged channel” and “dredged port basin” layers were also merged into this polygon because no evidence of sediment transport was significant at those locations. Stable areas are very common in the study area (67% of the mapped area) and are covered by benthic biota (mostly seagrass and macroalgae) to varying degrees.

The main outcome of the seabed mobility mapping is the exact identification of areas of sediment deposition offshore which adds environmental value to the reconnaissance of sediment transport pathways. In fact, sediment transport is likely to be oriented towards the deposition areas indicated in figure 25, following the northward oriented longshore sediment transport system which dominates the west coast of Australia. Moreover the seabed mobility mapping has helped in determining the boundaries of the sediment cells characterising the Geraldton coastal system, which will be further described in Chapter 4. A seabed mobility map with this high level of detail and significant spatial extent such as the one developed in this project is not commonly available for sediment budget studies, which often have a more limited understanding of the overall environmental characteristics of the systems.

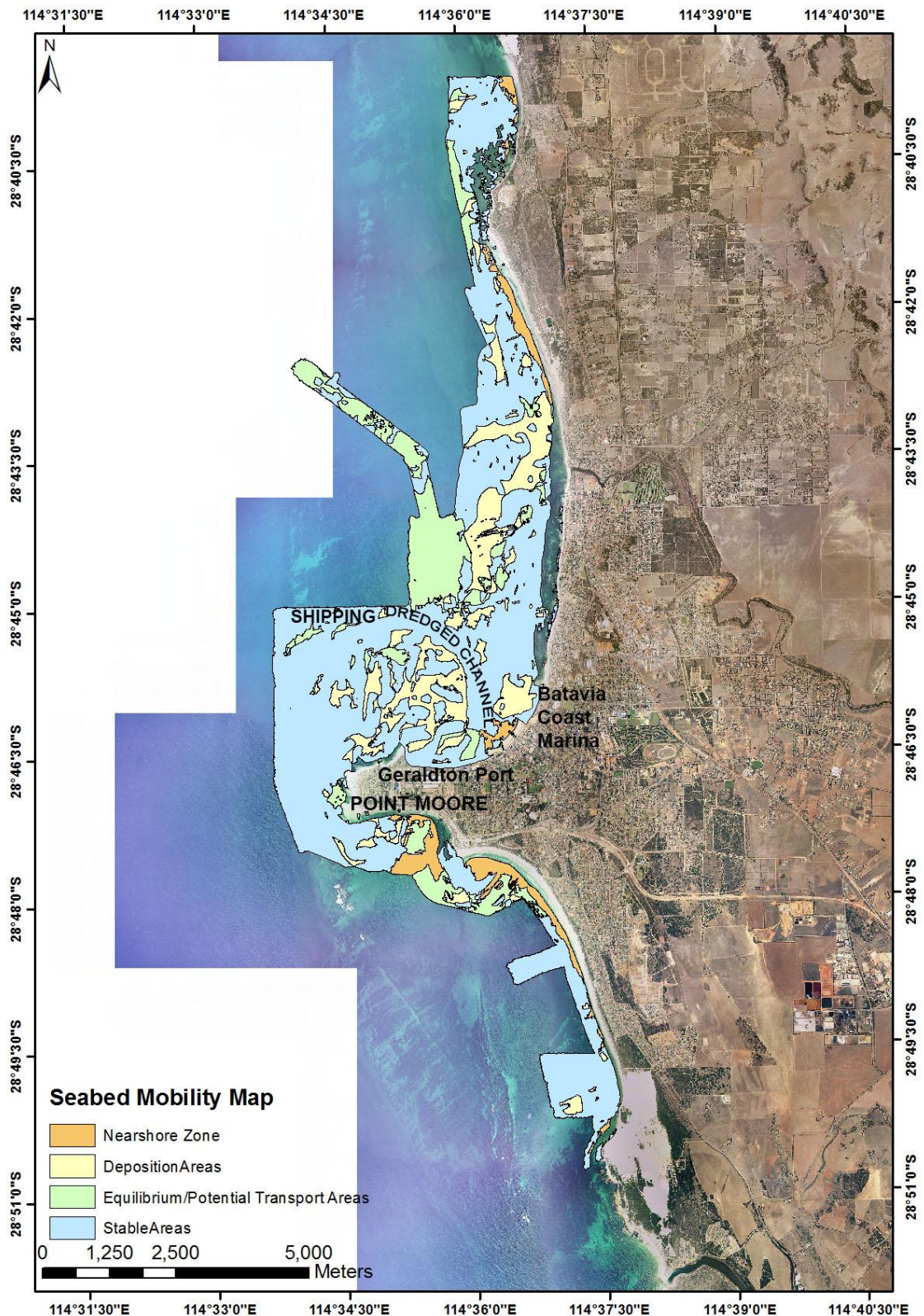


Figure 25: Seabed mobility map of the Geraldton coastal system. The GIS polygons are overlaid on the aerial photography. The nearshore zone indicates the seaward limit of sediment exchange between the beach system and the offshore based on bathymetry data. Sediment is transported towards the deposition areas, which represent sediment sinks. Sediment transport as bedload is visible on the bathymetry data within the zones mapped as equilibrium/potential transport areas. Finally, stable areas show no evidence of sediment deposition/erosion or bedload transport.

2.4 BENTHIC COVER AND PHYSICAL SUBSTRATES

The standard definition videography provided a depth consistent overview of the benthic cover of the Champion Bay embayment to 30 m depth (figure 26). The dominant biota is composed of macroalgae and seagrass, which may occur together or form dense monospecific communities. Seagrass meadows dominated by *Posidonia* sp. (PSP) were found between Pages Beach and the dredged channel, but *Amphibolis griffithii* (AG) and *Amphibolis antarctica* (AA) dominate elsewhere. *Halophila* sp. (HSP) is a coloniser seagrass which colonises more mobile substrates, and is common off the Chapman River mouth (figure 26). Whilst seagrass is common to ~10 m depth, macroalgae occur to ~30 m depth, colonising the reef systems on the coastal platform edge and the offshore high gradient slope. Macroalgae communities are patchy and form different assemblages at Champion Bay, with a general trend of denser and higher biota on the reef systems on the coastal platform edge where higher wave energy is available, and smaller and less dense biota on the coastal platform and offshore slope. The macroalgal cover of the Point Moore reef system has been especially well documented through underwater videography data and *Ecklonia* sp. was found to be a common species.

High-resolution videography data was collected throughout the study area within a shallower depth range (3–17.5 m water depth, with the majority of the data <10 m deep) than the standard definition videography (up to 30 m deep). This data has allowed a quantitative assessment of the benthic cover to be achieved and is presented herein using graphs of mean benthic percentage cover with associated standard errors amongst the four areas outlined below from south to north.

Greenough (from the Greenough River mouth to Separation Point; figure 27a). Six video transects were collected in this area and the results of their analysis (figure 27b) shows that 56% of the average benthic cover is composed of sand, 17% is a mixture of macroalgae and coralline algae, and the remaining 27% is composed of seagrasses. Two sites located off Southgate dune were sand-dominated and one site has dominant coloniser seagrass cover, which is consistent with the underwater morphology mapping that has identified a sand bar and sheet system at those locations. The remaining three sites were characterised by seagrass meadows (average seagrass cover 40%), with two sites dominated by AA (figure 28) and one by AG (figure 29).

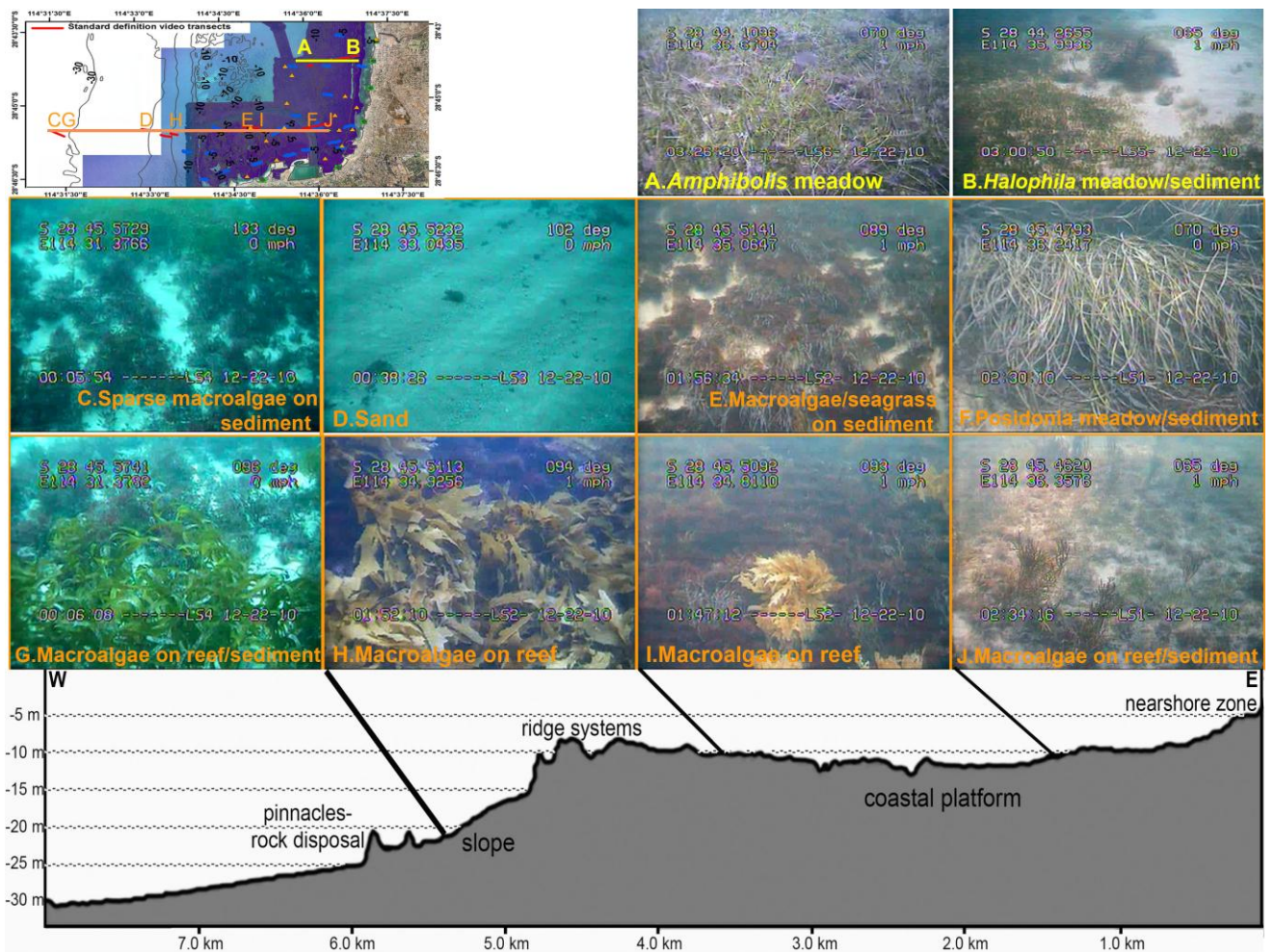


Figure 26: Habitat distribution across depth at Geraldton. Both seagrass meadows and macroalgae communities are patchy, showing a gradual density decrease while transitioning to sand-dominated substrates.

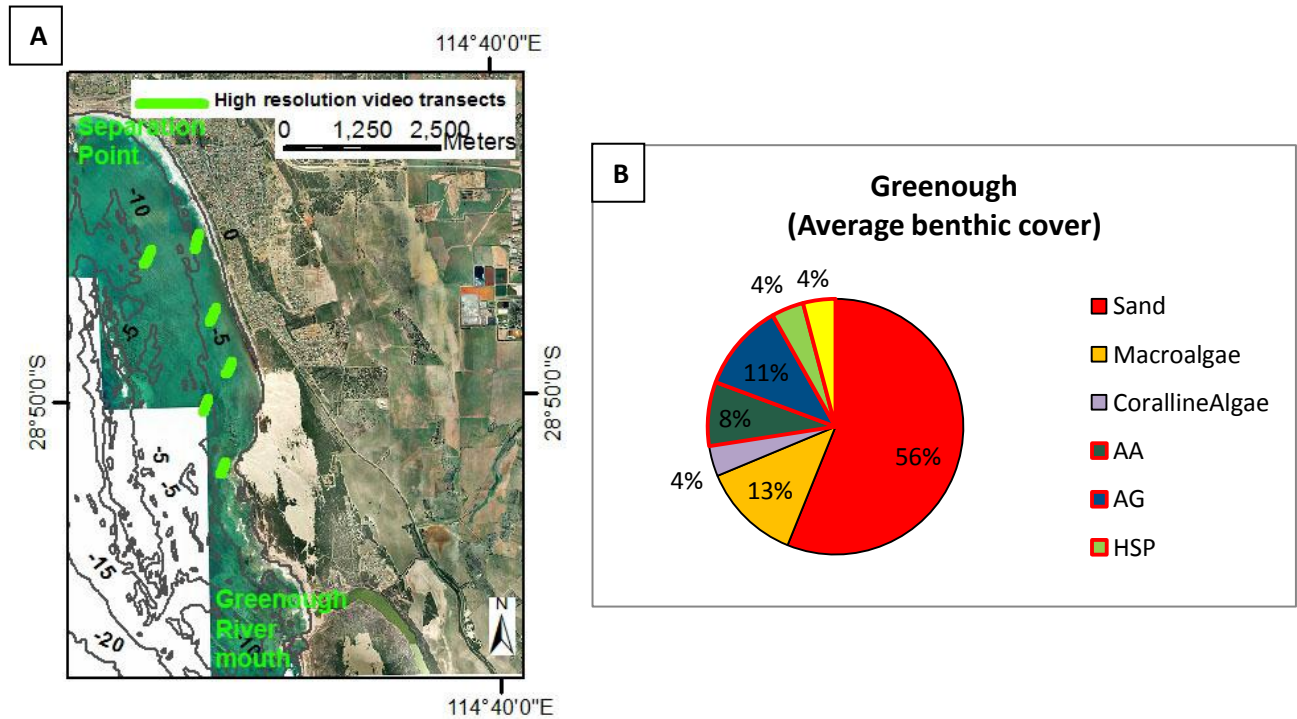


Figure 27: A) location map of the Greenough area (from the Greenough River mouth to Separation Point); B) mean percent cover of seagrass, algae and sand in the Greenough area. The red-bordered segments represent seagrasses: AG = *Amphibolis griffithii*; AA = *Amphibolis antarctica*, PSP = *Posidonia* sp. and HSP = *Halophila* sp.

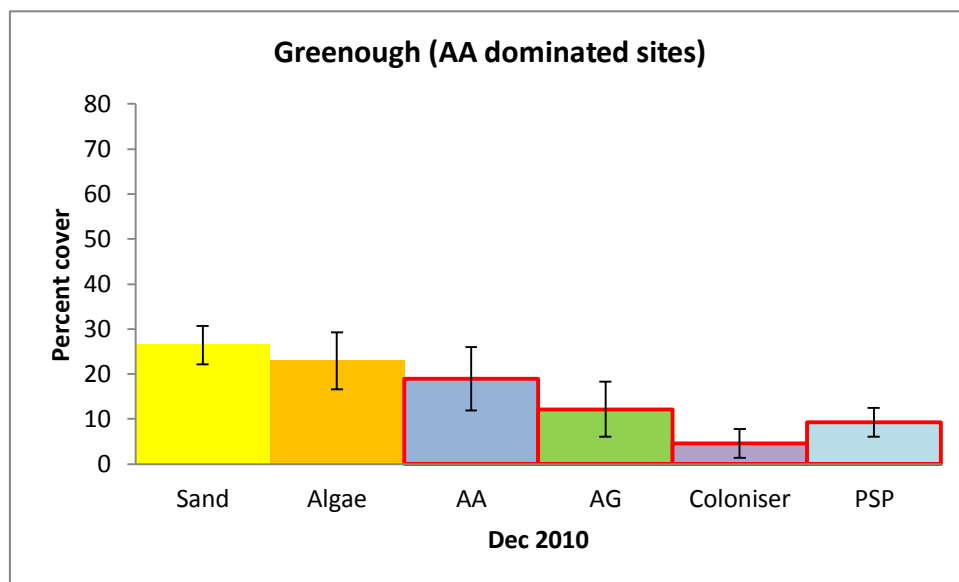


Figure 28: Mean percent cover of seagrass, algae and sand (\pm Standard Error) at *Amphibolis antarctica*-dominated sites in the Greenough area (from the Greenough River mouth to Separation Point). The red-bordered bars represent seagrasses: AG = *Amphibolis griffithii*; AA = *Amphibolis antarctica*; PSP = *Posidonia* sp.; and Coloniser = *Syringodium isoetifolium* + *Halophila decipiensis* + *Halophila* sp.

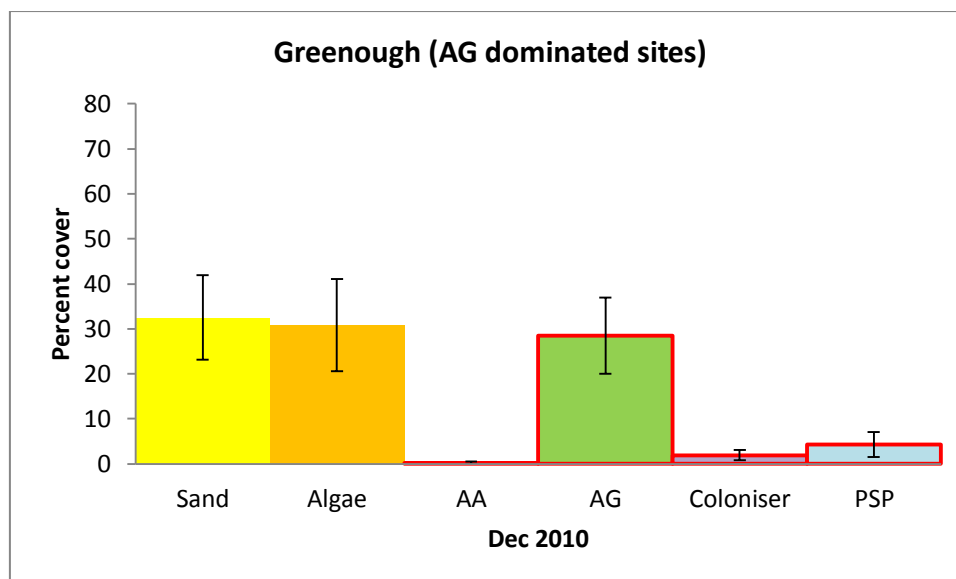


Figure 29: Mean percent cover of seagrass, algae and sand (\pm Standard Error) at *Amphibolis griffithii*-dominated sites in the Greenough area (from the Greenough River mouth to Separation Point). The red-bordered bars represent seagrasses: AG = *Amphibolis griffithii*; AA = *Amphibolis antarctica*; PSP = *Posidonia* sp.; and Coloniser = *Syringodium isoetifolium* + *Halophila decipiensis* + *Halophila* sp.

Separation Point (from Separation Point to Point Moore, figure 30a). It is dominated by sandy substrates (66%; figure 30b) and there is also a low percentage of rubble, outcropping pavement, and remains of dead vegetation (5% in total). Macroalgae are the most common biota found within this area (24%) together with a low percentage of coralline algae and seagrasses (5% in total). The sandy-dominated nearshore zone is the main geomorphic feature identified to the west of Separation Point as part of the underwater morphology mapping; shallow limestone reefs were also identified on the multibeam bathymetry models at locations where macroalgal communities are common on the video transects.

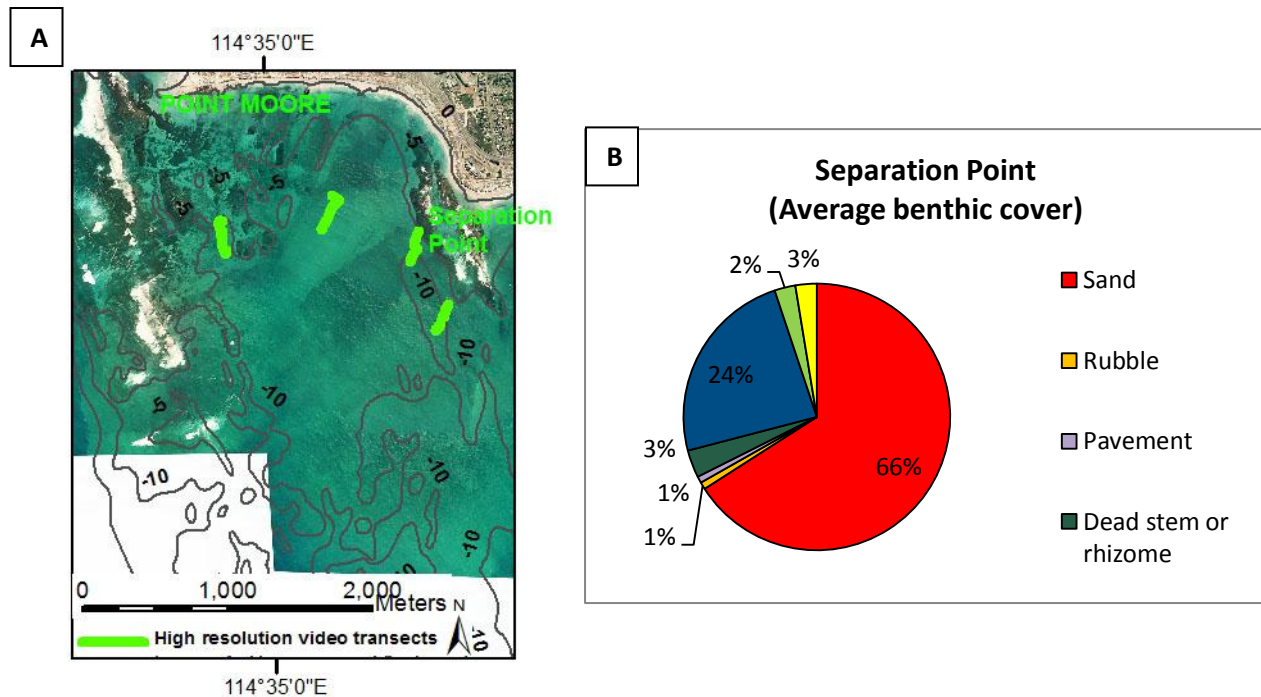


Figure 30: A) location map of the Separation Point area (from Separation Point to Point Moore); B) mean benthic percent cover in the Separation Point area.

Point Moore to Chapman River mouth (figure 31a). The majority of the underwater videography data collected in December 2010 falls within this region, with twenty-one transects recorded. As shown in figure 31b, sandy substrates are common (44%); macroalgae and coralline algae follow with 39% in total, and seagrasses constitute the remaining 17%. Important sandy patches were found off the Chapman River mouth, with mobile substrates mapped as part of the sand bar and sheet system in the underwater morphology investigations. Macroalgal communities with abundant *Ecklonia* sp. are common on the shallow reef system mapped on the multibeam bathymetry models to the north of Point Moore. A different assemblage of macroalgal communities, characterised by species with shorter canopies, was found closer to the town beaches and the port infrastructure. PSP-dominated meadows were only found on the flat substrates located between Pages Beach and the dredged channel (figure 32), as shown from data recorded at six survey sites. AA and AG-dominated seagrass meadows were found to the north of the dredged channel, where two video transects document the existence of relatively dense seagrass meadows (figures 33 and 34). Of note is that part of this habitat colonizes a low sloping limestone reef found on the multibeam bathymetry models off the Northern Beaches. Coloniser seagrasses are usually associated with low height macroalgal communities of the coastal town regions and with mobile sandy substrates found in the middle of Champion Bay and off the Chapman River mouth.

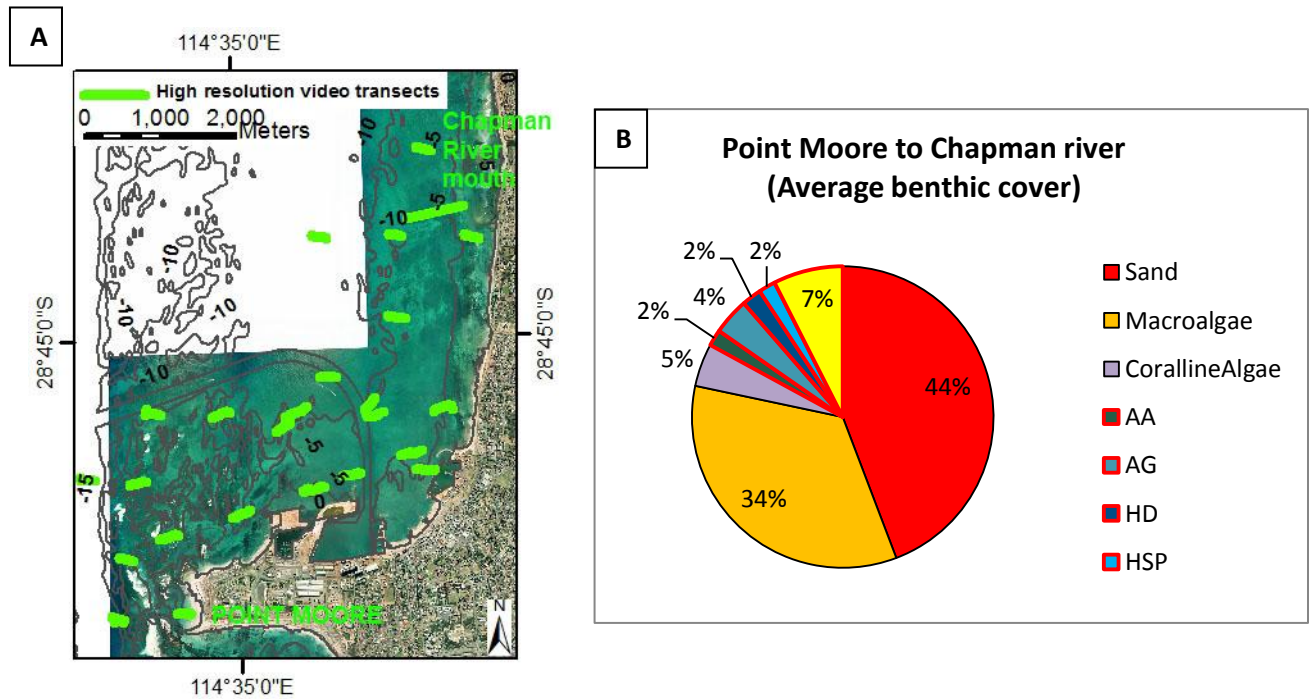


Figure 31: A) location map of the area between Point Moore and the Chapman River mouth; B) mean percent cover of seagrass, algae, and sand in the area between Point Moore and the Chapman River mouth. The red-bordered segments represent seagrasses: AG = *Amphibolis griffithii*; AA = *Amphibolis antarctica*; PSP = *Posidonia* sp.; HSP = *Halophila* sp.; and HD = *Halophila decipiensis*.

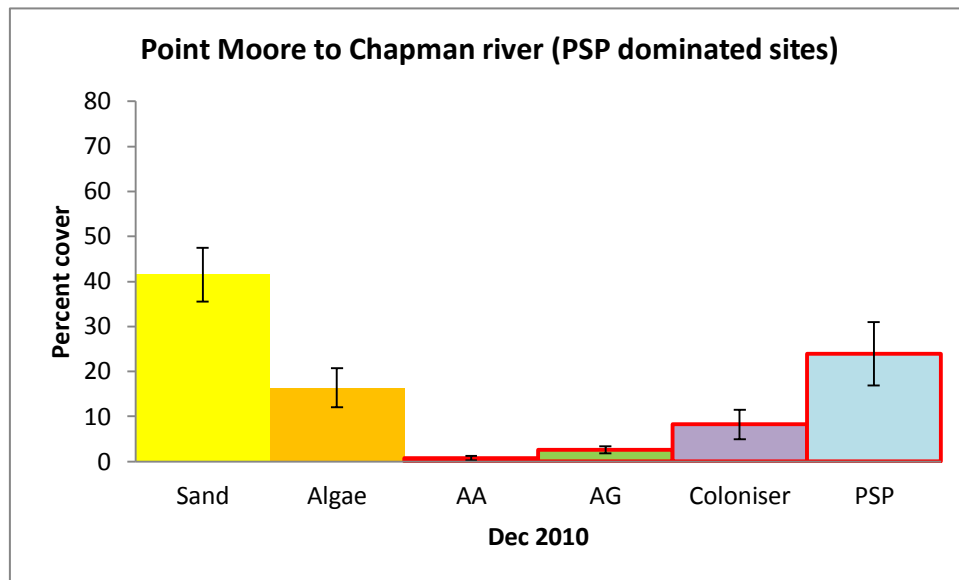


Figure 32: Mean percent cover of seagrass, algae and sand (\pm Standard Error) at *Posidonia* sp.-dominated sites, only found in the Point Moore to Chapman river area, more specifically between Pages beach and the dredged channel basin. The red-bordered bars represent seagrasses: AG = *Amphibolis griffithii*; AA = *Amphibolis antarctica*; PSP = *Posidonia* sp.; and Coloniser = *Syringodium isoetifolium* + *Halophila decipiensis* + *Halophila* sp.

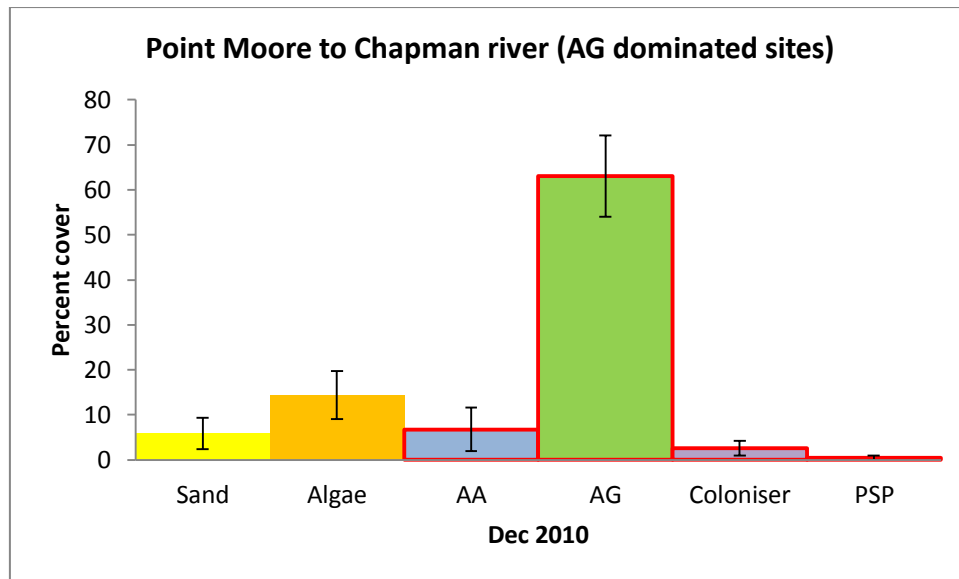


Figure 33: Mean percent cover of seagrass, algae, and sand (\pm Standard Error) at *Amphibolis griffithii*-dominated sites in the area between Point Moore and the Chapman River mouth. The red-bordered bars represent seagrasses: AG = *Amphibolis griffithii*; AA = *Amphibolis antarctica*; PSP = *Posidonia* sp.; and Coloniser = *Syringodium isoetifolium* + *Halophila decipiensis* + *Halophila* sp.

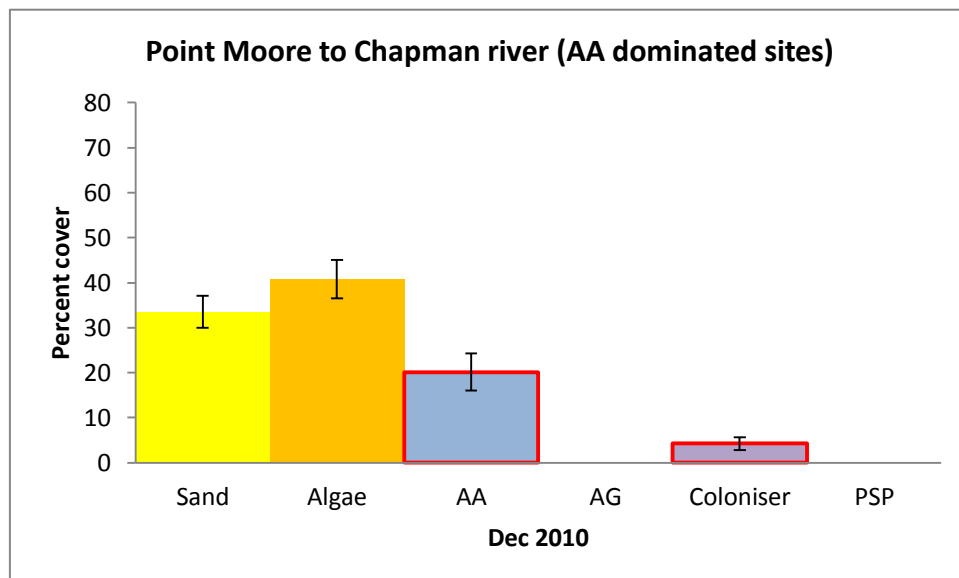


Figure 34: Mean percent cover of seagrass, algae, and sand (\pm Standard Error) at *Amphibolis antarctica*-dominated sites in the area between Point Moore and the Chapman River mouth. The red-bordered bars represent seagrasses: AG = *Amphibolis griffithii*; AA = *Amphibolis antarctica*; PSP = *Posidonia* sp.; and Coloniser = *Syringodium isoetifolium* + *Halophila decipiensis* + *Halophila* sp.

North of the Chapman River mouth (figure 35a) In this region, seagrass meadows are more abundant than in the previously described areas, with an average seagrass cover of 33% (figure 35b). Sandy substrates are also common (45%), with outcropping pavement also visible (4%). Macroalgal communities are the least occurring habitat in this region, with an

average benthic cover of 18%. Seagrass meadows are relatively dense, especially at the five AG-dominated sites (figures 36 and 37) and colonise shallow rocky areas.

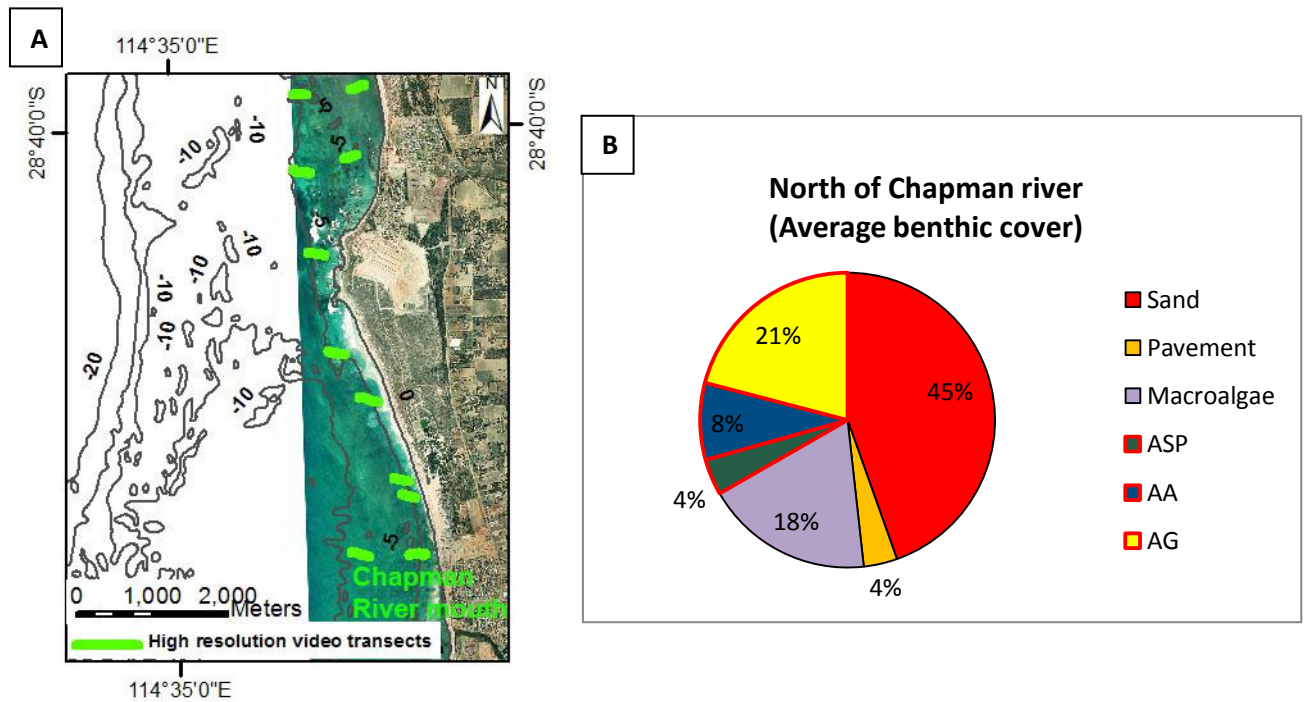


Figure 35: A) Location map of the area to the north of the Chapman River mouth; B) mean percent cover of seagrass, algae, sand and pavement in the area to the north of the Chapman River mouth. The red-bordered segments represent seagrasses: AG = *Amphibolis griffithii*; AA = *Amphibolis antarctica*; and ASP = *Amphibolis* sp.

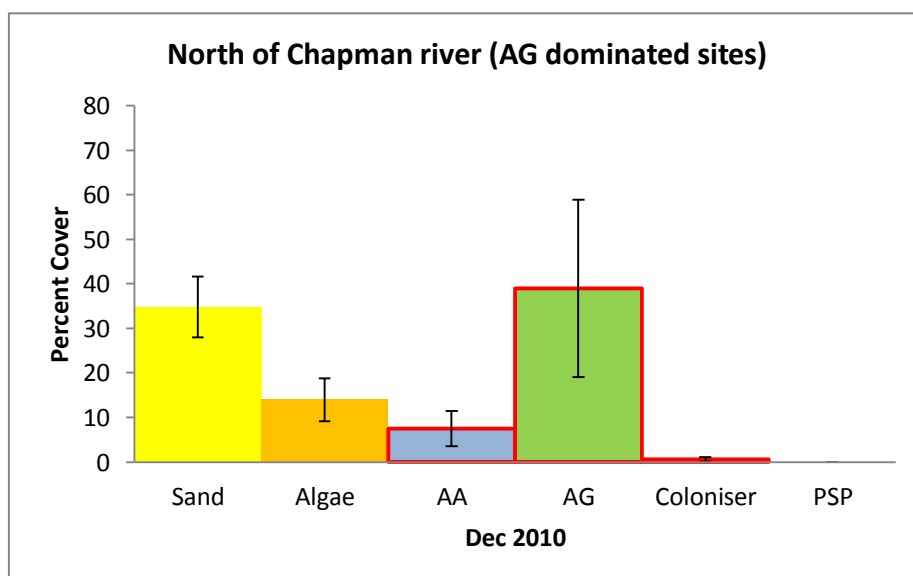


Figure 36: Mean percent cover of seagrass, algae and sand (\pm Standard Error) at *Amphibolis griffithii*-dominated sites in the area to the north of the Chapman River mouth. The red-bordered bars represent seagrasses: AG = *Amphibolis griffithii*; AA = *Amphibolis antarctica*; PSP = *Posidonia* sp.; and Coloniser = *Syringodium isoetifolium* + *Halophila decipiensis* + *Halophila* sp.

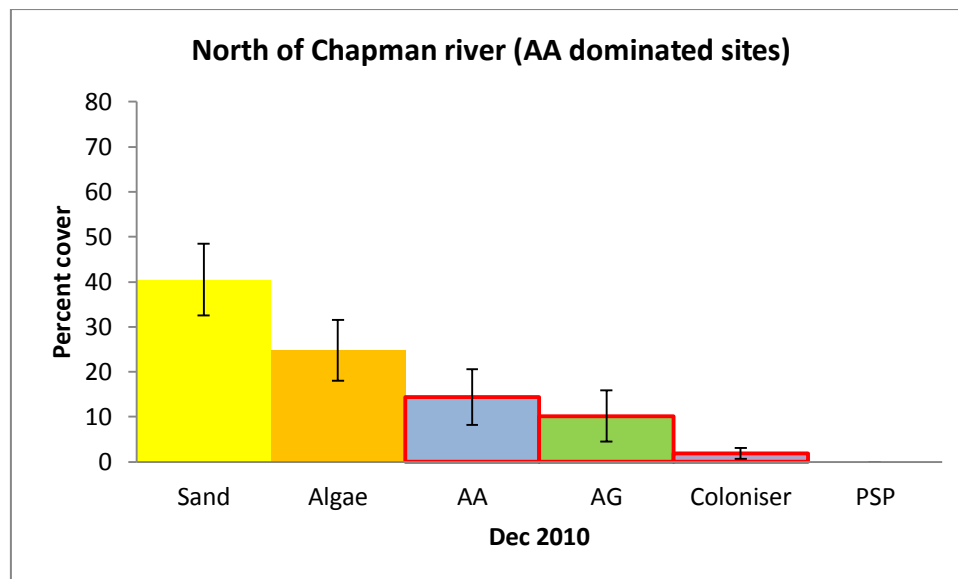


Figure 37: Mean percent cover of seagrass, algae and sand (\pm Standard Error) at *Amphibolis antarctica*-dominated sites in the area to the north of the Chapman River mouth. The red-bordered bars represent seagrasses: AG = *Amphibolis griffithii*; AA = *Amphibolis antarctica*; PSP = *Posidonia* sp.; and Coloniser = *Syringodium isoetifolium* + *Halophila decipiensis* + *Halophila* sp.

Other than supporting the acoustic habitat mapping procedures and providing an overview of the distribution of benthic biota at Geraldton, the underwater imagery has allowed the identification of variations in the benthic cover of seagrass, macroalgae and sand to be achieved. In particular, areas of increased sandy cover compared to literature data (CSIRO, 2007) were found off the Chapman River mouth which is an area identified as sediment sink for this coastal system. This finding indicates that the deposition of sand in the area is ongoing and sediment transport is likely to be oriented toward this location. Seagrass and macroalgal cover remain similar to the CSIRO (2007) literature data at other locations within the study area.

2.4.1 Geomorphological parameters and sediments as a surrogate for benthic habitat distribution

Geomorphological parameters, such as seabed topography and hardness, form useful surrogates where seabed structure and the distribution of benthic organisms are linked (McArthur et al., 2010). For example, it has been recently documented (James and Bone, 2011) that in South Australia macroalgae colonize lithified substrates, and seagrasses occupy adjacent sandy substrates. However, in the Mediterranean Sea seagrasses were found to be associated with sedimentary substrates and hardgrounds with the plant rooted in the troughs (De Falco et al., 2010). As the dominant biota in the study area is composed of seagrass meadows and macroalgal communities, data is provided below on the relationship

between substrate geomorphology and the distribution of these benthic communities. GIS techniques were used to count the number of occurrences of seagrass meadows and macroalgal communities, identified through underwater photography data, within polygons of the underwater geomorphic features mapped using high resolution multibeam bathymetry models, described in section 2.2.

Seagrass meadows (seagrass >69% from the photo analysis) were found to be mostly associated with low relief substrate (71%) and shallow limestone reef systems (24%, figure 38). Low-relief substrate is a flat or low sloping substrate with a rugose appearance on the bathymetry data, and consequently is not expected to be sand-dominated. The boundary between soft sediment and limestone pavement may be hard to define for the areas mapped as part of the low-relief substrate, as previously indicated for friable or semi-consolidated rocks partly covered by sediment, discussed in a review of abiotic surrogates for habitat mapping (McArthur et al., 2010). During the 2009 sediment sampling campaign, difficulties were reported in using the Van-veen sediment grab to collect sediment from the seabed, due to the consolidated nature of the substrate impeding sediment collection. Seagrass meadows were also found on the top of limestone reefs close to shore, possibly indicating that this biota can be associated with hardgrounds with the plant rooted in the troughs as indicated for some regions of the Mediterranean Sea. As suggested by Carruthers et al. (2007), the hydrodynamic energy plays an important role in the distribution of seagrass meadows, and seagrasses are mostly located in areas with lower wave heights compared to macroalgal communities.

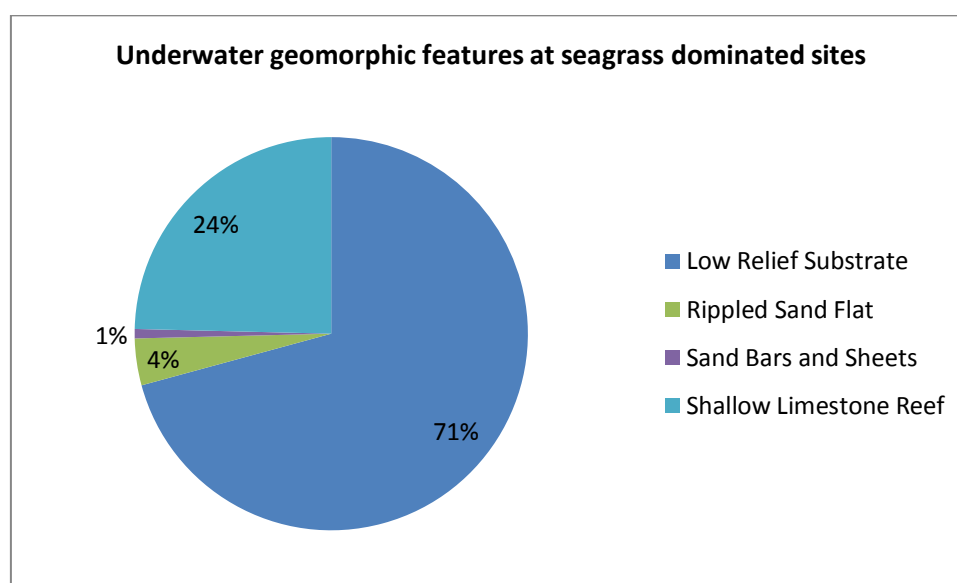


Figure 38: Count of broad scale geomorphic features associated with seagrass meadows (seagrass >69%), as resulting from a combination of GIS mapping of underwater geomorphology using multibeam bathymetry models and identification of benthic habitats through underwater photography data.

West Australian seagrass habitats occur over a range of sediment types (Carruthers et al., 2007), and at Geraldton, carbonate sediments are common with sediment structures linked to the distribution of limestone rock pavements (see Chapter 3 for more information). In particular, medium-coarse sands increase correspondingly to limestone reef systems and fine sands constitute a well-defined sediment belt close to shore, approximately 1 km wide and in water less than 10 m deep.

Figure 39 shows a significant correspondence between the distribution of seagrass meadows and highly-fine sandy substrates, with fine sand >70% of the bulk of the sample at 58% of the seagrass-dominated sites (seagrass >69% from the photo analysis). This result comes with the known capacity of trapping fine sediment by seagrass communities, and is considered particularly significant when studying seabed mobility. In particular, at Geraldton, fine sands dominate along the town beaches and the biogenic nature of this sediment is also linked to seagrass epiphytes deposited on the sea bottom (Chapter 3).

The results of this research, summarised in figures 38 and 39, show that seagrass communities colonize flat hardgrounds blanketed by consolidated fine sands and were also found on shallow limestone reefs close to shore. Fine sands derive from and are a proxy for seagrass communities, but the highly consolidated nature of these substrates places the transition from sediment cover to rock at shallow depths below the sea bottom (cm to dm scale).

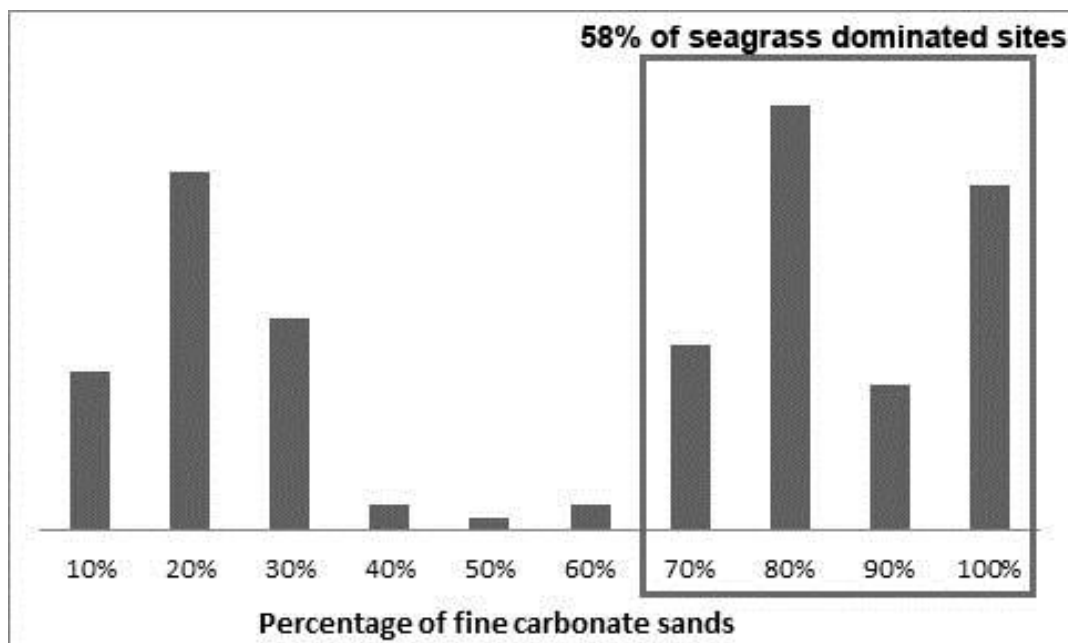


Figure 39: Percentage of fine carbonate sands at seagrass-dominated sites (seagrass >69%). Seagrasses were often found where fine sand >70% of the bulk of the sample (right-hand side of the plot). The minor mode of this bimodal plot (left-hand side) indicates that a minor percentage of seagrass meadows was found on coarser sediment substrates.

In terms of geomorphic features, macroalgal communities (macroalgae >69% from the photo analysis) were also found to be mostly associated with low-relief substrate (56%) and shallow limestone reef systems (30%, figure 40), which was also found in South Australia (James and Bone, 2011). However, a strong linkage between sediment grainsize and the distribution of this habitat was not found, but as suggested in previous studies sediment grainsize alone is often not a strong surrogate for species distribution (Post et al., 2006; Ryan et. al., 2007b). In general, medium-coarse carbonate sands were found at most of the macroalgal-dominated sites and fine sand constituted a minor part of the bulk of the samples, but the medium and coarse sand components varied significantly throughout macroalgae-dominated sites. As indicated above for seagrass meadows, this may be explained by the local hydrodynamic conditions as macroalgal reefs are located at the offshore extreme of the shallow coastal platform and are exposed to higher swell waves, mainly colonising mollusc-dominated limestone reef systems.

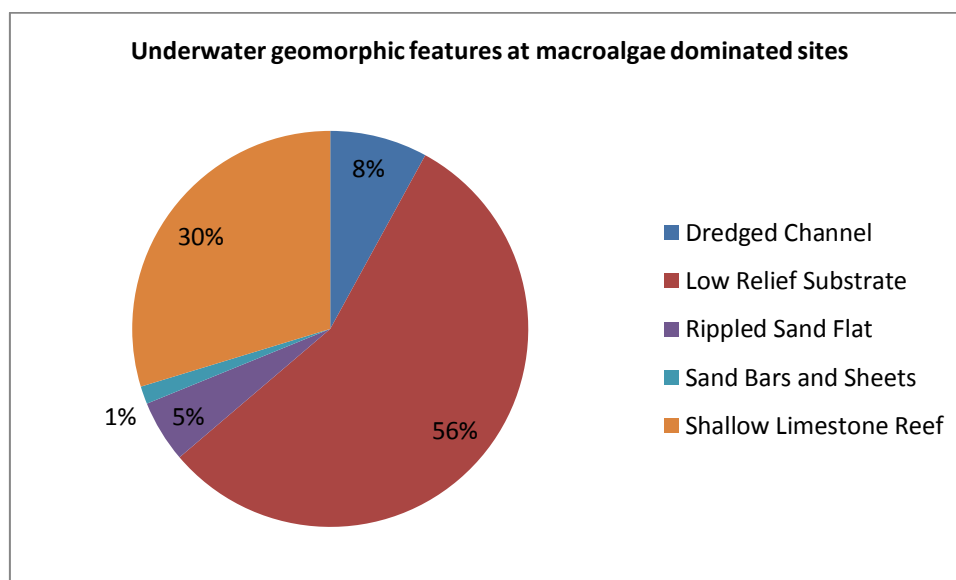


Figure 40: Count of broad scale geomorphic features associated with macroalgal communities (macroalgae >69%), as a result from a combination of GIS mapping of underwater geomorphology using multibeam bathymetry models and identification of benthic habitats through underwater photography data.

2.5 ACOUSTIC HABITAT MAPPING

A phenomenological approach for acoustic habitat mapping was adopted in this study, which consists of finding a correlation between geomorphic features, benthic cover, and acoustic data, with the aim of dividing data into acoustically different regions of the seabed. Underwater videography data was analysed and used to infer how the acoustic data relates to different seafloor types.

As a first step for acoustic habitat mapping, the main benthic habitats to be mapped were determined on the basis of ground truth and acoustic data and selected on the basis of the project needs. Due to the importance of seagrasses and macroalgal communities in the study area and also considering the sediment budget-oriented nature of this project, priority was given to the mapping of dense seagrass meadows, macroalgal colonized limestone reef systems and sandy substrates (figure 41). Consequently, the following habitat classes were selected for habitat mapping in this study: macroalgae >69%, seagrasses >69%, sand >69% (including fine sands and medium/coarse sands). However, due to the patchy distribution of the biota at Geraldton low density seagrass and macroalgal communities ($0 < \text{seagrass} < 70$, $0 < \text{macroalgae} < 70$, $0 < \text{sand} < 70$) are a common habitat which has also been mapped as part of this project. Previous habitat mapping studies (i.e. Phinn et al., 2008) have defined the map classes on the basis of project needs and considering the ability of raster and field data to consistently differentiate habitat classes, which support the methodology used in this project. The relationship between the selected habitats and the multibeam backscatter intensity is described in section 2.5.1. The backscatter intensity associated with the geomorphic features manually digitized on the multibeam bathymetry models in a GIS environment (section 2.2) was also analysed and is described in section 2.5.1.1.

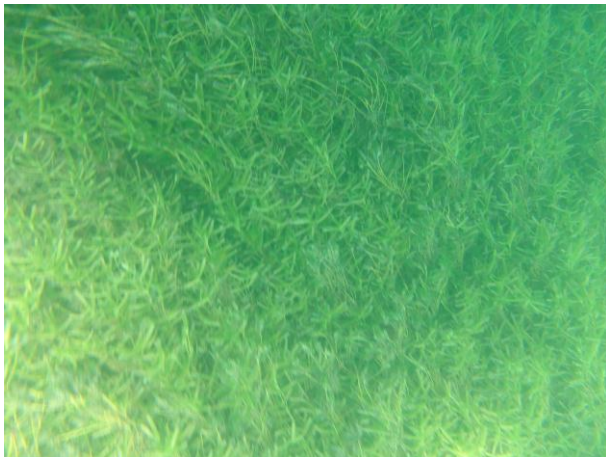
The phenomenological approach applied to habitat mapping practices includes the segmentation of selected benthic habitats and their acoustic attributes using either supervised or unsupervised classification algorithms. The application of both supervised and unsupervised classification algorithms has been assessed on the Geraldton data and is described in section 2.5.2. Due to the poor accuracy of the automatic classification techniques achieved in the Geraldton case study, data segmentation algorithms were applied to the datasets with the intent to group pixels with similar characteristics in the backscatter imagery. More specifically, a mean shift image segmentation technique based on the kernel density estimation was applied to the gridded raster of backscatter intensity through the Edge Detection and Image Segmentation System (EDISON) tool (<http://coewww.rutgers.edu/riul/research/code/EDISON/index.html>) which was described by Che Hasan et al. (2012) as an effective technique for benthic habitat mapping when combined with angular response data. A full explanation of the methodologies used to develop the acoustic habitat map of the study area is presented in section 2.5.2.1, and section 2.5.2.2 summarise the results of these methods when applied to mapping temperate water benthic habitats.



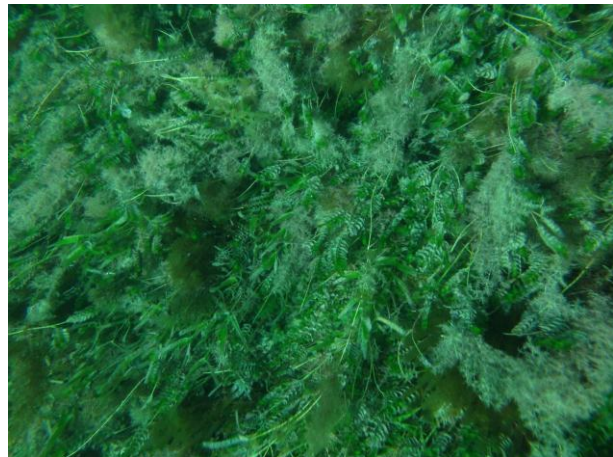
Sandy substrate (Sand >69%).



Dense vegetation: Case 1) Macroalgae >69%.



Dense vegetation: Case 2) Seagrass >69% (Dense *Amphibolis griffithii*).



Dense vegetation: Case 2) Seagrass >69% (Dense *Amphibolis antarctica*).



Dense vegetation: Case 2) Seagrass >69% (Dense *Posidonia sp.*).



Mixed communities: 0< Seagrass <70, 0< Macroalgae <70, 0< Sand <70.

Figure 41: Photos of representative habitat types used for the acoustic habitat mapping practices.

2.5.1 Relationship between benthic habitats and backscatter intensity

The habitat categories mapped in this study are summarised in table 8, and figure 42 shows the probability density distribution of the mean relative backscatter strength associated with these habitats. The backscatter strength as a function of incidence angle (known as angular response curve) was extracted at the ground truth locations for the seabed classes outlined in table 8 and is used below to relate benthic habitats and multibeam backscatter properties. At Geraldton, seagrass meadows (seagrass >69%) have the highest relative backscatter strength measured with approximately -8.5 dB at 35° incidence angle (figure 43). Macroalgal communities (macroalgae >69%) follow with approximately -9 dB at 35° incidence angle. The difference between seagrasses and macroalgae is only about 0.5 dB because these habitats occur over acoustically similar regions of the seabed, and as such were considered together and mapped as one category called “dense vegetation” on the habitat map produced in this study. Figure 42 also confirms the overlap between the relative backscatter strength of seagrass meadows and macroalgal communities, indicating that the identified biota is not individually driving the acoustic response of the seabed. Sandy substrates (sand >69%) record the lowest relative backscatter strength measured with values ranging between approximately -12 and -23 dB. The low density seagrass and macroalgal communities (0< seagrass <70, 0< macroalgae <70, 0< sand <70) have an intermediate relative backscatter strength between sandy substrates (lowest relative backscatter strength measured) and densely vegetated areas (highest relative backscatter strength measured). However, the probability density distribution of the mean relative backscatter strength measured for this habitat shows a significant overlap with the seagrass and macroalgal communities (figure 44), indicating that the density of the mapped biota is not the only factor influencing the acoustic response of these communities.

Table 8: Habitat classes used to classify the multibeam backscatter data. Refer to figure 41 for the habitat photos.

Habitat	Benthic cover	Relative backscatter intensity
Sandy substrate	Sand >69%	Lowest backscatter measured
Dense vegetation	Case 1) Macroalgae >69% Case 2) Seagrass >69%	Highest backscatter measured
Sparse vegetation	0< Seagrass< 70, 0< Macroalgae <70, 0< Sand <70	Intermediate backscatter values

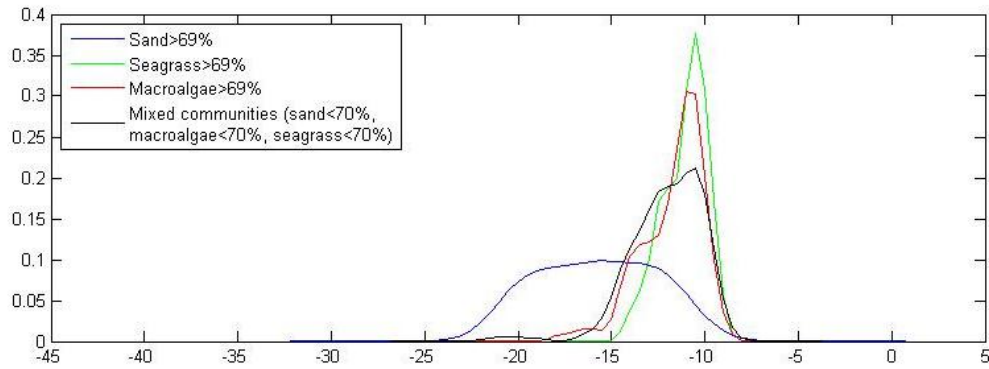


Figure 42: Probability density distribution of the mean relative backscatter strength values associated with the main habitat categories investigated in this study. This figure outlines the similarity of the acoustic response of seagrass meadows, macroalgal communities and mixed low density macroalgal and seagrass communities.

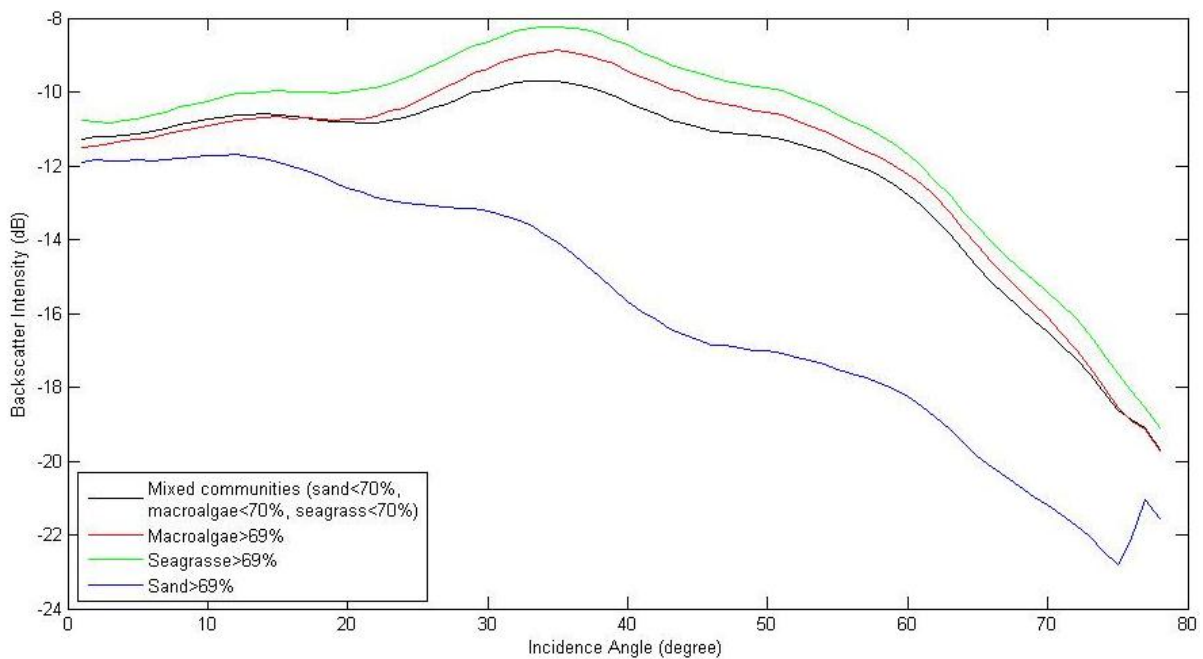


Figure 43: Angular response curves of the main seabed types found in the study area.

It is well known that the mean backscatter strength at the oblique angles is a key property in discriminating benthic habitats (Hughes Clarke et al., 1997; Parnum, 2007). It has also been widely demonstrated that, although the mean level of backscatter strength appears to best summarise the backscatter angular dependence, the slope of the angular response curves can provide additional information (Parnum, 2007). Consequently, the relationship between mean backscatter strength and slope of the oblique incidence angles of the angular response curves is shown in figure 44 for the seabed classes indicated in table 8. These properties were moderately correlated ($R = \sim 55\%$), which was also found in other studies (Parnum, 2007; De Falco et al, 2010). In particular, figure 44 supports the comparison of the acoustic properties of the four seabed classes mapped in this study (table 8). It further

demonstrates the distribution of relative backscatter strength values for the different classes, as indicated previously. Seagrass meadows and macroalgal communities have the highest values of relative backscatter strength measured, but the seagrass measurements are confined within a smaller range of backscatter strength and angular response data, which was not visible by looking at the angular response curves only.

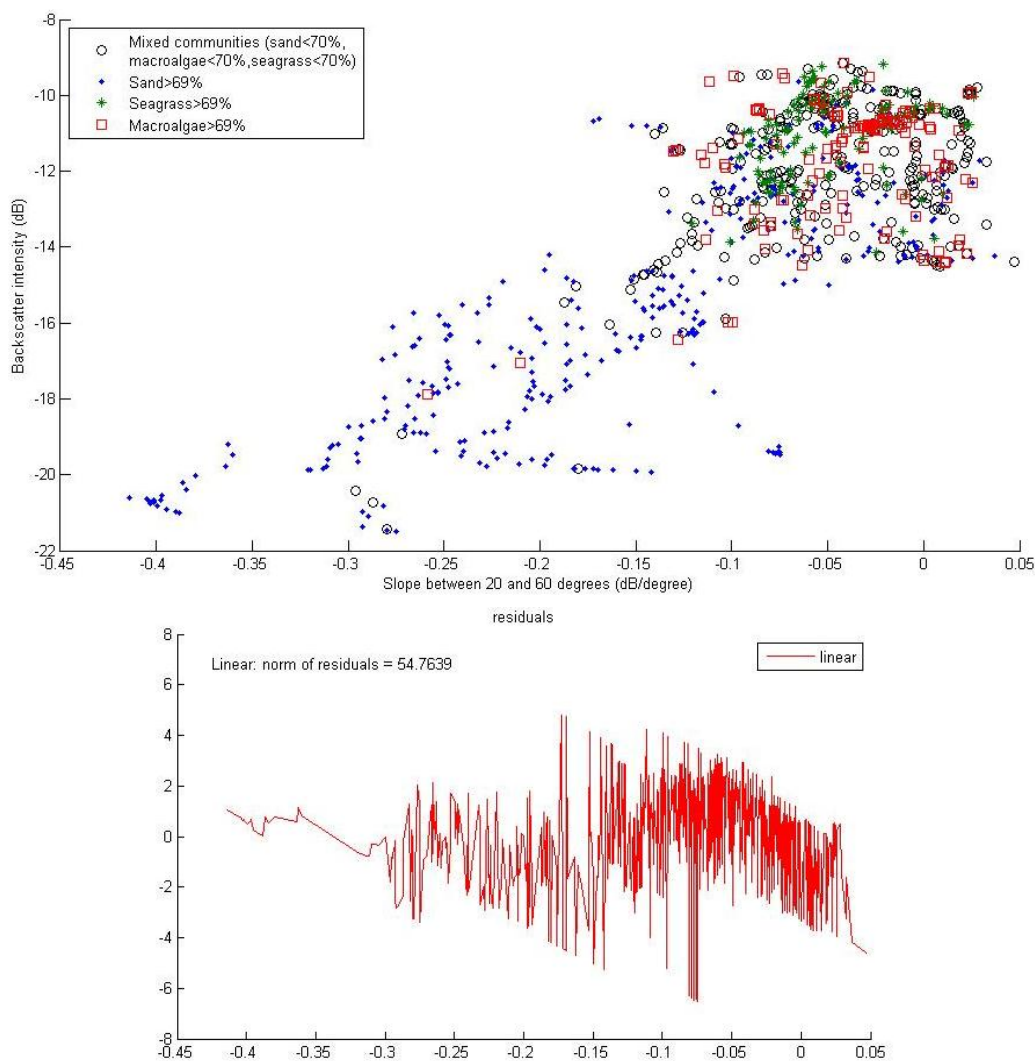


Figure 44: Mean backscatter intensity versus slope of the oblique incidence angles of the angular response curves for the seabed classes indicated in table 8 (top figure). The bottom figure shows a plot of the residuals.

Sandy substrates (sand >69%) record the lowest relative backscatter strength measured with mean values ranging between approximately -10 and -23 dB, within a range of -0.42 and 0.03 dB/deg for the slope of angular response curves at oblique incidence angles. This category includes fine, medium and coarse sized sands.

The heterogeneous habitats resulting from a combination of low seagrass and macroalgae cover ($0 < \text{seagrass} < 70$, $0 < \text{macroalgae} < 70$, $0 < \text{sand} < 70$) show a good correlation, with relative backscatter strength values between approximately -10 and -16 dB, and a range of

approximately -0.19 and 0.05 dB/deg for the slope of angular response curves at oblique incidence angles.

The mean relative backscatter strength values and slope of oblique incidence angles of macroalgal communities (macroalgae >69%) were mostly between -9 and -16 dB, and -0.13 and 0.04 dB/deg. Of note is that in the literature these communities are commonly associated with lithified substrates, and also at Geraldton their main occurrences were found on shallow limestone reef and low sloping hardgrounds (section 2.4.1). The nature of the substrates may play an important role in the high backscatter intensity described herein for this habitat.

The acoustic parameters described above for seagrass meadows (seagrass >69%) were slightly less dispersed than within macroalgal communities. Values recorded for macroalgal communities range between -9 and -14 dB for the relative backscatter strength and between -0.10 and 0.03 dB/deg for the slope of angular response curves at oblique incidence angles. At Geraldton, seagrasses were found to colonize flat hardgrounds blanketed by highly consolidated fine sands and were also established on shallow limestone reefs close to shore (section 2.4.1), and consequently the acoustic properties described here may be influenced by the characteristics of the substrate underneath the plants as well.

Finally, table 9 summarises and clarifies the relationships between benthic habitats and acoustic properties discussed above. Multivariate statistical analyses were carried out for these data (backscatter strength, angular response and benthic cover) and did not allow the recognition of the main parameters driving the seabed acoustic response. This result indicates that the biota type (i.e. seagrass or macroalgae) or the biota densities are not the dominant factors characterising the relative backscatter strength and angular response of the seabed. The characteristics of the identified biota form an integral part of the overall investigated benthic habitat, together with substrate type, sediment grainsize and thickness. As discussed in section 2.4.1, at Geraldton, macroalgal communities are mainly associated with limestone reef rocky substrates; seagrass meadows were also found to be common on hard grounds with a thin consolidated fine sandy cover, and low-density mixed seagrass and macroalgae communities are also common on hardgrounds. Sandy substrates range from fine to coarse sands in size, which is also reflected in varying seabed roughness, and subsequently in a high standard deviation of the probability density distribution of the mean relative backscatter strength measured for this habitat (figure 42). These considerations apply to the habitat categories mapped in this study and need to be taken into account for understanding the relationships between relative backscatter strength and benthic habitats discussed in this dissertation, which refer to the overall benthic habitat and not simply to the

biota. The following section discusses the relationship between relative backscatter strength and seabed substrates identified on the multibeam bathymetry data, adding further details to the characterization of the acoustic response of the Geraldton benthic habitats.

Table 9: Summary of the acoustic properties for the seabed classes analysed in this study.

Habitat/acoustic properties	Sand >69%	Sparse vegetation (sand <70%, macroalgae <70%, seagrass <70%)	Macroalgae >69%	Seagrass >69%
Min mean backscatter	-23 dB	-16 dB	-16 dB	-14 dB
Max mean backscatter	-10 dB	-10 dB	-9 dB	-9 dB
Angular response slope range of the oblique incidence angles	-0.42 – +0.03 dB/deg	-0.19 – +0.05 dB/deg	-0.13 – +0.04 dB/deg	-0.10 – +0.03 dB/deg

2.5.1.1 Relationship between geomorphic features and backscatter intensity

The relative backscatter strength of the geomorphic features described in section 2.2 was investigated in this study and is qualitatively compared in this section. The GIS polygons manually digitised on the multibeam bathymetry models were used to extract relative backscatter strength values for the seabed features described in section 2.2.

The overall results are consistent with what was previously described for the main benthic habitats occurring at Geraldton, with rocky substrates hosting dense vegetation showing high relative backscatter strength and uncolonised substrates showing low relative backscatter strength. This is also consistent with previously published data (Parnum, 2007; De Falco et al., 2010).

Areas mapped as shallow limestone reef and low relief substrate show the highest range of mean relative backscatter strength (between -5 and -10 dB; figure 45) and these rocky areas often host macroalgal and seagrass communities (section 2.4.1). As summarised in table 9, seagrass meadows and macroalgal communities recorded the highest relative backscatter strength measurements. However, from the data collected in this study, it is not evident whether the nature of the substrate or the actual benthic cover is most influential on the acoustic properties, but they seem to determine together the seabed acoustic response.

The remaining geomorphic features mapped at Geraldton (sand bars and sheets, nearshore zone, rippled sand flats, and sand dunes) are indicative of sandy substrates, and record a much lower relative backscatter strength over a wider range of values with average between -15 and -20 dB (figure 45). The sand bars and sheet polygon has shown the lowest standard deviation of the range of backscatter intensity measured compared to the remaining sandy features with an average value of approximately -16 dB. This might be due to the lower sediment thickness of the areas mapped as nearshore zone, rippled sand flats and sand dunes, which can be ascertained from the observation of bathymetry data. Of note is the bimodal distribution of the relative backscatter strength extracted from the areas mapped as rippled sand flats. There are two possible causes for this result, as these areas could be characterised by two different roughness or grainsize classes which would result in two modes in the relative backscatter strength measurements.

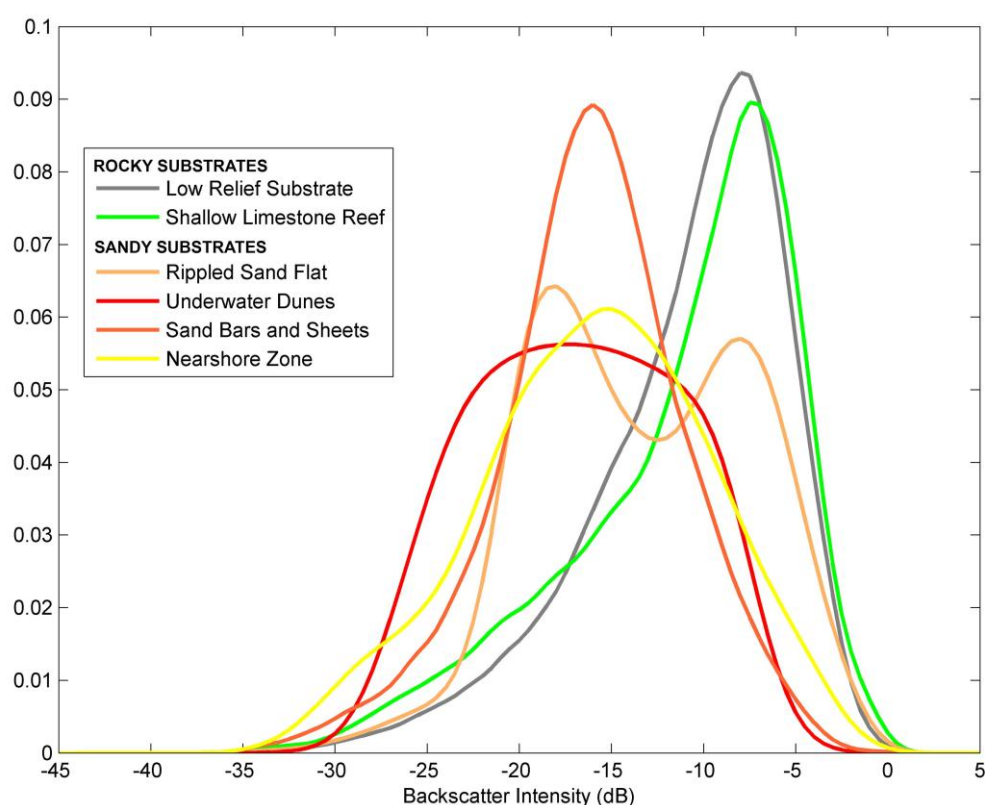


Figure 45: Probability density distribution of the mean backscatter intensity values associated with the underwater geomorphic features mapped on the multibeam bathymetry models. Refer to the main body of the text for an explanation of this figure.

2.5.2 Habitat map production

As seagrass meadows and macroalgal communities colonising shallow coastal embayments are common in South and Western Australia (Carruthers et al., 2007; Ryan et al., 2007b; James and Bone, 2011), it is considered useful for future studies of similar environments to

present data on habitat mapping of these communities based on acoustic data. Moreover, the application of supervised and unsupervised classification algorithms is widely accepted for classifying different kinds of datasets (i.e. aerial photography, landsat images, hyper-spectral data as well as marine acoustic data, etc.) stored as raster images (Thomson, 1998; Parnum, 2007; Phinn et al., 2008; Xie et al., 2008). Considering the significance of the temperate water habitats found at Geraldton and the routine application of the automatic classification procedures, habitat maps were developed for the studied area using ArcGIS techniques. The newer image segmentation techniques described by Che Hasan et al. (2012) were also used to classify the backscatter-derived raster image and the classification accuracies of the different methods are compared and discussed below.

Attempts were made to incorporate bathymetry and slope information to the raster classification analysis, on the basis of the habitat segregation principle described by James and Bone (2011), where macroalgae colonize lithified substrates (i.e. limestone reef systems) and seagrasses occupy adjacent sandy substrates. However, these operations were not successful as, at Geraldton, seagrasses were found on limestone reefs close to shore, similarly to the Mediterranean seagrass communities, previously described by De Falco et al. (2010), associated with sedimentary substrates and hardgrounds with the plant rooted in the troughs. At Geraldton, fine sandy substrates are highly consolidated and often the boundary between soft sediment and limestone pavement may be hard to define. Consequently the acoustic response of these substrates could be similar to that of friable rocks.

2.5.2.1 Methods

2.5.2.1.1 Supervised and unsupervised classification algorithms

The acoustic classification procedure was based on a 5 m spaced raster grid of angle-independent backscatter levels (figure 46) obtained following the procedures described in Chapter 1. This was imported into ArcMap 10™ and the unsupervised and supervised classification algorithms were applied on the basis of the habitat classes specified in table 8. Due to the similarity of the average relative backscatter strengths of seagrass meadows and macroalgae colonizing limestone reefs, the mapping of these habitats could not be performed separately by applying classification algorithms to a raster grid derived from angle-independent backscatter levels only, but these communities were mapped together as “dense vegetation”. As explained in section 2.5.1, seagrass meadows and macroalgal communities are only differentiated when considering the variability of relative backscatter

strength across track; however, the mean relative backscatter strength recorded at one specific point of the seabed is used for generating maps of angle-independent backscatter levels like the one produced for the study area and shown in figure 46, which does not include angular response data. However, seagrass and macroalgae percentage of cover resulting from the analysis of quantitative video transects were also overlain on the classified acoustic map, allowing the distinction of dense seagrass or macroalgal communities to be visualised (figure 47).

Unsupervised classification consists of data clustering in the form of raster cells into statistically-similar groups and is based on the premise that the input raster dataset includes natural statistical groups of backscatter patterns that represent particular habitat types. Supervised classification is based on user-defined classes (specified in table 8 for this study), and corresponding representative sample sets. The sample sets are specified by training raster data sets, which must be created, prior to entering the automatic acoustic data classification process. The training areas were selected in ArcMap 10™ by correlating ground truth information and backscatter properties, and are first processed by the software to define the statistical properties of each class. In the final classification stage, each cell in the input raster set is assigned to one of the training classes. Figure 47 shows the result of this procedure. Whilst section 2.6 describes the habitat distribution at Geraldton, section 2.5.2.2 focuses on the outcome of the acoustic habitat mapping.

2.5.2.1.2 Image segmentation

The Edge Detection and Image Segmentation System (EDISON) tool (<http://coewww.rutgers.edu/riul/research/code/EDISON/index.html>) was used to group pixels with similar characteristics in a 5 m spaced raster grid of angle-independent backscatter levels (figure 46). This tool uses a spatial parameter to define the search radius of processes described by kernel density estimation in the feature space, and then the mean shift vectors converge (Che Hasan et al., 2012). The main parameters were set as follows: spatial resolution = 9, colour resolution = 7.5, and minimum region = 250 pixels to obtain the segmented backscatter image shown in figure 48. The segmented raster was imported into ArcMap 10™ and converted to a polygon shapefile to allow data integration with ground truth information and polygon simplification. The ArcMap 10™ Geographically Weighted Regression (http://help.arcgis.com/en/arcgisdesktop/10.0/help/index.html#/Geographically_Weighted_Regression_GWR/005p00000021000000/) tool was applied to integrate acoustic data with the benthic cover information obtained from the underwater imagery (figure 48).

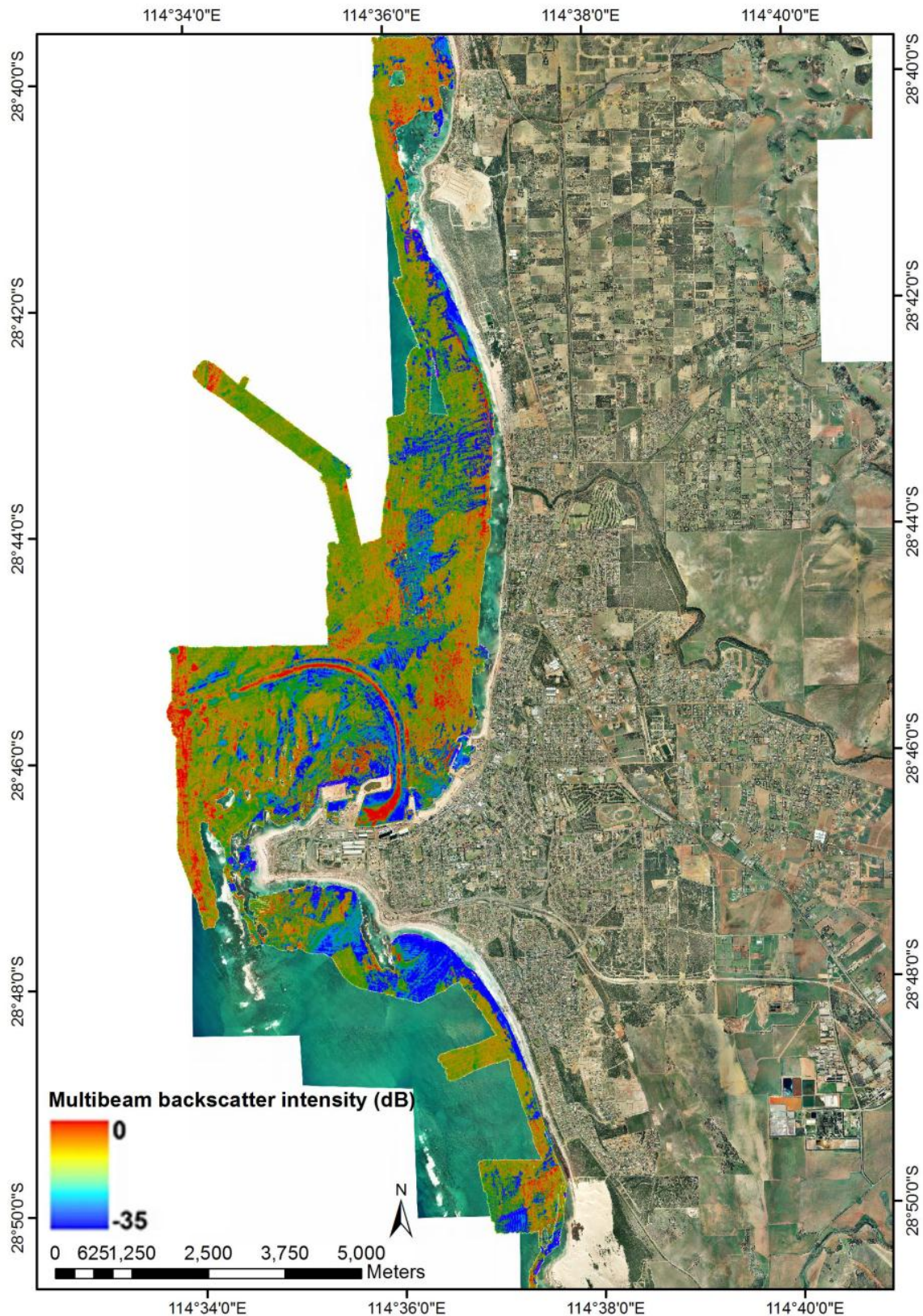


Figure 46: 5 m spaced raster grid of angle-independent backscatter levels resulting from the 2010 multibeam survey at Geraldton (data extent = $\sim 35 \text{ km}^2$ to $\sim 10 \text{ m}$ depth, reaching $\sim 25 \text{ m}$ depth in some locations) overlain on the aerial photography. Backscatter intensity values are relative only. Higher values are associated to dense vegetation, lower values to sandy substrates, and intermediate values to sparse vegetation.

2.5.2.1.3 Accuracy assessment

The accuracy of the automated classification techniques of raster images is commonly assessed through an error matrix which compares the acoustically classified regions of the seabed with benthic habitat classes obtained by classifying the underwater imagery, following the methodology described by Congalton (1991). Basically, ground truth data are compared to automatically-classified acoustic data and the percentage of data recording the same seabed class represents the classification accuracy. This approach was adopted in this study to evaluate the accuracy of acoustic habitat mapping resulting from the application of supervised classification algorithms and image segmentation techniques.

2.5.2.2 Results

2.5.2.2.1 Results of the application of supervised and unsupervised classification algorithms

The benthic habitat map resulting from the supervised classification of a raster of angle-independent backscatter levels (figure 47) only achieved an overall accuracy of ~54% (table 10), with the highest classification accuracy recorded for sand-dominated habitats (sand >69%; classification accuracy = ~79%), followed by sparse vegetation (0 < seagrass < 70, 0 < macroalgae < 70, 0 < sand < 70; classification accuracy = ~52%) and dense vegetation (seagrass >69% or macroalgae >69%; classification accuracy = ~25%). As shown in table 11, a higher mapping accuracy of 78% could be achieved by limiting the habitat categories to sand and vegetation only. However, the overall sediment budget study benefits from having information on the density of the main biota on the benthic habitat map, especially seagrass density which influences the seabed mobility, and this data was used for estimating the seabed roughness to be entered in the longshore sediment transport modelling. The increased mapping accuracy attainable by mapping sand and vegetation only indicates that a raster of angle-independent backscatter levels does not contain sufficient information to discriminate between different densities of seagrass or macroalgal communities.

The unsupervised classification algorithms applied to the Geraldton data were unable to identify the seabed classes which would have acoustically matched the ones specified in table 8, but could only separate between areas of data availability or unavailability.

Table 10: Error matrix for the benthic habitat map resulting from the supervised classification of angle-independent backscatter levels shown in figure 47. The bottom line summarises the classification accuracy for each habitat.

SAND	DENSE VEGETATION	SPARSE VEGETATION	
201	30	60	
11	51	35	
44	125	102	
78.52%	24.76%	51.78%	TOT. = 53.72%

Table 11: Error matrix derived from a reinterpretation of Table 10, showing the mapping accuracy increase which could be achieved by restricting the habitat categories to sand and vegetation only.

SAND	VEGETATION	
201	90	
55	313	
78.52%	77.67%	TOT. = 78.00%

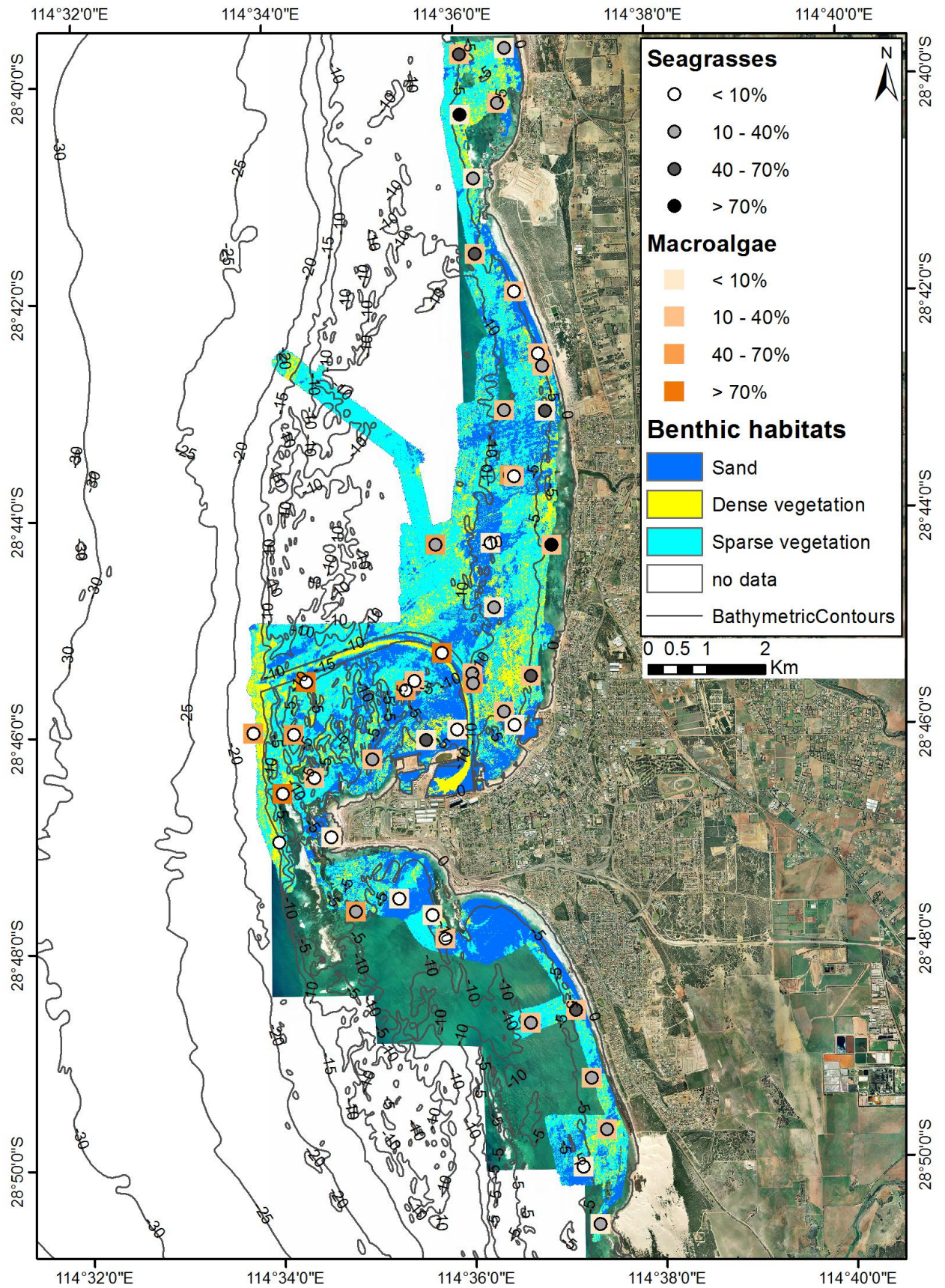


Figure 47: Benthic habitat map resulting from the supervised classification of a 5 m spaced raster of angle-independent backscatter levels. Seagrass percentage of cover and mean benthic cover resulting from the analysis of the quantitative video transects are overlain on the classified acoustic map.

2.5.2.2.2 Results of the application of image segmentation techniques

The segmented backscatter image shown in figure 48 (left-hand side) derives from the application of image segmentation techniques, with the polygons showing areas of similar angle-independent backscatter levels. The right-hand side of figure 48 shows the result of the combination of ground data with the polygons deriving from image segmentation. The spatial extent of the mapped habitats is based on acoustic data (i.e. grid of angle-independent backscatter levels segmented using the EDISON tool) and is limited to the polygons containing ground truth data. By observing figure 48, it is evident that not all of the polygons obtained through image segmentation contain ground truth data, as underwater video transects were only collected within some of the polygons deriving from image segmentation. The GIS tool used in this study to link polygons with similar angle-independent backscatter levels and underwater imagery information, limits the extent of the habitat map to the polygons containing ground data and consequently part of the acoustic data is lost as a result of this process and the habitat map does not represent the entire extent of the surveyed area. This map (figure 8, right-hand side) achieved an overall accuracy of ~54% (table 12), with the highest classification accuracy recorded for sand-dominated habitats (sand >69%; classification accuracy = ~67%), followed by dense vegetation (seagrass >69% or macroalgae >69%; classification accuracy = ~61%) and sparse vegetation (0 < seagrass < 70, 0 < macroalgae < 70, 0 < sand < 70; classification accuracy = ~28%). The similarity of the acoustic response from densely and sparsely vegetated substrates yields difficulties in distinguishing these habitats by using rasters of angle independent backscatter levels, as shown in figure 49 for data extracted within the habitat polygons obtained through image segmentation techniques and containing ground truth information.

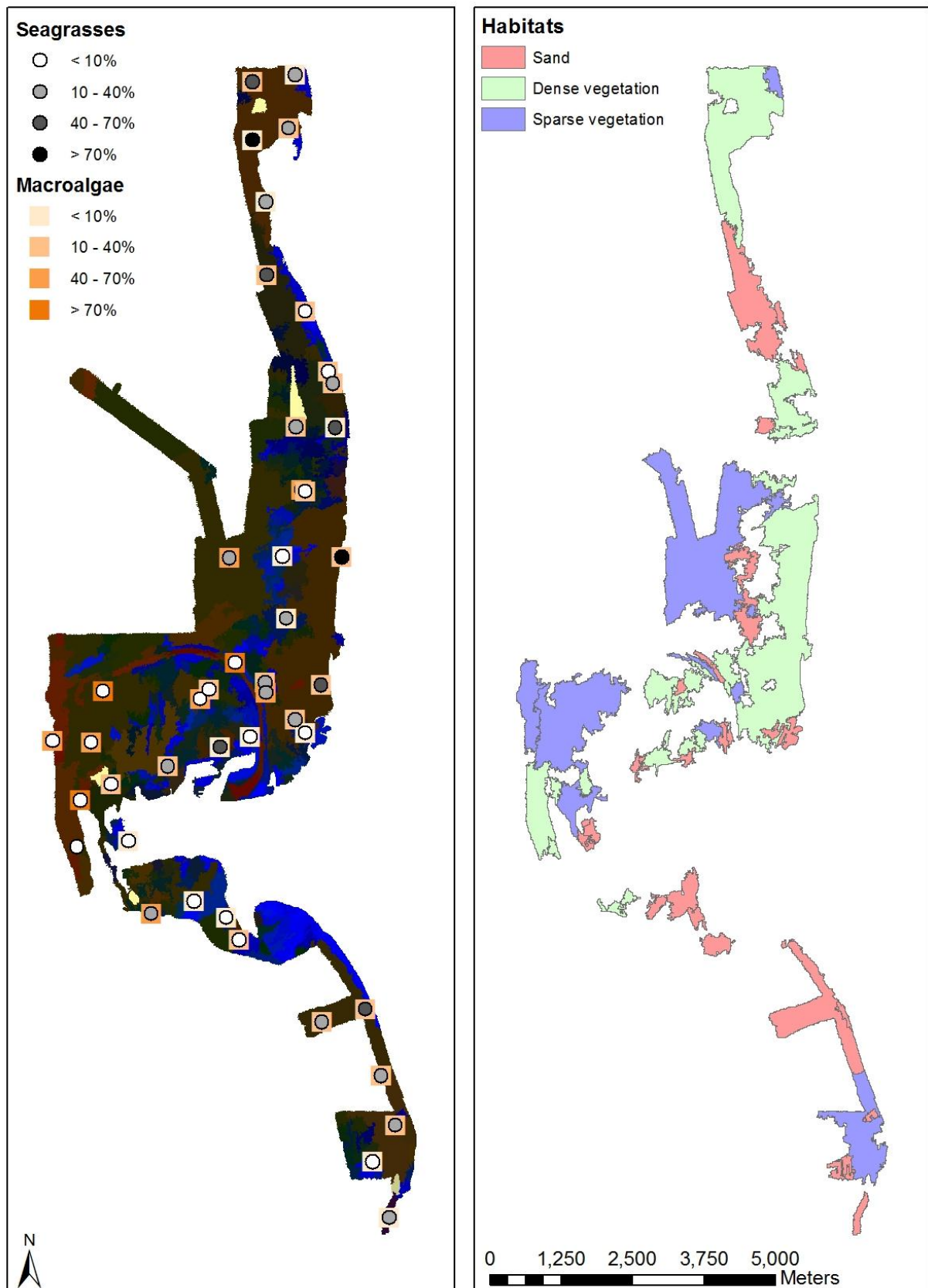


Figure 48: Polygons of acoustically similar regions of the seabed obtained from image segmentation with ground truth data overlain on it (left) and habitat map resulting from the association of ground data to the polygons using GIS techniques (right). Note the reduced data extent of the habitat map (right) due to limited availability of ground truth data.

Table 12: Error matrix for the benthic habitat map shown on the right hand side of figure 48. The bottom line summarises the classification accuracy for each habitat.

SAND	DENSE VEGETATION	SPARSE VEGETATION	
97	27	26	
32	74	52	
15	20	31	
67.36%	61.16%	28.44%	TOT. = 54.01%

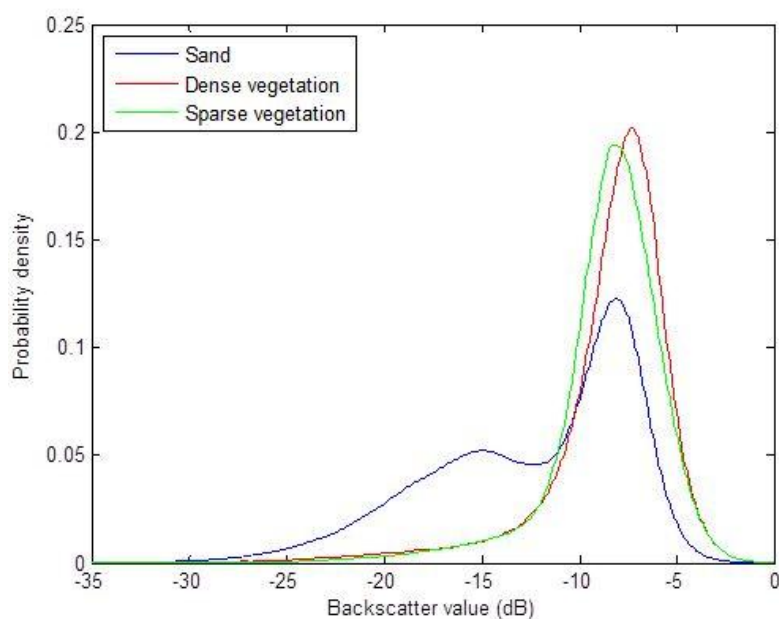


Figure 49: Probability density distribution of the angle-independent backscatter levels extracted within the polygons deriving from image segmentation (left-hand side of figure 48) for the main habitat categories investigated in this study. This figure outlines the similarity of the acoustic response of densely and sparsely vegetated substrates.

2.6 BENTHIC HABITAT DISTRIBUTION AND SIGNIFICANCE FOR SEDIMENT DYNAMICS

Due to the sediment budget-oriented nature of this project, the habitat classes used for the development of the habitat map (table 8) were chosen to facilitate the comparison of benthic habitats with the distribution of sediment facies and seabed mobility, and initial considerations of this kind are provided below. Given this premise and due to the patchy nature of the benthic community distributions at Geraldton, the following habitats were mapped using acoustic data and underwater imagery: sand (sand >69%), dense vegetation (seagrass >69% or macroalgae >69%) and mixed sandy, seagrass and macroalgae substrates (0 < seagrass < 70, 0 < macroalgae < 70, 0 < sand < 70). The habitat map resulting

from the application of supervised classification algorithms and shown in figure 47 is considered the best mapping output and will be referred to as the benthic habitat map for the study area throughout this dissertation. Moreover, since the availability of multibeam data has allowed the characterization of underwater geomorphology and benthic habitats, data on the seafloor geomorphology is also summarised below when describing the distribution of benthic communities.

Sandy substrates are widespread throughout the study area, and of significant extent are the sand bars and sheets found off Southgate dune, the nearshore zone developed to the west and east of the Separation Point ridge, the sand bar and sheet system found off the Chapman River mouth, and the nearshore zone developed at Glenfield Beach (see figures 19 to 21). It is important to note that sandy cover does not enhance vegetation development as it blankets the hard substrate where macroalgae are likely to attach, and indicates areas of greater sediment thickness than the surrounding vegetated areas. Unvegetated sediment bodies (nearshore zone, sand bars and sand sheets) are proxies for sediment accumulation and consequently indicate mobile areas of the seabed, which provide important clues in terms of sediment dynamics.

At Geraldton, densely vegetated (seagrass or macroalgae) substrates are often surrounded by areas with sparse vegetation (seagrass and/or macroalgae), showing a gradual transition from vegetated to sandy substrates. Dense seagrass meadows were found off Tarcoola Beach, off Pages Beach moving east towards the dredged channel, off the Northern Beaches, and at Drummond Cove (figure 47). *Posidonia sp.* dominates the seagrass meadows between Pages Beach and the dredged channel, whilst *Amphibolis griffithii* and *antarctica* are the dominant species of the remaining locations indicated above. As confirmed by sediment data analysed in this study (Chapter 3), seagrass-derived sediment input occurs at Geraldton, similarly to the South and Western Australia coasts where seagrass meadows are important sediment producers and warm-temperate carbonate sedimentation dominates the shallow littoral areas (Short, 2010; James and Bone, 2011). Consequently, the locations indicated above summarise some of the areas where fine modern skeletal carbonate sediment is currently being naturally supplied to the coastal system by seagrass-related organisms. Moreover, as noted in section 2.4.1, seagrass meadows mainly colonise low-relief substrate and shallow limestone reefs identified as part of the underwater morphology mapping which are considered stable areas in terms of seabed mobility due to the low sediment cover, together with the sediment trapping capacity provided by the seagrasses.

Macroalgal communities with dense vegetation colonise the Point Moore reef system, including the limestone ridge off Greys Beach. Also, these communities were found to contribute to sediment production at Geraldton (Chapter 3), similarly to the South and Western Australia coasts (Short, 2010; James and Bone, 2011), and consequently the locations indicated above are considered areas of sediment supply to the coastal system through organisms associated with macroalgal communities such as molluscs, foraminifera, encrusting coralline algae, etc. As noted in section 2.4.1, macroalgal communities mainly colonise shallow limestone reefs located ~4 km west of the shoreline, which are considered stable areas in terms of seabed mobility due to the low sediment cover and the lack of evidence of sediment erosion/deposition indicating a limited circulation of the sediment produced at these locations.

The mixed sandy, seagrass, and macroalgae substrates are common throughout the study area (figure 47), composed of smaller and less dense biota than habitats with dense marine vegetation and mainly associated with low-relief substrates. The sediment cover is not as thick as for sandy substrates, which assists certain biota, mainly low-density macroalgae and coloniser seagrasses, in colonising the seabed. This habitat is indicative of areas where sediment is more mobile than for densely-vegetated areas, due to the lack of trapping and stabilization provided by dense marine vegetation. Consequently, seabed mobility for this habitat is intermediate between sandy and densely-vegetated areas, and sediment production is also lower than for dense macroalgal and seagrass communities.

Whilst potentially mobile sandy substrates are widespread throughout the study area, areas of sediment deposition are limited to sand bars and sheet systems which are mostly located on the leeward side of shallow limestone reefs and in the middle of the coastal platform at Champion Bay. The nearshore zone is a dynamic environment of sediment exchange between the beach system and the offshore and is sand-dominated. However, the nearshore zone does not strictly indicate sediment accumulation, but it is a very mobile area of the seabed. Vegetated rocky substrates and sparsely-vegetated flat hardgrounds are abundant, indicating overall low seabed mobility and a relatively limited extent of the areas hosting dense vegetation and able to supply modern carbonate sediment to the coastal system. Bedforms were also found at Geraldton indicating bedload sediment transport; however, suspended sediment transport is likely to be more significant to account for the coastal evolution patterns recorded for the study area and described in Chapter 1.

Chapter 3

SEDIMENT CHARACTERISTICS AND GEOMETRY: the seagrass and macroalgal carbonate factories

3.1 REGIONAL CONTEXT

The western continental margin of Australia shows a significant sediment facies transition from cool to warm-water (James et al., 1994; Collins et al., 1997), and this gradational setting spans from the cool-water setting in the south (Collins, 1988) to the Ningaloo fringing reef in the north. The Abrolhos Shelf, comprising the Houtman Abrolhos coral reefs, lies in the biotic transition zone between the northern tropical and southern temperate environments and this is reflected in the carbonate facies, with cool-water carbonate shelf to the south and increasing coral development in the north (Collins et al., 1997). Geraldton is the closest coastal area to the Houtman Abrolhos and sedimentation is typically warm-temperate water dominated (figure 50).

The macroalgal and seagrass carbonate factories are recognized sediment producers of the south and western coasts of Australia (Carruthers et al., 2007; Short, 2010; James and Bone, 2011) and were also found in the study area. In the Esperance Bay, modern skeletal grains derived from seagrass beds were found mixed with quartz-dominated fine sands derived by the erosion of coastal cliffs at depths between 0 and 30 m (Ryan, 2007b) with increasing relict carbonate grains moving offshore, similarly to the Geraldton embayment. Over 100 sediment samples were collected between the onshore and the offshore, with the majority being shallow (5 to 20 m deep) offshore samples. Sediment grain size was carried out to look into the spatial relationship between different sediment facies and is reported here in section 3.2. Measurements of carbonate content were also undertaken for the entire dataset, and, as reported in section 3.3, the dominant carbonate composition of the analysed sediments has revealed the mostly biogenic nature of the shallow water sediments in the study area, providing important clues on sediment sources. X-ray diffraction analyses and microscopic characterisations of sediment petrology (section 3.4) were carried out for selected sediment samples to gain further insights on sediment composition and provenance (section 3.5). To distinguish between modern and relict sediment fractions was a primary objective of the analysis, so that the in-situ sediment input from living seagrass and macroalgal communities could be assessed.

Sediment thickness analyses were also undertaken at Geraldton (section 3.6), so that the volume of sediments lying on a consolidated bedrock interface could be evaluated and this helped in understanding the overall sediment accumulation rates. In fact, data of this kind were not available for the study area as most of the regional studies of this nature were previously carried out in the northern Western Australian regions within the Carnarvon Ramp, which is considered a “starved” tropical ramp (James et al., 1999) stretching from Shark Bay to Ningaloo Reef where, although bottom temperatures are tropical, the biota is largely subtropical with an absence of modern carbonate production on the mid-outer ramp. Biodegraded sediments are the main sediment components throughout the Carnarvon Ramp and represent carbonate production of the late Pleistocene. The sediment facies of the south-western Australian inner shelf in depths of 20-90 m were described by Collins (1988, p.25) as a “thin sediment blanket composed of quartz grainstone, lithoskel grainstone and skeletal grainstone”. At Geraldton, sediment facies were found to have a varying amount of modern and relict sediment components, with a remarkable trend of an increase in relict grains moving offshore and modern fraction dominance in the nearshore (section 3.7).

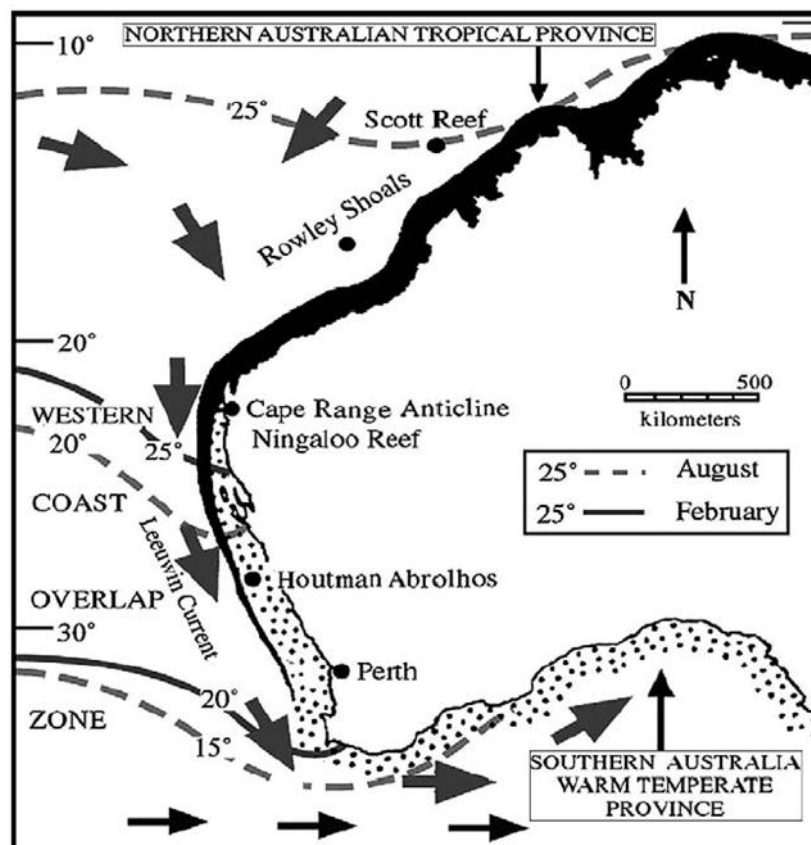


Figure 50: The western continental margin of Australia, showing regional oceanography and biotic zones (southern Australia warm temperate and northern Australia tropical provinces; from Collins, 2010).

3.2 SEDIMENT GRAINSIZE DISTRIBUTION

Sediment grainsize depends largely on the current strength in the local environment, together with size of available particles (Folk, 1974); consequently, sediment grainsize is an indicator of environmental energy and not strictly of sediment constituents, in that coarser sediment indicates higher wave energy compared to finer sediments. Modifications can apply to these generalisations in calcareous systems due to factors such as reduction of wave energy in seagrass meadows (Fonseca, 1989; Verduin and Backhaus, 2000; Madsen et al., 2001; van Keulen and Borowitzka, 2002; Carruthers et al., 2007) and specific inherited particle sizes applicable to bioproduction.

3.2.1 Underwater sediments

Most of the sediments in the study area are sand sized (figure 51). Dominance of gravel was only found in two samples (~72%), but a gravel range of ~1.5–25% is common throughout the study area. The carbonate mud component of sediments is ~4–10% between the Geraldton Port and the Batavia Coast Marina, and ~4–13% at Drummond Cove north toward the Buller River mouth. 1–4% of mud was also found at Separation Point and at the northern extreme of Tarcoola Beach.

The granulometric distribution of sands within the study area shows two separate sediment belts: one in the shallower areas within ~1km of the shoreline, and one at depths greater than 10 m. Fine sands dominate the shallowest areas and the beaches; medium and coarse sands are more abundant offshore. This indicates that fine sand is not being transported offshore, but is only interacting with the nearshore areas and littoral transport system.

Coarse sands dominate the 10 m deep ridge systems located offshore of Drummond Cove, and north of Point Moore to north of the dredged channel (figure 52). South of Geraldton, the seafloor offshore of the 10 m deep ridge system is covered by medium-coarse sands (figures 52 and 53).

North of Geraldton, fine sands dominate on the beaches and in the 1 km wide littoral belt starting from the shoreline down to 7 m of depth, with an interruption south of the Chapman River mouth where coarser and less sorted sand was found (figures 52 and 53), indicating higher environmental energy and sediment input from other sources (see section 3.5). Also, the area between the Geraldton Port and the Batavia Coast Marina, extending northward for ~2 km, is dominated by fine sands (figure 54). South of Geraldton, fine sands cover a wider area up to 2.5 km from the shoreline, including the beaches, with the exception of the area

off the northern extreme of Tarcoola Beach where the fine sand belt is only ~1 km wide (figure 54).

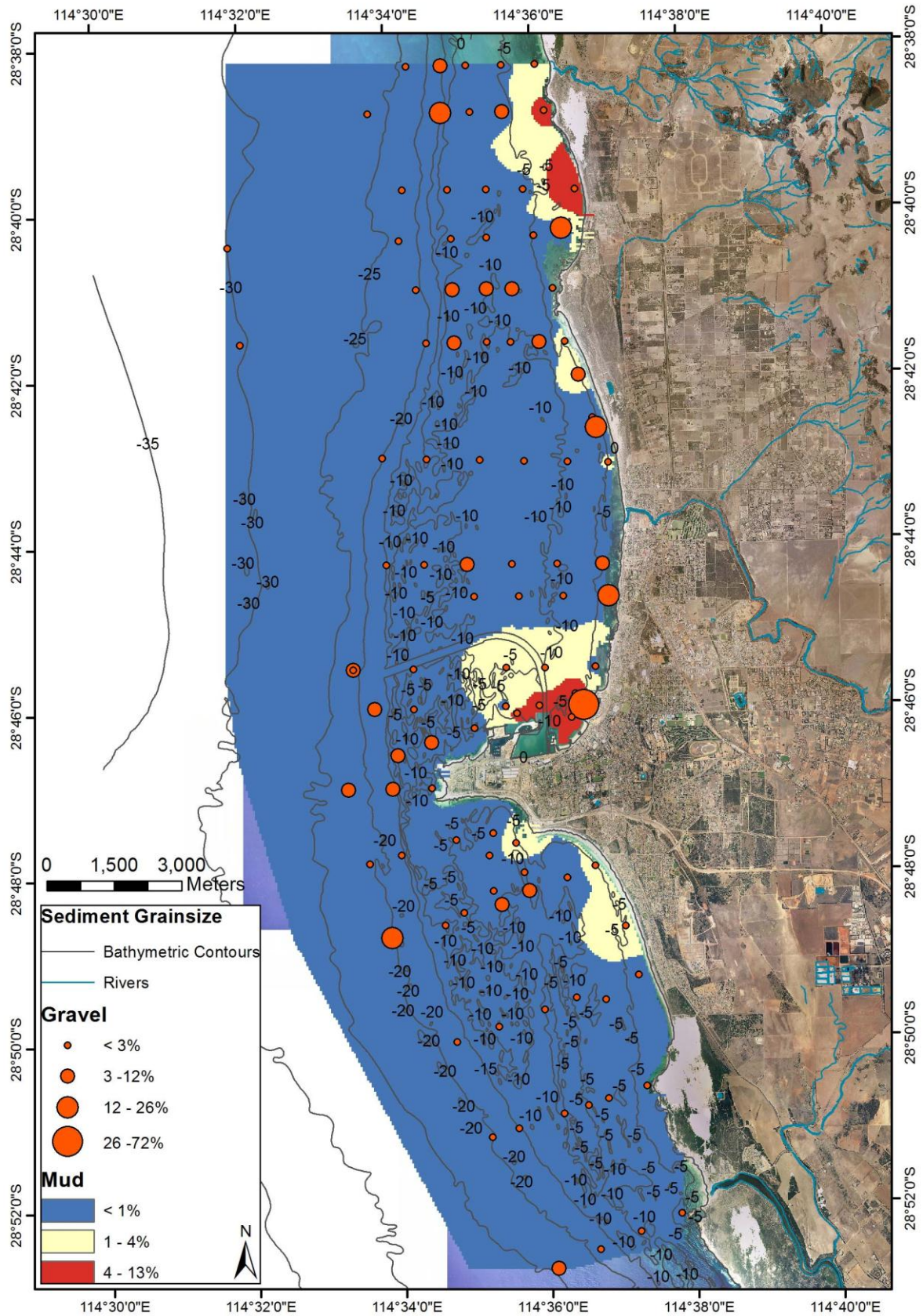


Figure 51: Sediment grainsize map of gravel and mud at Geraldton. The blue raster indicates <1% of mud.

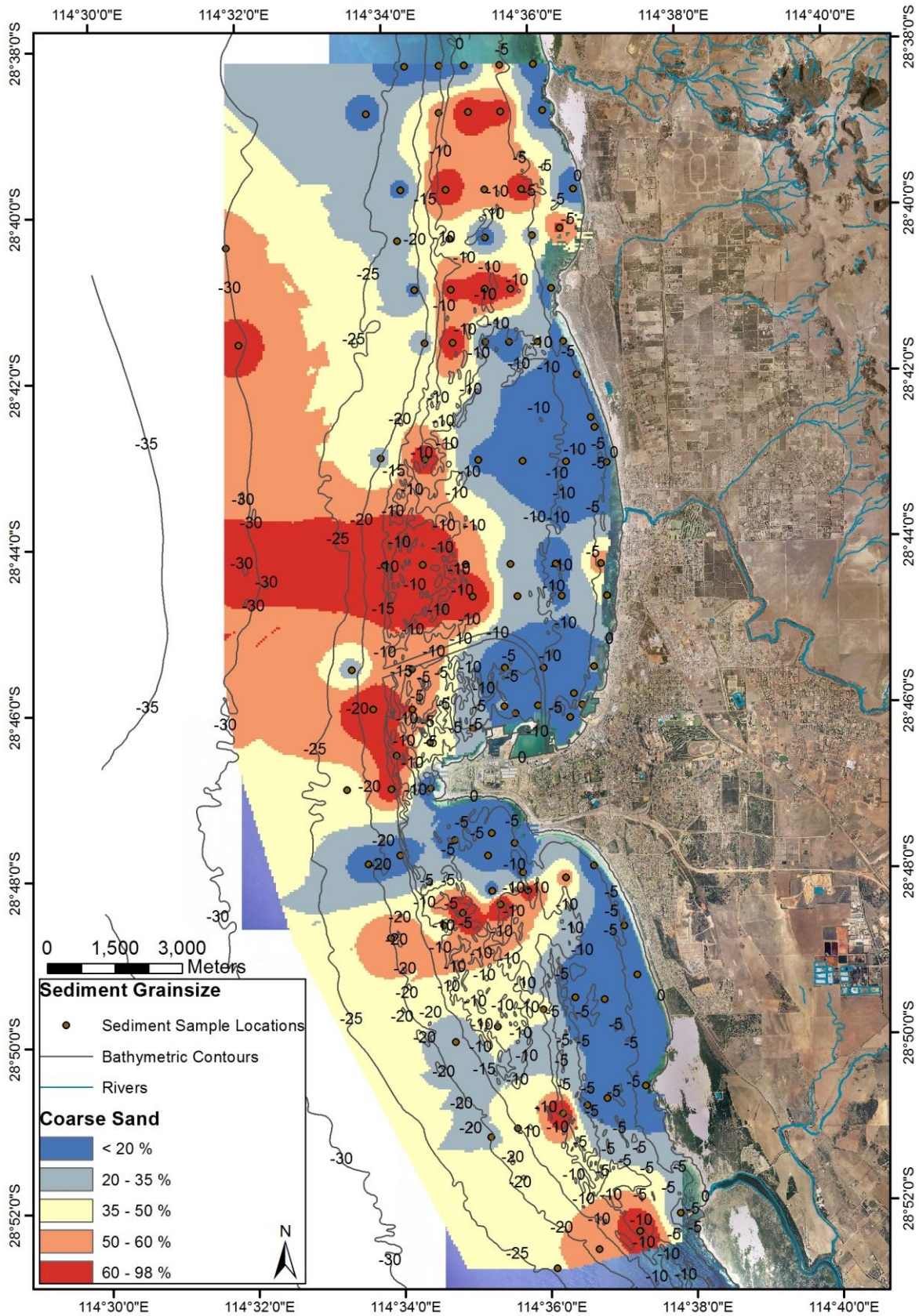


Figure 52: Sediment grainsize map of coarse and very coarse sands at Geraldton. Blue tones indicate low %, yellow tones intermediate %, and red tones high % of coarse sand.

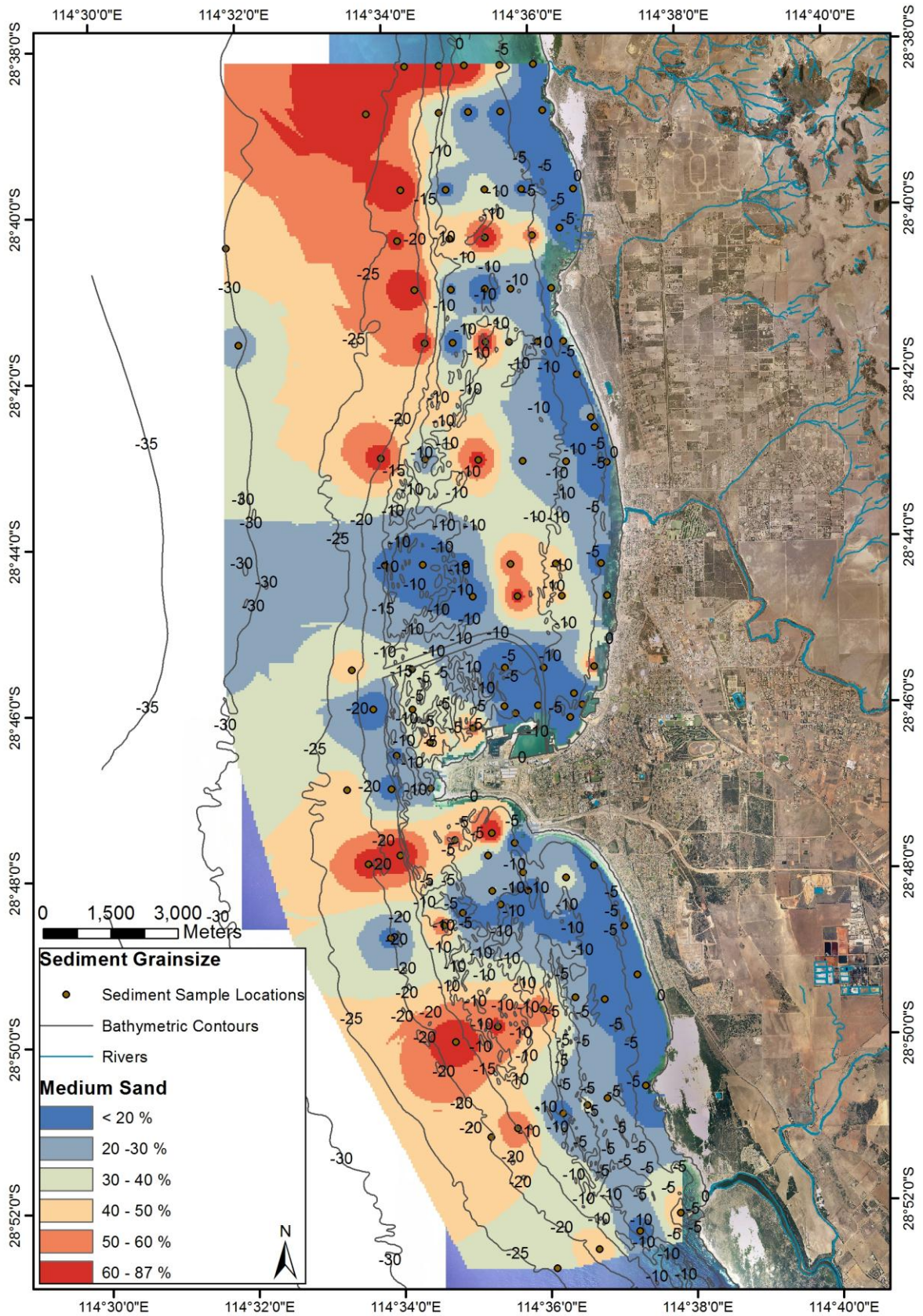


Figure 53: Sediment grainsize map of medium sand at Geraldton. Blue tones indicate low %, yellow tones intermediate %, and red tones high % of medium sand.

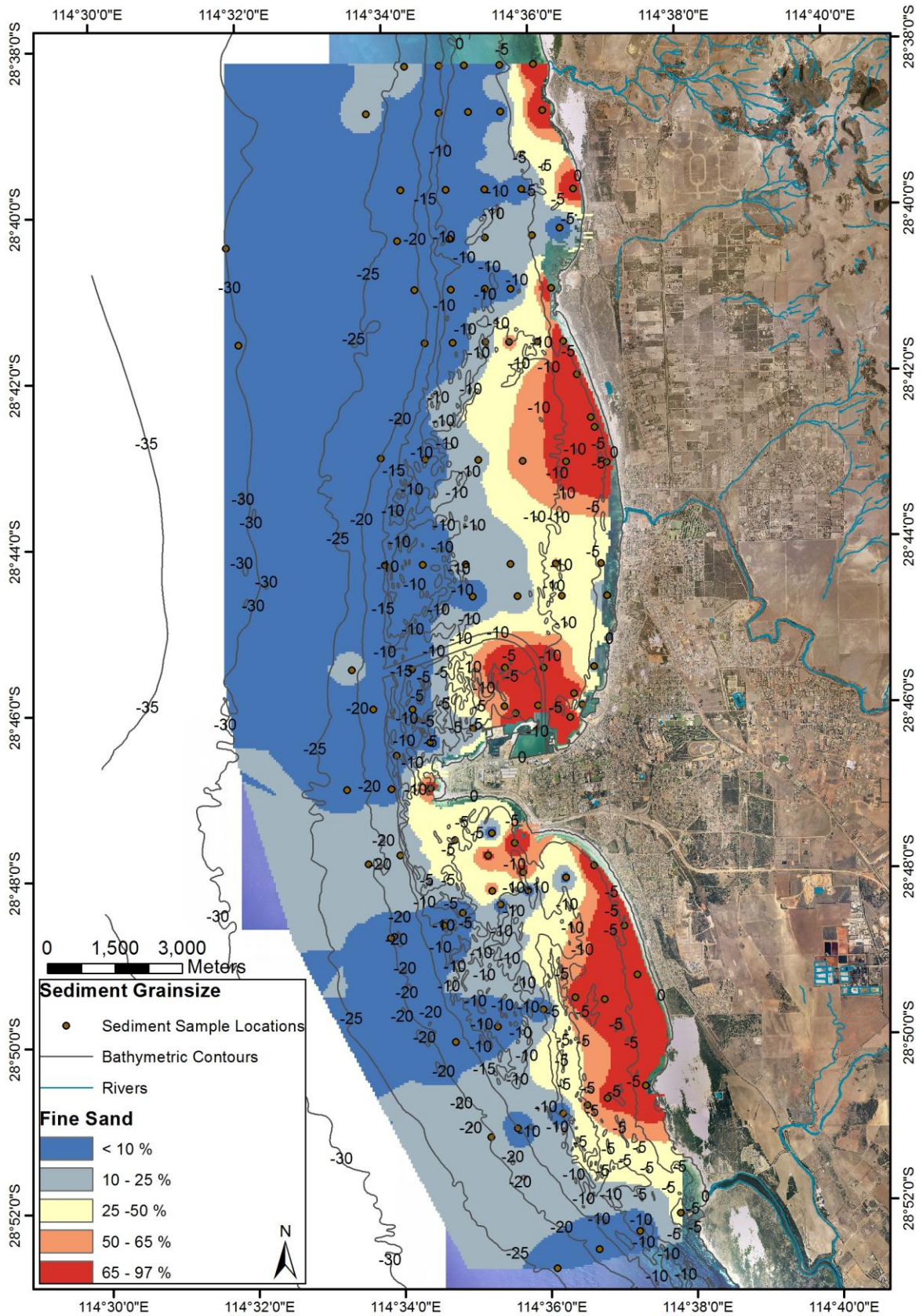


Figure 54: Sediment grainsize map of fine and very fine sands at Geraldton. Blue tones indicate low %, yellow tones intermediate %, and red tones high % of fine and very fine sand.

3.2.2 Coastal sediments

These sediment samples are located along the beaches only, as shown in figure 55. The May 2010 dataset is representative of the autumn sediment supply to the beaches and is comparable with the November 2009 and December 2010 datasets, which are representative of spring conditions.

This dataset confirms the prevalence of fine sand along the Geraldton beaches, with the exception of Sunset Beach which is characterised by medium-fine sand. As expected, the general trend indicates that the medium-coarse sand components increase in the autumn dataset, with the exception of Separation Point and Taroola Beach which are oriented to the south and consequently subject to higher wind-driven summer waves and swell.

It is worth noting that the Northern Beaches and Sunset Beach contained 50% of gravel to pebble sized, non-carbonate grains in samples collected after the February 2011 flooding of the Chapman River (see section 1.3.5), indicating an occasional river-derived sediment input at these locations, particularly in correspondence to flooding events.

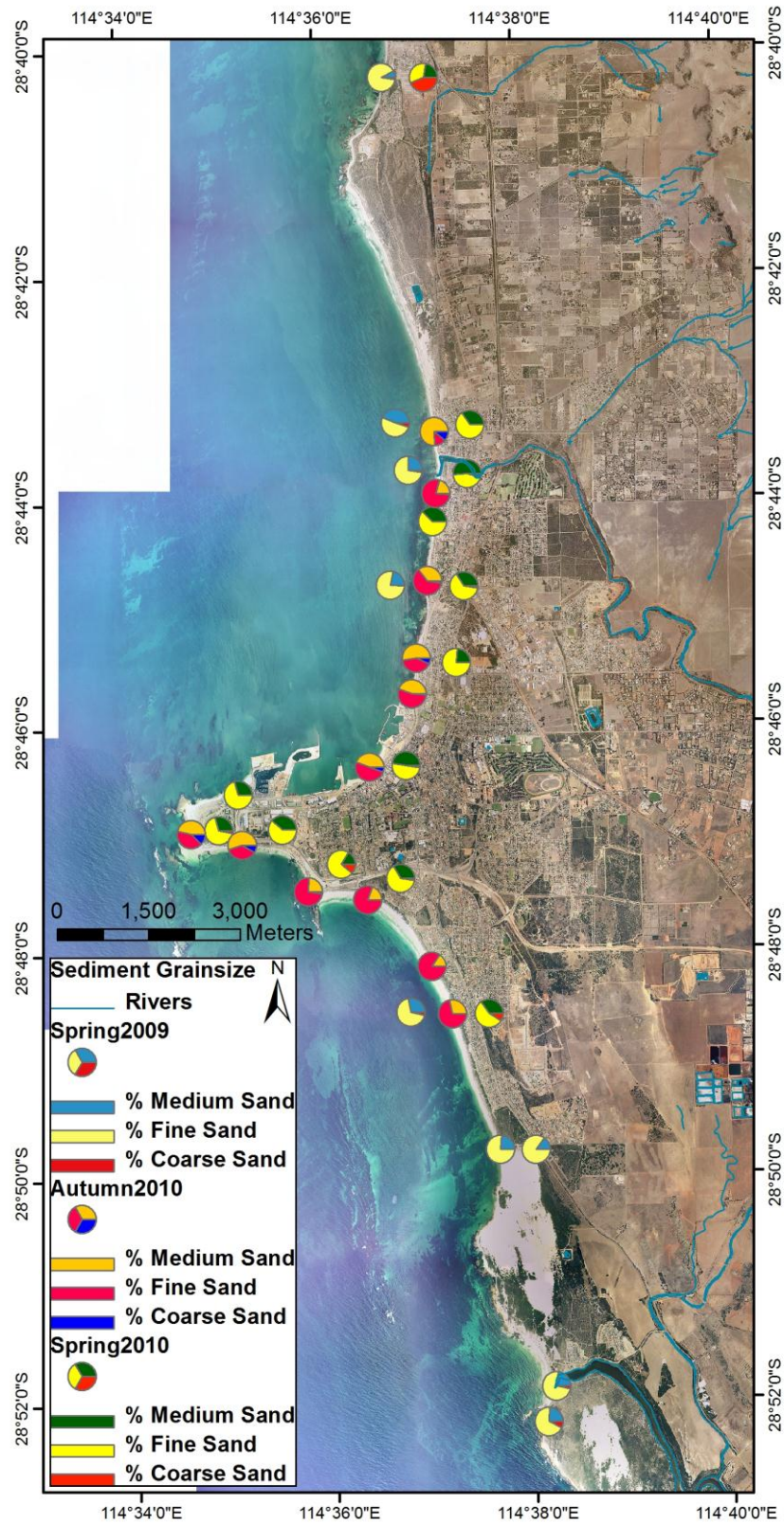


Figure 55: Sediment grainsize along the Geraldton beaches; a comparison of the results of spring (2009 and 2010) and autumn (2010) sediment deposition. Note: older to newer datasets from left to right at repeated sites.

3.3 CARBONATE CONTENT OF SEDIMENTS

The carbonate content of the sediment samples ranges between ~32.5 and 97% (figure 56), with an average value of ~74.5%. This is an indicator of carbonate-dominated sediments in the study area, composed of a mixture of modern and relict carbonate grains. Carbonate content not only reflects percentage of fresh bioclast grains, often seagrass-associated, but is also contributed to by limestone-derived particles and relict sediment mostly derived from the erosion of submersed limestone structures.

3.3.1 Underwater sediments

The highest carbonate percentages were found south of Geraldton, north of Point Moore to the dredged channel, eastward to the Geraldton Port, and at Drummond Cove (figure 56). In these areas, the carbonate content ranges between ~81.6 and 97.2% and corresponds to the zones dominated by fine sands; but, south of Point Moore to Separation Point more abundant medium sand was found.

South of Geraldton, the carbonate content decreases moving offshore, reaching the lowest measured values (~38.5%) at ~20 m depth and is ~60% at ~10 m depth west of the limestone ridge system. However, most of the sediments collected on the coastal platform south of Geraldton have a carbonate content of ~77–81.5%.

An important outcome of the carbonate content analysis is that the sediments situated offshore of the Chapman River mouth have the lowest carbonate content (~44-67%) of the shallow study area, indicating that other minerals compose part of the sediments, i.e. quartz. The proximity of the Chapman River suggests a correspondence between the river input of sediment into the coastal system and the high quartz content of the sediment, also supported by the coarser grain size of the samples collected in this location compared to the surrounding areas. Additional minor non-fluvial sources of quartz are from relict sediments or reworking of underlying limestones.

The ridge system offshore Drummond Cove shows a lower sediment percentage of carbonate (~72.4–77%) than the more inshore and offshore areas, even though the surrounding areas to the west are homogeneously rich in coarse sands. This might indicate the transport to the north of non-carbonate sediment supplied to the coastal system by the Chapman River.

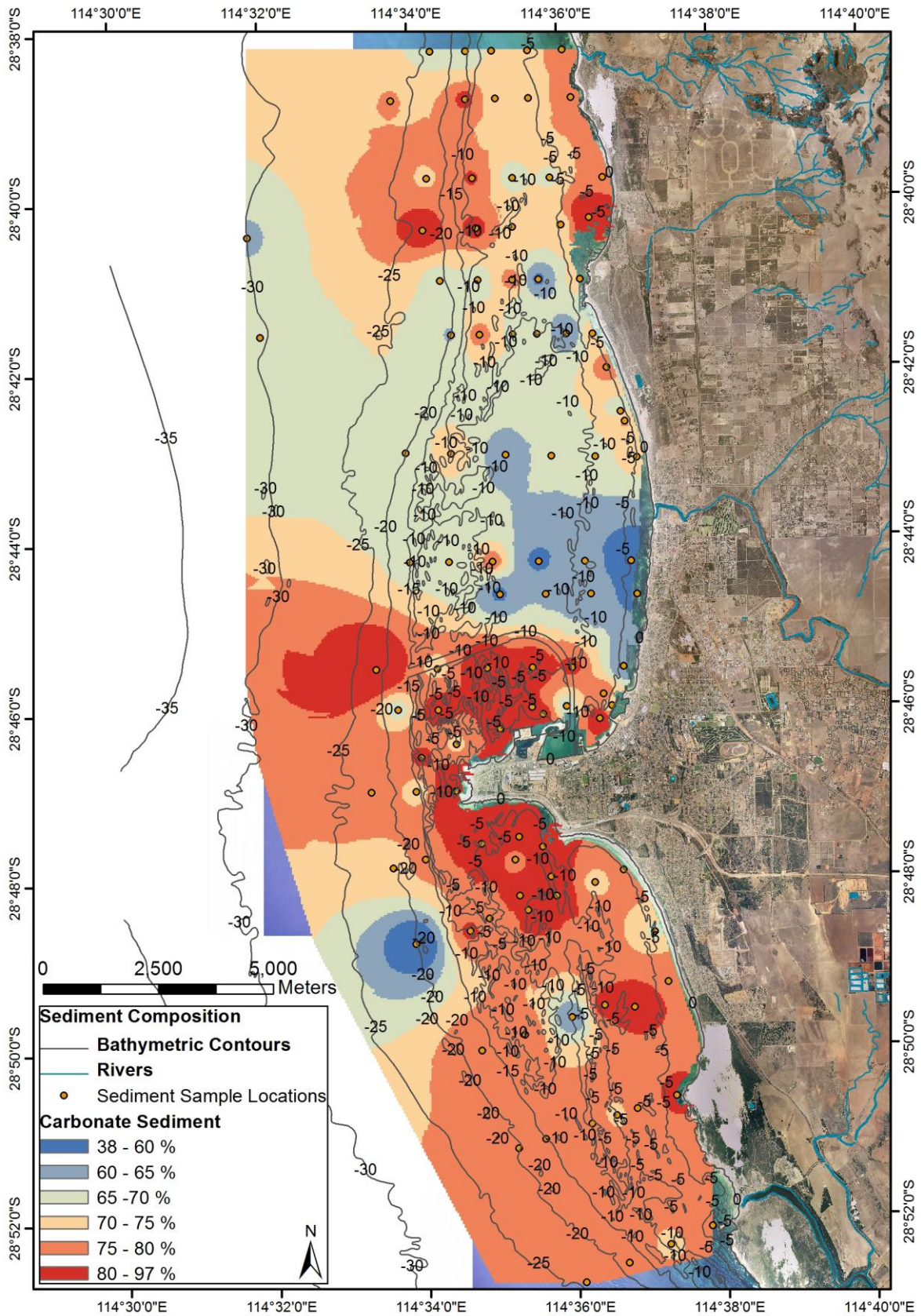


Figure 56: Sediment carbonate content map at Geraldton. Blue tones indicate low %, grey tones intermediate %, and red tones high % of carbonate sediment.

3.3.2 Coastal sediments

The carbonate content of the beach sediment (figure 57) reflects the offshore pattern outlined in section 3.3.1 with higher carbonate percentages south of Point Moore (>75%) and at Drummond Cove (80–88%). The lowest carbonate content was found at the Chapman River mouth (~32%) and at Sunset Beach (~50%), with the Northern Beaches and Town Beach within the range of 60–75%. Evidence of deposition of river-supplied gravel to pebble-sized, non-carbonate grains (mainly quartz, with a minor fraction of garnet and ilmenite) was found at Sunset Beach and on the Northern Beaches following the February 2011 flooding of the Chapman River (section 1.3.5); however, uncertainty about the provenance of non-carbonate minerals constituting the sediments on a non-seasonal basis remains. Non-carbonate minerals might have been constituents of the sands used for the nourishment activities, and the lack of information in this regard (section 1.3.1) does not assist identification of sediment provenance in this area. A significant variation was not noted between the spring and autumn datasets, and when such occurred it was lower than 10%.

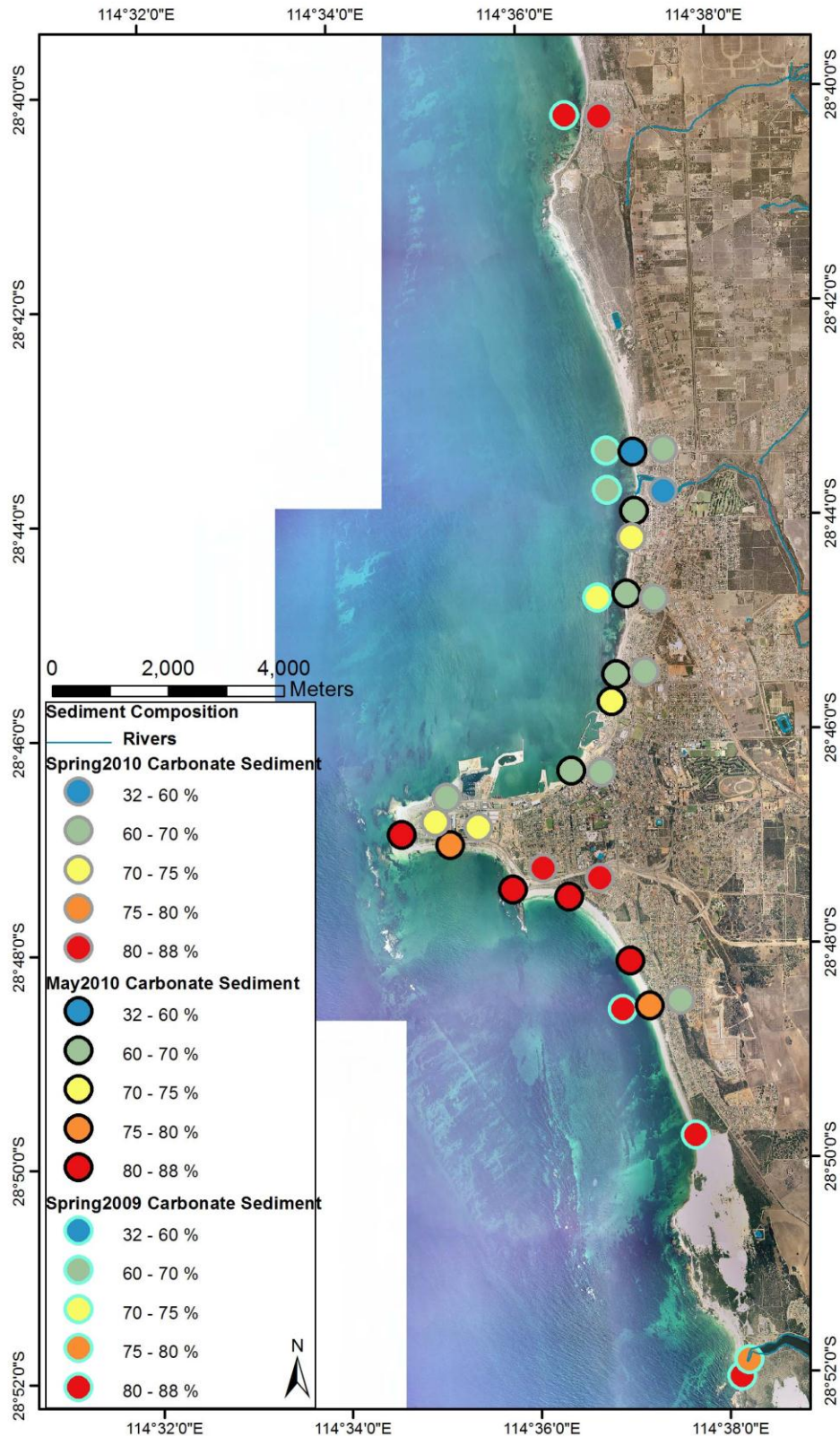


Figure 57: Sediment carbonate content along the Geraldton beaches; a comparison of the results of spring (2009 and 2010) and autumn (2010) sediment deposition. Note: older to newer datasets from left to right at repeated sites.

3.4 SEDIMENT COMPONENTS: PETROLOGICAL AND X-RAY DIFFRACTION ANALYSES

Carbonate sediments dominate the Geraldton coastal platform and beaches, and are mainly composed of the skeletons of modern and relict marine organisms, together with grains deriving from the abrasion of submerged limestone structures. Low and high-Mg calcite, aragonite, and quartz are the minerals constituting the Geraldton sediment. As summarised by Chave (1962), molluscs and bryozoans provide the aragonitic component, benthic foraminifera and coralline algae produce dominantly high-Mg calcite, and planktonic foraminifera produce low-Mg calcite. Sponge spicules are responsible for the amorphous component of the sediments and are abundant in the shallowest sediment samples, although the greatest errors in the XRD analysis were found when the amorphous sediment fraction was most abundant. Quartz is a terrigenous mineral supplied to the coastal system by river discharge of material collected inland, and it accumulates in the sediments over consecutive sedimentary cycles due to its low deterioration properties. In the study area, quartz is more common offshore (>20 m depth) and in the Geraldton northern embayment, where relatively low carbonate content was found in the sediments, especially off the Chapman River mouth and in nearby areas (section 3.3).

Whilst low Mg calcite is stable under varying pressure and temperature conditions, aragonite and high Mg calcite are commonly unstable (Chave, 1962; Preda and Cox, 2005). Carbonate material can reprecipitate as low-Mg calcite when mobilised and correlation with petrological observation of sediment constituents is necessary to correlate mineralogy and skeletal composition (Preda and Cox, 2005). Data of this kind was made available for this project; however, sediment composition was not undertaken to a species level but was assessed through visual estimation of the percentages of modern bioclasts, reworked grains and relict bioclasts. These three classes have similar abundances (figures 58 and 59) and consequently a clear pattern in the distribution of sediment facies based exclusively on grain type percentages was not obvious. Modern bioclasts represent an important fraction of the sediment as they range from 30 to 70% for 33 out of the 36 samples petrologically analysed in this study (locations shown in figure 59). Molluscs (most commonly bivalve fragments 1–45%, and secondly gastropods 1–13%), calcareous red algae (5–30%), benthic foraminifera (1–30%), bryozoans (1–18%), and sponge spicules (1–15%) are common modern bioclasts, which is what is expected in a temperate water carbonate environment. Reworked grains are also common as they constitute between 18 and 60% of most of the samples, with the deepest sample collected in this study containing 80% of reworked grains. Of these sediment grains, 15 to 45% are carbonate intraclasts together with quartz (3–60%) and rare feldspar (max. 1%). Relict skeletal grains are also common and their abundance ranges

between 15 and 63%, with fragmented benthic foraminifera, bivalves and bryozoans as main constituents.

As shown in figure 60, there is a limited variability in terms of sediment mineralogy in the study area. There is an overall predominance of high-Mg calcite which can be attributed to the abundance of modern and relict foraminifera and fragments of modern calcareous red algae. Modern skeletal grains do not only explain the high-Mg calcite fraction of the Geraldton sediments but also contribute to the aragonite component, as aragonitic molluscs and bryozoans were commonly found through the microscope observations. Low-Mg calcite and aragonite show similar abundances (10–25%), indicating that the sediment mineralogy is not changing significantly from modern to relict grains, but the sediment constituents are maintaining the same mineralogical phase after being exposed on the seabed and subjected to erosive cycles, and there is no apparent inversion to low-Mg calcite. Limestone intraclasts are expected to be constituted by low-Mg calcite as these grains are remains of previous sedimentary cycles and are deemed to have been subjected to varying diagenetic conditions, which are usually responsible for grain reprecipitation into the more stable low-Mg calcite phase. This is particularly evident in the samples collected along the northern edge of Southgate dune, where intraclasts and relict benthic foraminifera dominate the sediment composition and high- and low-Mg calcite are the dominant minerals (figures 59 and 60).

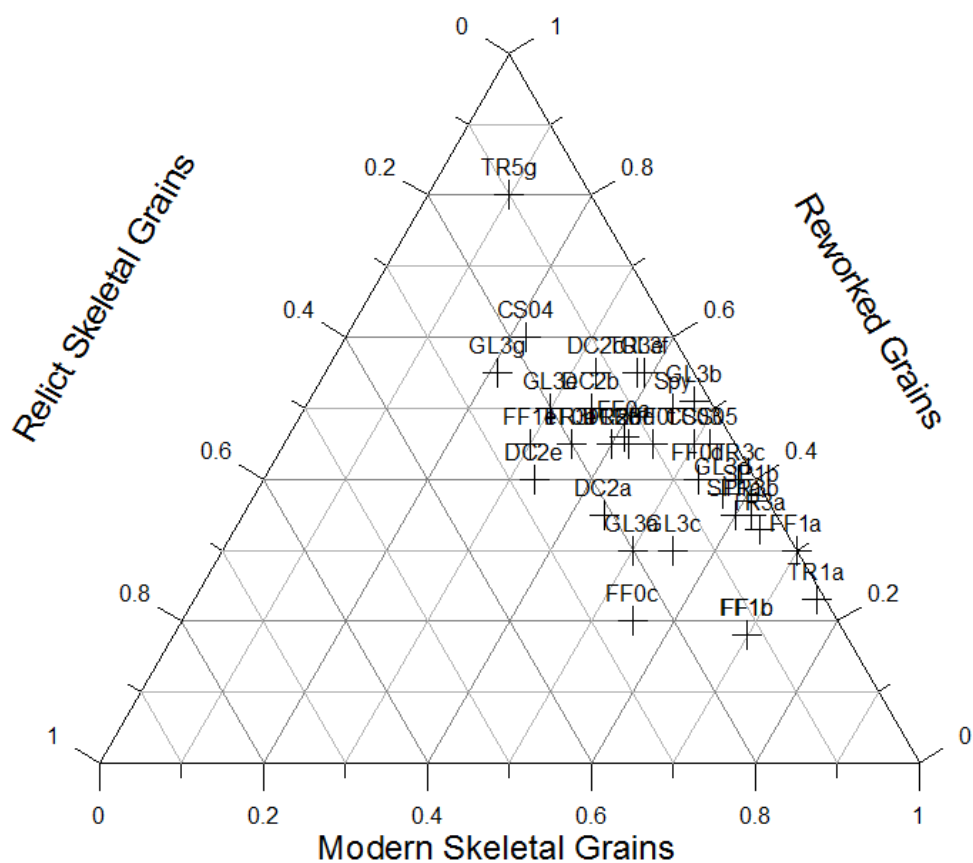


Figure 58: Sediment composition based on visual estimation of the percentages of modern bioclasts, reworked grains and relict bioclasts. Note poor discrimination of sediment types in this plot.

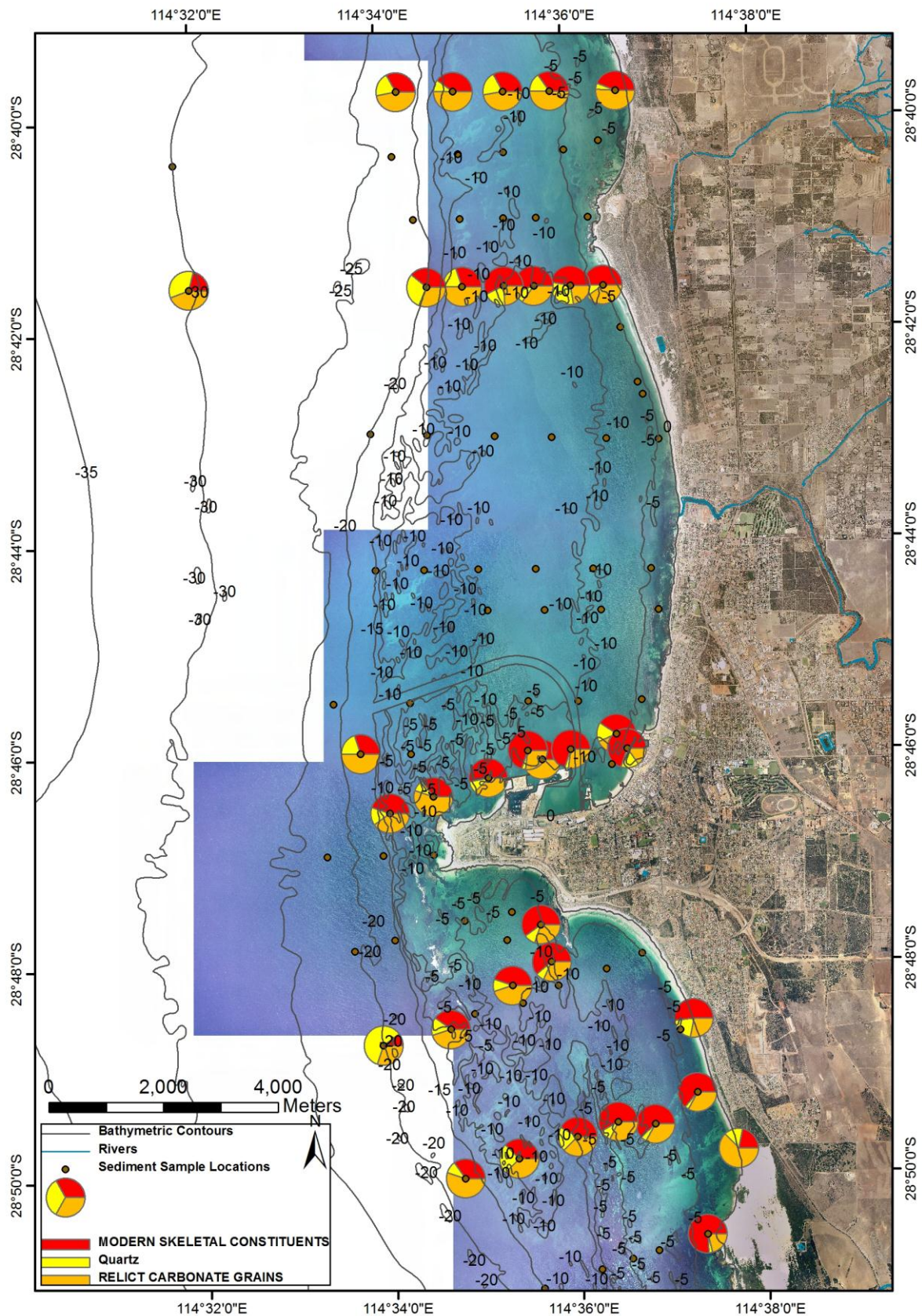


Figure 59: Sediment composition resulting from the microscopic observation of sediment samples. Sediment composition was not undertaken to a species level but was assessed through visual estimation of the percentages of modern bioclasts, reworked grains and relict bioclasts.

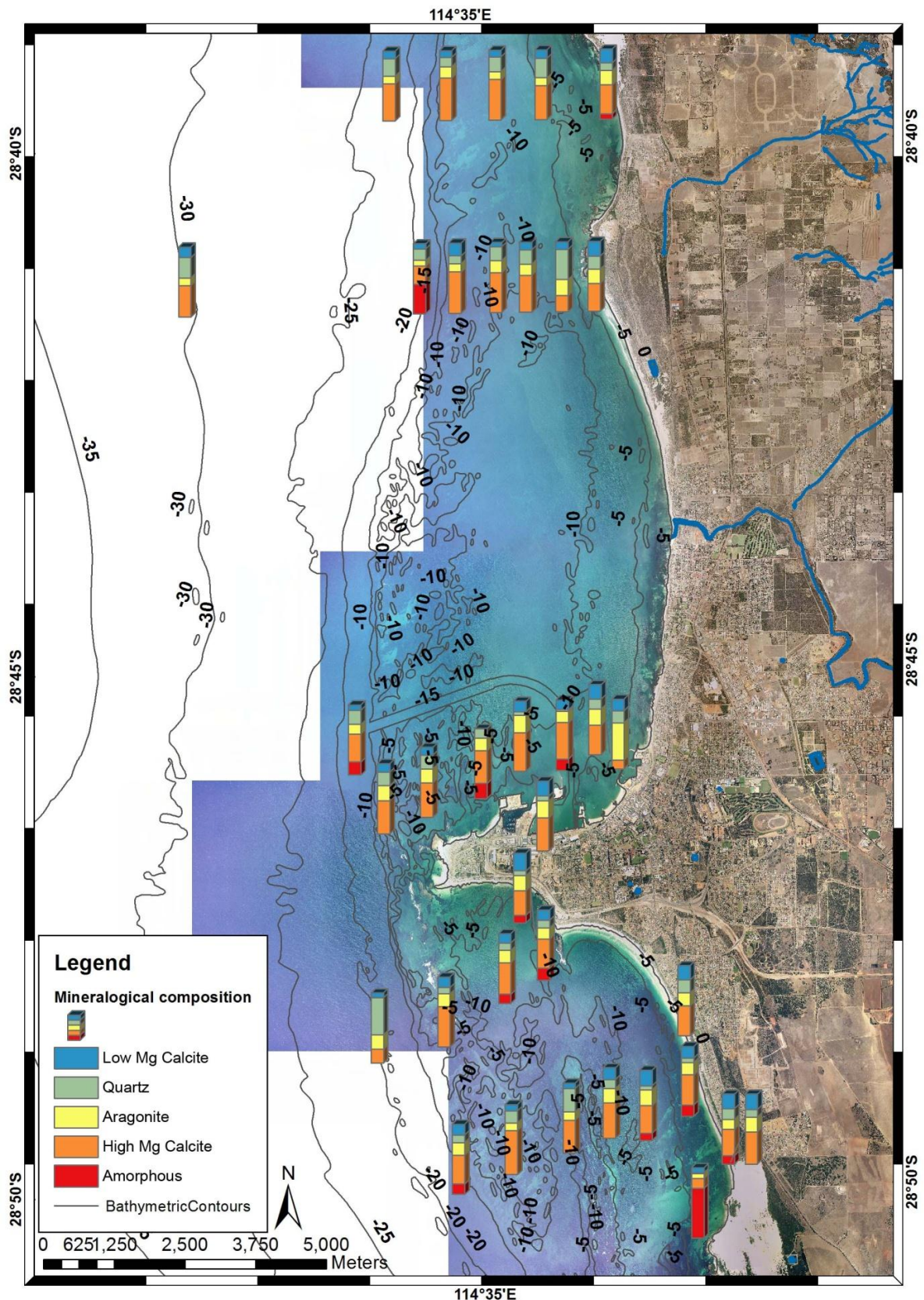


Figure 60: Mineralogical composition of selected sediment samples derived from the XRD analysis. Amorphous material includes silica from sponges, and other non-crystalline materials. Of note is the dominance of High Mg Calcite and the similarity in the abundances of Aragonite and Low Mg Calcite. This seems to indicate that sediment mineralogy is not changing significantly from modern to relict grains, and there is no apparent inversion of Aragonite and High Mg Calcite to Low Mg calcite.

3.5 SEDIMENT FACIES

Due to the poor discrimination of sediment classes based on the petrological and mineralogical analyses, sediment facies were determined by considering percentage of fine, medium, and coarse sands, percentage of modern skeletal grains, and sediment carbonate content (see Chapter 1 for further details on the methodology).

Based on figure 61, fine modern skeletal sand, medium-coarse modern and relict skeletal sand, and fine-medium quartzose and modern skeletal sand are the most common sediment types at Geraldton. Coarse quartzose and relict skeletal sand is mainly representative of the offshore sediments (>15 m depth) and could not be extensively mapped due to the limited amount of samples at those depths. The distribution across depth of these sediment facies is illustrated in figure 62; however, as the fine-medium quartzose and modern skeletal sand sediment facies is only representative of the Champion Bay area and was mapped at similar depths as fine modern skeletal sand and medium-coarse modern and relict skeletal sand, it was not included in figure 62. Moreover, the fine-medium quartzose and modern skeletal sand visible in figure 61 in the southern Geraldton embayment is an artefact of the mapping techniques, and these areas are likely to be part of the surrounding fine modern skeletal sand and medium-coarse modern and relict skeletal sand polygons.

Based on the results of the petrologic analysis, modern grains comprise ~60% of the fine modern skeletal sand and ~40% of the medium-coarse modern and relict skeletal sand, with the remaining consisting of reworked grains (figure 62). The so called “fine-medium quartzose and modern skeletal sand” sediment facies is composed of ~45% river-supplied sand (i.e. quartz), with the remaining consisting of modern bioclasts and some reworked grains. Modern grains are “bioclasts” associated with in situ sediment production connected to marine vegetated areas, particularly seagrass meadows and macroalgal communities. Calcified benthic organisms are attached and live on the vegetation as epiphytes and accumulate within the sediment when they die, constituting the so-called bioclast.

The fine modern skeletal sand was mapped on the most protected coastal areas close to shore (0–10 m depth, figure 61) and is sponge spicule rich, with abundant foraminifera, molluscs and coralline algae (figure 63A and figures 64A, B, and C). This sediment type develops correspondently to *Amphibolis* and *Posidonia*-dominated seagrass meadows (see Chapter 2 for habitat maps) and is redistributed along the shore by the littoral currents.

The middle part of Champion Bay is largely covered by fine-medium quartzose and modern skeletal sand (figure 61), correspondently to the lower carbonate content/higher quartz content of the seabed sediments. This sediment facies occupies sparsely vegetated areas

with mainly coloniser seagrass and macroalgae present. Sandy substrates as part of a sand sheet and bar system are also common where this facies was mapped (see Chapter 2).

The medium-coarse modern and relict skeletal sand was mapped in higher energy areas (~10 m depth, figure 61), correspondently to limestone ridge systems colonised by dense macroalgae communities, and in the northern extreme of the study area where higher wave heights are common. Calcareous red algae and molluscs are the most common modern grain types found within this facies (figure 63B and figures 64D, E, and F), and are commonly part of macroalgae communities.

Table 13 summarises the main characteristics of the sediment facies described above.

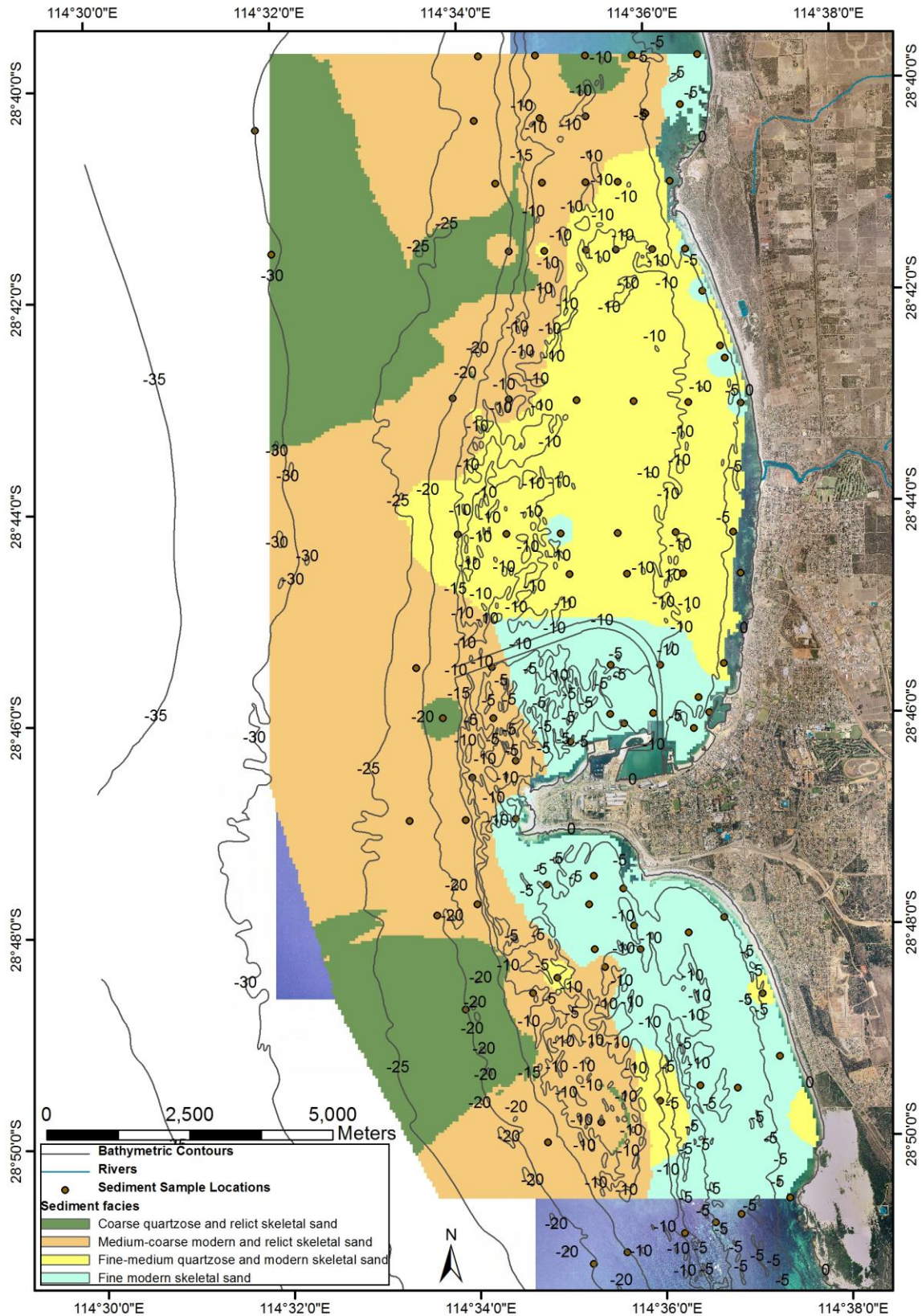


Figure 61: Sediment facies map at Geraldton. Sediment facies were determined by considering percentage of fine, medium, and coarse sands, percentage of modern skeletal grains, and sediment carbonate content. The distribution of fine-medium quartzose and modern skeletal sand south of Geraldton is an artefact of data interpolation, and these areas are likely to be part of the surrounding fine modern skeletal sand and medium-coarse modern and relict skeletal sand polygons.

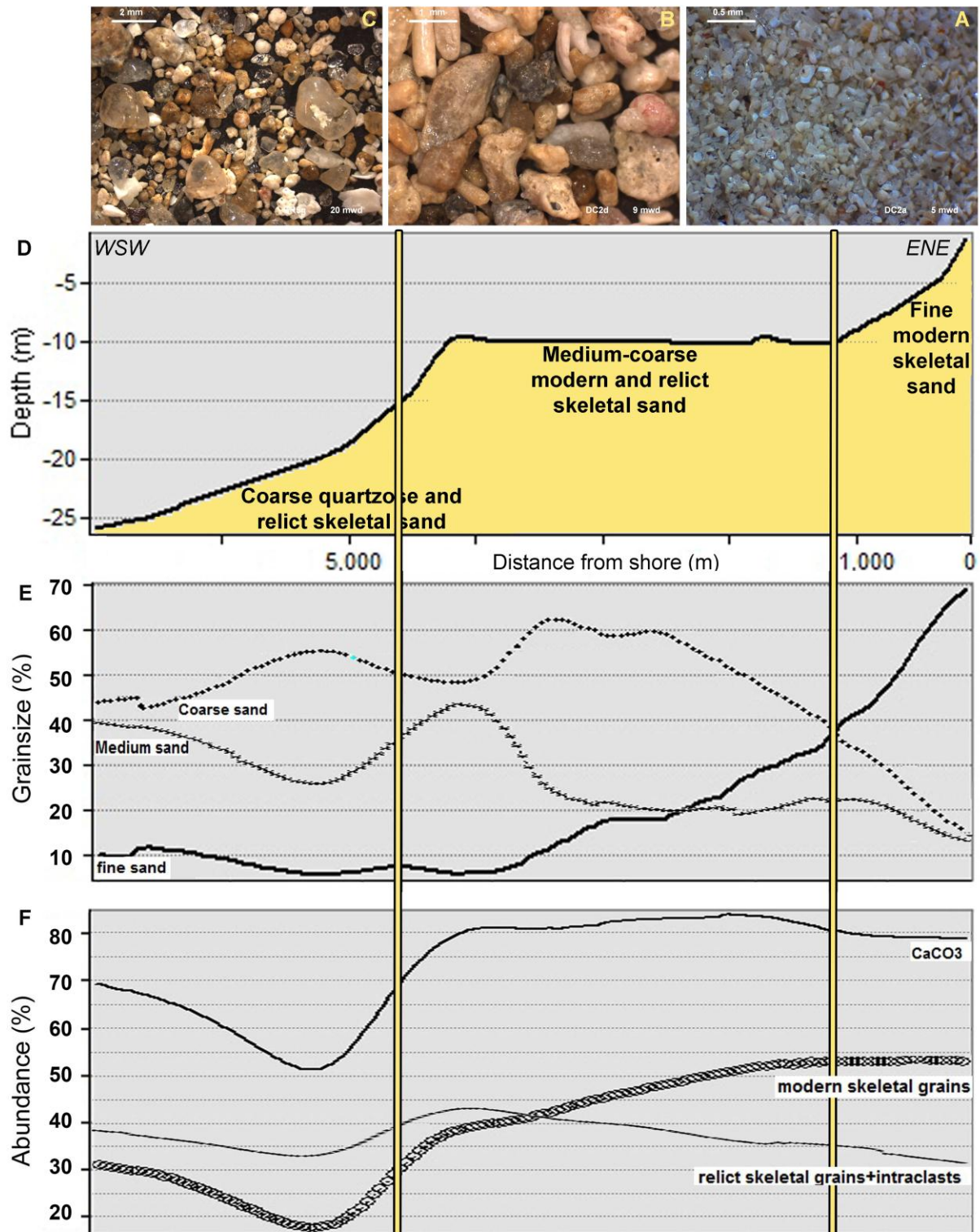


Figure 62: Microscope photos of loose grains of the following sediment facies: A) Fine modern skeletal sand; B) Medium-coarse modern and relict skeletal sand; C) Coarse quartzose and relict skeletal sand; D) Cross-shore transect showing the distribution of sediment facies across depth at Geraldton; E) Line plots of sediment grainsize across depth showing percentage of fine, medium, and coarse sands; F) Line plots across depth showing carbonate content (CaCO_3), percentage of modern skeletal grains, and percentage of relict carbonate grains (intraclasts + relict skeletal grains). Whilst this profile represents an average sediment distribution across depth throughout the study area, off the Chapman River mouth the “fine-medium quartzose and modern skeletal sand” sediment facies dominates the coastal platform (refer to the main body of the text for further explanations).

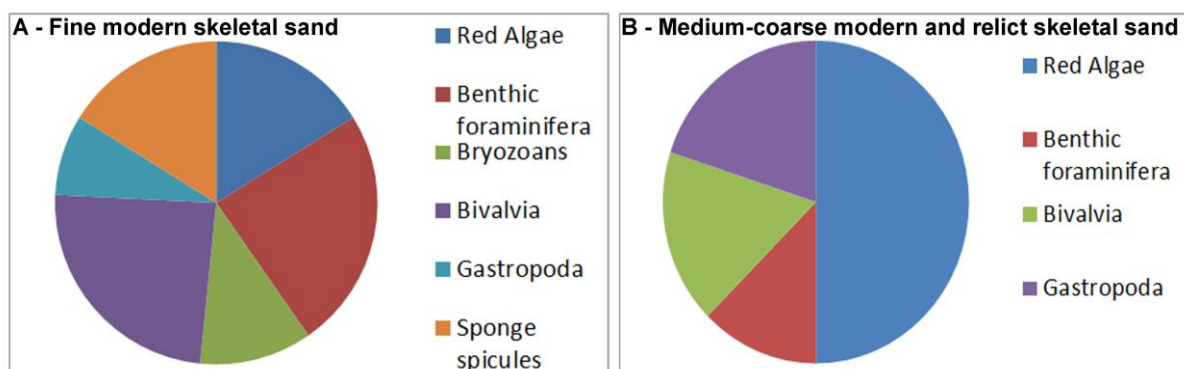


Figure 63: Fossil composition of the modern skeletal grain sediment fractions for A) Fine modern skeletal sand and B) Medium-coarse modern and relict skeletal sand.

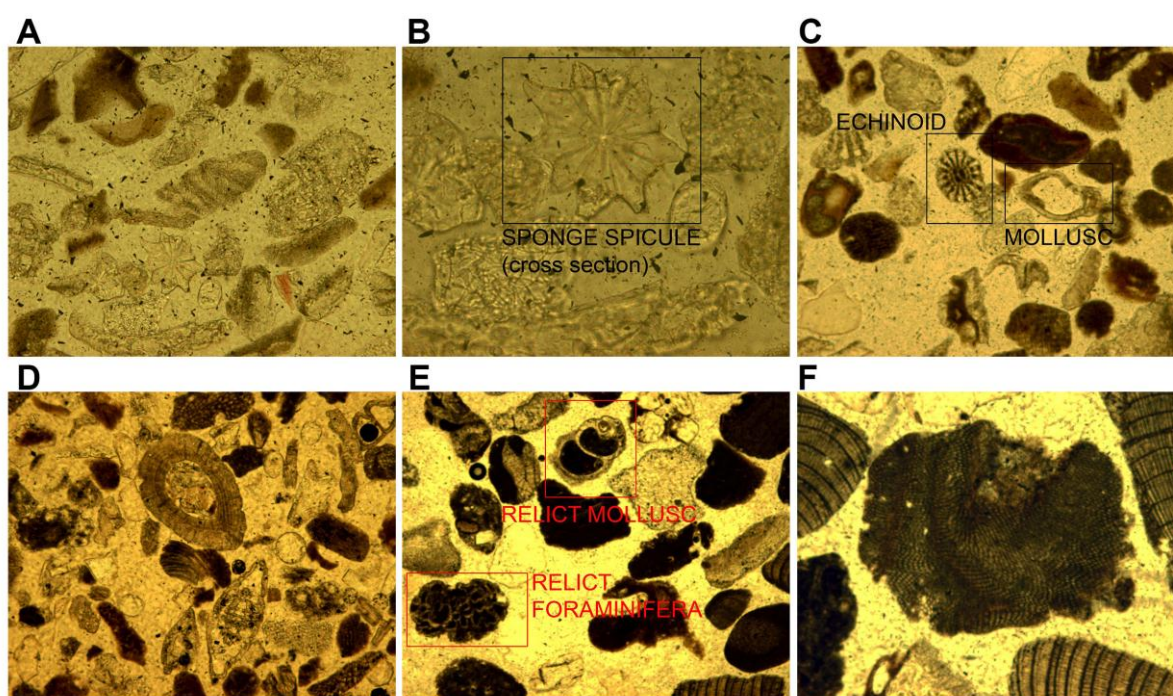


Figure 64: Microscope photos of the two most common sediment facies found at Geradlton: fine modern skeletal sand (A, B and C) and medium-coarse modern and relict skeletal sand (D, E and F). A, C, D & E – 10x enlargement on high power; B & F – 40x enlargement.

Table 13: Summary of the main characteristics of the Geraldton sediment facies.

SEDIMENT FACIES	MEAN WATER DEPTH	CARBONATE CONTENT	AVERAGE MAIN CONSTITUENTS	DEPOSITIONAL ENVIRONMENT
Fine modern skeletal sand	0-10 m	70-100%	60% modern skeletal grains + 40% reworked grains	<i>Amphibolis</i> and <i>Posidonia</i> seagrass meadows
Medium-coarse modern and relict skeletal sand	5-15 m	65-100%	40% modern skeletal grains + 60% reworked grains	Macroalgal communities
Fine-medium quartzose and modern skeletal sand	0-10 m	38-65%	45% quartz+30% modern skeletal grains + 25% reworked grains	Sand plain (Chapman River supplied sand)
Coarse quartzose and relict skeletal sand	>15 m	38-70%	80% reworked grains + 20% modern skeletal grains	Offshore from the coastal platform

3.6 OFFSHORE SEDIMENT THICKNESS

The isopach map produced in this study (figure 65) shows that the sediment thickness within most of the project area ranges between 1 and 2 m; however, a trend could be identified and is linked to the bathymetric gradient as the sediment cover is greater at the seaward end of the coastal platform (>15 m depth) and decreases to landward (0–15 m depth).

Data was available at depths greater than 15 m in two different locations: north of the dredged channel and at the northern extreme of the study area, and showed that a thicker sedimentary cover occurs offshore (2 to 3.7 m). The most indicative unconformities, which provided geometric evidence on the position of the sediment-rock interface, were found at the data's northern extremity at about 19 m depth, approximately 3 km off the Drummond Cove coast. Figure 66 shows an example of those unconformities. This stratigraphic evidence supported the interpretation of the data north of the Chapman River mouth, which shows up to four discontinuous concordant reflectors outlining sediment thickness increase offshore and decrease moving landwards.

The sediment thickness ranges between 1 and 1.5 m between 5 and 15 m depth throughout most of the investigated area north of Geraldton. The majority of the seismic lines analysed between the Chapman River mouth and the Geraldton Port area show two concordant

reflectors. The deeper of the two visible reflectors coincides with the acoustic basement and has a higher continuity than the sediment base recognized north of the Chapman River mouth, which has low continuity and variable amplitude. Higher sediment thickness was found north of the dredged channel, where 2 m of sediment occurs landwards of the submerged ridge system 10 m deep (figure 65). The sedimentary cover ranges between 0.5 and 1 m at depths shallower than 5 m in the area north of Point Moore, but two locations have a greater thickness of sediment:

- 2 m in the inshore waters south of Glenfield Beach and
- 1.5 m in the inshore waters at Drummond Cove.

Both sides of the dredged channel are covered with about 1 m of sediment, but the thickness varies in areas closer to the port. Greater sediment thicknesses (approximately 1.5 m) were found north of the dredged channel and off Town Beach. According to the seismic data, the sediment cover is only 0.5 m north and west of the Geraldton Port; however, the data recorded at these locations show a higher signal penetration, with evidence of a more complex structure which could not be fully interpreted due to the lack of well data. The general trend in the area surrounding the Port is for an increasing sediment thickness from west to east and from south to north, i.e. toward the dredged channel.

South of Geraldton, the geological structure is similar to the Champion Bay area structure, with two concordant reflectors and the deeper of the two coinciding with the acoustic basement and having a higher continuity and intensity. The sediment thickness is commonly around 1 m, but it reaches about 2 m off the northern extreme of Tarcoola Beach. An area of sediment accumulation has been identified adjacent to the northern end of the Southgate dune system, where up to 2.5 m of sediment thickness was found (figures 65 and 67) adding value to previous studies which show that Southgate dune is supplying sediment to the ocean (Chapter 1). South of Point Moore, the isopach map also outlines a few areas with 0.5 m of sediment thickness (i.e south of Separation Point, north of the sediment accumulation area correspondent to the northern part of Southgate dune system, between the Greenough River mouth and the southern extreme of the Southgate dune system) which seem to correlate well with the bathymetry and habitat mapping results.

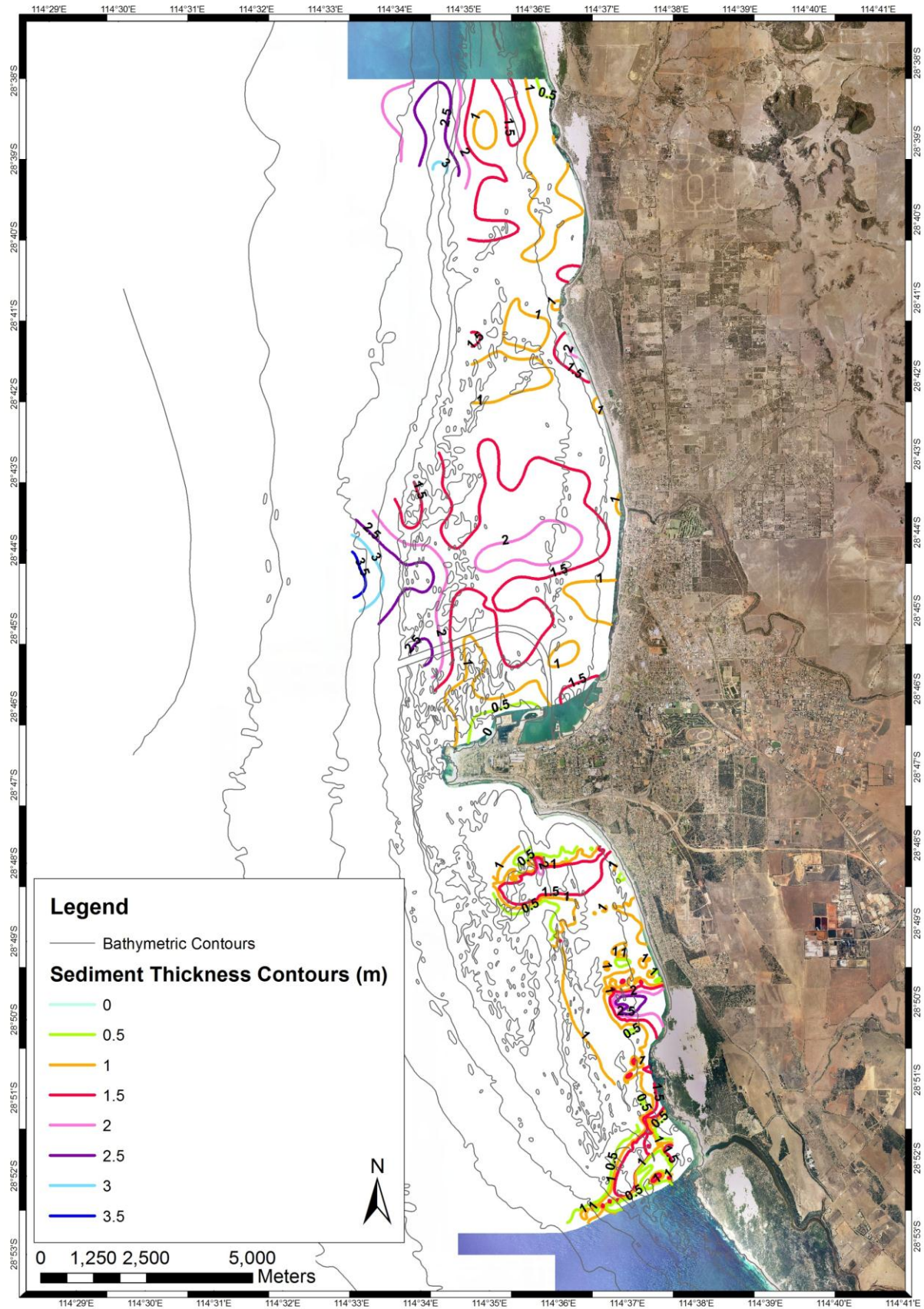


Figure 65: Isopach map of sediment thickness based on seismic data at Geraldton. Commonly sediment thickness is 1 m (orange contour), but it increases to 2 m (pink contour) where sediment accumulation occurs.

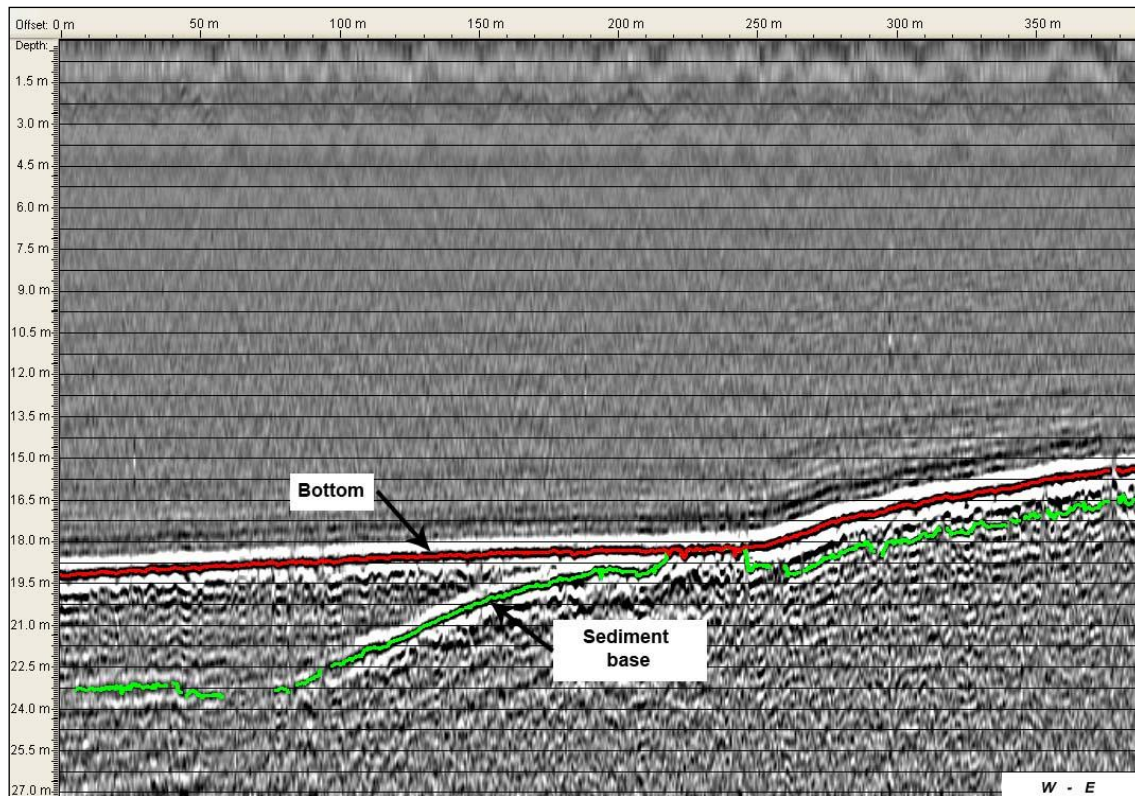


Figure 66: Example of the unconformities indicating the sediment rock interface (green) found at the northern extreme of the study area, off the Drummond Cove coast. For locations of seismic lines see figure 14.

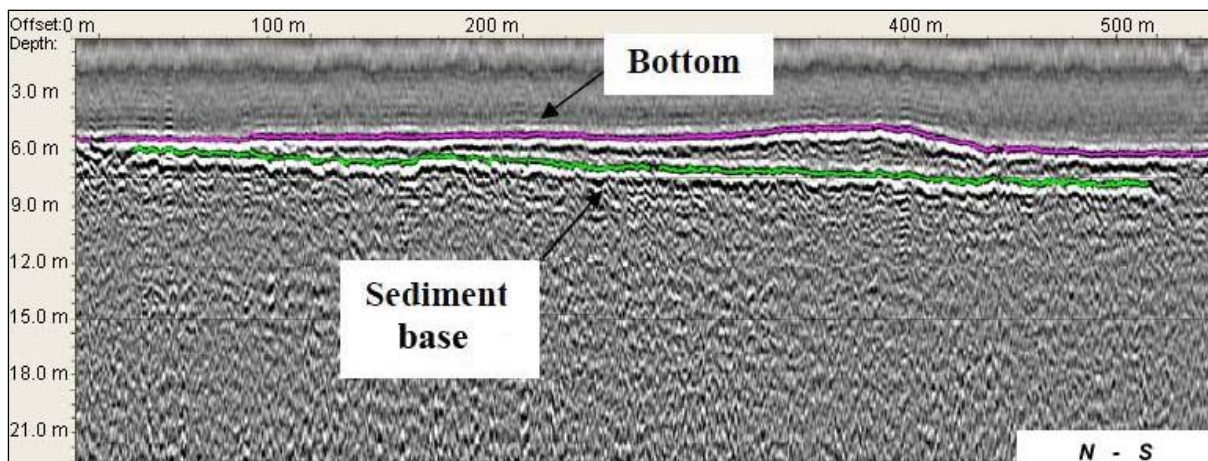


Figure 67: Sediment wedge overlying the sediment base reflector (green) off the Southgate dune system. For locations of seismic lines see figure 14.

3.7 CARBONATE SEDIMENT PRODUCTION AND ACCUMULATION RATES

Modern carbonate sedimentation is linked to seagrass and macroalgal communities colonising the shallow coastal platform <10 m deep, which provide habitats for molluscs, red

algae, benthic foraminifera, bryozoans, and others to secrete their carbonate skeletons and contribute to sediment production, together with non-carbonate secreting organisms such as sponges. Whilst *Posidonia* sp., *Amphibolis actarctica*, and *Amphibolis griffithii* meadows are mostly located within a narrow belt of maximum 2 km from shore, macroalgal communities dominate the shallow limestone reef situated along the edge of the coastal platform ~4km from shore at ~10 m water depth. The sediment facies identified in the area reflect this habitat distribution, with fine modern skeletal sand mapped within a narrow belt of maximum 2 km from shore and this sediment facies is composed of ~60% of modern bioclasts supplied to the coastal system by seagrass meadows with the remaining composed of palimpsest biogenic sediments, mainly limestone-derived intraclasts and relict skeletal grains. Macroalgal communities are located in areas of higher environmental energy where the medium-coarse modern and relict skeletal sand sediment facies have been identified. Macroalgal communities supply different and less bioclasts (~40%) to the coastal system, which are mainly mixed to palimpsest biogenic sediments. Carbonate sediments produced by seagrass meadows are trapped within this habitat but are also transported towards the shore by the wave motion, and consequently seagrass-derived modern bioclasts supply and constitute the Geraldton beaches. In contrast, macroalgal-derived sediments are produced far from shore and are mainly found in situ. In fact, the limestone reef systems which support the development of macroalgal communities also constitute an obstacle for sediment transport, supporting the sediment facies partitioning.

The sediment thickness (min. ~0.5 m, max. ~2 m) found on the coastal platform at Geraldton shows that the coastal environment is sediment starved, as previously recognized for the southern and western margins of Australia (James et al., 1994). Published estimates of accumulation rates for seagrass related sediment are 20–100cm/1000 years (average 60cm/1000 years) for Australian cool-water carbonate environments and 90–150cm/1000 years (average 120 cm/1000 years) for Australian tropical carbonates (Rao, 1996). The west Australian continental shelf was completely exposed during the Pleistocene sea level regression as the sea level dropped to ~125m below the current sea level position, and sediment production and deposition only restarted following the Holocene transgression, with sediment transport towards the Geraldton coastal area during the Holocene sea level rise. Due to the lack of sediment dating and assuming that the sediment was transported since the Holocene transgression, minimum accumulation rates can be estimated for the Geraldton area. Considering that the last sediment accumulation cycle is ~6,000 years long (figure 68), approximately 3.6 m of sediment would be expected at Geraldton if a deposition rate of 60cm/1000 years would have occurred, but only 1 to 1.5 m thick accumulations are common on the Geraldton inshore platform where seagrass banks have been mapped. This

finding suggests a low sedimentation rate for the studied area, as the local sediment accumulation rate is approximately 20 cm/1000 years, at the lower extremity of the published range for Australian seagrass banks of cool-water environments.

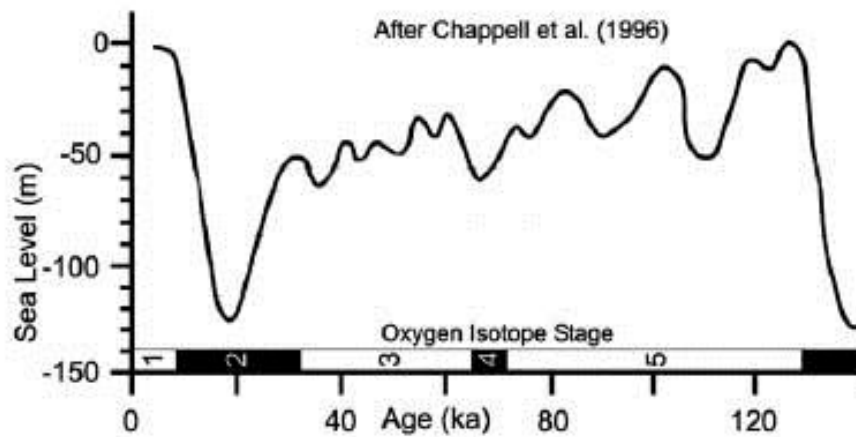


Figure 68: Quaternary eustatic sea level curve after Chappell et al. (1996). The study area was above mean sea level until the Holocene transgression started ~20 Ka ago.

Chapter 4

SEDIMENT DYNAMICS: an integrated analysis of hydrodynamic modelling, sediments, geomorphology and habitat data

4.1 INTRODUCTION

Sediment dynamics are mainly controlled by coastal processes such as nature, level, and direction of wave, tide, and wind energy, but are also a function of: the size of the material being transported on the seabed and throughout the water column (Hallermeier, 1981; Carter, 1988; Jiménez and Madsen, 2003; Short and Woodroffe, 2009); the underwater and coastal topography (Cooper and Pontee, 2006; Velegrakis et al., 2007); and the benthic habitats, especially when seagrass beds are developed within the study site (Fonseca, 1989; Hilton and Hesp, 1996; Verduin and Backhaus, 2000; Madsen et al., 2001; van Keulen and Borowitzka, 2002; Carruthers et al., 2007; Chen et al., 2007). As outlined in Chapter 1, along most of the Western Australian coast, including the study area, the combination of swell waves and strong sea breeze wave fields drives the prevalent northward-oriented longshore sediment transport (Short and Woodroffe, 2009; Short, 2010). Significant year-round swell waves coming from south-southwest are attenuated by coastal limestone ridges which are common in the study area at ~4 km from the shore (Chapter 2), reaching depths of ~4 m at the western edge of a 10 m deep coastal platform. Close to shore, wind waves generated by the strong prevailing south-south-westerly winds are superimposed on swell waves. The net littoral transport direction is determined by the angle between the local shoreline and the dominant incident wave and is not always to the north; however, there is an overall south to north transport pattern.

The nature of the data available for this study (hydrodynamic modelling, coastal topography, sediments, bathymetry, offshore sediment thickness and habitat data) led to a detailed understanding of cross-shore and alongshore sediment dynamics on the basis of geomorphological and sedimentological evidence. Hilton and Hesp (1996, p.497) state that “the boundary between wave-worked and non-wave-worked sediment may be apparent from the sediment size, grain preservation or faunal community structure”, and this was evident within the study area. Any seabed mobility study should be based upon an accurate sediment distribution map (Velegrakis et al., 2007), especially when the bioclastic input of sediment has been indicated as the main sediment source for the coast of Western Australia (Short, 2010). As part of sediment dynamics studies, the measurement of seabed bedform

parameters such as bedform height, wavelength and symmetry/asymmetry are used to identify water flows determining sediment transport on the seabed (Ashley, 1990; Ryan et al., 2007b). Beach profiles have also been widely applied in the past to qualitatively and quantitatively estimate longshore and cross-shore sediment transport (Masselink and Pattiaratchi, 2001; Pacheco et al., 2008; Rao et al., 2009; Rodriguez and Dean, 2009; Aagaard, 2011). When studying sediment dynamics it is important to consider the offshore boundary of sediment movement by using multiple approaches (Hilton and Hesp, 1996; U.S. Army Corps of Engineers, 2008), and consequently the theoretical calculation of the depth of closure was also carried out for the study area; this data is compared to sediment, bedform and nearshore geomorphology data in section 4.2.

A conceptual sediment budget model has been described as the first step in the development of a quantitative sediment budget for a stretch of the coast (Rosati, 2005; U.S. Army Corps of Engineers, 2008; Aagaard, 2011) and consists of a qualitative model describing the general processes regulating the sediment input, transport and accumulation within the study area (Rosati, 2005). The formulation of a conceptual sediment budget model is recommended prior to any quantitative sediment-budget calculation, to better understand the processes regulating sediment exchange between adjacent sediment cells (Rosati, 2005; Aagaard, 2011). This model is outlined in section 4.3 for the study site and includes identification of sediment sources, reconnaissance of artificial and natural sinks of sediment, and assessment of longshore sediment transport pathways on the basis of literature and environmental data, together with shoreline evolution data, to be used as a background for further analysis. It is a common routine to develop historical shoreline change analyses to assess areas of coastal retreat and accretion over a given period of time, and obtain useful information about longshore sediment transport to add certainty to the results of the longshore sediment transport modelling (Rao et al., 2009; Rodriguez and Dean, 2009; Aagaard, 2011). Historical shoreline change analysis of the study area was carried out as part of the "Geraldton Embayments Coastal Sediment Budget Study" (Tecchiato et al., 2012), carried out for the Western Australian Department of Transport by Curtin University, and data was made available for this thesis.

The understanding of littoral processes and the correct addressing of management issues are based upon the identification of coastal sediment cells, and recently an integrated approach which takes into account the characterisation of geomorphology, sediments, shoreline evolution, and local hydrodynamics has been regarded as the most appropriate method for delineating littoral sediment cells (Rosati, 2005; Cooper and Pontee, 2006; U. S. Army Corps of Engineers, 2008; Anfuso et al., 2011). In this study, the considerations made in sections 4.2 and 4.3, and based on the environmental characterisation of the Geraldton

coastal system, are brought together in section 4.4 to describe the sediment cells of the study site. Sediment cells were defined along the Geraldton coastal system using standard concepts and methodologies. Sediment cells were defined by McInnes et al. (1998, p.295) as: “a length of coastline which is relatively self-contained as far as the movement of sand or shingle is concerned, and where interruption to such boundaries should not have a significant effect on adjacent sediment cells”. Bray et al. (1995, p.386) presented a comprehensive overview of sediment cell boundaries which are used in this study (section 4.4) and state that “cells are identified according to morphological and process information and defined as relatively self-contained units within which sediment circulates”. The concept of sediment cells serves the quantitative determination of a coastal sediment budget, because a complete self-contained sediment budget exists within its boundaries (U.S. Army Corps of Engineers, 2008). In other words, the volume of sediment controlled (i.e. transported, sinking or supplied) by a sediment cell constitutes an entry element in that sediment tally which is a quantitative sediment budget.

A sediment budget is “a tally of sediment gains and losses, or sources and sinks” (Rosati, 2005, p.308) and the following equation is commonly used for calculating a sediment budget in terms of volume or as volumetric rate of change:

$$\Sigma Q_{\text{source}} - \Sigma Q_{\text{sink}} - \Delta V + P - R = \text{Residual}$$

where Q_{source} and Q_{sink} are the sources and sinks to the control volume respectively, ΔV is the net change in volume within the coastal cell, P and R are the amounts of material placed in and removed from the cell respectively, and Residual represents the degree to which the cell is balanced. Several approaches have been developed that solve Rosati’s (2005) sediment-budget equation which is considered the final aim of this study, and these methods often require longshore sediment transport modelling to gain quantitative data on sediment transport volumes set to the depth of closure. As such, quantitative modelling of longshore sediment transport was carried out in this study and its results are presented in section 4.5. Longshore sediment transport can be regarded as a sediment source when it supplies sediment to the coastal system, but it can also cause sediment losses when the downdrift-directed sediment transport is larger than the supply from updrift (Rosati, 2005; Aagaard, 2011). Sediment transport modelling carries large uncertainties (Thieler et al., 2000; Pilkey and Cooper, 2002; Aagard, 2011; Appendini et al., 2012), and field measurements to constrain transport models are scarce and not available for this study.

Finally, the quantitative sediment budget model for the identified littoral cells is outlined in section 4.6 providing a comprehensive overview of the littoral processes influencing the

sediment dynamics of the Geraldton coastal embayments. Aagard (2011, p.143) states that the “determination of the individual components of the sediment budget is not a trivial exercise because many of the source and loss terms are difficult to estimate”.

The results of this chapter were brought together in a paper submitted to *Geomorphology* and titled “An integrated approach to coastal dynamics in temperate Midwestern Australia: Sediment budget of a wave-dominated carbonate system” for which the candidate is first author. Appendix 3 shows a list of the project outcomes.

4.2 CROSS-SHORE SEDIMENT TRANSPORT

The depth of closure is widely used as an empirical measure of the offshore limit of significant cross-shore sediment transport on sandy beaches (Hallermeier, 1981; Hilton and Hesp, 1996; Nicholls et al., 1998; Phillips and Williams, 2007; Rodriguez and Dean, 2009; Short and Woodroffe, 2009). The depth of closure has been defined by Kraus et al. (1999, p.272) as “the most landward depth seaward of which there is no significant change in bottom elevation and no significant net sediment exchange between the nearshore and the offshore”. Figure 69 shows the relationship between the position of the depth of closure and the extent of the nearshore beach zone. The depth of closure is given by the term d_l of Hallermeier (1981, p.258) and it occurs where “intense bed activity is caused by extreme near-breaking waves and breaker-related currents”. It is to be noted that most research into the closure depth was carried out on sandy beaches with a thick sand layer in wave-dominated environments; consequently, variations may apply for beaches where the morphology is largely controlled by underlying geology (Schwartz, 2006). As described in Chapters 2 and 3, the Geraldton coastal platform is characterised by a veneer of active sand above a rocky limestone substrate and this may influence the morphology of the nearshore concave surface.

Sediment and bathymetry data are recognised indirect indicators of beach processes and provide useful data for the prediction of the seaward limit of a sandy beach (Hallermeier, 1981). In fact, variations in sediment facies are often found in the different beach zones (Carter, 1988; Hilton and Hesp, 1996). Bedform measurements were undertaken as part of this study and are indicative of areas with active bedload sediment transport when bedforms are asymmetric; however, bedforms are only indicative of wave shoaling when showing a symmetric morphology.

Repeated beach and nearshore profiles allow identification of the depth of closure as the depth at which topographic changes become insignificant (Nicholls et al., 1998; Krauss et al., 1999; Schwartz, 2006). Repetitive bathymetric surveys were not carried out in the study area; however, the nearshore concave-upward surface was observed on the multibeam bathymetry data. The term “nearshore” refers to a zone of active bedload sediment transport and is widely recognised as a concave-upward surface, described as an equilibrium response of an unconsolidated coast to the typical local wave and current regime (Niedoroda and Swift, 1981; Niedoroda et al., 1984; Short, 1984; Niedoroda and Swift, 1991; Hilton and Hesp, 1996). Figure 70 shows the cross-shore zonation of the beach environment and the nearshore zone corresponds to a dynamic zone dominated by wave shoaling processes (Krauss et al., 1999; Schwartz, 2006; Short and Woodroffe, 2009). Wave shoaling commences when deep-water ocean waves begin to interact with the seabed forming ripples and transporting sand landward (Short and Woodroffe, 2009). Whilst figure 69 shows a cross-shore zonation of the beach on the basis of hydrodynamic data, figure 70 is a cross-section of the beach where zones are defined on the basis of geomorphological features. The shoal zone of figure 69 coincides with the nearshore zone of figure 70, dominated by wave shoaling processes. The littoral zone of figure 69 includes the surf zone and subaerial beach of figure 70. The depth of closure (d_l of figure 69) is located at the landward boundary of the nearshore zone where shoaling waves transform into breaking waves inducing shoreward sediment transport.

In the following sections the results of sediment analyses (section 4.2.1), geomorphological mapping of bathymetry data (sections 4.2.2 and 4.2.3), and theoretical formulae (section 4.2.4) are discussed to understand the cross-shore sediment transport system within the study area. The setup of the longshore sediment transport modelling carried out in this project is based on these data.

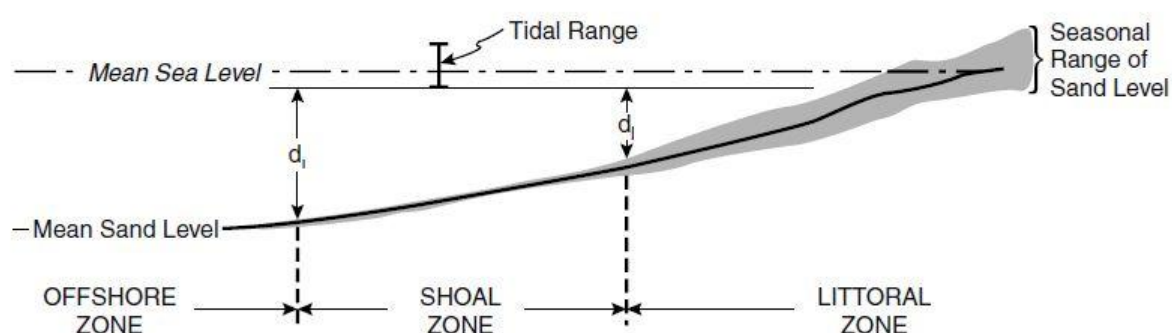


Figure 69: Sketch showing the limits of the nearshore zone and the position of the depth of closure, coincident with the d_l limit depth of Hallermeier (1981) and indicating a depth where “intense bed activity is caused by extreme near-breaking waves and breaker-related currents” (source: Schwartz, 2006).

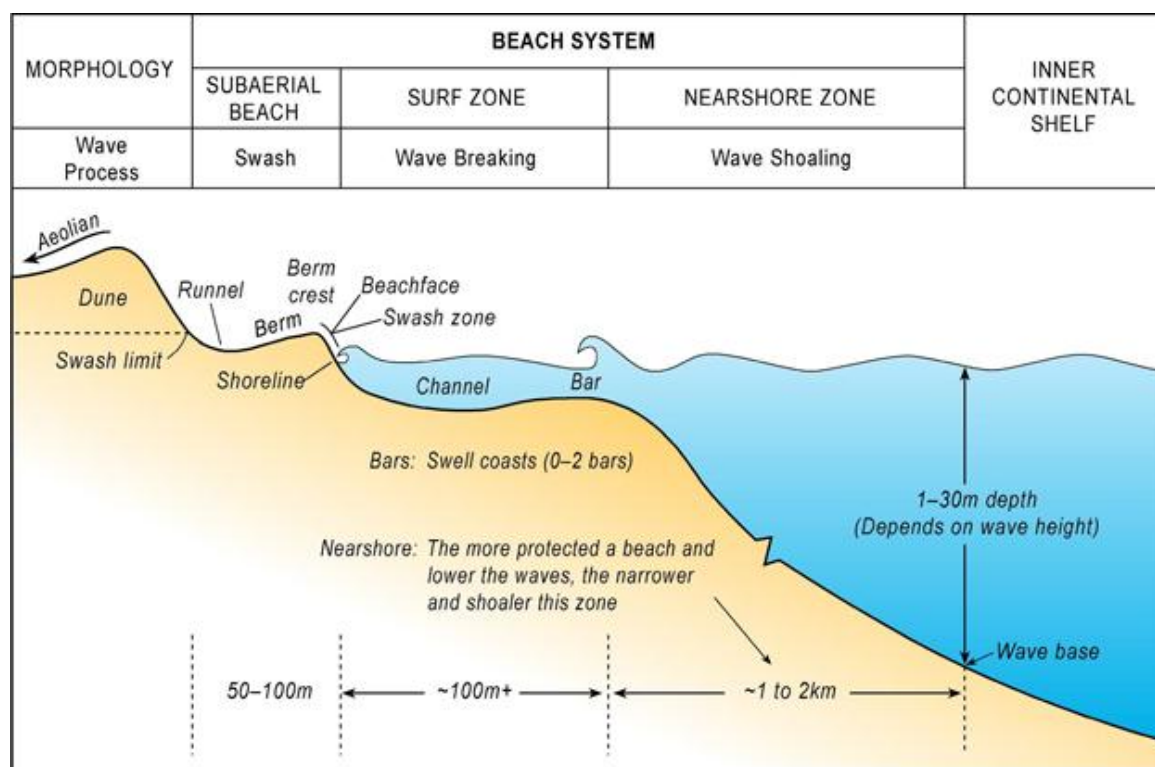


Figure 70: An idealised cross-section of a wave-dominated beach system outlining the nearshore zone, which extends out to wave base, where waves shoal to build a concave-upward slope (source: Short and Woodroffe, 2009).

4.2.1 Sediments

As shown in Chapter 3, four sediment facies were mapped at Geraldton: fine modern skeletal sand, medium-coarse modern and relict skeletal sand, fine-medium quartzose and modern skeletal sand, and coarse quartzose and relict skeletal sand. The latter sediment type was only found at depths greater than 15 m, and the relict constituents of this sediment together with the higher sediment thickness found through the seismic investigations at those depths demonstrate that this sediment facies has an independent transport mechanism compared to the shallower sediment facies. The medium-coarse modern and relict skeletal sand was also mapped at the seaward edge of the 10 m deep coastal platform found at Geraldton and does not interact with the shallower sediment transport mechanisms.

The largely continuous belt of fine modern skeletal sands close to the Geraldton shoreline is not common further offshore. This sediment has high carbonate content and most of the sediment constituents are modern bioclasts, consisting of calcified organisms living in association with seagrass meadows (Chapter 3); consequently, this habitat is considered a natural source of sediment for the Geraldton coastal system. This sediment facies was also found along the beaches where nourishment activities have not been previously undertaken,

especially south of Geraldton, at Point Moore and Pages beaches and north of the Chapman River mouth. This indicates that the sediment produced by the seagrass communities is transported shoreward onto the beaches by wave motion, but no evidence of relevant offshore transport of this type of sand was found. Consequently, the fine carbonate sand belt appears to have a separate dynamic to the surrounding areas and the sediment supplying the beaches is expected to be transported between 0 and ~10 m depth and within an area extending to a maximum of 2 km offshore (figure 71).

A major fraction of the fine-medium quartzose and modern skeletal sand sinks in the middle of Champion Bay, where a relatively high sediment thickness was found (~2 m; Chapter 3). This sediment facies extends mostly off the Chapman River mouth with limited sediment redistribution to the north. Offshore sediment transport is occurring at this location which allows the deposition of quartzose sand from the Chapman River mouth to ~2 km offshore (see section 4.3 for further details), thereby impeding a clear identification of the seaward limit of the longshore sediment transport system to be established on the basis of sediment data.

In summary, the fine modern skeletal sand and the fine-medium quartzose and modern skeletal sand sediment facies contribute to the nearshore sediment transport system, with the difference that the fine-medium quartzose and modern skeletal sand sediment facies is limited to the middle part of the northern Geraldton embayment, and the fine modern skeletal sand sediment facies dominates elsewhere. The sediment supplying the shore consists largely of fine modern skeletal sand and is expected to be transported between 0 and maximum 10 m depth and within an area extending to a maximum of 2 km out at sea. The fine-medium quartzose and modern skeletal sand largely sinks in an area 5–10 m deep, located in the middle of Champion Bay and is expected to be only partly redistributed along the shore by littoral currents. Little data exists to compare the results of this highly-detailed analysis of a non-tropical carbonate system at a regional scale, as many of the studies previously carried out in Western Australia concerned the continental shelf or deeper regions of the seabed.

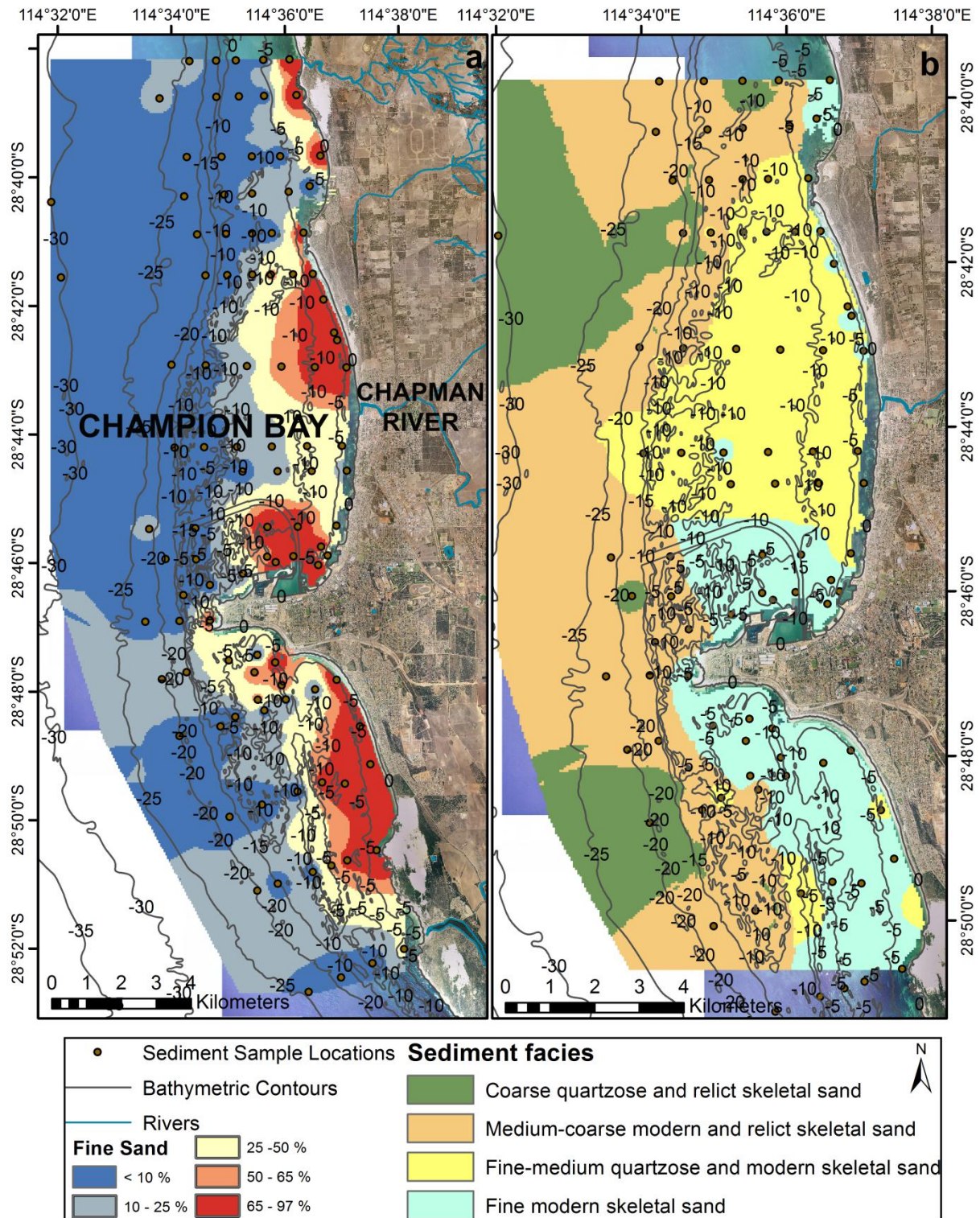


Figure 71: A) Interpolated % fine sand at Geraldton. The seaward limit of the nearshore based on sediment data is approximately coincident with the extent of >65% fine sand-dominated sediment class. B) Sediment facies at Geraldton. The distribution of fine-medium quartzose and modern skeletal sand south of Geraldton is an artefact of data interpolation, and these areas are likely to be part of the surrounding fine modern skeletal sand and medium-coarse modern and relict skeletal sand polygons.

4.2.2 Nearshore geomorphology

For open ocean beaches, the depths of the upper and lower boundaries of the nearshore are primarily controlled by wave and current climates, but the offshore bathymetry also influences sediment transport. In the study area, the significant slope terminating the coastal platform located ~4 km from the shore, extending from 10 to 30 m depth, acts as a topographic obstacle for sediment movement, obstructing the interaction between offshore currents and the littoral system. Moreover, the configuration of the coastal platform at Geraldton, with shallow limestone ridges ~4 km from shore, reduces the wave heights at the coast, thereby sheltering the beaches. Discontinuously along the shoreline, the nearshore concave surface was observed mostly at a distance of ~400 m offshore and at ~5 m depth in the northern Geraldton embayment; however, a depth range between 3.5 and 6.5 m was observed in the southern Geraldton embayment. As stated previously, the Geraldton coastal platform is characterised by a veneer of active sand above a rocky limestone substrate and the morphology of the nearshore concave surface results from the deposition of the available sediment on the pre-existing limestone topography, as regulated by wave and current characteristics.

Limestone ridges are also common in close proximity to the beaches (Chapter 2) and were mapped on the multibeam bathymetry at locations where the nearshore concave surface was not visible, as summarised in table 14. Where a poor sandy cover was noted along the shore, sand bar and sheet systems were found further offshore and the nearshore concave surface was not visible. As described in table 14, the locations where the limit of the nearshore could be clearly identified on the bathymetry data are scarce, especially due to the frequent rock exposure along the coast, and consequently this data needs to be used with caution.

The offshore boundary of the nearshore can vary greatly at small temporal and spatial scales. For example, Stul et al. (2012) identified a hierarchy of coastal compartments for the Western Australian coast based on broadscale geological and geomorphologic settings and identified three offshore limits of the nearshore zone. However, the 5 m isobath was the most common boundary used by Stul et al. (2012) and was considered to approximately correspond with the extent of the nearshore. This agrees with some of the geomorphological observations gained in this study on the basis of the multibeam bathymetry data.

Table 14: Offshore geomorphology and beach characteristics throughout the study area.

Beach	Beach typology (Short, 2006)	Offshore geomorphology (as resulting from the mapping of multibeam bathymetry data)
Southgate	PERCHED	Offshore ridges and sand bar and sheet system
South Tarcoola Beach	REFLECTIVE	Nearshore zone developed to 170 m offshore to -3.5 m depth
North Tarcoola Beach	DISSIPATIVE	Nearshore zone developed to 400 m offshore to -6.5 m depth
Grey's Beach	REFLECTIVE	Offshore ridges
Point Moore	DISSIPATIVE	Offshore ridges
Page's Beach	REFLECTIVE	Offshore ridges
Town Beach	REFLECTIVE	Nearshore zone developed to 400 m offshore to -5 m depth
Northern Beaches opposite Mark St	PERCHED	Offshore ridge
Northern Beaches opposite Hosken St	REFLECTIVE	Offshore ridge
Northern Beaches opposite Morris St	REFLECTIVE	Offshore ridge
Chapman River mouth	REFLECTIVE	Offshore sand bar and sheet system
Sunset Beach	REFLECTIVE	Offshore sand bar and sheet system
Drummond Cove North	REFLECTIVE	Nearshore zone developed to 400 m offshore to -4.8 m depth, offshore ridges also present

4.2.3 Bedforms

The asymmetry of seabed bedforms reflects the dominance of bottom currents (i.e. offshore versus onshore currents) oriented transversally to the bedform crests (Ashley, 1990; Hilton and Hesp, 1996). The transition from symmetric to asymmetric bedforms seems to be linked to variations in water depth, grain size, bottom current velocity, wave period, and wave asymmetry; however, modal wave base is generally interpreted to occur when asymmetric bedforms become dominant (Ashley, 1990; Hilton and Hesp, 1996). As outlined in Chapter 2 (figures 22 to 24), rippled sand flats were found to ~10 m depth throughout the study area indicating that the wave action influences the whole coastal platform at Geraldton which is ~10 m deep. These sandy areas are dominated by symmetric ripples (wavelength <1 m; cf.

Ashley, 1990), with the exception of one location off the Batavia Coast Marina <1 km from the shore at 5 m depth where asymmetrical ripples were mapped, indicating a northward oriented bottom current. Larger bedforms (underwater sand dunes; wavelength = 1–10 m; cf. Ashley, 1990) were mapped to the east of Separation Point at 7–10 m depth and are asymmetric to the north-east, indicating a stronger bottom current and higher sand availability in this location, where a gap in shelter from the shallow limestone ridges exists. These larger bedforms are not representative of the average wave climate at Geraldton, as the bay to the east of Separation Point is influenced by higher wave energy than the rest of the coast.

Overall the coastal system shows symmetrical ripple dominance with no clear transition from symmetric to asymmetric ripples moving toward the coast as commonly found in nearshore systems (Short, 1984; Hilton and Hesp, 1996). This is probably because seagrass meadows and sparsely-vegetated seagrass and macroalgae substrates are common in the study area and limit sediment movement and bedform development (Chapter 2).

4.2.4 Depth of closure

Hallermeier (1981) developed the first empirical formula for the depth of closure using laboratory data and limited field results. However, based on field data, Birkemeier (1985) demonstrated that the formula of Hallermeier (1981) provides a conservative estimate of the depth of closure. Birkemeier (1985) also indicated that a simple formula based on H_e (nearshore storm-wave height that is exceeded only 12 hours per year) provides a reasonable estimate of the depth of closure. The data available for this study is suitable to the application of the Birkemeier (1985) formula and this was used to predict the depth of closure (DoC) in the study area as indicated below.

$$\text{DoC} = 1.57 H_e = 1.57 * 3.32 = 5.21 \text{ m}$$

The coastal configuration landward of the coastal platform at Geraldton produces wave breaking ~4 km from the coastline, and reduced wave heights reaching the coast are responsible for sediment transport, possibly explaining why a shallow depth of closure is expected for the study area and rendering the depth of closure value of 5.21 m a representative assessment. The topographic elevation of the pre-existing limestone of the coastal platform may also be an ancestral control. It is likely that high-energy events are accompanied by significant cross-shore and alongshore sediment redistribution and transport, but this is difficult to estimate or model, especially considering wave penetration through gaps in the reef barrier at the coastal platform edge. Both the reef barriers and the

ancestral limestone topography of the coastal platform distinguish the Geraldton area from an “ideal” sandy coast.

At Geraldton, theoretical formulae show some agreement with sedimentological and geomorphological data in determining the depth of closure. Sediment data clearly show sediment exchange between the shore and the fine modern skeletal sand sediment facies developed between 0 and maximum 10 m depth and within an area extending to a maximum of 2 km from the shore. The calculated depth of closure value of 5.21 m falls within <2 km of the Geraldton shoreline where the sediment facies supplying the nearby beaches was mapped. Observation of bedform morphologies has demonstrated that the overall wave climate has sufficient heights and periods to initiate bottom sediment particle movement over the entire (10 m deep) coastal platform with no clear transition from symmetric to asymmetric ripples moving toward the coast. However, asymmetrical ripples were only found at 5 m depth in the northern Geraldton embayment, and this observation supports the calculated depth of closure value of 5.21 m.

A range of depth of closure values published in Hilton and Hesp (1996) quote 6.6 m for the northeast New Zealand coast, which has a similar wave climate to that of Geraldton.

4.3 CONCEPTUAL SEDIMENT BUDGET MODEL

4.3.1 Sediment sources

Based on the description of sediment facies (Chapter 3), the input of modern sediment into the coastal system is linked to living marine communities, such as seagrass meadows and macroalgal communities colonising shallow reef systems, contributing up to ~60% of the sediment supply in the areas mapped as fine modern skeletal sand and exchanging sediment with the coast. This sediment is then redistributed along-shore by the littoral currents and as such the input of sediment deriving from the living biota needs to be accounted for as part of the longshore sediment transport calculated in section 4.5.

The Chapman River input of sediment into the coastal system is clearly evidenced by the presence of quartz in the sediments deposited off its mouth. The lower carbonate content found in the sediments mapped off the Chapman River mouth indicates the presence of minerals other than carbonate in the sediments, and quartz is a clear indicator of riverine input. The circled area on the isopach map of sediment thickness (figure 72) shows that 2 m of sediment cover is present off the Chapman River mouth, but the surrounding areas only have ~1m sediment thickness. Figure 72 shows the correlation between low carbonate

content and a thicker sediment volume on the isopach map off the Chapman River mouth. The correspondence between higher sediment thickness and lower carbonate content led to the conclusion that river-derived sediment does not seem to significantly contribute to the littoral transport, but is more likely to sink in the middle of Champion Bay. Part of the river-supplied sediment is expected to be redistributed along the shore by the littoral currents and deposit along the Northern Beaches and Sunset Beach. Unpublished data suggests an average sediment input of $Q_{\text{source}} = 10,600 \text{ m}^3/\text{year}$. A complex history of sand bypassing and nourishment activities along the town beaches has made the Northern Beaches and Town Beach artificially supplied systems; however, sediment data has shown limited transport of quartzose-rich sand towards the Northern Beaches and Sunset Beach when the Chapman River floods disrupt the sand bar, normally closing the river mouth.

The isopach map of sediment thickness, together with the multibeam bathymetry and backscatter maps, show sediment accumulation off Southgate dune (figure 73), which together with the historical evolution of this coastal landform supports the identification of the dune system as a sediment source for the Geraldton southern embayment (see Chapter 1). It is known that the dune system is migrating northwards and oceanwards, with demonstrated vegetation loss and sediment supply to the ocean (Short, 2006a; Stevens and Collins, 2011). The non-modern skeletal sand (~20%) component of the areas mapped as fine modern skeletal sand off Tarcoola Beach is considered coincident with the Southgate dune sediment input. The fine modern skeletal sand facies in the area is mainly carbonate (average ~80%, up to ~98%) and, due to the offshore limestone ridge isolating the coastal environment, a limited sediment input is expected from processes of shelf erosion in the area. Consequently, the non-modern skeletal sand component of the fine modern skeletal sand sediment facies off Tarcoola Beach is likely to derive from Southgate dune. Petrologic observation of sediment samples from these locations was also indicative of this finding. Based on unpublished data, an average sediment input of $Q_{\text{source}} = 38,500 \text{ m}^3/\text{year}$ is suggested for this landform.

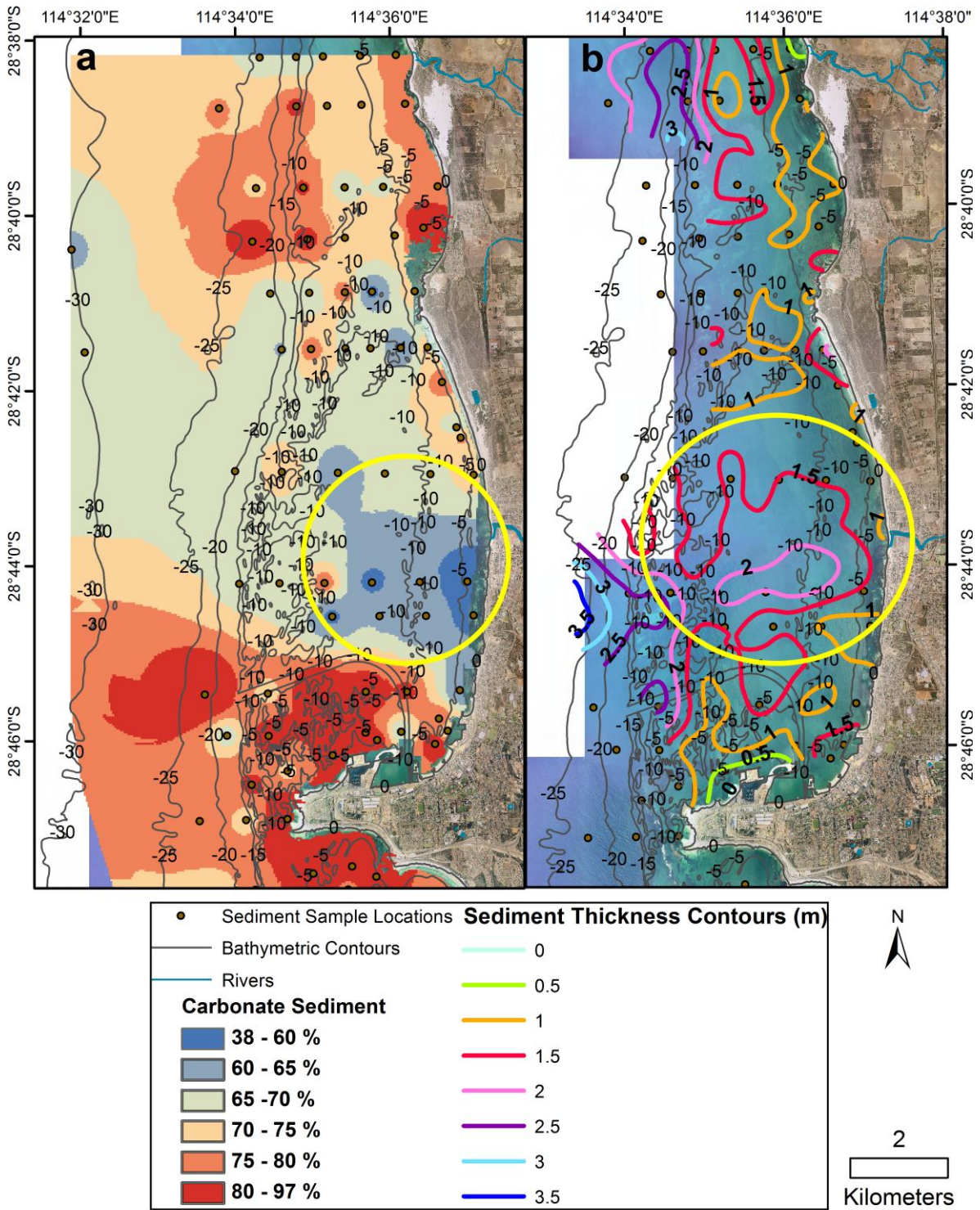


Figure 72: Correspondence between Chapman River input of sediment identified through low carbonate content (a) and higher sediment thickness found at the same locations on the Geraldton coastal platform (b). On the carbonate content map (a), blue tones indicate low %, grey tones intermediate %, and red tones high % of carbonate sediment. On the isopach map of sediment thickness (b), the average sediment thickness of 1 m is indicated by the orange contour, and areas of sediment accumulation (2 m thickness) are shown by the pink contour.

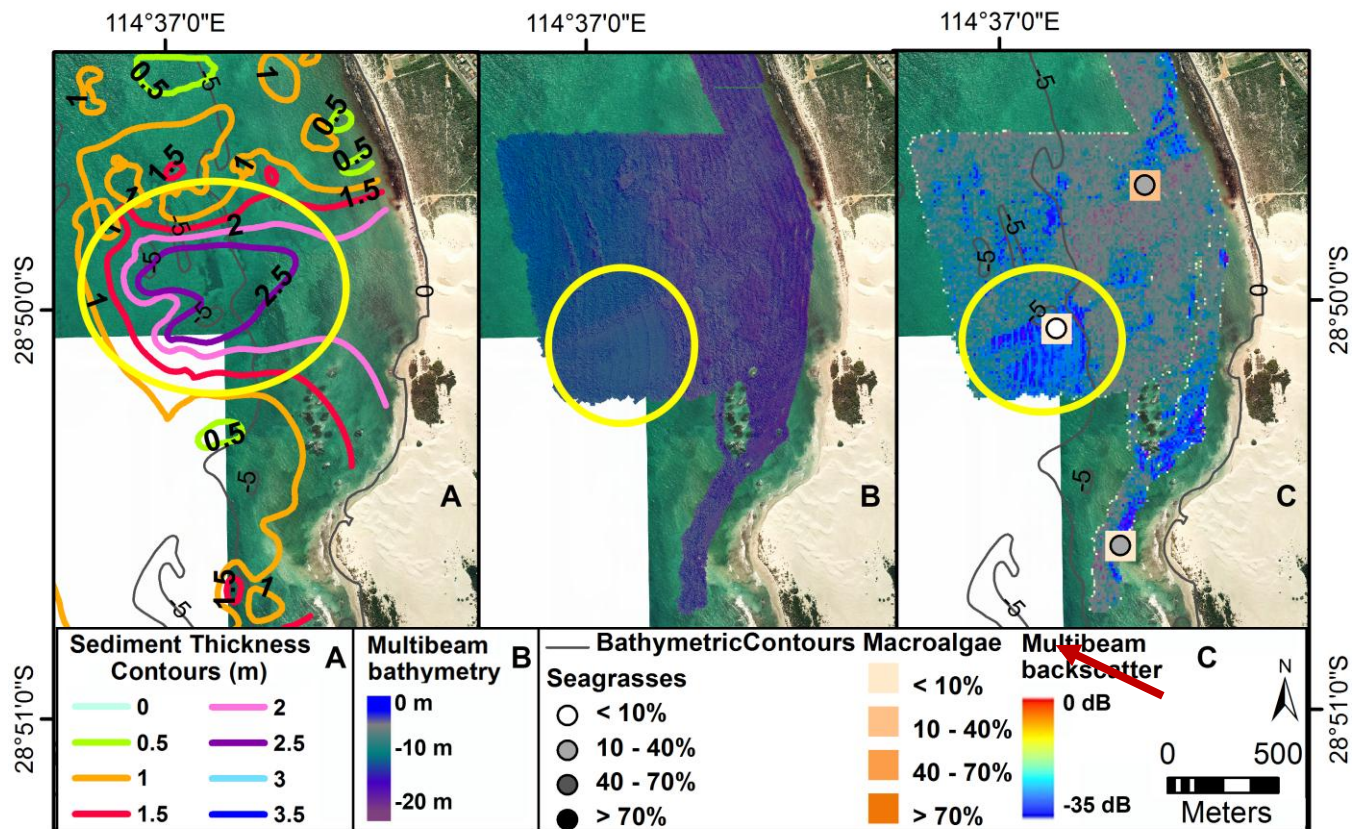


Figure 73: Correspondence between the Southgate dune inputs of sediment found through morphology and habitat mapping and a higher sediment thickness on the isopach map. The circled area on the isopach map (A) shows 2 m of sediment thickness, with the surrounding areas at ~1 m. An offshore limestone ridge is also evident and is likely to limit the exchange of sediment supplied by Southgate dune with the offshore. A sand bar and a few sand sheets are visible at the same location on the bathymetry data (B), with the sand dominance confirmed by the low backscatter values (C) and the results of underwater imagery analyses.

4.3.2 Sediment storage

The comparison of multibeam bathymetry data from 2002–2003 and 2010 within the Port basin and dredged channel has shown that there is sediment accumulation at the following locations (shown in red on figures 74 to 76): within the Port basin, a few hundred meters north of the port entrance, and where the channel bends curving westwards, about 3 km north of the Geraldton Port entrance. These regions were also mapped as part of the sand bars and sheet system when undertaking underwater morphology mapping which confirms sediment accumulation. Moreover, a W-E oriented bathymetric profile of the channel ~350 m north of the Geraldton Port entrance (figures 77 and 78) shows the asymmetric morphology of the dredged channel margins. The western margin has a gentler slope than the eastern margin, and this morphology is related to the higher sediment coverage on the western margin of the channel. Also, where the channel bends curving westwards, about 3 km north of the Geraldton Port entrance, the multibeam bathymetry shows a similar channel

morphology, but with sediment depositing on the southern margin of the channel (figures 77 and 79). The above-mentioned data allows us to consider the dredged channel and Port basins as artificial sinks for the eastward and northward littoral sediment transport systems from Point Moore towards the shoreline. A Geraldton Port Authority communication and information from JFA Consultants have advised that the estimated volume for the maintenance dredging works of 2012 was 125,000 m³, and this is the first dredging activity since the 2002–2003 campaign, making the average accumulation equal to $Q_{\text{sink}} = 12,500 \text{ m}^3/\text{year}$. The volume is to be split between the channel (~71,000 m³) and harbour basin (~54,000 m³), with the main areas of sediment accumulation within the channel corresponding to the “channel bend” and the entrance to the Port basin.

The sand bar and sheet system developed in between the limestone ridge system north of Point Moore is also trapping a significant amount of sediment, and has been identified as a natural sediment sink in the study area which has been assessed to be trapping sediment at an average rate of $Q_{\text{sink}} = 210 \text{ m}^3/\text{year}$. In fact, the results of this study outline the role of Point Moore as a “permeable barrier” to sediment (cf. Bray et al., 1995; Anfuso et al., 2011; Anfuso et al., 2013) which is transported from the southern to the northern embayment, and “sinks” in between the limestone reef system to the north of Point Moore (figure 80). The rate indicated for this feature is a long-term average of sediment erosion and deposition based on sediment thickness data, and consequently it is difficult to assess its accuracy.

The Batavia Coast Marina is also trapping sediment as indicated by the seabed mobility mapping and visible in figure 80. In fact, the sandy substrate dominance and the presence of sand bars in the area indicate sediment accumulation; however, an estimate of the accumulation rate is not possible due to the lack of sediment thickness data.

A natural sediment sink was also identified in the middle of Champion Bay which has been assessed to be trapping sediment at an average rate of $Q_{\text{sink}} = 250 \text{ m}^3/\text{year}$. Figure 72 shows the correspondence between quartz abundance and thicker sedimentary cover off the Chapman River mouth, which led to the conclusion that sediment transported to the ocean by the Chapman River is depositing in the middle of Champion Bay and not significantly interacting with the littoral transport system. A sand bar and sheet system was mapped in the area as part of the underwater morphology and habitat mapping, which is also indicative of sediment accumulation (figure 81). The rate indicated for this feature is a long term average of sediment erosion and deposition based on sediment thickness data, and consequently it is difficult to assess its accuracy.

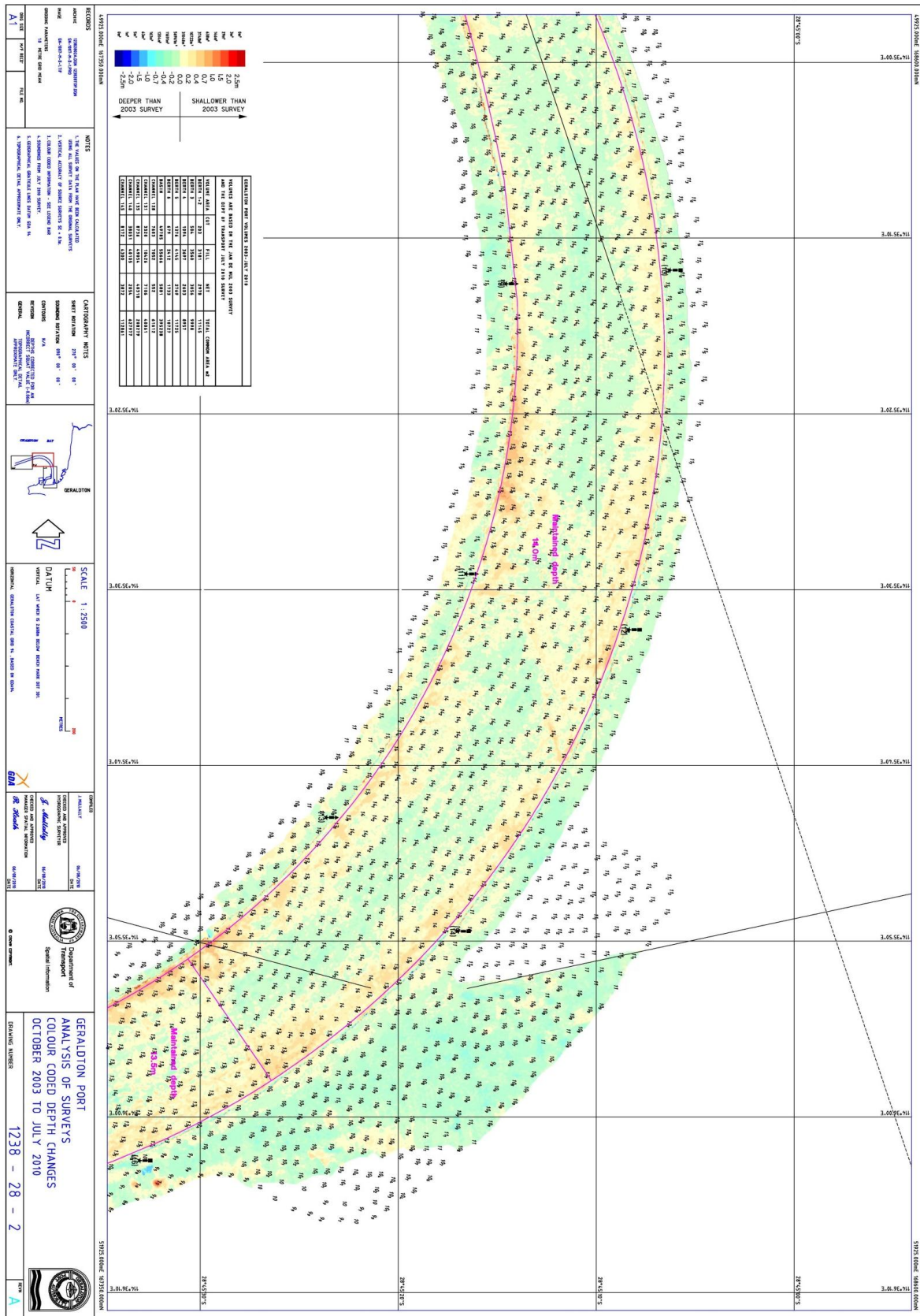


Figure 75: Comparison of multibeam bathymetry data from 2002–2003 and 2010 within the port basin and dredged channel areas (provided by the Western Australian Department of Transport). Blue tones indicate areas deeper in 2010 than in 2003, yellow tones indicate areas of no bathymetry change, and red tones indicate areas shallower in 2010 than in 2003. Consequently sediment accumulation occurs in the areas in the red zones.

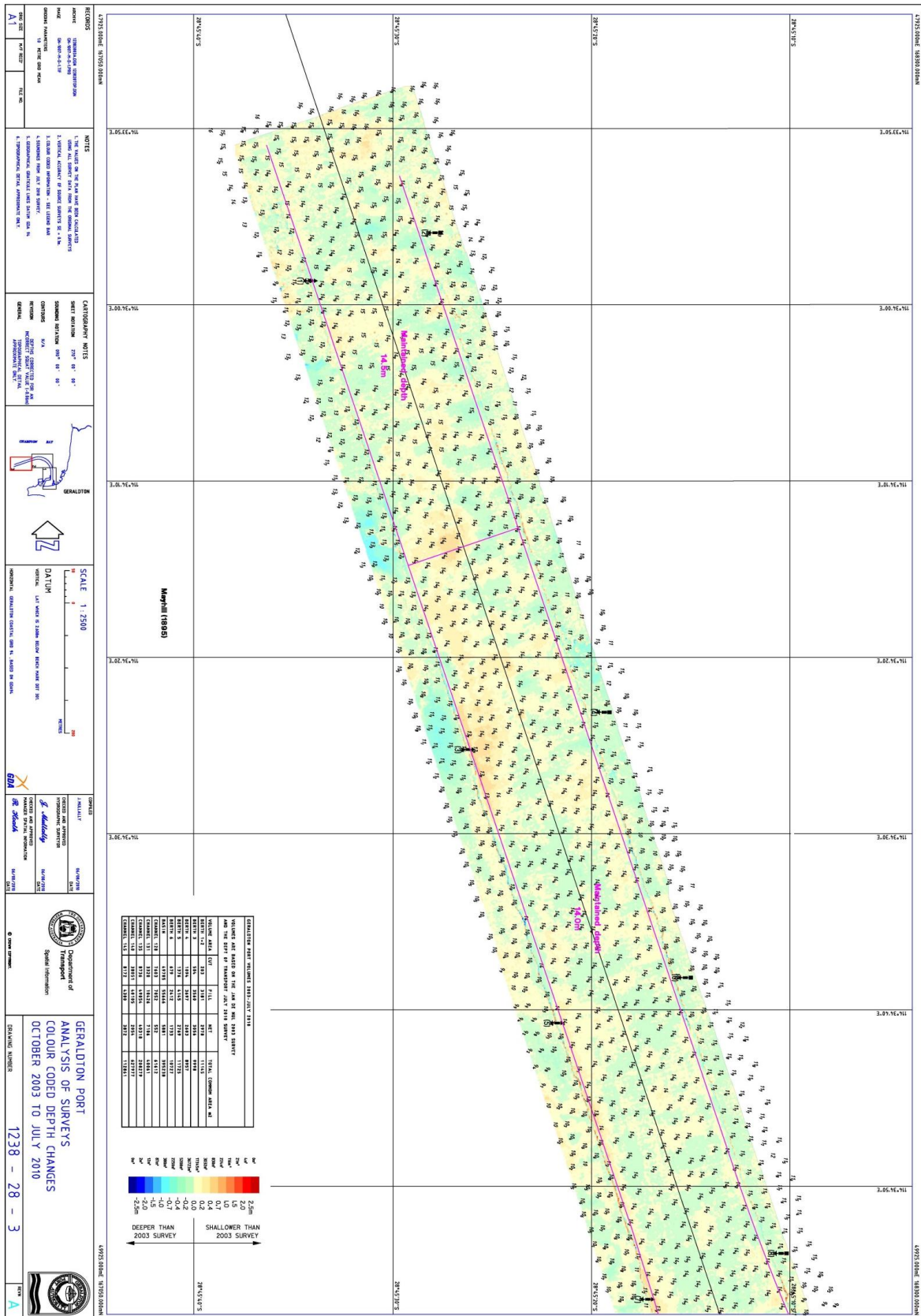


Figure 76: Comparison of multibeam bathymetry data from 2002–2003 and 2010 within the port basin and dredged channel areas (provided by the Western Australian Department of Transport). Blue tones indicate areas deeper in 2010 than in 2003, yellow tones indicate areas of no bathymetry change, and red tones indicate areas shallower in 2010 than in 2003. Consequently sediment accumulation occurs in the areas in the red zones.

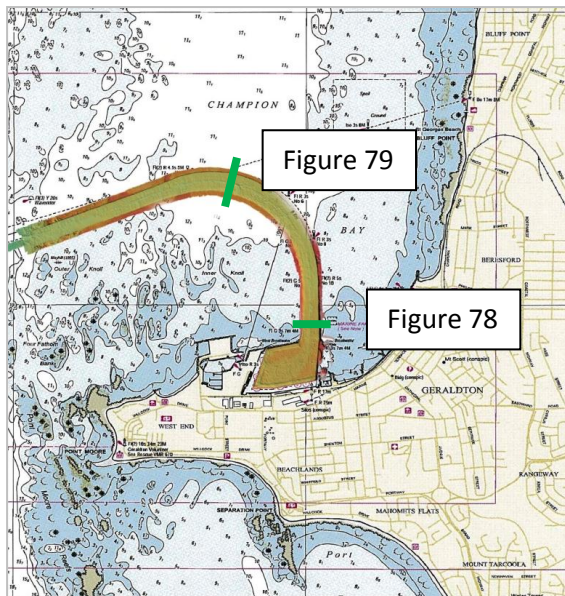


Figure 77: Location of figures 78 and 79.

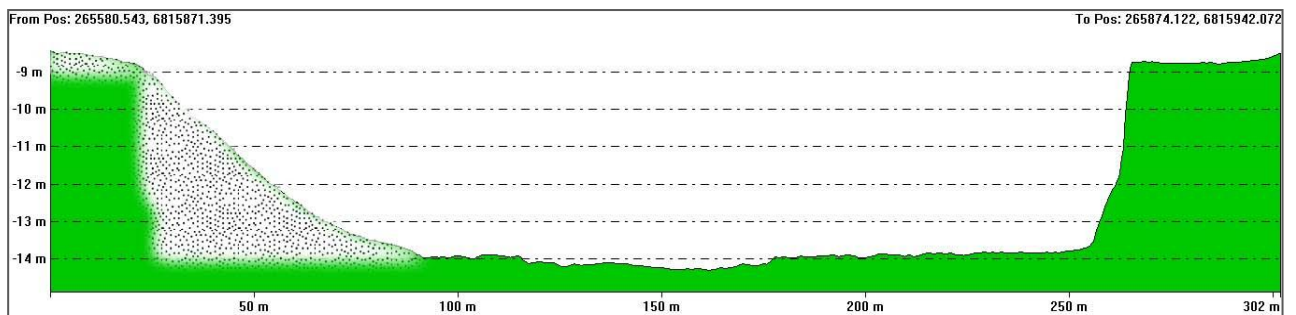


Figure 78: W-E bathymetric profile of the dredged channel (location on figure 73). The dotted area indicates the sediment cover.

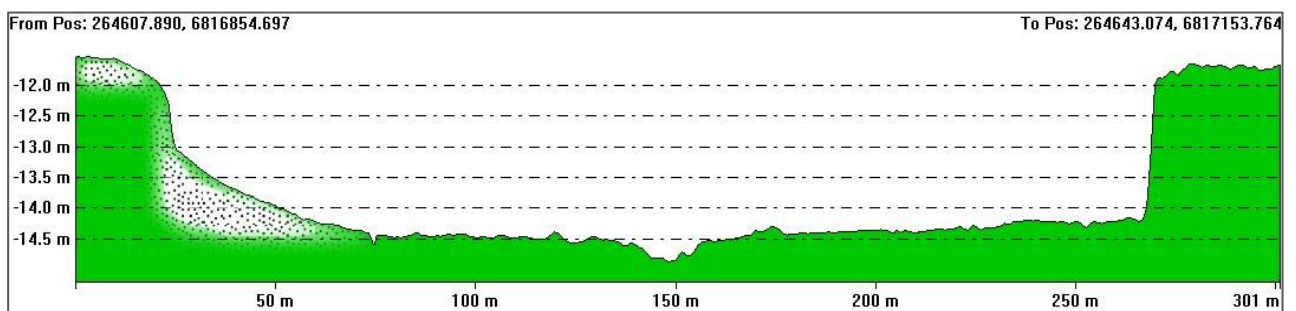


Figure 79: SSW-NNE bathymetric profile of the dredged channel (location on figure 73). The dotted area indicates the sediment cover.

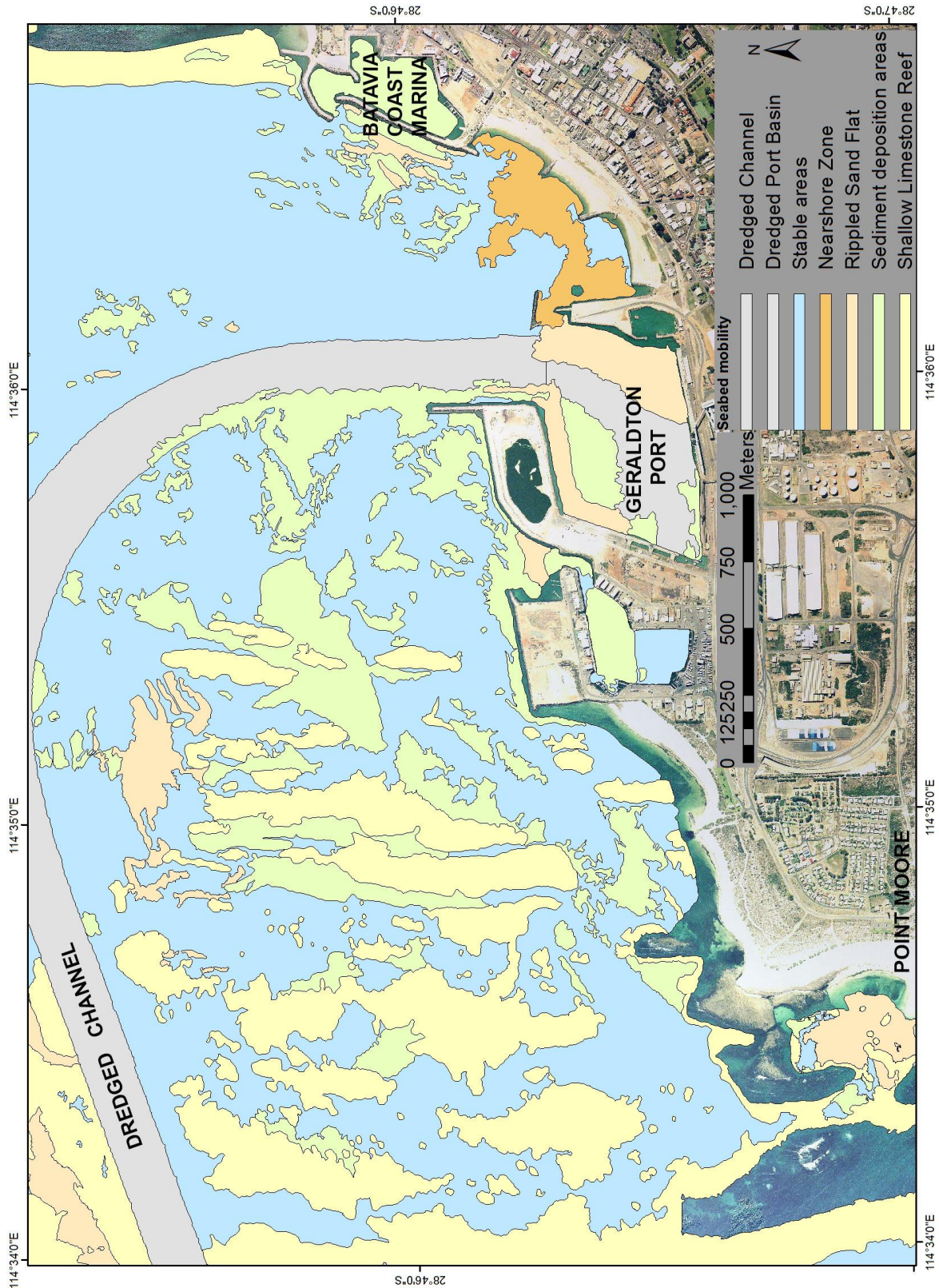


Figure 80: Detail of a modified version of the seabed mobility map discussed in Chapter 2 to allow the location of shallow limestone reefs to be visualised (yellow polygons). The map outlines the sediment deposition areas (green polygons) developed in between the limestone reef to the north of Point Moore, which are natural sediment sinks for the coastal system. The dredged channel and Port basins are indicated by the grey polygons where sediment deposition does not occur; however, the green polygons falling within their basins indicate areas of sediment deposition. The Batavia Coast Marina also includes a green polygon and it was recognised as an artificial sediment sink for the coastal system.

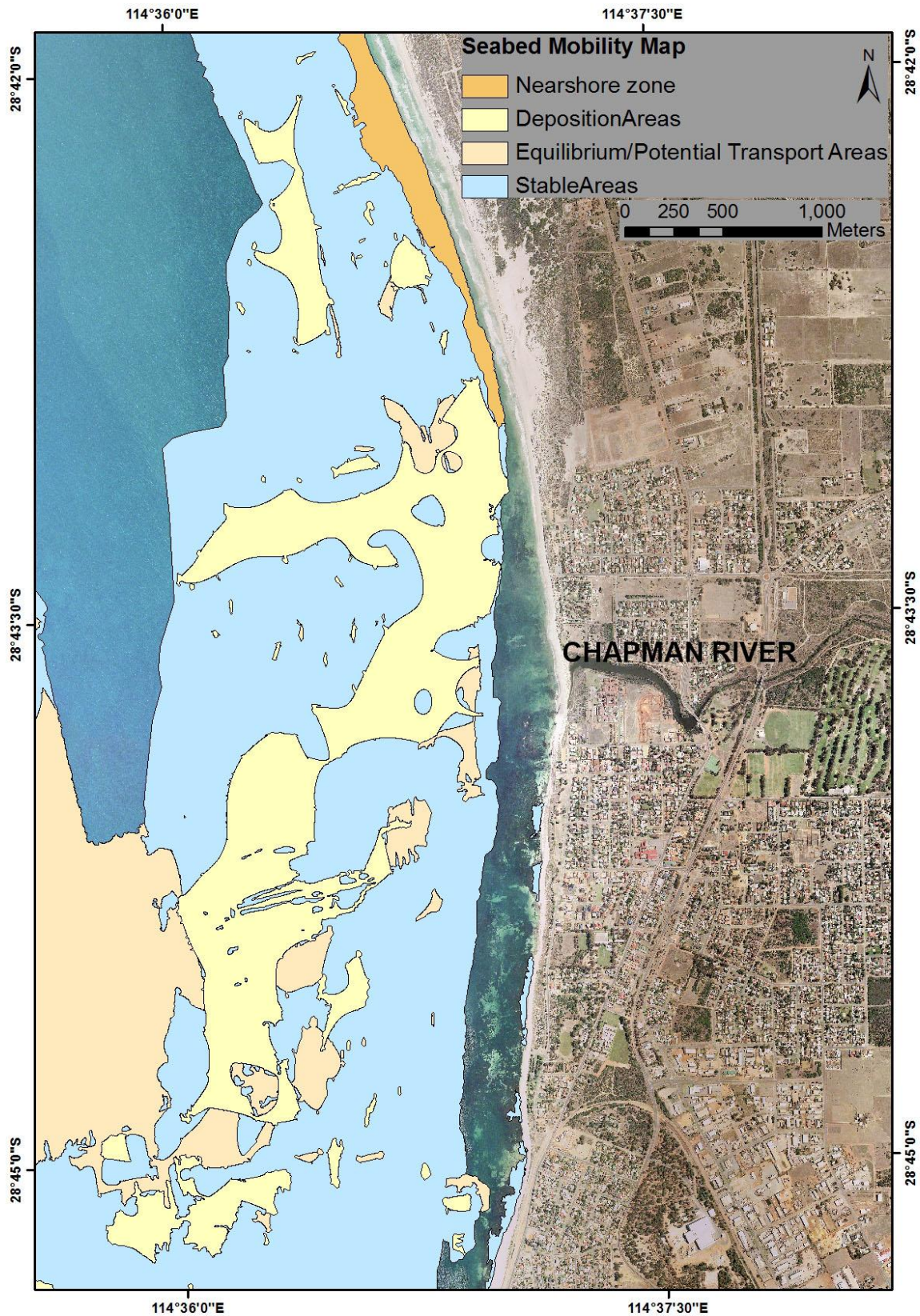


Figure 81: Detail of the seabed mobility map discussed in Chapter 2 outlining the sediment deposition areas (yellow polygons) off the Chapman River mouth. These are natural sediment sinks for the coastal system.

4.3.3 Longshore sediment transport pathways

Longshore sediment transport can be regarded as a sediment source when it supplies sediment to the coastal system, but it can also cause sediment losses when the downdrift-directed sediment transport is larger than the supply from updrift (Aagaard, 2011). At Geraldton, the overall sediment transport pathway appears mainly driven by northward-oriented currents. Short term variations can apply to this model, especially during the winter months or when storms occur, and transport direction is reversed.

Sediment storage occurs if the beach is prograding and/or the upper shoreface is aggrading (Aagaard, 2011), and in the study area cross-shore profiles show wide variability in their characteristics with varying slopes and irregular nearshore bathymetry (figure 82). North and south of Point Moore, the beaches show different characteristics in terms of morphology, extent, and evolution pattern. In terms of swash-zone width, there is an average of 30 m south of Point Moore and about 15 m in the northern embayment, with the widest beach width recorded at Point Moore (~84 m).

Southgate and Tarcoola Beaches show similar profiles with a number of offshore bars present in the surf zone and a relatively well-defined nearshore, indicating that this section of the coast is quasi-uniform alongshore with a general trend of stability or localised accretion/erosion (figures 82a, 82b, and 83e) and no significant input from the longshore sediment transport. The localised cases of shoreline erosion are connected to beach access tracks. The inner bar at Southgate is broader and shallower than at Tarcoola, suggesting higher sediment accumulation in the area. Sediment deposition was observed in the area, and the presence of a broad inner bar also confirms that Southgate dune is a source of sediment for this coastal compartment (as discussed in section 4.3.1).

The understanding of beach evolution patterns achieved in this study allowed the recognition of the natural northward and westward migration of Point Moore, with beaches naturally eroding on the southern side and accreting on the northern side (figure 84). Greys Beach shows an irregular substrate offshore with very little bars (figure 82c) and has shown significant erosion in the past decades (figure 83d). There is a general trend of sediment transport to the north of Point Moore, with sediment deposition and subsequent wide beaches at Point Moore and Pages beaches. These beaches show well developed bars offshore as well as a limestone reef system which protects the shoreline from high ocean swell waves (figures 82d and 82e). Sand is naturally accumulating at Pages Beach and is mined for nourishing the Northern Beaches with an average sand volume of $R = 12,500 \text{ m}^3/\text{year}$. The littoral current flowing from south of Point Moore and feeding Point Moore and Pages beaches continues northwards and eastwards, transporting sediment towards the

dredged channel, with sediment deposition documented within the channel at two locations: 350 m north of the port entrance and 3 km north of the port entrance where the channel bends (section 4.3.2). The littoral current flowing from south of Point Moore and filtering between the ridge systems of the area is likely to continue north of the dredged channel oriented towards the middle of Champion Bay.

Town Beach is a highly modified beach and has shown significant accretion linked to infrequent nourishment activities and placement of groynes in the 2000s. The cross-shore profile visible in figure 82f is indicative of a reflective beach as defined by Short (2006b), with a simple morphology and the boundary of the nearshore at ~5m depth.

The Northern Beaches are also reflective according to the classification by Short (2006b) and are stabilised by regular nourishment activities ($P = 12,500 \text{ m}^3/\text{year}$). Of note is a major sand placement of $89,000 \text{ m}^3$ in 2004. The relatively low carbonate content of the sediment characterising the Northern Beaches (Chapter 3) might indicate a limited redistribution southward of the quartzose sand supplied by the Chapman River to the coast. The cross-shore profiles (figures 82g, 82h, and 82i) show a relatively narrow beach system with irregular small sand bars present, indicating little sediment accumulation in the submerged beach zone; however, the morphology of the profiles indicates that most of the sediment deposition is occurring in the upper beach zone, allowing shoreline stability to be maintained. Evidence of a northward littoral transport at shallow depths along the Northern Beaches is provided by the asymmetrical deposition of sand adjacent to the island breakwater (figure 85), which is a qualitative indicator of sand accumulation south of the island breakwater. Evidence of this process is also provided by the asymmetrical ripples mapped off the Batavia Coast Marina as part of the multibeam bathymetry data analysis (Chapter 2).

The Sunset Beach area is similar to the region off the Chapman River mouth (figures 82j and 82k), with a relatively steep, narrow beach profile and four small sand bars indicating significant cross-shore sediment transport in the area with offshore sediment deposition, well-balanced by the high erosion rate recorded at Sunset Beach, with an average of 1.5 m/year. Glenfield Beach has a stable coastline and shows two well-developed sand bars offshore (figures 82l and 82m), indicating significant sediment storage in the area; however, the overall shoreline evolution trend indicates stability (figure 83a).

Cross-shore profiles were not repetitively surveyed in time and so volumetric calculations and morphological comparison were not obtained from this data, as the profiles repeated in time available within the study area did not reach the depth of closure and consequently do not take into account the evolution of the submerged part of the beach system which has been shown to store a significant amount of sediment at Geraldton.

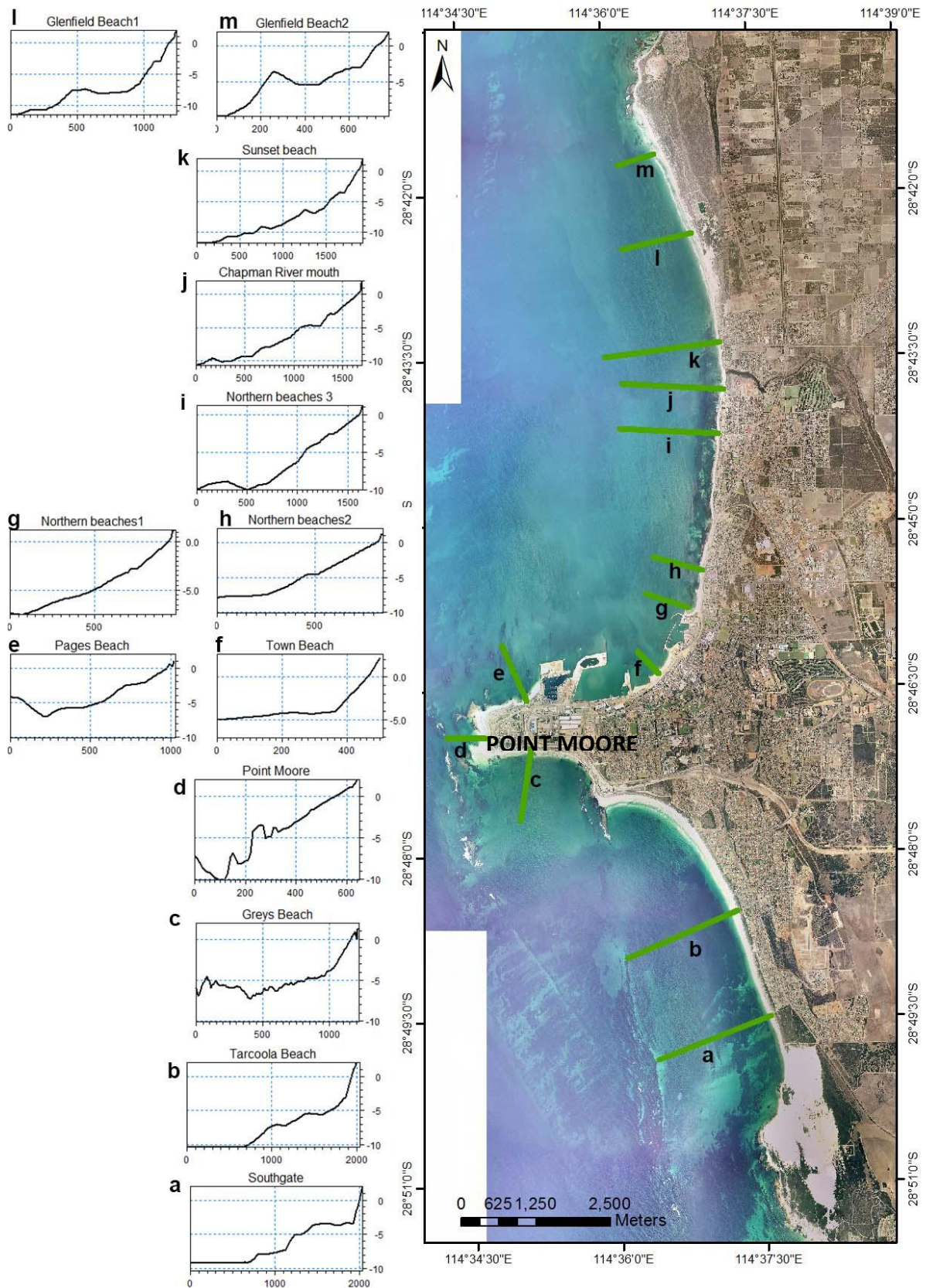


Figure 82: Cross-shore profiles extracted from multibeam bathymetry and coastal topographic surveys. Vertical and horizontal scales are in meters. The profiles are used to identify patterns of sediment transport alongshore and cross-shore. Refer to the main body of text for further explanation.

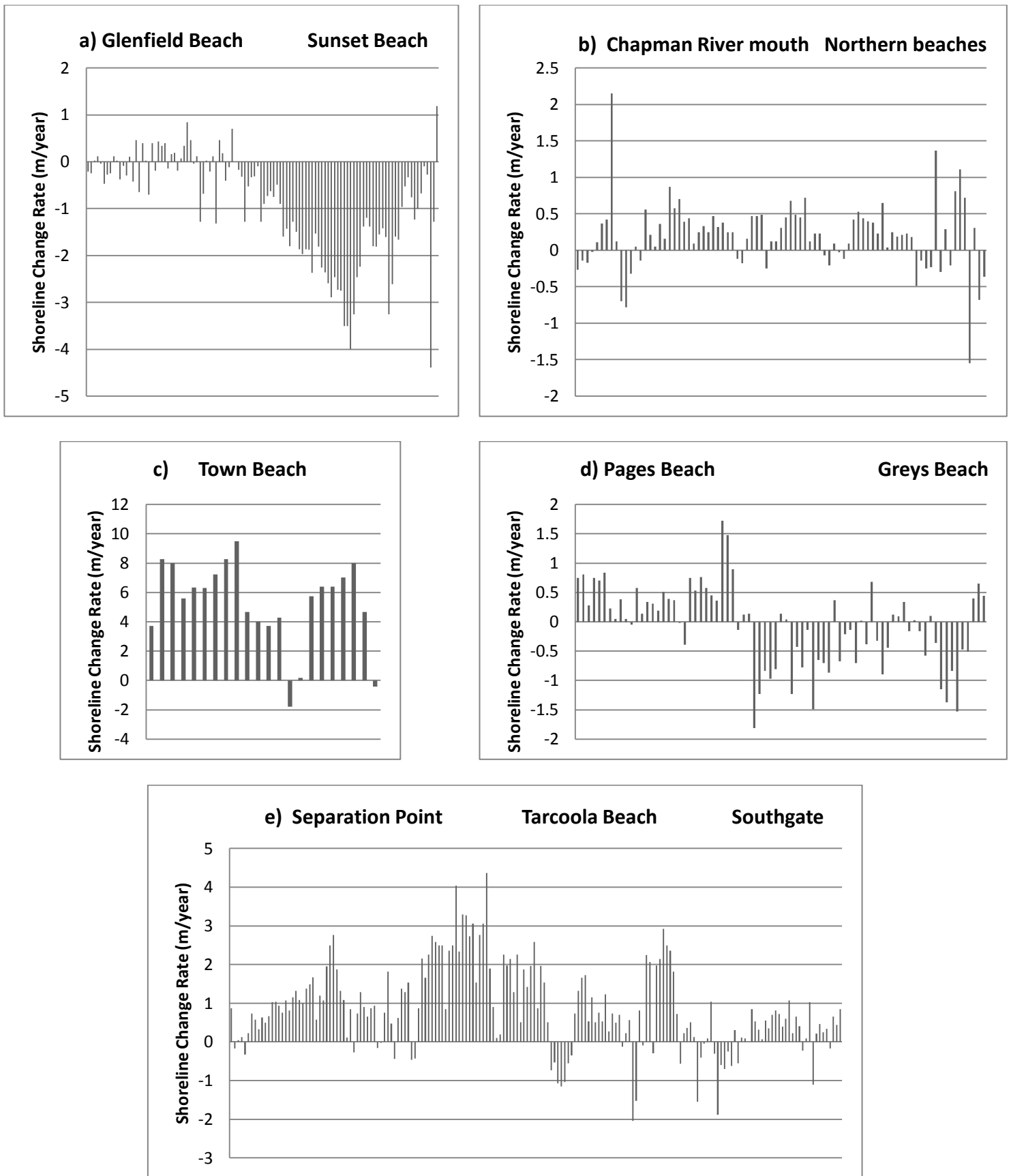


Figure 83: Shoreline change rate deviations along the Geraldton coastline from 1942 to 2010 (data developed as part of Tecchiato et al., 2012). The horizontal axis shows the distance between the locations indicated on the top of the graphs and outlined in figure 1.

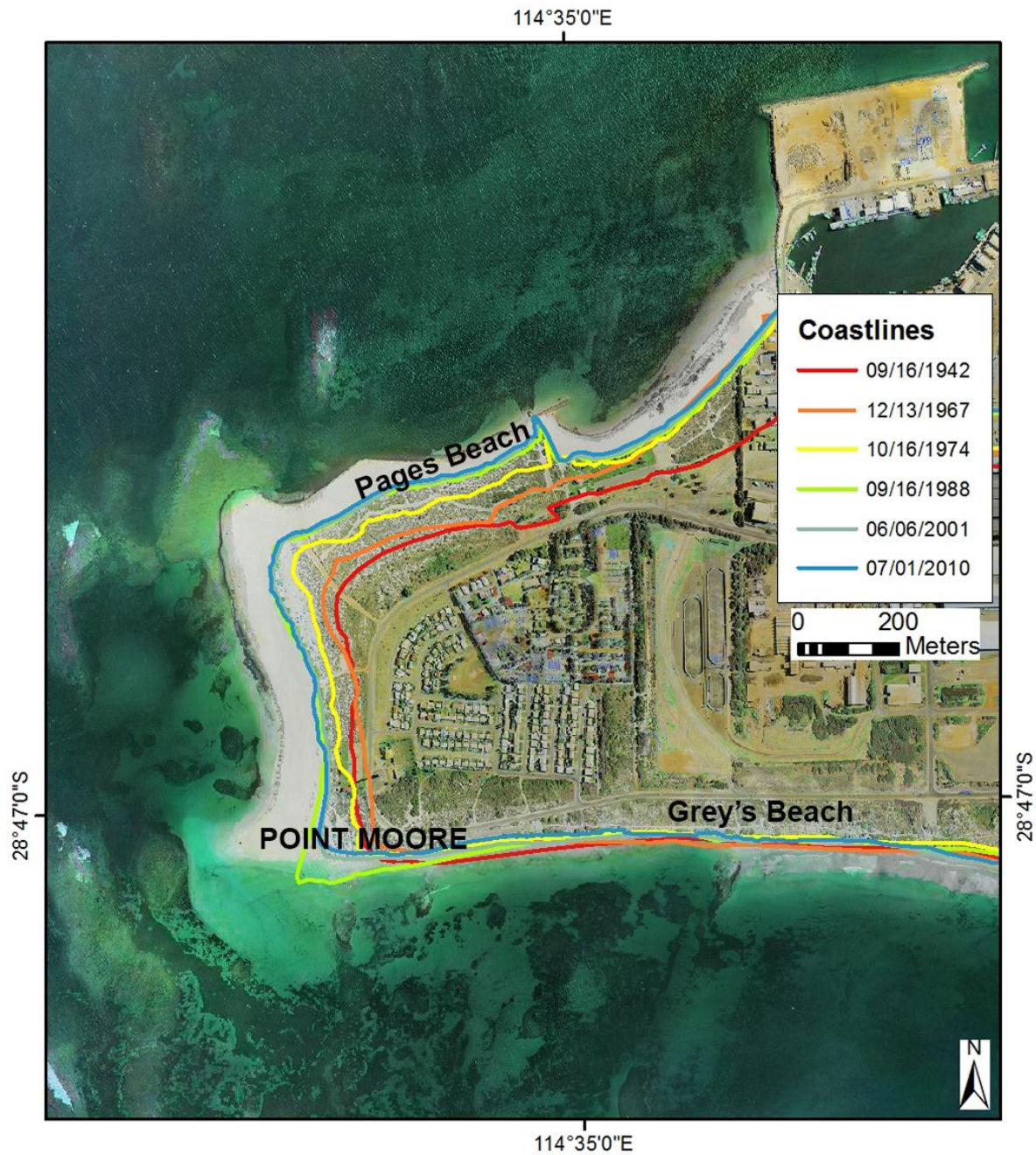


Figure 84: Migration of the area surrounding Point Moore at Geraldton over ~70 years from 1942 to 2010. Note the northward and westward movement of the coastlines in the area, with stability reached from 1988.

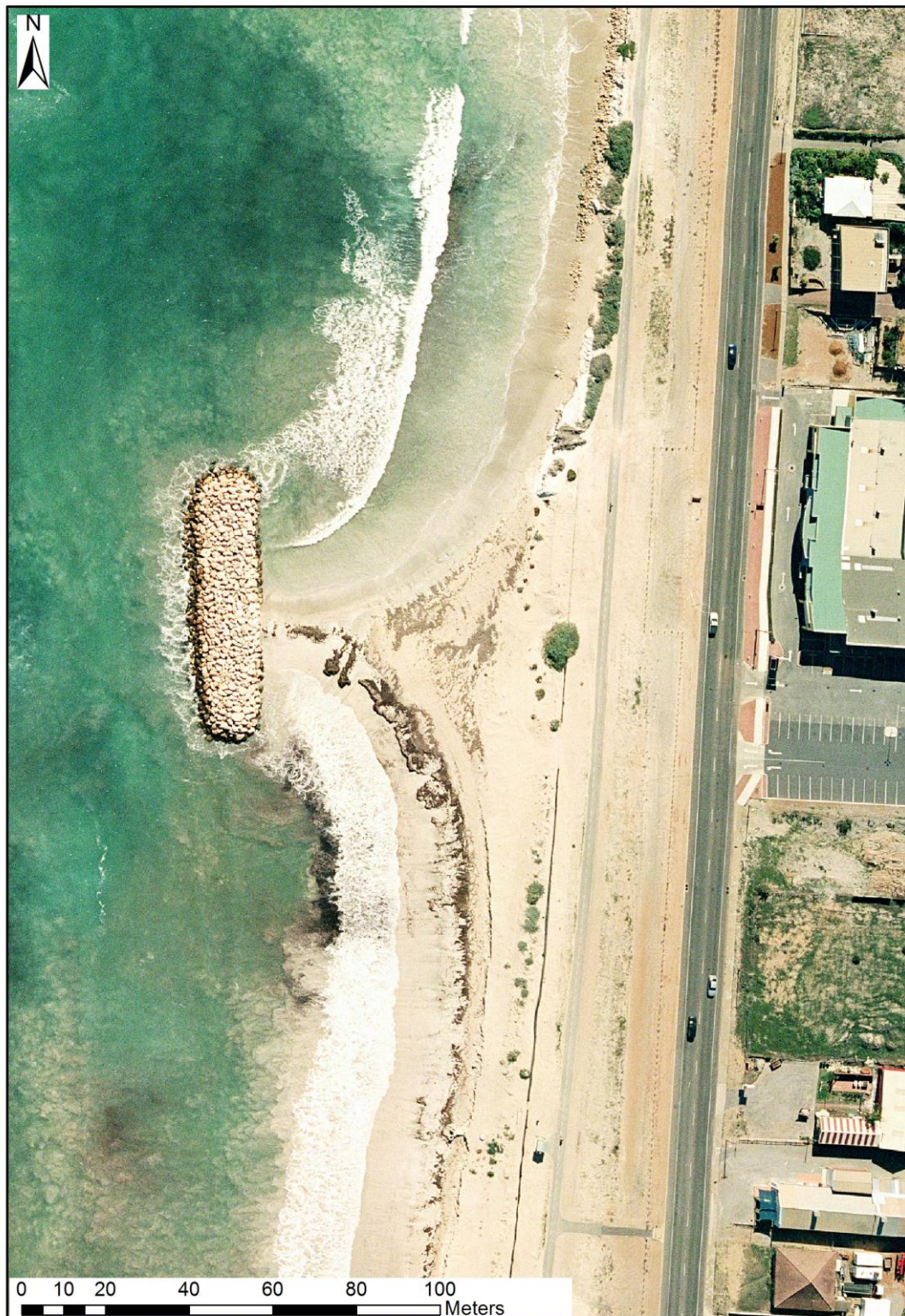


Figure 85: The asymmetry of the beach north and south of the island breakwater, located north of the Batavia Coast Marina, is a qualitative indicator of prevalent northward littoral transport. The image is an enlargement from the July 2007 aerial photograph.

4.3.4 Conceptual sediment budget model

The following conceptual sediment budget model (figure 86) summarises the sediment transport pathways under the prevalent swell direction from the south west. The shallow reef system, developed along the edge of the coastal platform approximately 4 km from the shore, attenuates the swell waves coming from the open ocean, although the wave heights are sufficient to generate sediment movement over the entire Geraldton coastal platform. The calculated depth of closure for the study area is 5.21 m depth, extending to <2 km from the shoreline. The south to north sediment transport pattern driven by the prevalent year-round SW swell is the dominant feature of the system, followed by the modifying effect of the Point Moore salient on an otherwise N-S oriented coast

In situ sediment production linked to seagrass meadows and macroalgal communities is considered a sediment source and this sediment is redistributed along the coast by the longshore currents, consequently the contribution of the living biota in terms of sediment budget is accounted for as part of the longshore sediment supply. Southgate dune supplies sediment to the coastal system which deposits offshore and is distributed to the north by the littoral currents. The Chapman River is also considered a sediment source; however, the sediment supplied by this river is accumulating in the middle of Champion Bay and is being partly redistributed to the north, contributing to sand accumulation as part of the nearshore beach zone at Glenfield Beach.

There is a major sediment volume that is being transported north of Point Moore and is sinking in the deposition areas found in between the limestone ridge systems and in the dredged channel and port basins, which appear to interrupt the sediment exchange to the east. The well-developed nearshore beach system at Town Beach and the sediment accumulation within the Batavia Coast Marina might indicate the areas where the sediment, artificially supplied to the coastal system through the nourishment activities is depositing, however more data are needed to confirm sediment provenance.

The longshore drift drives northward oriented sediment transport, with limited sediment deposition in the submerged beach zone of the artificially stabilised Northern Beaches but significant sediment deposition should contribute to beach stability at Glenfield Beach. A small amount of sediment is expected to filter through the shallow reef system at Drummond Cove and deposit to the north.

There is evidence of sediment transport onshore at the northern extreme of Tarcoola Beach, to the east of Separation Point, on the basis of bedform data on bottom currents. This sediment accumulates to the east and west of Separation Point ridge contributing in the

extensive nearshore beach zone mapped in the area. However the lack of sheltering by the limestone reef system in this location might also contribute to sediment lost offshore, as indicated by sediment data.

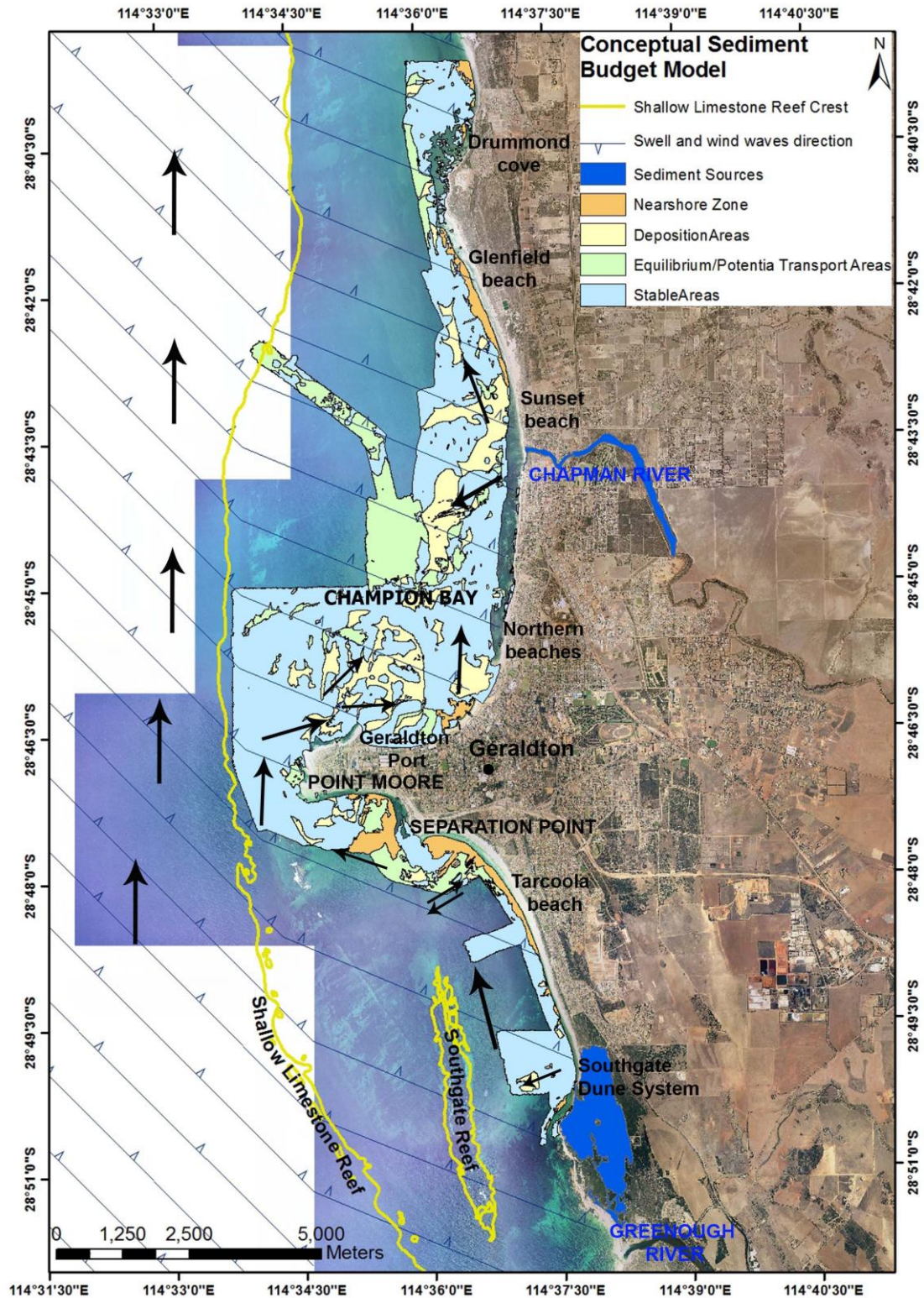


Figure 86: The conceptual sediment budget model is summarised in this figure, using the seabed mobility map discussed in Chapter 2 as a background layer. Swell waves come from SW and the wind component in the Champion Bay area is mainly from S-SW. There are two sediment sources: Southgate dunes and Chapman River (GIS layer courtesy of GSWA). In situ sediment production linked to seagrass meadows and macroalgal communities is also considered a sediment source but could not be indicated on the map as it is accounted as part of the longshore sediment supply. The sediment deposition areas are accurately located on this map and include the dredged channel, the Geraldton port, and the Batavia Coast Marina basins. Black arrows indicate sediment transport pathways.

4.4 SEDIMENT CELLS

4.4.1 Methodologies for identifying sediment cell boundaries

Bray et al. (1995) presented a comprehensive overview of sediment cell boundaries based on the identification of discontinuities in the rate or direction of sediment transport, and this classification is used in this study. Sediment transport boundaries are to be based on the full range of morphological, sedimentological, historical, hydraulic, and process information available for the studied area (Carter 1988; Bray et al., 1995; Stul et al., 2005). Sediment cell boundaries are considered *fixed* if they present a great temporal stability (20–100 years; Bray et al., 1995; Anfuso et al., 2011; Anfuso et al., 2013) and *free* if their position changes in time according to the characteristics of approaching waves (Carter 1988; Bray et al. 1995). Limits are *absolute* when they act as barriers to all sediments, while *partial* or *permeable* boundaries permit bypassing or periodic throughput (Bray et al., 1995; Anfuso et al., 2011; Anfuso et al., 2013). Examples of fixed absolute cell boundaries include hard rock headlands and artificial structures (Bray et al., 1995). Fixed permeable boundaries are also represented by headlands and artificial inlets, but admit sediment bypassing and deposition updrift (Bray et al., 1995). Free permeable boundaries usually delineate minor sub-cells, as by definition they are partial barriers and form where discontinuities in littoral sediment transport patterns occur (Bray et al., 1995). Free permeable sediment cell boundaries are classified as *divergent* when littoral drift divides in correspondence with the limit, and *convergent* when opposite littoral drifts converge at limit (Bray et al., 1995; Anfuso et al., 2011; Anfuso et al., 2013). Free permeable boundaries can also be *transit* when accretion is recorded at one side and erosion at the other side of the limit (Anfuso et al., 2011; Anfuso et al., 2013).

The boundaries of the Geraldton sediment cells were determined by considering geological (i.e. shoreline attached reefs and rocky platforms, sand dunes, and cusped forelands) and engineered structures, the results of the shoreline evolution analysis developed as part of the “Geraldton Embayments Coastal Sediment Budget Study” (Tecchiato et al., 2012), sediment characteristics, beach typology, and wave characteristics based on the hydrodynamic modelling performed by Cardno Pty Ltd.

The seabed mobility mapping completed in this study has allowed identification of the areas of sediment deposition offshore. Positioning of the offshore cell boundaries was based on sediment characteristics, underwater morphology, and habitat mapping, also considering the calculated depth of closure for the study area (5.21 m).

4.4.2 Sediment cells

Five major sediment cells, limited by fixed and free limits and containing sub-cells, were identified at Geraldton. A detailed cell by cell explanation of boundary positioning and sediment transport processes is outlined below from south to north (refer to figure 87 for visualising the cell boundaries).

Cell 1. The southern boundary of this cell could not be identified due to the lack of data at the southern extreme of the study area; however, the northern boundary is a *fixed permeable* artificial limit represented by the shipping dredged channel and the eastern breakwater of the Port basin. Although infrastructure could be regarded as a fixed absolute artificial cell boundary, sediment bypassing around the shipping dredged channel and the eastern breakwater of the Port basin is occurring at Geraldton. In fact, sediment transported as bed load is infilling the channel and Port basin, but the sediment suspended through the water column continues to be transported to the east and north of the Port infrastructure. Further information about this process is provided in section 4.5. The sediment bypassing around the shipping dredged channel and the eastern breakwater of the Port basin makes these structures *fixed permeable* artificial limits of Cell 1.

Cell 1 is dominated by the fine modern skeletal sand facies and the similarity of the sediments found within the cell—but not offshore or elsewhere—supported the identification of the area as part of a single open cell. In the Geraldton southern embayment, the offshore cell limit is defined by the N-S elongated shallow ridge (Southgate Reef) located ~2 km off Tarcoola Beach, which obstructs sediment exchange with the offshore and protects the bay from wave action. There is evidence of sediment input from the offshore due to bottom currents to the east of the Separation Point ridge where the Southgate limestone ridge does not exist; however, sediment loss offshore might also occur in the area as a result of the lack of sheltering. These settings make Cell 1 an open cell with sediment input from the offshore at Separation Point.

Whilst the north-western edge of Southgate dune is eroding (Chapter 1) and supplying sediment to the ocean (section 4.3.1), the northern end of Tarcoola Beach and the beach west of Separation Point are accreting significantly. Sediment is transported northwards and accumulates east and west of the Separation point ridge, with the longshore sediment transport continuing to the north. The sediment accumulation occurring to the east and west of the Separation Point ridge impedes the placement of a major cell boundary in the area. However, the hydrodynamic modelling suggested the presence of eddies in the Separation Point area and the coastal evolution pattern changes from accretion at Tarcoola Beach to

erosion at Greys Beach. On the basis of these processes, a *free permeable divergent* minor sub-cell limit can be placed in the area just north of Separation Point.

The fine modern skeletal sand found at Point Moore and Pages Beaches has different characteristics to the sediment found offshore; hence offshore sediment exchange is obstructed by limestone ridges off Point Moore but sediment input to the northern embayment is provided by the longshore sediment transport from the Geraldton southern embayment. Whilst Greys Beach is eroding, Pages Beach and Point Moore are accreting beaches, indicating that a significant sediment volume is transported from the southern embayment to the north of Point Moore, whilst also considering that Pages Beach has been subjected to ongoing sediment mining for nourishing the northern town beaches. Consequently Point Moore is a *free permeable transit* minor sub-cell limit to sediment transport within Cell 1.

Cell 2. This small sediment cell encompasses Town Beach and the area directly offshore from it, mapped as nearshore beach zone as part of the underwater morphology mapping. This cell is bounded by two *fixed permeable* artificial limits: the eastern breakwater of the Port basin and the southern breakwater of the Batavia Coast Marina. Sediment is supplied to this system by the longshore drift and through infrequent nourishment activities which mostly source sand at Pages Beach. This sediment accumulates off Town Beach to form the sediment wedge included in this cell and is partly transported north toward Cell 3.

Cell 3. This cell encompasses the Batavia Coast Marina and is bounded by two *fixed permeable* artificial limits—the Marina's breakwaters. Bathymetry and habitat data have shown a dominant sandy cover off and within the Marina basin, indicating areas of sediment accumulation. The northward-oriented ripples mapped off the marina entrance suggest the sediment provenance is from the south.

Cell 4. This cell extends from the northern groyne of the Batavia Coast Marina (*fixed permeable* artificial boundary) to the beach north of the Chapman River mouth (*free permeable divergent* boundary) and is 1–1.5 km wide E-W. The sediment mapped within this area has relatively low carbonate content and there is a similar wave climate for this part of the coast, which justifies the definition of this area as one single major cell. There is mixed natural and artificial sediment input into the area, with the longshore sediment drift following the south to north transport system. However, the relatively high quartz content found along the Northern Beaches suggests some redistribution of the Chapman River-derived sand to the south. Consequently, a divergent drift occurs at the northern extreme of this cell and allows the northern sediment cell boundary to be classified as *free permeable divergent*.

Cell 5. This cell includes Sunset Beach and Glenfield, as this part of the coast shows similar wave climate and sediment characteristics. Whilst Glenfield Beach is accreting, Sunset Beach is subject to erosion. The quartzose sediment supplied to this system by the Chapman River accumulates offshore (see Deposition areas of figure 87) and a smaller fraction is transported northward towards Glenfield. Sediment is transported into this cell from the adjacent Cell 4 through the northward-oriented longshore sediment transport, and contributes to the wide nearshore beach zone mapped south of the Glenfield cusped foreland. Sediment accumulation is limited at Sunset Beach as a result of the dominant northward transport and of the shoreline configuration.

The northern boundary of this sediment cell is a *free permeable transit* natural limit located to the north of a cusped foreland. In general, cusped forelands enhance sediment deposition on the up-drift side and this model applies at Glenfield. However, some sediment filters through the gaps in the reef system located off the Glenfield cusped foreland and sediment accumulation occurs down-drift of this feature, as outlined by the accretion pattern documented in the area. Consequently, a *free permeable transit limit* was identified to the north of the cusped foreland and associated offshore reef system. This feature is deemed to represent a minor sub-cell boundary of a major cell continuing to the north. The limited data available there does not allow the northwards sediment cell boundary to be defined; however, the eroding beach suggests that the northwards-oriented littoral transport carries sediment north of the Drummond Cove bay.

It is important to highlight that the sediment cells identified at Geraldton are limited by natural and artificial structures; consequently, development of infrastructure has modified natural sediment transport processes previously occurring in the study area. In particular, the shipping dredged channel, and Port and Batavia Coast Marina basins are human-made structures which have generated new areas of sediment deposition which did not occur in the previously existing natural coastal system. These modifications of natural processes are likely to have influenced coastal evolution patterns at Geraldton.

Point Moore and the cusped foreland at Glenfield are two free permeable barriers to sediment transport, as they allow sediment transport to the north and their position is likely to change in the long term.

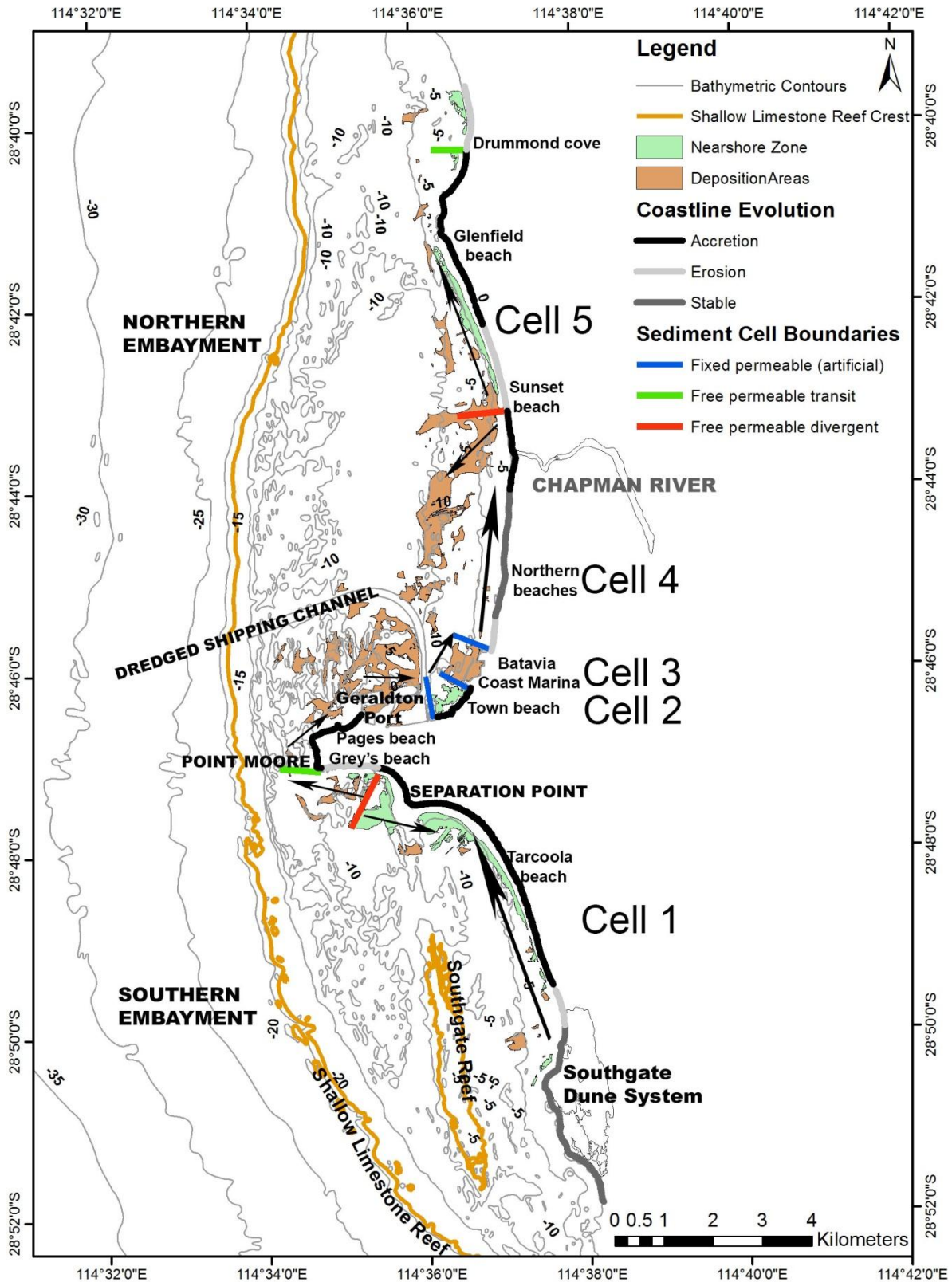


Figure 87: Sediment cells of the Geraldton coastal system (see the text for a detailed explanation of sediment pathways). The identified sediment cell boundaries and their characteristics are also indicated: blue and light blue lines are fixed permeable boundaries and define major cells; green and red lines indicate free permeable limits and delineate sub-cells. The coastline evolution pattern is summarised in this figure, with accreting, eroding, and stable areas. The black arrows indicate transport pathways, and areas of sediment deposition within the littoral sediment cells are also indicated. Of note is that sediment nourishment is ongoing within Cell 4 and provides occasional sediment input within Cell 2.

4.5 LONGSHORE SEDIMENT TRANSPORT MODELING

Several approaches have been developed that solve Rosati's (2005) sediment budget equation and these are usually based on hydrodynamic and sediment transport models, which allow the estimation of sediment volumes transported within the studied littoral environment by the longshore sediment transport (Q_y). In this study, the annual longshore sediment transport of the Geraldton embayments was simulated using a numerical model for wave-driven longshore sediment transport called LITDRIFT developed by DHI Pty Ltd (DHI, 2010). LITDRIFT includes a number of user-specified options and the parameters used in this study are described in section 1.4. The calculations of the annual sediment drift were carried out along 13 cross-shore profiles placed at representative locations for the processes dominating the coastline and shown in figure 88. The values next to the profile lines in figure 88 represent the volume of sediment in cubic meters (m^3) transiting across the profile over 1 year, and indicate northward-oriented sediment transport if positive, or southward-oriented sediment transport if negative.

Overall, there is a majority of northward-oriented sediment transport with only one profile showing southward oriented littoral drift off Greys Beach, to the south of Point Moore. The amount of sediment being transported is higher in the southern embayment where higher waves infringe on the coast and decreases in the more sheltered northern embayment, reaching maximum values in the area surrounding Point Moore which is more exposed to swell waves. Minimum values were recorded off Glenfield towards the northern extreme of the area considered in the simulation.

Table 15 summarises the volume of sediment transported within the identified sediment cells; sediment is accumulating in the cell when the values are positive, or contrarily is transiting and then exiting the sediment cell when negative. According to the LITDRIFT simulation, the sediment volume transported within Cell 1 by the littoral drift is $Q_y = -0.69 \times 10^6 \text{ m}^3/\text{year}$ with the dominant transport direction oriented to the north. Some sediment is also lost offshore, indicating that a significant amount of sediment is transiting this cell and is transported towards the northern embayment. The coast within Cell 1 is mostly stable with the exception of Greys Beach where offshore sediment loss is likely to occur and a lack of sheltering by the offshore limestone reefs occurs at this location.

Cell 2 is being supplied with sediment coming from the east at an annual rate of $Q_y = 0.2 \times 10^6 \text{ m}^3/\text{year}$ which correlates well with the accretion pattern of Town Beach, although significant infrastructure is present which induce sediment accumulation.

Cell 3 is accumulating sediment at an annual rate of $Q_y = 0.12 \times 10^6 \text{ m}^3/\text{year}$ and this sediment is mostly sinking in the Marina basin.

Cell 4 has a negative balance with $Q_y = -0.06 \times 10^6 \text{ m}^3/\text{year}$, indicating that the sediment transported northwards and lost offshore is greater than the sediment entering this cell due to longshore sediment transport. This agrees with the overall coastal situation, showing erosion in some areas, and with the Northern Beaches in need of ongoing nourishment activities to maintain the shoreline at a stable position.

Finally, Cell 5 shows a $Q_y = 0.08 \times 10^6 \text{ m}^3/\text{year}$, indicating sediment accumulation in this cell, which correlates well with the sedimentological findings and geomorphology mapping undertaken as part of this study.

Although the results of the LITDRIFT simulation agree with the conceptual model built for the study area, the data available for calibration were scarce as discussed below. Several attempts were made to correlate the modelling results with volumetric calculations deriving from annually repeated beach profiles, simplified calculations of longshore sediment transport based on the CERC and Kamphius formulae (Wang et al., 2002), and shoreline evolution data.

Beach profiles were surveyed annually between 2004 and 2007 within Cells 2 and 4; however, the extent of the profiles did not reach the depth of closure, and consequently the volumetric calculations of beach change do not take into account the submerged part of the beach where significant sediment transport is expected. For this reason, the volumes of sediment transported by the littoral drift, estimated through beach profile data, were lower than the LITDRIFT results; however, there was agreement between the patterns of sediment accumulation for Cell 2 and good agreement with the simulated value for Cell 4.

Comparison of the LITDRIFT simulation and longshore sediment transport volumes calculated through the CERC and Kamphius formulae (Wang et al., 2002) did not return good results either, possibly because the empirical formulae are simplistic and do not take into account various factors, such as the roughness of the seabed, which is an important feature at Geraldton considering the wave attenuation and sediment trapping functions of the seagrass beds that are widespread in the area.

The only quantitative data available for calibration of the model is the amount of sediment accumulating in the dredged channel and port basins ($Q_{\text{sink}} = 0.0125 \times 10^6 \text{ m}^3/\text{year}$). However this volume is considerably lower than the estimates made through the LITDRIFT simulation, reducing the validity of the estimated rates. One possible reason for the high

rates estimated in the LITDRIFT simulation is that the modelled wave height data inputted in the simulation could have been overestimated; however the Cardno Pty Ltd data is considered reliable.

The annual sediment volume change calculated on the basis of shoreline evolution data has shown good agreement with the LITDRIFT model within Cell 2; however, significant differences were found in the remaining cells. Reasons for these discrepancies are likely associated with the significant sediment transport occurring in the submerged beach zone, which cannot be assessed through shoreline evolution data. Aagard (2011, p.143) states that “little is known about the cross-shore sediment exchange between the upper and the lower shoreface”, which is the section of the coast this study lacks information about. Consequently, the volume estimates discussed herein must be used with caution and the results presented in this study represent the best outcome considering the data available.

The results of the LITDRIFT model have confirmed that northward-oriented sediment transport is dominant, with the highest simulated volumes recorded off Pages Beach. At the up-drift boundary of the studied area, Cell 1 supplies $Q_y = -0.69 \times 10^6 \text{ m}^3/\text{year}$ of sediment through northward directed littoral drift. Part of the sediment supplied by Cell 1 is transported alongshore and accumulates within Cell 2 ($Q_y = 0.2 \times 10^6 \text{ m}^3/\text{year}$) and Cell 3 ($Q_y = 0.12 \times 10^6 \text{ m}^3/\text{year}$), and the remaining sediment volume is likely to be transported through the water column towards the middle of Champion Bay. Cells 4 and 5 are relatively well-balanced with similar amounts exiting Cell 4 ($Q_y = -0.06 \times 10^6 \text{ m}^3/\text{year}$) and entering Cell 5 ($Q_y = 0.08 \times 10^6 \text{ m}^3/\text{year}$) due to longshore sediment transport.

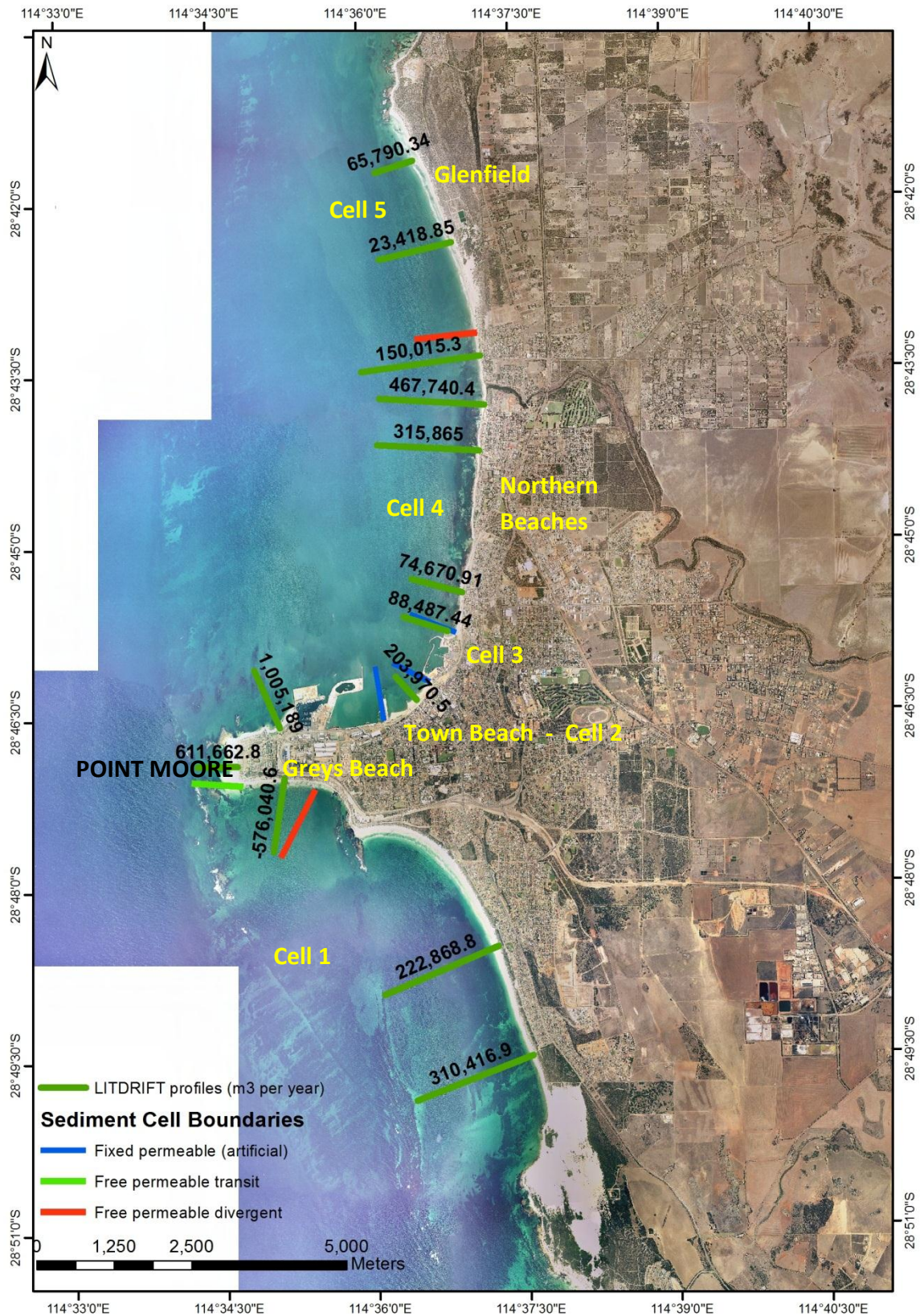


Figure 88: Results of the longshore sediment transport modelling by LITDRIFT, indicating the volume of sediment transiting across the investigated profiles in cubic meters (m^3). Positive values indicate northward-oriented sediment transport and were recorded for most of the investigated locations. Negative values indicate southward-oriented sediment transport and were only measured at one profile south of Point Moore.

Table 15: Summary of the volume of sediment input into a sediment cell or transported out of a sediment cell, as simulated by the longshore sediment transport modelling.

Sediment Cell	Longshore Sediment Transport based on LITDRIFT results (m ³ /year)	
	INPUT	OUTPUT
1		-0.69 x 10 ⁶
2	0.2 x 10 ⁶	
3	0.12 x 10 ⁶	
4		-0.06 x 10 ⁶
5	0.08 x 10 ⁶	

4.6 SEDIMENT BUDGET MODEL

The sediment budget equation (Rosati, 2005) applied to the Geraldton coastal system has returned the values shown in figure 89 for the sediment cells identified in the area. These results were obtained by considering the results of the LITDRIFT simulation to account for longshore sediment transport volumes Q_y , and a range of datasets to evaluate Q_{source} and Q_{sink} , ΔV , P , and R (i.e. pre- and post-dredging bathymetric charts, records of sand bypassing and nourishment activities, and environmental reports).

As outlined in the previous section, the data available for calibration of the LITDRIFT model were scarce. Sediment transport occurring in the submerged beach zone is deemed to be significant, and could not be assessed because of the lack of repetitive coastal topographic surveys extending to the depth of closure. Volume estimates must be viewed with caution; however, previously-published studies of this nature return similar orders of magnitude for the sediment volumes exchanged between adjacent coastal sediment cells of wave-dominated open ocean embayments (Pacheco et al., 2008; Rao et al., 2009; Aagaard, 2011). However the offshore limestone ridge barrier reduces wave heights and sediment transport volumes at Geraldton, therefore volume estimates must be treated with caution and represent the best outcome considering the data available.

The system is complex with seagrass beds colonising the shallower areas, offshore limestone ridges sheltering the coast, significant infrastructure, sand mining, and nourishment activities. The modern sediment fraction found on the beaches and in the shallow coastal areas is a product of carbonate sedimentation within seagrass meadows, which is redistributed along the coast by the wave-driven littoral drift. This sediment predominantly consists of fine carbonate sand, moderately sorted. Other sediment sources identified for the study area consist of a dune system (Southgate) in the southern embayment and a small stream (Chapman River) in the northern Geraldton embayment.

At the up-drift boundary of the study area, Cell1 is supplying sediment by longshore transport to the northern Geraldton embayment and partly losing sediment offshore. Considering that the amount of offshore sediment lost is hard to assess, the estimated volume of $-0.63 \times 10^6 \text{ m}^3/\text{year}$ indicates that a significant amount of sediment is transiting through this cell and is being transported towards the northern embayment. Although some sediment is being intercepted by the dredged channel and port basins which have been identified as sediment sinks ($Q_{\text{sink}} = 0.0125 \times 10^6 \text{ m}^3/\text{year}$), a significantly higher sediment volume filters through the limestone reef system to the north of Point Moore and is transported northwards towards the middle of Champion Bay and eastwards towards Town Beach. Cell 1 also provides sediment for nourishing the Northern Beaches at an average rate of $R = 0.0125 \times 10^6 \text{ m}^3/\text{year}$ with sediment mining occurring at Pages Beach. Whilst the sediment input from Southgate Dune ($Q_{\text{source}} = 0.0385 \times 10^6 \text{ m}^3/\text{year}$) contributes to stabilising the shoreline, the longshore sediment transport is significant and determines the overall coastline stability and sediment output from this cell ($Q_y = -0.69 \times 10^6 \text{ m}^3/\text{year}$).

Cell 2 is being supplied with sediment transported from the east at an annual rate of $Q_y = 0.2 \times 10^6 \text{ m}^3/\text{year}$, together with occasional sediment input from nourishment activities. The balance for this cell is $0.21 \times 10^6 \text{ m}^3/\text{year}$ and agrees with the beach accretion pattern recorded in the area.

Cell 3 is storing sediment at an annual rate of $0.12 \times 10^6 \text{ m}^3/\text{year}$ and this sediment is mostly being supplied from the south and accumulates within the Batavia Coast Marina basin.

Cell 4 has a balance of $-0.03 \times 10^6 \text{ m}^3/\text{year}$, with the volume of sediment transported longshore estimated at $Q_y = -0.06 \times 10^6 \text{ m}^3/\text{year}$. This indicates that the sediment transported northwards and lost offshore is greater than the sediment entering this cell due to longshore sediment transport. The coast within Cell 4 is being stabilised by regular nourishment activities at a rate of $P = 0.0125 \times 10^6 \text{ m}^3/\text{year}$. Nourishment ensures that the upper beach zone is maintained at its current location as beach profiles have shown sediment accumulation in this shallow zone with most of the sediment transport occurring further offshore (see section 4.3.3 for a description of the beach profile).

Finally, Cell 5 shows a positive balance of $0.08 \times 10^6 \text{ m}^3/\text{year}$ indicating sediment accumulation within this cell, as previously indicated by the sedimentological findings and geomorphology mapping undertaken as part of this study. This cell is being supplied by the Chapman River at an average rate of $Q_{\text{source}} = 0.0106 \times 10^6 \text{ m}^3/\text{year}$. The area off the Chapman River has been identified as a sink where sediment accumulation is driven by natural processes at an average rate of $Q_{\text{sink}} = 250 \text{ m}^3/\text{year}$.

Keeping in mind that the calculations of volume are likely to contain errors, the sediment budget of the Geraldton embayments is moderately balanced. An annual amount of $0.63 \times 10^6 \text{ m}^3$ enters the northern embayment and a total of $0.41 \times 10^6 \text{ m}^3$ is stored within Cells 2, 3 and 5. An additional $0.03 \times 10^6 \text{ m}^3$ is transported within Cell 4, with some of this sediment lost offshore and some accumulating within Cell 5.

A combination of sediment transport pathways, coastal geomorphology, and infrastructure controls coastal evolution at Geraldton. Whilst most of the beaches are stable or accreting, erosion is recorded at Greys Beach, along the southern part of the Northern Beaches and at Sunset Beach. Infrastructure has been identified as a sink for the studied area and is likely that the sediment volume being transported to the Northern Beaches and Sunset Beach have decreased since the placement of infrastructure. On the up-drift side of the Port groynes, Pages Beach has accreted significantly. Shoreline movement analysis has shown that erosion rates have tripled since the shipping dredged channel was deepened, confirming the linkage between beach erosion and infrastructure development.

The erosion pattern recorded at Greys Beach is more likely to be linked to natural processes, as the beach is located down-drift of a limestone ridge attached to shore which is likely to obstruct sediment transport to the area. Wave-driven currents show eddies correspondently to this ridge system, and consequently offshore sediment transport is also likely to occur in the area.

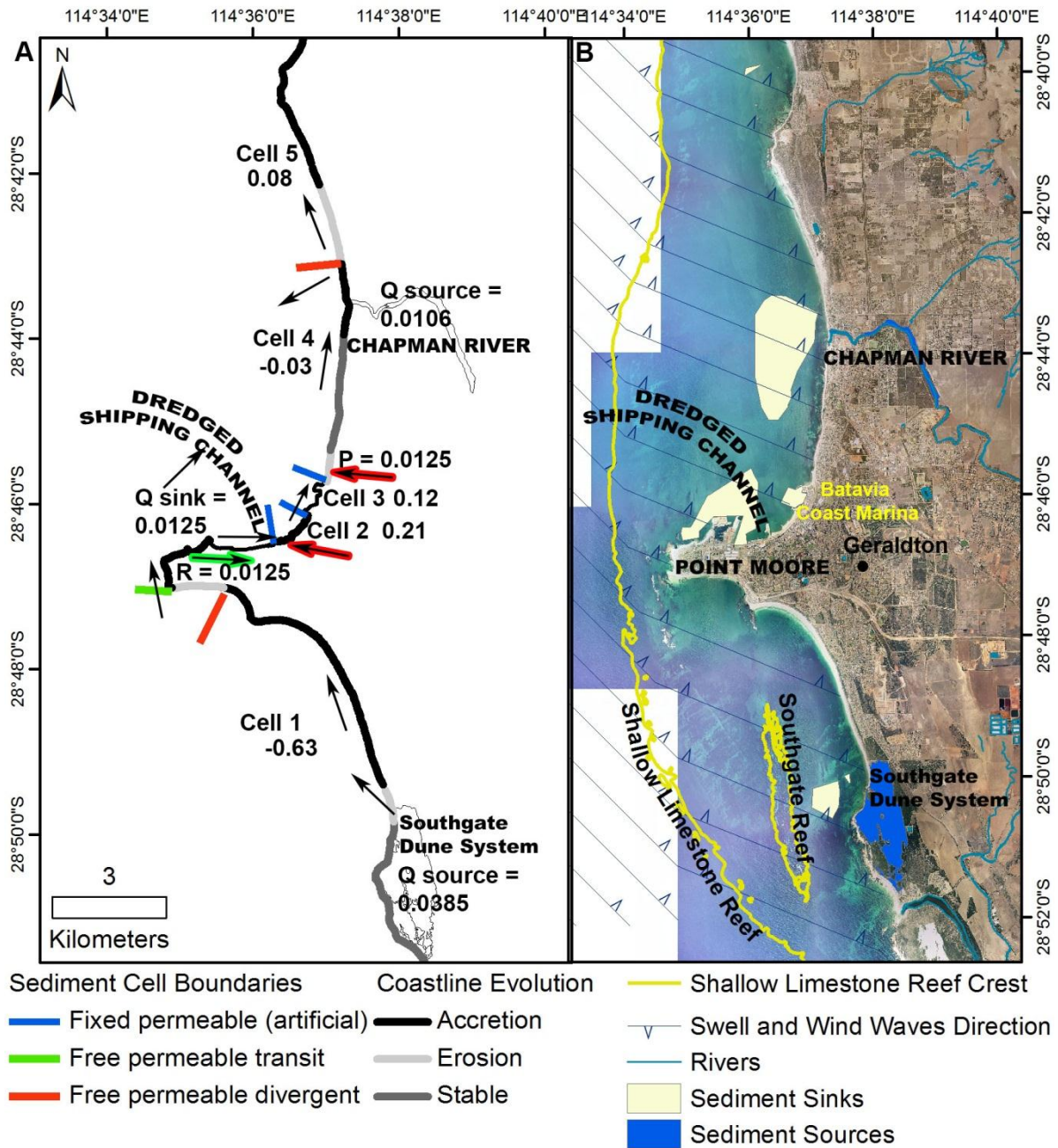


Figure 89: Quantitative sediment budget model of the Geraldton embayments. A) The black arrows indicate sediment transport pathways, the red arrows locations of sediment nourishment, and the green arrow the beach where sediment is mined. The balance of each sediment cell is indicated next to the cell name (106 m³/year), as well as the amount of sediment supplied (Q_{source} and P), sinking (Q_{sink}), and artificially removed from the beach (R). B) This conceptual map shows location of sediment sources and sediment sinks identified on the basis of sediment, bathymetry, habitat, and seismic data. The approximate location of the offshore reefs sheltering the coast is also visible on the map, as well as the main swell and wind waves direction.

Chapter 5

CONCLUSIONS

5.1 SHALLOW WATER GEOMORPHOLOGY, HABITATS, AND SEDIMENT DISTRIBUTION OF A TEMPERATE WATER LITTORAL ENVIRONMENT

5.1.1 Seabed geomorphology

The western margin of Australia is a continent-scale passive margin with a ~50 km wide continental shelf (Collins, 1988) exposed to swell waves, and its tectonic stability has resulted in the shelf and coastal geomorphology being strongly related to pre-existing topography and sea-level fluctuations of the last 1.8 million years (Ryan, 2008). The Geraldton coastal area was generated by this history, with the geology and geomorphology of the coastal platform deriving from karstification and erosion of pre-existing Pleistocene limestone surfaces, including reef systems. Paleo reef systems might form the shallow limestone reef systems identified at Geraldton (Langford, 2001; Johnson et al., 1995).

The coastal platform is 10 m deep and ~4 km wide, and becomes narrower to reach ~2km width towards the northern and southern ends of the study area. Topographic features characterising the coastal platform comprise either unconsolidated sediment accumulations (i.e. rippled sand flats, underwater sand dunes, nearshore beach zone, sand bars and sheets), low sea-level cemented shoreline features (i.e. shallow limestone reefs), or flat or low-sloping areas with a shallow sandy cover, called “low relief substrate” herein. Such geomorphological features have been reported elsewhere on the southern and western margins of Australia (Collins, 1988; Ryan, 2008; James and Bone, 2011), especially the shallow limestone reef systems developed at ~10 m depth along the edge of the coastal platform and in close proximity to the beaches. These features have been widely reported in adjacent regions with the known function of sheltering the Western Australian coast (Short, 2006b), and constitute an extensive area available for colonisation by a range of benthic organisms contributing to carbonate sediment production. The macroalgal carbonate factory which has developed on shallow limestone reefs contributes to modern sediment production, which dilutes the relict carbonate grains derived from prior erosion and sedimentation. Bathymetry and sediment data show that much of this carbonate sediment accumulates on the leeward side of the reef systems contributing to the formation of sand bars. Limestone reefs attached to the shoreline contribute to sand accumulation in the nearshore beach zone. Sediment accumulation around those reefs is common, and in general these features

influence sediment transport and deposition by obstructing the sediment flow and creating topographic barriers which support sediment accumulation in the surrounding areas. Shallow limestone reefs also host sessile biota, and are usually considered biodiversity hotspots for fisheries management. Sand bars and sheets indicate areas of sediment accumulation and were extensively mapped off the Chapman River mouth, where riverine quartz sediment is common. The presence of nearshore asymmetric underwater dunes indicates that some sediment is transported toward the shore where no shelter from the limestone reef system is present; however, offshore sediment loss may also occur at the same location as part of the sediment transported throughout the water column. Overall, the wave-driven longshore sediment transport controls the distribution of sand bodies in the nearshore, with shallow limestone reefs also influencing sediment deposition. Wave-induced sediment transport seems to be most influential in determining the formation of sand bars on the leeward side of limestone reef systems. Sediment accumulation is mostly restricted at these locations, with the exception of the area off the Chapman River mouth and there are large regions of the seabed with exposed limestone hardgrounds.

5.1.2 The macroalgal and seagrass carbonate factories: depositional environments and habitat characteristics

The macroalgal and seagrass carbonate factories are widely reported for the southern and western Australian coasts (Collins, 1988; Ryan, 2008; James and Bone, 2011) and at Geraldton modern carbonate sedimentation is linked to these communities, which provide habitats for molluscs, red algae, benthic foraminifera, bryozoans, etc. to secrete their carbonate skeletons and contribute to sediment production, together with non-carbonate secreting organisms such as sponges. Whilst seagrasses are common to ~10 m water depth, macroalgae occur to ~30 m depth, colonising the limestone reef systems on the coastal platform edge and the offshore high-gradient slope. The distribution of these habitats is well correlated to seabed topography, hydrodynamic energy, and sediment characteristics as summarised in figure 90.

Seagrass meadows in the study area are dominated by *Posidonia sp.*, *Amphibolis griffithii*, and *Amphibolis antarctica*. Seagrass meadows were found to be mostly associated with a flat or low-sloping substrate with shallow consolidated sandy cover and shallow limestone reef systems located in proximity to the shoreline, indicating that this biota can be associated with hardgrounds with the plant rooted in the bedrock depressions as found in some regions of the Mediterranean Sea (De Falco et al., 2010). Macroalgal communities are patchy and form different assemblages at Geraldton, and are mostly associated with rocky substrates

such as a flat or low-sloping substrate with shallow consolidated sandy cover and shallow limestone reef systems. Consequently, the partitioning of warm-temperate macroalgal and seagrass communities on the basis of the substrate types (i.e. macroalgae) colonize rocky substrates and seagrasses occupy adjacent sandy substrates, summarised in James and Bone (2011) for the south Australian coast, does not fully reflect the Geraldton distribution of benthic habitats, as it is representative of macroalgal communities, but not of seagrass meadows, which colonize sediment veneer over rocky substrates. Mixed seagrass and macroalgal communities are also common at Geraldton and colonize sediment veneer over rocky substrates, similarly to seagrass meadows.

As suggested by Carruthers et al. (2007), the hydrodynamic energy plays an important role in the distribution of seagrass meadows and, at Geraldton, seagrasses colonise more sheltered areas compared to macroalgal communities. A significant correspondence between the distribution of seagrass meadows and very fine sandy substrates was found in this study, indicating that fine sands derive from and are a proxy for seagrass communities. In fact, the fine carbonate sand belt characterising the shallow 1 km wide zone close to shore is constituted by ~60% of modern skeletal grains supplied to the coastal system by seagrass meadows, comprising fragmented red algae, benthic foraminifera, bryozoans, molluscs, and sponge spicules. Whilst sediment grain size did not provide a consistent surrogate for macroalgal distribution, hydrodynamic energy is higher and denser biota is commonly developed in association with the limestone reef systems ~4 km from shore at ~10 m water depth. Macroalgal derived sediments are mostly composed of fragmented red algae, benthic foraminifera, and molluscs, and are mainly found in situ representing ~40% of the sediment facies surrounding the shallow limestone reefs along the coastal platform edge. Whilst the sediment produced by the seagrass carbonate factory is transported onshore supplying the adjacent and updrift beaches, the sediment supplied by the macroalgal carbonate factory accumulates offshore in between or on the leeward side of the reef systems contributing to the formation of sand bar and sheet systems.

The modern Geraldton embayments are a useful analogue for the interpretation of high-energy carbonate-dominated palaeoenvironments, as the results presented in this study indicate that wave energy, sediment types, and local geomorphology are important proxies for carbonate facies reconstructions. However, sediment accumulation rates are lower than the published range for Australian cool-water seagrass banks, indicating a low sedimentation rate in the area.

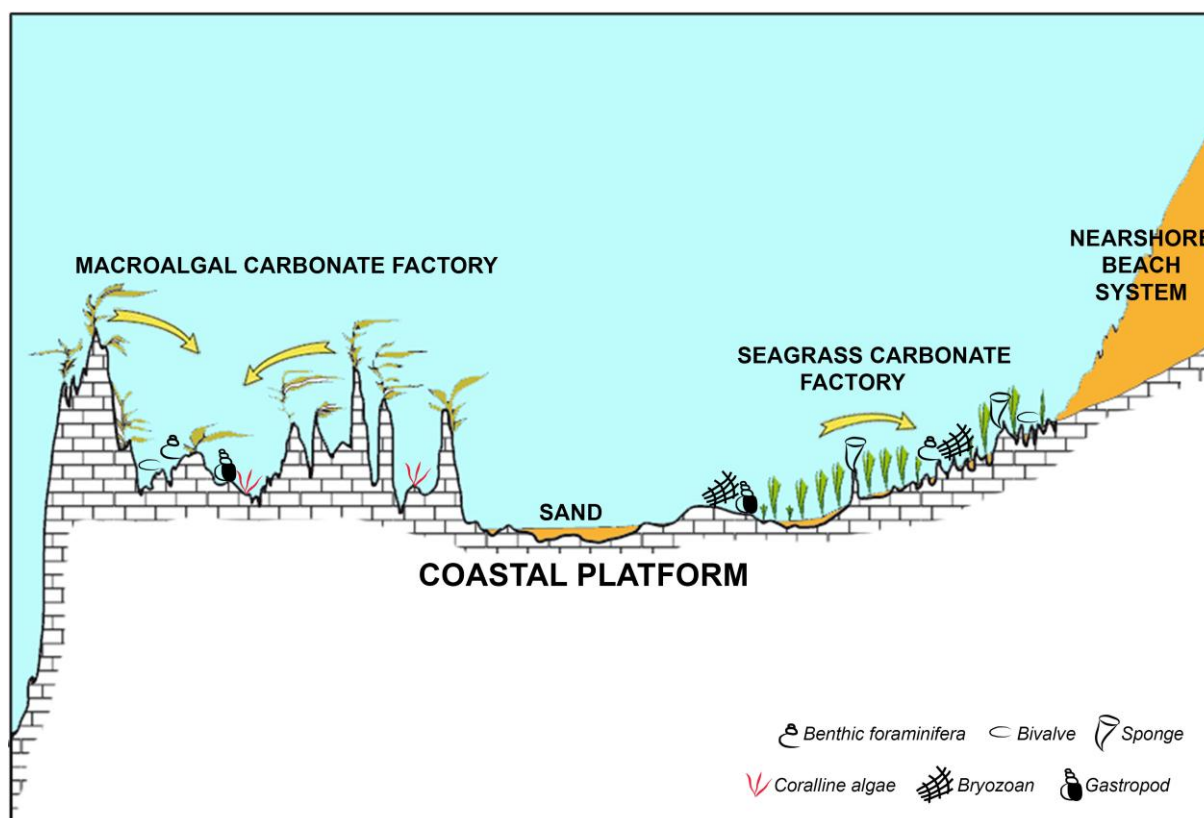


Figure 90: Shore normal sketch illustrating the nature of shallow water carbonate sediment production in the studied shallow water warm-temperate marine embayments. Both the macroalgal and seagrass carbonate factories are producing similar, but somewhat different, carbonate sediments with higher production rates for seagrass meadows. The arrows indicate sediment transport directions. A lack of mixing of the particles deriving from these benthic communities occurs in the study area, with fine sands dominating the seagrass sites and medium-coarse sands occurring where macroalgal communities are prevalent. The figure also summarises the substrate-related partitioning of these communities with macroalgae located on the high-energy shallow limestone reef systems at the seaward edge of the coastal platform and seagrasses rooted in the troughs of flat or low sloping hardgrounds with sediment veneers at sheltered locations close to shore. Mixed seagrass and macroalgal communities are also common at Geraldton and colonize sediment veneer over rocky substrates, similarly to seagrass meadows.

5.2 ABILITY OF THE MULTIBEAM ECHO-SOUNDER BACKSCATTER DATA TO DISCRIMINATE BETWEEN SANDY SUBSTRATES, SEAGRASS MEADOWS, AND MACROALGAL COMMUNITIES

An integrated analysis of the relationships between relative backscatter strength of temperate water benthic habitats constituted by sandy substrates, macroalgal communities, and seagrass meadows was carried out in this study and was supported by sediment, habitat, and geomorphology data. One of the main results is that benthic cover and substrate geomorphology need to be considered together, as they both influence the acoustic response of the seabed. Uncolonised sandy substrates are the most easily discernible habitats, as they retain the lowest relative backscatter strength values measured in this study (between -10 and -23 dB). At Geraldton, macroalgal communities and seagrass

meadows colonise hardgrounds with shallow consolidated sediment cover and show similar relative backscatter strengths (-9 and -14 dB for seagrasses; -9 and -16 dB for macroalgae). These habitats cannot be mapped separately by applying automated classification algorithms to a raster of angle-independent backscatter levels. The low-density mixed seagrass and macroalgal communities are also common on hardgrounds, and show similar acoustic properties to dense macroalgal communities and seagrass meadows (between -10 and -16 dB). This finding indicates that the biota density is not the main determinant of acoustic parameters, but the underlying substrates need to be taken into account. Moreover, the similarity of the acoustic response from macroalgal communities, seagrass meadows, and low-density mixed seagrass and macroalgae communities has caused a low accuracy to be achieved for the habitat maps completed in this study. Three mapping methodologies were tested for these data, as unsupervised and supervised classification algorithms, as well as the newer image segmentation techniques, were applied to a grid of angle-independent backscatter levels. The mapped habitats were sandy substrates, dense vegetation (including dense seagrass and macroalgae communities), and low density mixed seagrass and macroalgal communities. The application of supervised classification algorithms and image segmentation both achieved ~54% mapping accuracy, but the spatial extent of the habitat map resulting from image segmentation does not represent the entire study area. For this reason the habitat map resulting from the application of supervised classification algorithms is considered the best output. It has been shown that the mapping accuracy could be increased by reducing the mapped habitat categories to sandy substrates and vegetated areas (i.e. not considering the biota density); however, this would not enhance the overall study outcomes and consequently it was not performed.

5.3 INVESTIGATION OF LITTORAL SEDIMENT DYNAMICS: RESULTS OF AN INTEGRATED ANALYSIS

5.3.1 Cross-shore sediment transport

The cross-shore sediment transport system may be understood by analysing variations in sediment facies and stratigraphy, bathymetry and coastal geomorphology, benthic habitats, bedform characteristics, and by theoretical calculations of the depth of closure. The analysis of these parameters for the Geraldton embayments was essential to overcome the lack of previously published studies of sediment dynamics for similar environments of the Western Australian coast. The coastal geomorphology of Western Australia results from exposure to wind and waves of pre-existing Pleistocene limestone surfaces, including reef systems. The 10 m deep and ~4 km wide coastal platform bordered by shallow limestone reef identified at

Geraldton is an extensive feature along the coast of Western Australia, as the geological history of this passive continental margin was uniform at a regional scale. This coastal platform influences cross-shore sediment transport processes by inducing wave breaking offshore and reducing wave heights reaching the coast.

The calculated depth of closure is 5.21 m, which is considered relatively shallow for wave-dominated open-ocean systems. The morphology of the coastal platform with a wide 10 m deep coastal plain bordered by shallow shore parallel limestone reefs significantly reduces the depth of sediment transport onshore, although sediment movement occurs on the seabed as confirmed by the presence of symmetrical ripples on the bathymetry data. Asymmetrical ripples were only found at 5 m depth, and this data correlates well with the calculated depth of closure. Exceptions would occur where higher energy waves are able to penetrate “gaps” in the limestone barrier.

Sediment analyses in terms of grain size, mineral composition, and petrological identification have provided important clues for spatially locating the boundary between wave reworked and non-wave reworked sediments. An important outcome of the sediment analyses was the identification that the littoral sediment transport is separate from the offshore sediment movement, as fine carbonate sand was not found offshore, indicating a clear separation between littoral (0–10 m depth) and offshore (>10 m depth) transport systems. Fine carbonate sands were also found along the beaches, where nourishment activities have not been undertaken previously, indicating that the sediment dominating the shallowest part of the coastal platform is transported onto the beaches by wave motion.

These concepts are summarised in figure 91, where the cross-shore distribution of shallow habitats, sediment, and geomorphic features is related to the calculated depth of closure. As discussed in section 4.3, most previous research into the closure depth was carried out on sandy beaches with a thick sand layer in wave-dominated environments; however, at Geraldton the beach morphology is largely controlled by underlying geology. The coastal platform is characterised by a veneer of active sand above a rocky limestone substrate, with only a few locations showing a thick sandy cover.

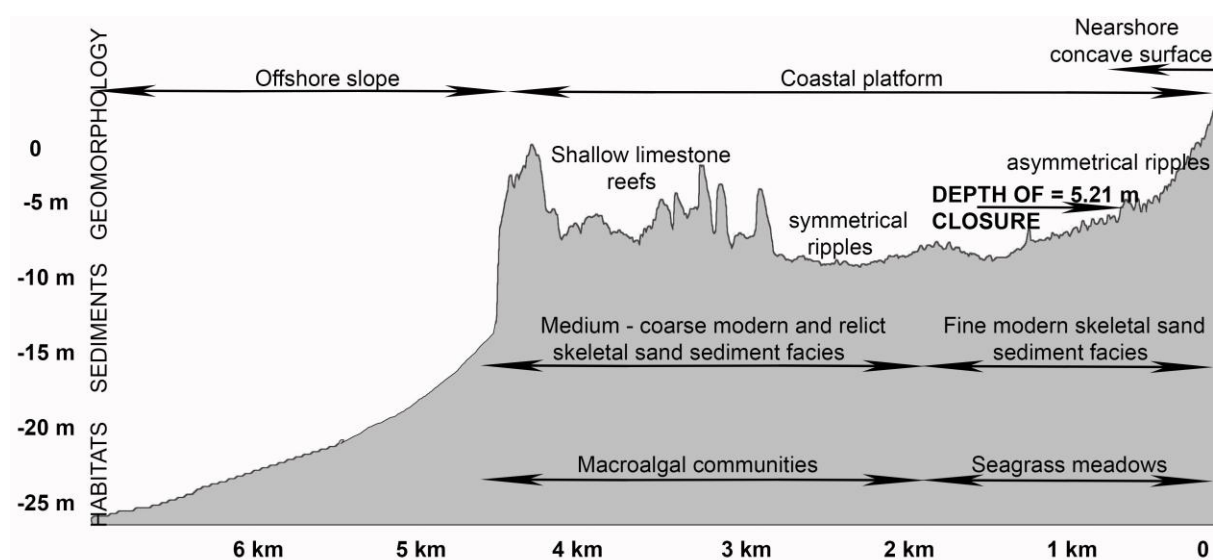


Figure 91: Shore normal sketch illustrating the cross-shore distribution of sediments, benthic habitats, and geomorphological features. The calculated depth of closure is also indicated, to allow a linkage with the environmental parameters to be made. Distance from shore is given on the horizontal axis.

5.3.2 Relationship between coastal geomorphology, sediment characteristics and longshore sediment transport

The environmental investigations undertaken as part of this study are not commonly part of sediment budget analyses, but there is a lack of literature for shallow coastal areas of Western Australia. The available literature is limited to the pioneer studies on coastal geomorphology and sediment transport by Short (2006a; 2006b; 2010), Sanderson et al. (2000), Sanderson and Eliot (1999), and some localised studies on coastal sediment dynamics in areas closer to Perth (Masselink and Pattiaratchi, 2001; Gallop et al., 2011; Gallop et al., 2012). Consequently, a greater understanding of the coastal system in terms of sediment input, transport, and storage and its linkage to geomorphological features and sediment facies was needed. Moreover, an integrated approach which takes into account the characterisation of geomorphology, sediments, shoreline evolution, and local hydrodynamics has been regarded as the most appropriate method for understanding littoral processes (Rosati, 2005; Cooper and Pontee, 2006; U.S. Army Corps of Engineers, 2008; Anfuso et al., 2011). This section summarises the relationship between coastal geomorphology, sediment characteristics, sediment geometry, and longshore sediment transport pathways.

The geomorphology and benthic habitats of the coastal platform influence sediment transport, and identification of substrate types, and topographic features on the seabed have provided useful information for understanding sediment transport pathways. For example,

sand bar and sheet systems indicate areas of sediment accumulation, and are areas where the sediment cover is mobile and do not contribute to stabilizing the seabed. Sediment transport pathways are directed towards areas of sediment accumulation, and the identification of underwater bedforms (rippled sand flats and underwater sand dunes) has supported the localisation of bottom currents at specific locations on the seabed. Limestone reefs influence sediment transport and deposition by obstructing the sediment flow and creating topographic barriers which support sediment accumulation in the surrounding areas. The seabed mobility map (Chapter 2) compiled in this study depicts the conceptual insights of the mapped geomorphic features in regard to sediment dynamics and shows areas of sediment deposition indicated by the sand bars and sheet system, stable areas in terms of sediment transport represented by limestone reefs, and low relief substrate, and zones with evidence of sediment transport on the seabed coinciding with the areas mapped as rippled sand flats and underwater sand dunes.

Important findings were obtained from the integrated analysis of bathymetry and sediment data, further emphasising the importance of an integrated approach to coastal sediment dynamic studies. Sediment stratigraphy supported the differentiation of areas of active sediment movement to sediment accumulation regions, and further information about these areas was obtained through sediment grain size, mineral composition, and bathymetry data. For example, it was found that the offshore sediment movement (>10 m deep) does not interact with the shallower coastal system due to topographic segregation, as the seaward-oriented slope at the edge of the coastal platform impedes the sediment transference from deeper locations. Higher sediment volumes were found at the bottom of the coastal platform slope through seismic data and these sediments are coarser and have a more abundant relict component than the shallower sediment facies mapped at Geraldton.

The use of different types of environmental data was useful for the identification of sediment sources and sediment sinking areas. For example, the Chapman River input of sediment and the sediment sink located off the Chapman River mouth were identified on the basis of seismic, sediment, bathymetry, and habitat data. Seismic data indicates higher sediment volumes off the Chapman River mouth than in the surrounding areas. Sediment data indicates the presence of quartzose sediment off the Chapman River mouth and on the nearby beaches. Bathymetry/habitat data allowed identification and mapping of a widespread sand bar and sheet system located off the Chapman River mouth.

The formulation of a conceptual sediment budget model and the identification of individual components of the coastal sediment budget were based on environmental data. Sediment transport modelling was necessary to fully understand the processes regulating coastal

erosion and to add quantitative data to the conceptual model. The integrated approach to sediment dynamics used in this study outlines the importance of analysing a wide range of data to achieve a comprehensive understanding of the processes regulating sediment input, transport, and storage in shallow coastal embayments.

5.4 ASSESSMENT OF THE GERALDTON COASTAL EVOLUTION USING SEDIMENT BUDGET COMPUTATIONS: IMPLICATIONS FOR COASTAL MANAGEMENT

Important natural processes have been identified in this study and should be taken into account for future environmental planning decisions at Geraldton and at locations with similar environmental and urban settings in coastal Western Australia. This project supports local and regional planning and management regarding the coast and shallow marine environments, and provides a background for future studies of sediment dynamics in the region as little data exists on sediment budgets along the coast of Western Australia. Moreover, this is the first comprehensive study on an area of Western Australia characterised by ongoing sediment bypassing and regular maintenance dredging activities, which are common practices in regional Western Australia.

The high latitude swell waves, associated with wind waves close to shore, drive a northward-oriented sediment transport along the entire coast of Western Australia (Short, 2010) which, together with the underwater morphology and coastal topography, determines the location of sediment sinks and sediment cell boundaries. In particular, the shallow reef systems, developed along the edge of the coastal platform located between 4 and 10 km offshore, induce wave refraction and subsequent formation of sandy salients, tombolos, barriers, banks, etc. (Sanderson and Eliot, 1996; Short, 2010), such as the Point Moore tombolo at Geraldton. These features experience sediment erosion on the southward facing side and deposition on the northern side, as a result of the northward-oriented sediment transport and persistent southerly winds and waves. Evidence of these processes occurring at Geraldton was found in this project. For example, sand banks were mapped on the northern side of the Point Moore tombolo, in between the limestone reef systems, indicating areas of sediment deposition. Moreover, Greys Beach on the south side of Point Moore is eroding and Pages Beach on the northern side of Point Moore is accreting. These results indicate that features such as Point Moore at Geraldton act as permeable barriers to littoral sediment movement. Infrastructure located on the downdrift side of this sediment transport system is regularly infilled by sediment, such as the Geraldton dredged channel and Port basin in the northern

embayment which are in need of ongoing maintenance dredging operations, and sand bypassing activities are also required to stabilise eroding beaches located further north. Future planning of coastal infrastructure such as dredged channels, which are common features of the Western Australian coast, should take into account this sediment transport pathway, so that potential coastal erosion and subsequent remediation costs can be minimised.

When a coastal system is in dynamic equilibrium, the general trend of the beach is to remain stable over the medium-long term, with variations in the short term. The Geraldton coastal system is wave-dominated, with mostly swash-aligned beaches, some subject to erosion (e.g. Sunset Beach), and little or no sediment input to the shore. The complex architecture of reef systems on the seaward edge of the coastal platform influences wave refraction along the Geraldton coast, and the Point Moore tombolo also contributes to these processes. The integrated approach used in this study to formulate a quantitative sediment budget and to identify sediment transport pathways at Geraldton has supported the understanding of processes regulating localised coastal erosion phenomena. Coastal erosion appeared to be mainly driven by the interaction of coastal configuration and infrastructure with the cross-shore and longshore sediment transport pathways. For example, the Point Moore tombolo shows eroding beaches on the southern sides and accreting beaches on the northern side, and the LITDRIFT longshore sediment transport modelling has identified a significant amount of sediment transported from the southern to the northern Geraldton embayment. This sediment volume is substantially higher than the sediment trapped by the Port infrastructure, indicating that sediment transported through the water column may be an important component of the coastal sediment budget and is not interacting with the coastal infrastructure. This information should also be taken into account for future planning of coastal infrastructure which could obstruct the transport of suspended sediment. Moreover, this information also indicates that not all the sediment coming from the Geraldton southern embayment is supplying the beaches of the northern embayment. More examples on the interaction between littoral transport pathways, coastal configuration, infrastructure and nourishment are provided in Chapter 4.

Carbonate dunes are common along most of the Western Australian coast, including the Geraldton embayments, and were generated by the persistent high Southern Ocean swell transporting carbonate sediment from the shelf to the coast soon after the Holocene sea-level transgression. The offshore wind regime results in a weak transport system compared to the onshore winds and year-round swell responsible for transporting sediment toward the coast; however, favourable winds and coastal configuration may result in sediment supply from the dune to the ocean. The Southgate dune system is a significant mobile dune sheet

to the south of the city of Geraldton, just north of the Greenough River, and has been identified as a source of sediment down-drift, particularly feeding the Geraldton southern embayment and participating in beach stability. This trend should not be interrupted by human development as it could interfere with the coastal stability of adjacent and down-drift situated beaches.

Seagrass meadows are highly productive benthic habitats and generate an important source within the sediment budget of the Geraldton embayments. Coastal stability is further enhanced by the stabilization function that this habitat provides for the offshore seabed substrates. The protection of this habitat should be ensured by environmental managers, as sediment input and coastal stability should be maintained at their current status to avoid coastal erosion in the future.

This study has contributed to the local knowledge by outlining the influence of coastal infrastructure on coastal erosion patterns. The linkage between natural processes and ongoing sediment bypassing and maintenance dredging activities was also explained, and future planning should use this information to develop infrastructure at locations less susceptible to intercept sediment transport pathways. Carbonate sand dunes and seagrass meadows contribute in beach stability and their protection should be ensured by coastal authorities.

5.5 SUMMARY OF OUTCOMES

Overall, this study has generated new data on temperate water habitat distribution, carbonate sedimentation, coastal geomorphology, cross-shore and longshore sediment transport processes for regional Western Australia which are beneficial to the scientific community and can be regarded as a reference for future studies of similar nature.

This project supports local and regional planning and management regarding the coast and shallow marine environments, and provides a background for future studies of sediment dynamics in the region. Natural features contributing to the coastal sediment supply have been identified, and managers should ensure their protection.

This research has documented the interaction between infrastructure and natural sediment transport patterns, providing useful data on the processes regulating regular dredged channel infilling. Data of this kind were not previously available to local and regional coastal managers, as this is the first sedimentological study on dredged channels and sediment bypassing, which are common features of the Western Australian coast.

The key findings of this research are:

- Geomorphic characterisation and high resolution mapping of two shallow (<30 m) wave-dominated coastal embayments.

Wave-driven longshore sediment transport controls the distribution of sand bodies in the nearshore, with shallow limestone reefs also influencing sediment deposition.

- Sediment characterisation and mapping: sources of sediment for the coastal sediment budget.

Useful insights on sediment provenance were obtained from the sediment analyses. Sediment input by a local river was identified, as well as in-situ sediment production linked to the seagrass and macroalgal carbonate factories.

- New data on the use of geomorphological parameters and sediments as a surrogate for benthic habitat distribution.

At Geraldton, macroalgal communities are associated with rocky substrates (flat or low-sloping substrate and shallow limestone reef systems) with shallow consolidated sandy cover, as documented previously for other regions of the Australian coast. Seagrass meadows colonize sediment veneer over rocky substrates at Geraldton; however these communities are commonly associated with sand flats in the literature.

- Description of a modern analogue for the interpretation of high-energy carbonate-dominated palaeoenvironments.

Wave energy, sediment types, and local geomorphology are important proxies for carbonate facies reconstructions.

- Acoustic habitat mapping of seagrass, macroalgae and sandy substrates using multibeam bathymetry and backscatter data.

Benthic cover and substrate geomorphology need to be considered together to understand the acoustic response of temperate water benthic habitats, such as seagrass and macroalgal communities.

- Identification of cross-shore sediment dynamics.

A shallow 10 m deep 4 km wide coastal platform characterises the seabed geomorphology at Geraldton and was documented for most of the Western Australian coast. An integrated analysis of geomorphology, sediment and hydrodynamics data outlined that this feature influences cross-shore sediment dynamics by reducing the wave heights reaching the coast.

- Identification of the relationship between coastal geomorphology, sediment characteristics and longshore sediment transport.

Seabed mobility, longshore sediment transport and geomorphic features are strictly related. Areas of sediment deposition are indicated by the sand bars and sheet system, and sediment transport is oriented towards these locations. Stable areas in terms of seabed mobility are represented by limestone reefs, which are topographic obstacles for sediment transport.

- Identification of sediment cells.

The sediment cells identified at Geraldton are limited by natural and artificial structures, as the development of infrastructure modified natural sediment transport processes previously occurring in the study area.

- Formulation of the coastal sediment budget.

Seagrass meadows and coastal sand dunes are sediment sources for the coastal sediment budget. The protection of these features should be ensured by coastal authorities, as they contribute to maintain beach stability.

- Identification of the link between infrastructure and coastal erosion.

Coastal erosion appeared to be mainly driven by the interaction of coastal configuration and infrastructure with the cross-shore and longshore sediment transport pathways.

- Identification of the processes regulating dredged channel infilling under fair weather conditions with one prevalent sediment transport direction.

Shoreline salients, cusped forelands and tombolos act as permeable barriers to littoral sediment movement. Shipping dredged channels and groynes located on the downdrift side of these features trap and reduce sediment volumes transported downdrift. Sand bypassing activities are often required to stabilise eroding beaches as a consequence of the interruption of the sediment supply due to the placement of infrastructure.

References

- Aagaard, T. (2011). Sediment transfer from beach to shoreface: The sediment budget of an accreting beach on the Danish North Sea Coast. *Geomorphology*, 135(1), 143–157.
- Anfuso, G., Martínez-del-Pozo, J. Á., & Rangel-Buitrago, N. (2013). Morphological cells in the Ragusa littoral (Sicily, Italy). *Journal of Coastal Conservation*, 17(3), 369–377.
- Anfuso, G., Pranzini, E., & Vitale, G. (2011). An integrated approach to coastal erosion problems in northern Tuscany (Italy): Littoral morphological evolution and cell distribution. *Geomorphology*, 129(3), 204–214.
- Appendini, C. M., Salles, P., Mendoza, E. T., López, J., & Torres-Freyermuth, A. (2012). Longshore sediment transport on the northern coast of the Yucatan Peninsula. *Journal of Coastal Research*, 28(6), 1404–1417.
- Ashley, G.M. (1990). Classification of large-scale subaqueous bedforms: a new look at an old problem. *Journal of Sedimentary Petrology*, 60(1), 160–172.
- Bailey, J. (February 2005). Report on coastal sand migration Oct 2004 – Jan 2005 associated with southern transport corridor sand placement in September 2004. Prepared for the City of Geraldton.
- Birkemeier, W. A. (1985). Field data on seaward limit of profile change. *Journal of Waterway, Port, Coastal, and Ocean Engineering*, 111(3), 598–602.
- Blott S.J. & Pye K. (2001). Gradstat: a grain size distribution and statistics package for the analysis of unconsolidated sediments. *Earth Surface Processes and Landforms*, 26, 1237–1248.
- BoM, (2011). Bureau of Meteorology website, <http://www.bom.gov.au/wa/geraldton/climate.shtml>
- Bray, M. J., Carter, D. J., & Hooke, J. M. (1995). Littoral cell definition and budgets for central southern England. *Journal of Coastal Research*, 381–400.
- Cardno, (2012a). Beresford foreshore coastal protection and enhancement project, master plan report. Prepared for the City of Greater Geraldton.
- Cardno, (2012b). Beresford foreshore coastal protection project – Curtin University additional modelling work – wave modelling outputs, Letter to the Department of Transport on 9 February 2012.
- Carruthers, T.J.B., Dennison, W.C., Kendrick, G.A., Waycott, M., Walker, D.I., & Cambridge, M.L. (2007). Seagrasses of south–west Australia: a conceptual synthesis of the world's most diverse and extensive seagrass meadows. *Journal of Experimental Marine Biology and Ecology*, 350: 21–45.
- Carter W.G. (1988). *Coastal environments: an introduction to the physical, ecological, and cultural systems of coastlines*. Academic Press, London.

-
- Chappell, J., Omura, A., Esat, T., McCulloch, M., Pandolfi, J., Ota, Y., & Pillans, B. (1996). Reconciliation of late Quaternary sea levels derived from coral terraces at Huon Peninsula with deep sea oxygen isotope records. *Earth and Planetary Science Letters*, 141(1), 227–236.
- Chave, K. E. (1962). Factors influencing the mineralogy of carbonate sediments. *Limnology and Oceanography*, 7(2), 218–223.
- Che Hasan, R., Ierodiaconou, D., & Laurenson, L. (2012). Combining angular response classification and backscatter imagery segmentation for benthic biological habitat mapping. *Estuarine, coastal and shelf science*, 97, 1–9.
- Chen, S. N., Sanford, L. P., Koch, E. W., Shi, F., & North, E. W. (2007). A nearshore model to investigate the effects of seagrass bed geometry on wave attenuation and suspended sediment transport. *Estuaries and Coasts*, 30(2), 296–310.
- Collins, L. B. (1988). Sediments and history of the Rottneest Shelf, southwest Australia: a swell-dominated, non-tropical carbonate margin. *Sedimentary Geology*, 60(1), 15–49.
- Collins, L.B. (2010). Controls on morphology and growth history of coral reefs of Australia's western margin. In Morgan, W. A., et al. (ed), *SEPM, Special Publication 95: Cenozoic Carbonate Systems of Australasia: 195-217. USA: Society for Sedimentary Geology (SEPM)*.
- Collins, L.B., France, R., Zhu Z.R. & Wyrwoll K.H. (1997). Warm-water platform and coolwater carbonates of the Abrolhos shelf, southwest Australia. In James, N.P., Clarke, J.D.A. (ed), *SEPM, Special Publication 56(1), Cool-Water Carbonates: 23–36. USA: Society for Sedimentary Geology (SEPM)*.
- Congalton R. G. (1991). A review of assessing the accuracy of classifications of remotely sensed data. *Remote Sensing of the Environment*, 37, 35–46.
- Cooper, N. J., & Pethick, J. S. (2005). Sediment budget approach to addressing coastal erosion problems in St. Ouen's Bay, Jersey, Channel Islands. *Journal of coastal research*, 112–122.
- Cooper, N. J., & Pontee, N. I. (2006). Appraisal and evolution of the littoral 'sediment cell' concept in applied coastal management: experiences from England and Wales. *Ocean & coastal management*, 49(7), 498–510.
- Cox, M. E., Johnstone, R., & Robinson, J. (2004, January). Effects of coastal recreation on social aspects of human well-being. In *Proceedings of the Coastal Zone Asia Pacific Conference 2004: Improving the Quality of Life in Coastal Areas*, 156–162.
- CSIRO, 2007. Post-dredging recovery of seagrasses in the Geraldton region – Year 3 Report. Prepared for Geraldton Port Authority by CSIRO Marine Research, Perth, Western Australia, September 2007.
- DCC, 2009. Climate change risks to Australia's coast – A first pass national assessment. Department of Climate Change.
- De Falco, G., Tonielli, R., Di Martino, G., Innangi, S., Simeone, S., & Michael Parnum, I. (2010). Relationships between multibeam backscatter, sediment grain size and *Posidonia oceanica* seagrass distribution. *Continental Shelf Research*, 30(18), 1941–1950.

-
- DHI, 2010. LITDRIFT User Guide: Longshore Current and Littoral Drift. DHI Software. .
- EPA (2009), City of Geraldton-Greenough Town Planning Scheme No. 1A Amendment 4 – Brand Highway, Cape Burney. Report and recommendations of the Environmental Protection Authority. *Prepared by Environmental Protection Authority, Report 1326*, Perth, Western Australia, May 2009.
- Ferrini, V. L., & Flood, R. D. (2006). The effects of fine-scale surface roughness and grain size on 300 kHz multibeam backscatter intensity in sandy marine sedimentary environments. *Marine geology*, 228(1), 153–172.
- Folk, R. L. (1954). The distinction between grain size and mineral composition in sedimentary-rock nomenclature. *The Journal of Geology*, 344–359.
- Folk, R.L. (1974). *Petrology of sedimentary rocks*. Hemphill Publishing Company, Austin, Texas..
- Folk, R. L., Andrews, P. B., & Lewis, D. (1970). Detrital sedimentary rock classification and nomenclature for use in New Zealand. *New Zealand journal of geology and geophysics*, 13(4), 937–968.
- Fonseca, L., Brown, C., Calder, B., Mayer, L., & Rzhanov, Y. (2009). Angular range analysis of acoustic themes from Stanton Banks Ireland: A link between visual interpretation and multibeam echosounder angular signatures. *Applied Acoustics*, 70(10), 1298–1304.
- Fonseca, M. S. (1989). Sediment stabilization by *Halophila decipiens* in comparison to other seagrasses. *Estuarine, Coastal and Shelf Science*, 29(5), 501–507.
- Foote, K. G., Chu, D., Baldwin, K. C., Mayer, L. A., McLeod, A., Hufnagle Jr, L. C., & Michaels, W. (2003). Protocols for calibrating multibeam sonar. *The Journal of the Acoustical Society of America*, 114(4), 2307–2308.
- Gallop, S. L., Bosserelle, C., Eliot, I., & Pattiaratchi, C. B., 2012. The influence of limestone landforms on storm erosion and recovery of a perched beach. *Continental Shelf Research*, 47, 16–27.
- Gallop, S. L., Bosserelle, C., Pattiaratchi, C., & Eliot, I., 2011. Hydrodynamic and morphological response of a perched beach during sea breeze activity. *Journal of Coastal Research*, Special, 64, 75–79.
- GEMS (2001). Geraldton port enhancement and town beach redevelopment: hydrodynamic modelling study, *Prepared for URS Australia by Global Environmental Modelling Systems*, Report no. 18/01, October 2001.
- Goff, J. A., Kraft, B. J., Mayer, L. A., Schock, S. G., Sommerfield, C. K., Olson, H. C., & Nordfjord, S. (2004). Seabed characterization on the New Jersey middle and outer shelf: correlatability and spatial variability of seafloor sediment properties. *Marine Geology*, 209(1), 147–172.
- Hallermeier, R. J. (1981). A profile zonation for seasonal sand beaches from wave climate. *Coastal engineering*, 4, 253–277.
- Harvey, N., & Caton, B. (Eds.). (2010). *Coastal management in Australia*. University of Adelaide Press.
-

-
- Hilton, M. J., & Hesp, P. (1996). Determining the limits of beach-nearshore sand systems and the impact of offshore coastal sand mining. *Journal of Coastal Research*, 496–519.
- Hughes-Clarke J, Danforth BW, & Valentine P. (1997). Areal seabed classification using backscatter angular response at 95 kHz. In: Pace NG, Pouliquen E, Bergen O, Lyons AP, editors. In: SACLANTCEN conference proceeding CP-45. Lerici (1997), 243–50.
- James, N. P., & Bone, Y. (2011). Carbonate production and deposition in a warm-temperate macroalgal environment, Investigator Strait, South Australia. *Sedimentary Geology*, 240(1), 41–53.
- James, N. P., Boreen, T. D., Bone, Y., & Feary, D. A. (1994). Holocene carbonate sedimentation on the west Eucla Shelf, Great Australian Bight: a shaved shelf. *Sedimentary Geology*, 90(3), 161–177.
- James, N. P., Collins, L. B., Bone, Y., & Hallock, P. (1999). Subtropical carbonates in a temperate realm; modern sediments on the Southwest Australian shelf. *Journal of Sedimentary Research*, 69(6), 1297–1321.
- Jiménez, J. A., & Madsen, O. S. (2003). A simple formula to estimate settling velocity of natural sediments. *Journal of waterway, port, coastal, and ocean engineering*, 129(2), 70–78.
- Johnson, M. E., Baarli, B. G., & Scott, J. H. (1995). Colonization and reef growth on a Late Pleistocene rocky shore and abrasion platform in Western Australia. *Lethaia*, 28(1), 85–98.
- Kendrick, G. W., Wyrwoll, K. H., & Szabo, B. J. (1991). Pliocene-Pleistocene coastal events and history along the western margin of Australia. *Quaternary Science Reviews*, 10(5), 419–439.
- Krauss, N.C., Larson, M., and Wise, R., 1999. Depth of closure in beach fill design. *Proceedings of the 12th National Conference on Beach Preservation Technology*. Florida Shore and Beach Preservation Association, 1568–1583.
- Langford, R.L. (2001). Regolith-landform resources of the Geraldton 1:50 000 sheet. *Geological Survey of Western Australia*.
- Madsen, J. D., Chambers, P. A., James, W. F., Koch, E. W., & Westlake, D. F. (2001). The interaction between water movement, sediment dynamics and submersed macrophytes. *Hydrobiologia*, 444(1–3), 71–84.
- Masselink, G., & Pattiaratchi, C. B. (2001). Seasonal changes in beach morphology along the sheltered coastline of Perth, Western Australia. *Marine Geology*, 172(3), 243–263.
- Mazzullo, J., Graham, A. G., & Braunstein, C. (1988). Handbook for shipboard sedimentologists. Ocean Drilling Program technical note no. 8.
- McArthur, M. A., Brooke, B. P., Przeslawski, R., Ryan, D. A., Lucieer, V. L., Nichol, S., & Radke, L. C. (2010). On the use of abiotic surrogates to describe marine benthic biodiversity. *Estuarine, Coastal and Shelf Science*, 88(1), 21–32.

-
- McInnes, R. G., Jewell, S., & Roberts, H. (1998). Coastal management on the Isle of Wight, UK. *Geographical Journal*, 291–306.
- Mount, R., Bircher, P. & Newton, J. (2007). National intertidal/subtidal benthic habitat classification scheme. School of Geography and Environmental Studies, University of Tasmania.
- MRA (2001). Geraldton Northern Foreshore Stage 1. *Prepared for City of Geraldton, Geraldton Port Authority & Department for Planning and Infrastructure* by M.P. Rogers & Associates, Perth, Western Australia, November 2001.
- Niedoroda, A. W., & Swift, D. J. (1981). Maintenance of the shoreface by wave orbital currents and mean flow: observations from the Long Island coast. *Geophysical Research Letters*, 8(4), 337–340.
- Niedoroda, A. W., & Swift, D. J. (1991). Shoreface processes. In Herbich, J.B. (ed.), *Handbook of Coastal and Ocean Engineering*. Houston: Gulf Publishing Company, 735–768.
- Niedoroda, A. W., Swift, D. J., Hopkins, T. S., & Ma, C. M. (1984). Shoreface morphodynamics on wave-dominated coasts. *Marine Geology*, 60(1), 331–354.
- Nicholls, R. J., Birkemeier, W. A., & Lee, G. H. (1998). Evaluation of depth of closure using data from Duck, NC, USA. *Marine Geology*, 148(3), 179–201.
- Orme, A. R. (1988). Coastal dunes, changing sea level, and sediment budgets. In *Dune/Beach Interaction*, ed. N. P. Psuty, *Journal of coastal research*, Special Issue No. 3, 127–129.
- Pacheco, A., Vila-Concejo, A., Ferreira, Ó., & Dias, J. A. (2008). Assessment of tidal inlet evolution and stability using sediment budget computations and hydraulic parameter analysis. *Marine Geology*, 247(1), 104–127.
- Parnum, I.M. (2007). Benthic habitat mapping using multibeam sonar system. PhD Thesis Curtin University of Technology, Department of Imaging and Applied Physics, Centre for Marine Science and Technology..
- Phillips, M. R., & Williams, A. T. (2007). Depth of closure and shoreline indicators: empirical formulae for beach management. *Journal of Coastal Research*, 487–500.
- Phinn, S., Roelfsema, C., Dekker, A., Brando, V., & Anstee, J. (2008). Mapping seagrass species, cover and biomass in shallow waters: An assessment of satellite multi-spectral and airborne hyper-spectral imaging systems in Moreton Bay (Australia). *Remote sensing of Environment*, 112(8), 3413–3425.
- Pilkey, O. H., & Cooper, J. A. G. (2002). Longshore transport volumes: a critical view. *Journal of Coastal Research*, 36, 572–580.
- Playford, P. E., Horwitz, R. C., Peers, R., & Baxter, J. L. (1970). *1: 250,000 Geological Series - Explanatory notes on the Geraldton Geological sheet*. Geological Survey of Western Australia.
-

-
- Post, A. L., Wassenberg, T. J., & Passlow, V. (2006). Physical surrogates for macrofaunal distributions and abundance in a tropical gulf. *Marine and Freshwater Research*, 57(5), 469–483.
- Preda, M., & Cox, M. E. (2005). Chemical and mineralogical composition of marine sediments, and relation to their source and transport, Gulf of Carpentaria, Northern Australia. *Journal of Marine Systems*, 53(1), 169–186.
- Rao, C.P., 1996. *Modern carbonates – tropical temperate polar, introduction to sedimentology and geochemistry*. Howarth, Tas.: Carbonates.
- Rao, V. R., Murthy, M. V., Bhat, M., & Reddy, N. T. (2009). Littoral sediment transport and shoreline changes along Ennore on the southeast coast of India: Field observations and numerical modeling. *Geomorphology*, 112(1), 158-166.
- Rodríguez, E. L., & Dean, R. G. (2009). A sediment budget analysis and management strategy for Fort Pierce Inlet, Florida. *Journal of Coastal Research*, 870–883.
- Rosati, J. D. (2005). Concepts in sediment budgets. *Journal of Coastal Research*, 21(2), 307–322.
- Ryan, D. A. (2008). Geomorphic evolution and benthic environments of two carbonate systems on the Australian continental shelf. PhD Thesis Curtin University of Technology, Department of Applied Geology.
- Ryan, D. A., Brooke, B. P., Bostock, H. C., Radke, L. C., Siwabessy, P. J., Margvelashvili, N., & Skene, D. (2007a). Bedload sediment transport dynamics in a macrotidal embayment, and implications for export to the southern Great Barrier Reef shelf. *Marine geology*, 240(1), 197–215.
- Ryan, D. A., Brooke, B. P., Collins, L. B., Kendrick, G. A., Baxter, K. J., Bickers, A. N., Siwabessy, P.J.W, & Pattiaratchi, C. B. (2007b). The influence of geomorphology and sedimentary processes on shallow-water benthic habitat distribution: Esperance Bay, Western Australia. *Estuarine, Coastal and Shelf Science*, 72(1), 379–386.
- Sanderson, P.G., & Eliot, I. (1996). Shoreline salients, cusped forelands and tombolos on the coast of Western Australia. *Journal of Coastal Research*, 12(3), 761–773.
- Sanderson, P. G., & Eliot, I. (1999). Compartmentalisation of beachface sediments along the southwestern coast of Australia. *Marine Geology*, 162(1), 145–164.
- Sanderson, P. G., Eliot, I., Hegge, B., & Maxwell, S. (2000). Regional variation of coastal morphology in southwestern Australia: a synthesis. *Geomorphology*, 34(1), 73–88.
- Schwartz, M. (Ed.). (2006). *Encyclopedia of Coastal Science*. Springer.
- Short, A.D. (2006a). *Beaches of the Western Australian coast: Eucla to Roebuck Bay*. Coastal Studies Unit of the University of Sydney, NSW.
- Short, A.D. (2006b). Australian beach systems – nature and distribution. *Journal of Coastal Research*, 22(1), 11–27.

-
- Short, A.D. (1984). Beach and nearshore facies: South-East Australia. *Marine Geology*, 60, 261–282.
- Short, A.D. (2010). Sediment transport around Australia – sources, mechanisms, rates, and barrier forms. *Journal of Coastal Research*, 26(3), 395–402.
- Short, A. D., & Woodroffe, C. D. (2009). *The Coast of Australia*. Cambridge University Press.
- Short, F.T., McKenzie, L.J., Coles, R.G., & Vidler, K.P. (2002). *SeagrassNet manual for scientific monitoring of seagrass habitat*. Queensland Department of Primary Industry, Queensland Fisheries Service, Cairns.
- Stevens, A.M., & Collins, L.B. (2011). Development and application of GIS datasets for assessing and managing coastal impacts and future change on the central coast of Western Australia. *Journal of Coastal Conservation*, 15, 671–685.
- Stul, T. (2005). Physical characteristics of Perth beaches, Western Australia. Thesis (Hons, unpublished), University of Western Australia.
- Stul, T., Gozzard, J.R., Eliot, I.G., & Eliot, M.J. (2012) Coastal Sediment Cells between Cape Naturaliste and the Moore River, Western Australia. Report prepared by Damara WA Pty Ltd and Geological Survey of Western Australia for the Western Australian Department of Transport, Fremantle.
- Tecchiato S., Collins L., & Parnum I. (2013). Application of multi-beam echo sounder data to studies of sediment dynamics: an example from Geraldton, Midwestern Australia. *International Congress on Natural Sciences and Engineering*; Taipei, Taiwan, January 2013.
- Tecchiato, S., Collins, L.B., & Stevens, A. M. (2012). Geraldton embayments coastal sediment budget study. Applied Sedimentology, Coastal and Marine Geoscience Group Report 2012/01, Curtin University"©, Department of Applied Geology Western Australia School of Mines. Prepared for Department of Transport, Marine House, Fremantle, WA.
- Tecchiato, S., Parnum, I.M., Collins, L., & Gravitov, A. (2011). Using multibeam echosounder to map sediments and seagrass cover in shallow coastal areas. *Proceedings of the Fourth Underwater Acoustic Measurements: Technologies and Results*, Kos Island, June 2011.
- Thieler, E., Himmelstoss, E. A., Zichichi, J. L., & Ergul, A. (2009). The Digital Shoreline Analysis System(DSAS) Version 4.0 - An ArcGIS Extension for Calculating Shoreline Change. U. S. Geological Survey.
- Thieler, E. R., Pilkey Jr, O. H., Young, R. S., Bush, D. M., & Chai, F. (2000). The use of mathematical models to predict beach behavior for US coastal engineering: a critical review. *Journal of Coastal Research*, 48–70.
- Thomson, A. G. (1998). Supervised versus unsupervised methods for classification of coasts and river corridors from airborne remote sensing. *International Journal of Remote Sensing*, 19(17), 3423–3431.

-
- UNEP (2006). Marine and coastal ecosystems and human wellbeing: A synthesis report based on the findings of the Millennium Ecosystem Assessment. United Nations Environment Programme (UNEP).
- URS (2001). Port enhancement project and preparatory works for town beach foreshore redevelopment. *Prepared for Geraldton Port Authority* by URS Australia Pt Ltd, Report no. R859, Perth, Western Australia, November 2001.
- U. S. Army Corps of Engineers (2008). *Coastal Engineering Manual*.
<http://140.194.76.129/publications/eng-manuals/>
- van Keulen, M., & Borowitzka, M. A. (2002). Comparison of water velocity profiles through morphologically dissimilar seagrasses measured with a simple and inexpensive current meter. *Bulletin of Marine Science*, 71(3), 1257–1267.
- Veevers, J.J, Powell C. Mca., Roots S. R. 1991. Review of seafloor spreading around Australia. I. Synthesis of the patterns of spreading. *Australian Journal of Earth Sciences*, 38, 373–389.
- Velegrakis, A. F., Collins, M. B., Bastos, A. C., Paphitis, D., & Brampton, A. (2007). Seabed sediment transport pathway investigations: review of scientific approach and methodologies. In: Balson, P.S. and Collins, M.B. (Eds.), Coastal and shelf sediment transport. *Geological Society, London, Special Publications*, 274(1), 127–146.
- Verduin, J. J., & Backhaus, J. O. (2000). Dynamics of Plant–Flow Interactions for the Seagrass *Amphibolis antarctica*: Field Observations and Model Simulations. *Estuarine, Coastal and Shelf Science*, 50(2), 185–204.
- Wang, P., Ebersole, B. A., & Smith, E. R. (2002). Longshore sand transport-initial results from large-scale sediment transport facility (No. ERDC/CHL-CHETN-II-46). Engineer research and development center Vicksburg ms coastal and hydraulics lab.
- Wilson, P. S., & Dunton, K. H. (2009). Laboratory investigation of the acoustic response of seagrass tissue in the frequency band 0.5–2.5 kHz. *The Journal of the Acoustical Society of America*, 125 (4), 1951-1959.
- WorleyParsons (2010). Coastal processes study – Greys Beach to Sunset Beach, a project of the coastal vulnerability and risk assessment program. Prepared for City of Geraldton-Greenough, July 2010.
- Xie, Y., Sha, Z., & Yu, M. (2008). Remote sensing imagery in vegetation mapping: a review. *Journal of Plant Ecology*, 1(1), 9–23.

APPENDIX 1 – Tecchiato et al. (2013). Application of multi-beam echo sounder data to studies of sediment dynamics: an example from Geraldton, Midwestern Australia. International Congress on Natural Sciences and Engineering; Taipei, Taiwan, January 2013.

Application of multi-beam echo sounder data to studies of sediment dynamics: an example from Geraldton, Midwestern Australia

Sira TECCHIATO^a, Lindsay B. COLLINS^a and Iain M. PARNUM^{2b}

^a**Applied Sedimentology and Marine Geoscience Group, Department of Applied Geology, Curtin University, GPO Box U1987, Perth, WA 6845 Australia,**
sira.tecchiato@postgrad.curtin.edu.au

^b**Centre for Marine Science and Technology, Department of Applied Physics, Curtin University, GPO Box U1987, Perth, WA 6845 Australia.**

Abstract

The identification of sediment transport pathways is vital for coastal sediment budget studies and depends upon a comprehensive knowledge of seabed geomorphology and of the benthic communities, especially where modern sediment production contributes to the local sediment supply. The multi-beam echo sounders record high resolution bathymetry and backscatter data, which have been widely used to describe seabed morphology and are becoming more common in the acoustic habitat mapping practices. This paper presents an application of multi-beam echo sounder data to a sediment budget study undertaken at Geraldton, in Western Australia. Sediment accumulation areas were successfully mapped on the bathymetry models and the sandy nature of the identified areas was confirmed through the backscatter data, adding value to the bathymetry mapping. Geraldton has a temperate water environment, where seagrasses and macroalgae communities contribute to sediment production and influence sediment mobility. The distribution of these habitats was mapped through the combined analysis of multi-beam bathymetry and backscatter data supported by underwater videography. The acoustic habitat mapping capability of the multi-beam echo sounder combined with the morphological investigation of the seabed provides an efficient tool for investigating the seabed mobility of coastal temperate water environments.

Keywords: multibeam echo sounder, sediment budget, seabed mobility, sediment dynamics, seagrass meadows

1. Introduction

Sediment budget studies aim to identify sediment sources, sinks and transport pathways for a coastal system within a defined period of time [1], and often represent fundamental tools for coastal planning [2] and management of human impacted shorelines. The first step in defining a sediment budget is the development of a conceptual sediment budget [3, 4, 5], which is a qualitative model describing the coastal processes on a regional basis (i.e. prevalent sediment transport directions, areas of sediment deposition, sediment exchange between adjacent littoral cells). Important clues to sediment dynamics are provided by the understanding of seabed mobility [2]: i.e. sediment accumulation areas indicate locations to where the sediment is being transported by the littoral currents, and consist of uncolonized sediment bodies; benthic communities often influence the seabed mobility and their distribution is often linked to the morphological features of the sea bottom. This paper presents a study of underwater geomorphology and habitat mapping which has provided important clues toward the understanding of sediment dynamics of a shallow coastal system.

A sediment budget study was undertaken at Geraldton in Midwestern Australia (Figure 1), an expanding urban and industrial complex, which serves an important port facility of the state of Western Australia (WA). The important coastal infrastructure and the coastal erosion phenomenon that is threatening the town beaches make Geraldton a hot spot for local environmental managers, but similar situations are reported across the state as maritime transport is vital for sustaining international commercial activities of WA. The Geraldton sediment budget study used environmental indicator of seabed mobility to assess sediment dynamics and transport pathways. The novel aspect of this study was the introduction of multi-beam echo sounder (MBES) data, providing high resolution bathymetry and backscatter (BS) data which were used for seabed characterization. Previous sediment budget studies used side scan sonars to investigate the seafloor geomorphology [6, 1] which provide lower resolution data compared to MBES [7, 8]. Moreover, MBESs not only record bathymetry data but the modern techniques of acoustic habitat mapping provide seabed mapping capabilities which are beneficial to seabed mobility studies [2].

Geraldton is characterized by temperate water sedimentation and the coastal platform is colonized by seagrass and macroalgae communities. Seagrass meadows and macroalgae communities colonizing shallow rocky substrates are common in south and west Australia, where significant sections of the coast are fringed by seagrass meadows [9], which supply carbonate sediment to the coastal systems [10] constituting a sediment source in terms of sediment budget. On a global scale seagrasses colonize most of the nearshore environments [11] and have the capacity to reduce water flow and therefore increase sediment deposition [9, 12, 13, 14 and 15] which must be taken into account when undertaking seabed mobility studies. Recent acoustic habitat mapping studies of seagrass meadows were based on MBES BS data [16, 17] and were able to differentiate bare sand to *Posidonia* seagrass cover. This paper presents the outcomes of the application of MBES bathymetry and backscatter data to the development of a seabed mobility map, and outlines the significance and repeatability of this method for the assessment of sediment dynamics of coastal temperate water environments.

2. Methods

The Western Australian Department of Transport (DoT) founded this study and provided a Reson Seabat 8101 MBES system, set up aboard a DoT hydrographic vessel specifically designed for MBES data acquisition. A MBES survey was carried out in November 2010 covering the embayments north and south of the city of Geraldton, between 2 and 30 m depth. Only part of these data is presented in

this paper, located in an area of significant complexity, in terms of morphology and habitat distribution.

Underwater photography was collected in December 2010 through 250 m long transects distributed along a 1km x 1km spaced grid and used to ground truth the MBES data. The relative abundance of benthic cover was assessed through visual comparison of still photographs with a photo guide specifically developed for seagrass dominated habitats [18].

2.1 MBES bathymetry data

MBES bathymetry data were dynamically corrected for boat pitch, roll and heave during acquisition using the QUINSy™ software interface, and further removal of signal spikes was carried out at the processing center. These main geomorphic features were mapped in the ArcGIS 10™ environment using 0.5 m grid spaced DEMs (Figure 1) as base layers.

2.2 MBES BS data

MBES BS data were processed using the Centre for Marine Science and Technology's (CMST) multibeam sonar processing toolbox. The BS strength as a function of incidence angle (known as Angular Response curve, AR) was extracted at the ground truth locations for the main seabed habitats found in the study area (Figure 2): macroalgae $\geq 70\%$, seagrasses (*Halophila sp.*, *Posidonia sp.*, *Amphibolis antarctica* and *Amphibolis griffithii*) $\geq 70\%$, sand $\geq 70\%$ (including fine sands and medium/coarse sands). The AR curves and the underwater imagery helped in identifying the BS intensity associated with the main habitat categories found in the study area and indicated above.

2.3 Seabed mobility

The combined observation of bathymetry and BS data provided the input data for a seabed mobility map (Figure 3) to be generated by distinguishing:

- Sediment deposition areas: mapped as sand bars and sheets on the basis on the MBES bathymetry data with the sandy substrate dominance confirmed by the MBES BS data. Unvegetated sediment bodies (banks, bars and sheets) are proxies for sediment accumulation.
- Stable areas: are rocky or vegetated zones of the coastal platform where no evidence of sediment erosion/deposition was found, such as shallow limestone reefs and flat areas.

3. Results

MBES data allowed the geomorphology of the Geraldton coastal platform to be analyzed at high detail and linked to the living communities and seabed mobility. An example from a selected region of the study area is described in this paper with the intent of providing an overview of how the data were used for the overall sediment budget study.

3.1 MBES bathymetry data

The Point Moore area at Geraldton has a shallow coastal platform (~10 m deep) with a complex outcropping limestone ridge and pinnacle system (0-3 m depth) at the seaward edge of the coastal platform. These features are made of the Pleistocene Tamala Limestone [19] and are N-S elongated structures representing the remains of paleoreef systems [20].

Sand bars and sheets are deposited in between the ridge and pinnacle systems, and generate a difference in depth of up to 1 m on the surrounding sea bottom. The easternmost features of this kind are asymmetric to the east indicating sediment transport from west to eastwards, which was expected in the area as the main ocean swell direction is from the SW.

The seabed surrounding these features (0-10 m depth) is flat and mostly composed of calcarenite of the Pleistocene Tamala Limestone [19]; no evidence of sediment deposition/erosion was found correspondently to the flat substrate.

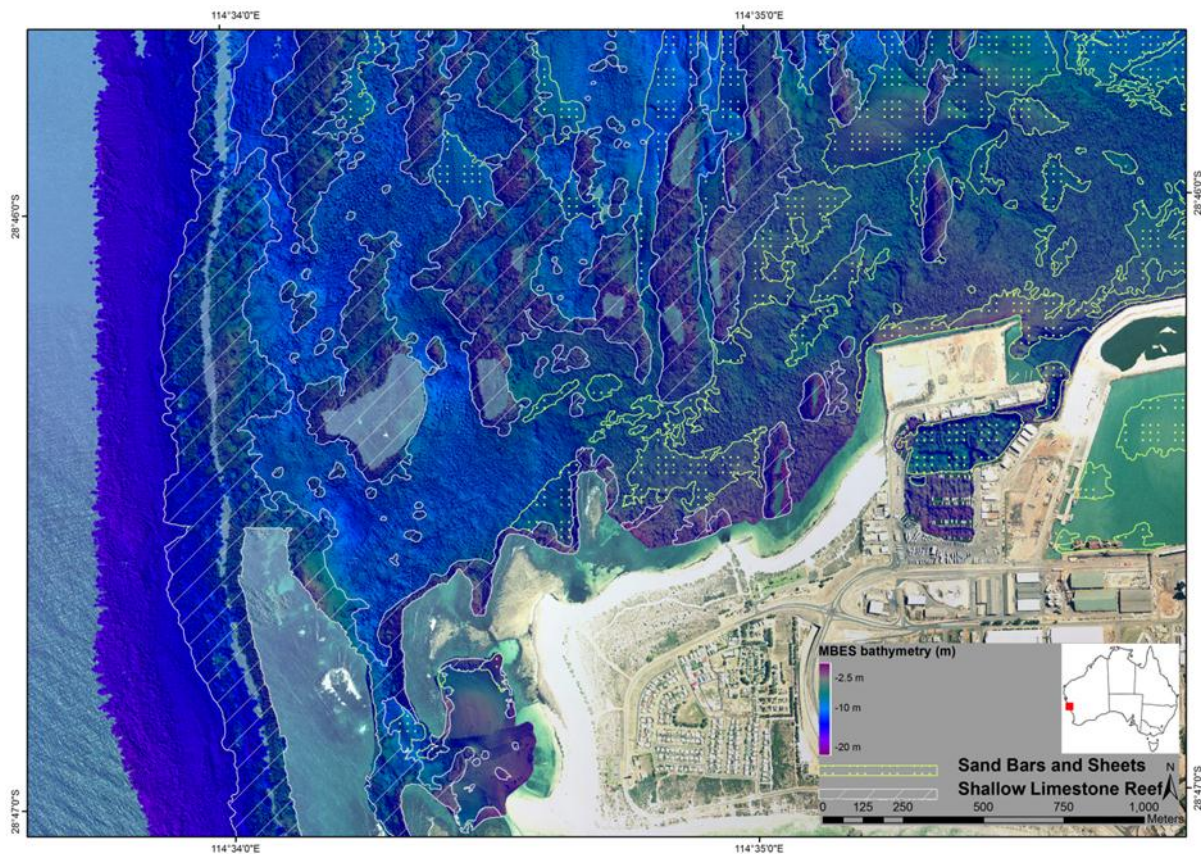


Figure 1: underwater morphology mapped on a DEM of MBES bathymetry (resolution 0.5 m). On the right, the map of Australia indicates the location of the study area.

3.2 MBES BS data

The different BS intensity and AR curves associated with the habitat categories identified through the underwater imagery data were relatively compared to each other and used to map the spatial distribution of seabed substrates and benthic cover. Dense seagrass meadows have the highest BS intensity measured in the study area, but have a similar AR curve as macroalgae communities. Sandy substrates have the lowest range of BS intensity measured and a very distinct AR curve compared to

seagrass meadows and macroalgae communities. Also [21] identified sandy substrates as areas of lower BS intensity compared to rocky substrates, seagrass and macroalgae communities.

Seagrass meadows and macroalgae communities are also associated with different morphological features. In fact, macroalgae communities colonize shallow limestone reefs whilst seagrass meadows were found over flat substrates closer to the shoreline. Sandy substrates are sparse in between the limestone ridge systems and over the flat areas; the spatial distribution of sandy substrates found on the MBES BS data overlaps the locations of sand bars and sheets systems mapped on the MBES bathymetry adding value to the morphological identification of these sediment bodies.

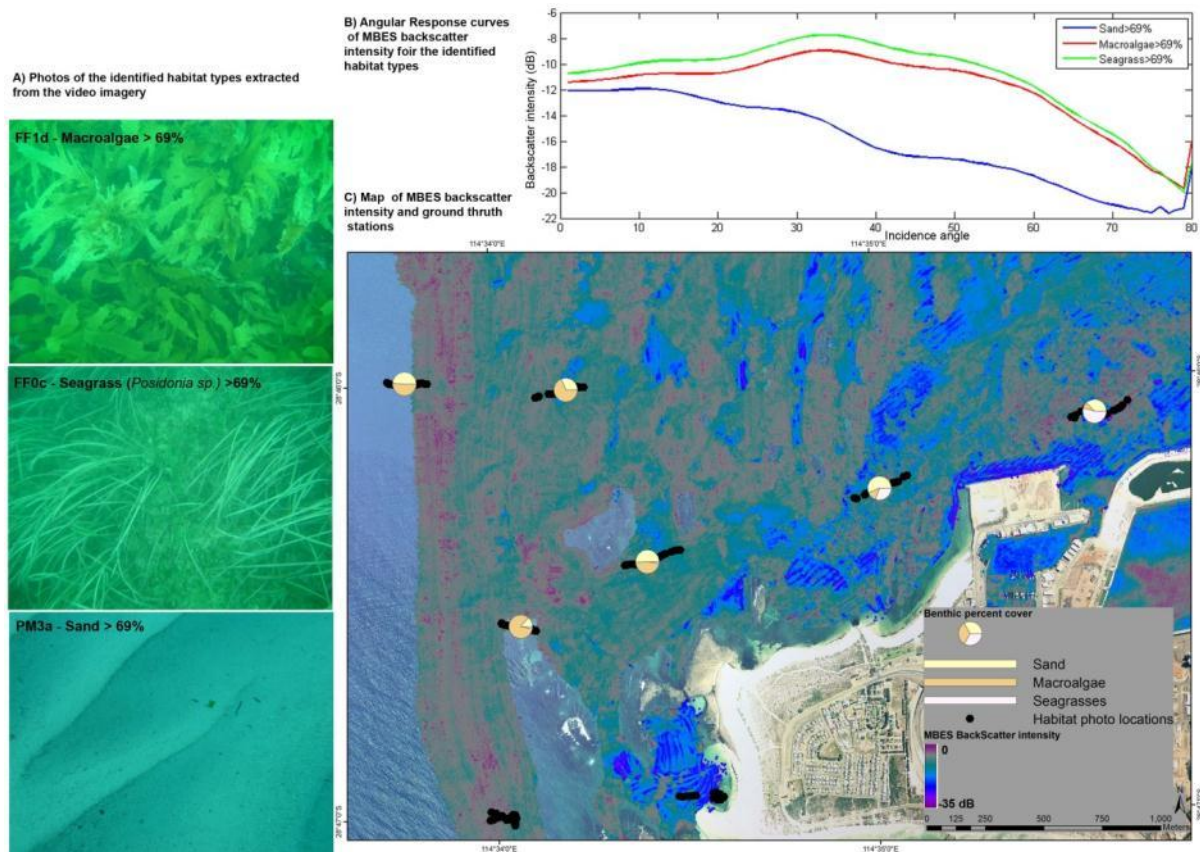


Figure 2: Macroalgae communities, seagrass meadows and sandy substrates were the main habitat types identified at Geraldton through MBES BS data and underwater imagery. A) photos of the identified habitats; B) AR curves extracted from the MBES data with a search radius of 20 m; C) map of MBES BS intensity (resolution 1 m) which shows the ground truth station locations and average benthic cover of the towed video transect.

3.3 Seabed mobility

Figure 3 shows the seabed mobility map generated in this study. Stable areas show no evidence of sediment deposition or erosion and include limestone reef systems and flat rocky substrates. Shallow limestone reef colonized by macroalgae communities shelter the coastal platform from the ocean waves and are considered areas of significant hydrodynamic energy. Sediment deposition is not expected in these areas as shallow reef systems influence sediment transport pathways by constituting a topographic barrier to sediment movement [2]. In fact, sediment accumulation occurs in the calmer areas in between the limestone ridges, where sandy substrates dominate. Moreover, sediment deposition is more abundant in the eastern and more protected areas of the bay. The flat substrate

close to shore is covered by a sand veneer and occasionally colonized by seagrasses, and is considered an area of overall stability in terms of seabed mobility, with sediment production and trapping correspondently to the seagrass communities, but not significant sediment deposition or erosion noted.

Sediment deposition areas are constituted by uncolonized sand bodies and indicate mobile areas of the seabed, where sediment accumulation is enhanced by the littoral currents. Sediment transport occurs towards these bodies and as such sediment transport pathways are active at these locations.

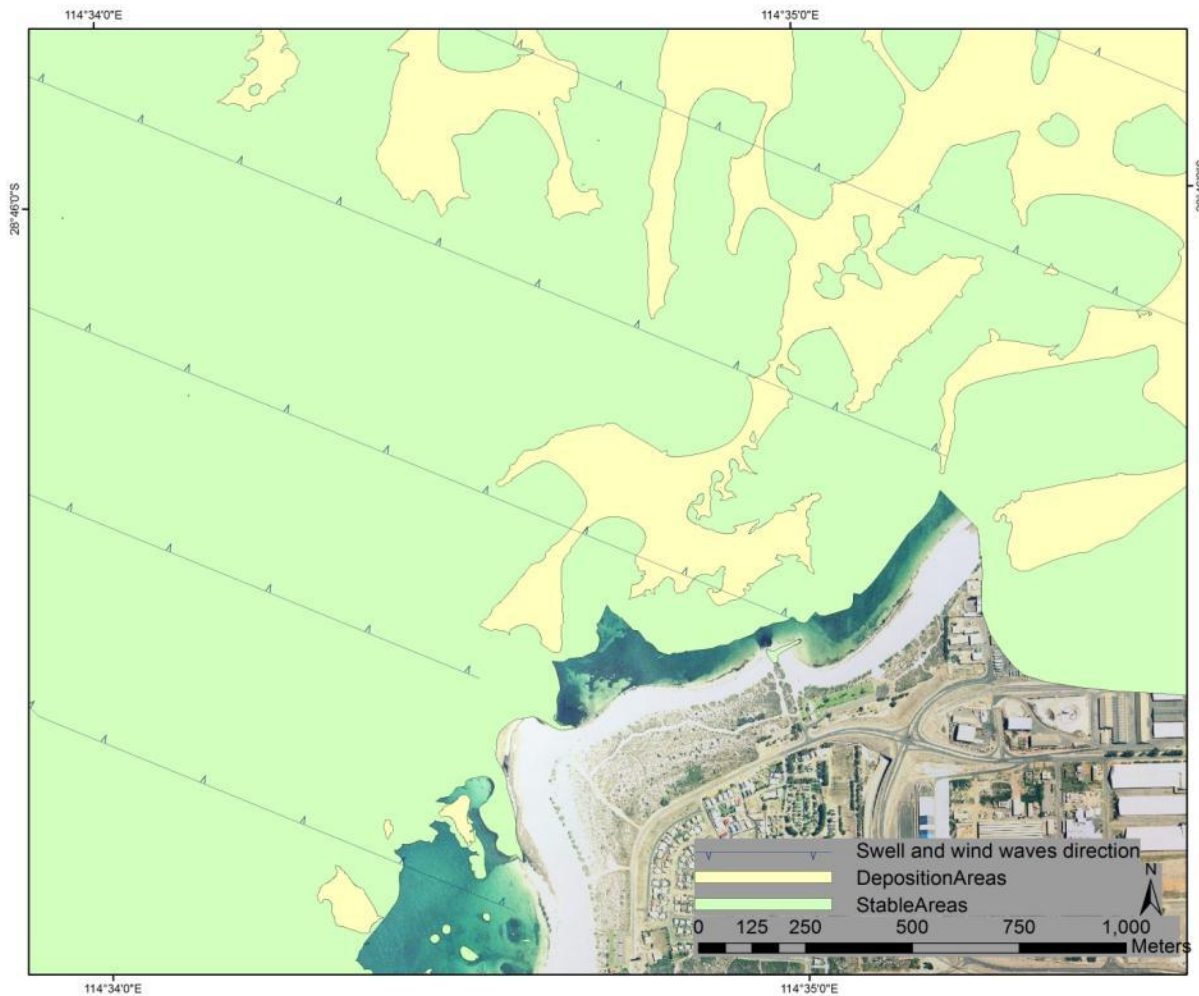


Figure 3: Seabed mobility map with dominant swell and wind wave direction. Note that sediment deposition areas occur on the upstream side of stable areas.

4. Discussion

A combination of MBES bathymetry and BS data allowed a seabed mobility map to be completed by indicating sediment deposition areas and stable areas in terms of sediment dynamics (i.e. no evidence of sediment erosion/deposition).

Sediment deposition areas are considered sediment sinks in terms of coastal sediment budget, and consist of unvegetated sediment bodies (banks, bars and sheets) [2]. Sand bar and sheet systems were identified on the MBES bathymetry in the study area, and the sandy nature of these sediment bodies was confirmed through the BS data. These features are considered important when studying sediment dynamics, as sand bars and sheets are indicative of sediment accumulation and point out areas of

sediment deposition within a coastal system, indicating that the local currents are transporting sand where they are located.

Limestone ridges and pinnacles were also identified through the MBES bathymetry and they are commonly colonized by macroalgal communities. These ridges are considered stable areas in terms of seabed mobility and sediment deposition around these features is common [2].

Seagrass meadows are known to be sediment producers and are considered sediment sources in terms of sediment budget in WA [10]. This habitat also supports fine sand trapping and enhances substrate stability [9, 12, 13, 14 and 15], and as such the distribution of seagrass meadows needs to be incorporated in seabed mobility studies. Moreover, the detailed mapping of seagrass distribution allowed by the analysis of MBES BS data provides a reference for future comparison of the habitat distribution within the studied coastal system which may become necessary as environmental conditions will change and these changes may influence the local sediment dynamics and seabed mobility.

5. Conclusions

The integration of sediment erosion, transport and depositional processes with pre-existing topography shapes the seabed morphology [2], hence the bathymetry of the study area was analyzed at high detail through MBES data providing important clues on sediment dynamics. Moreover, MBES BS data with appropriate ground truth have allowed the development of habitat maps which provide a valuable tool for monitoring the future impact of environmental condition changes on the coastal system, which may affect seabed mobility and coastal assets. Side scan sonars which have been more commonly used for seabed mobility studies are only able to record an acoustic image of the seafloor, lacking of the bathymetry data and the high resolution habitat mapping capability of MBESs, and consequently MBESs are considered more efficient for mapping coastal systems as part of seabed mobility studies. Finally, the data presented in this paper were used to understand the sediment dynamics of a temperate water environment, and the repeatability of this method in similar environments is foreseen as it is based on simple sedimentological principles.

6. Acknowledgments

This project was funded by the Western Australian Department of Transport. This PhD project is supported by the Curtin International Postgraduate Research Scholarship (CIPRS).

7. References

- [1] Rosati, J.D., 2005. CONCEPTS IN SEDIMENT BUDGETS. *Journal of Coastal Research*, 21(2), pp.307-322.
- [2] Velegrakis, A.F., Collins, M.B., Bastos, A.C., Paphitis, D. and Brampton, A., 2007. Seabed sediment transport pathway investigations: review of scientific approach and methodologies. In: Balson, P.S. and Collins, M.B. (Eds.), *Coastal and shelf sediment transport*. London, UK, Geological Society of London, 127-146. (Geological Society Special Publication 274.
- [3] KANA, T. and STEVENS, F., 1992. Coastal Geomorphology and Sand Budgets Applied to Beach Nourishment. *Proceedings Coastal Engineering Practice '92* (Reston, VA, ASCE), pp. 29-44.
- [4] DOLAN, T.J.; CASTENS, P.G.; SONU, C.J., and EGENSE, A.K., 1987. Review of Sediment Budget Methodology: Oceanside Littoral Cell, California. *Proceedings, Coastal Sediments '87* (Reston, VA, ASCE), pp. 1289-1304.

-
- [5] U. S. Army Corps of Engineers (2008). Coastal Engineering Manual. <http://140.194.76.129/publications/eng-manuals/>
- [6] COOPER, N.J. and PETHICK, J.S., 2005. Sediment budget approach to addressing coastal erosion problems in St. Ouen's Bay, Jersey, Channel Islands. *Journal of Coastal Research*, 21(1), 112–122. West Palm Beach (Florida), ISSN 0749-0208.
- [7] Brown C. J., and Blondel P., 2009. Developments in the application of multibeam sonar backscatter for seafloor habitat mapping. *Applied Acoustics*, Volume 70, Issue 10, October 2009, pp. 1242–1247.
- [8] Le Bas T., and Huvenne V., 2009. Acquisition and processing of backscatter data for habitat mapping – comparison of multibeam and sidescan systems. *Applied Acoustics*, Volume 70, Issue 10, October 2009, pp. 1242–1247.
- [9] Carruthers, T.J.B., Dennison, W.C., Kendrick, G.A., Waycott, M., Walker, D.I., Cambridge, M.L., 2007. Seagrasses of south–west Australia: A conceptual synthesis of the world's most diverse and extensive seagrass meadows. *Journal of Experimental Marine Biology and Ecology* 350: 21–45.
- [10] Short, A.D., 2010. SEDIMENT TRANSPORT AROUND AUSTRALIA – SOURCES, MECHANISMS, RATES, AND BARRIER FORMS. *Journal of Coastal Research*, 26(3), pp.395-402.
- [11] Short, F.T., and Coles, R.G., 2001. *Global seagrass research methods*. Amsterdam; London: Elsevier.
- [12] Verduin, J.J., Backhaus, J.O., 2000. Dynamics of plant-flow interactions for the seagrass *Amphibolis antarctica*: Field observations and model simulations. *Estuarine, Coastal and Shelf Science* 50 (2), 185–204.
- [13] van Keulen, M., Borowitzka, M.A., 2002. Comparison of water velocity profiles through morphologically dissimilar seagrasses measured with a simple and inexpensive current meter. *Bulletin of Marine Science* 71 (3), 1257–1267.
- [14] Madsen, J. D., Chambers, P. A., James, W. F., Koch, E.W. and Westlake, D. F., 2001. The interaction between water movement, sediment dynamics and submersed macrophytes. *Hydrobiologia* 444: 71–84.
- [15] Fonseca, M.S., 1989. Sediment stabilization by *Halophila decipiens* in comparison to other seagrasses. *Estuarine, Coastal and Shelf Science* Volume 29, Issue 5, November 1989, Pages 501-507.
- [16] Di Maida, G., Tomasello, A., Luzzu, F., Scannavino, A., Pirrotta, M., Orestano, C., and Calvo, S., 2011. Discriminating between *Posidonia oceanica* meadows and sand substratum using multibeam sonar. *ICES Journal of Marine Science* (2011), 68(1), 12–19.
- [17] De Falco, G., Tonielli, R., Di Martino, G., Innangi, S., Simeone, S. and Parnum, I. M., Relationships Between Multibeam BS, Sediment Grainsize and *Posidonia Oceanica* Seagrass Distribution, *Continental Shelf Research*, 30, pp.1941-1950, 2010.
- [18] Short, F.T., McKenzie, L.J., Coles, R.G., and Vidler, K.P., 2002. *SeagrassNet Manual for Scientific Monitoring of Seagrass Habitat*, Queensland Department of Primary Industry, Queensland Fisheries Service, Cairns, pp.56.
- [19] Langford, R.L., 2001. *REGOLITH-LANDFORM RESOURCES OF THE GERALDTON 1:50 000 SHEET*. Geological Survey of Western Australia.
- [20] JOHNSON, M. E., BAARLI, B. G., and SCOTT, J. H., 1995. Colonization and reef growth on a Late Pleistocene rocky shore and abrasion platform in Western Australia. *Lethaia*, 28, p.85–98.
- [21] Parnum, I.M., 2007. *BENTHIC HABITAT MAPPING USING MULTIBEAM SONAR SYSTEM*. PhD Thesis Curtin University of Technology, Department of Imaging and Applied Physics, Centre for Marine Science and Technology, pp. 213.

APPENDIX 2 – Tecchiato et al. (2011). Using multibeam echo-sounder to map sediments and seagrass cover in shallow coastal areas. Proceedings of the Fourth International Conference on Underwater Acoustic Measurements: Technologies and Results. Kos Island, Greece, June 2011.

USING MULTI-BEAM ECHO SOUNDER BACKSCATTER DATA TO MAP SEDIMENTS AND SEAGRASS COVER IN COASTAL ENVIRONMENTS

Sira Tecchiato^a, Iain Parnum^b, Lindsay Collins^a and Alexander Gavrilov^b

^a Department of Applied Geology, Curtin University of Technology, GPO Box U1987, Perth, WA 6845, Australia

^b Centre for Marine Science and Technology, Department of Imaging and Applied Physics, Curtin University of Technology, GPO Box U1987, Perth, WA 6845, Australia

Sira Tecchiato, Department of Applied Geology, Curtin University of Technology, GPO Box U1987, Perth, WA 6845, Australia. Tel.: +61 8 9266 3710; fax: +61 8 9266 3153.

E-mail addresses: S.Tecchiato@curtin.edu.au, sira.tecchiato@gmail.com

***Abstract:** A sediment budget study in the coastal zone off Geraldton in Western Australia aims to identify sediment sources, sinks and transport pathways within shallow coastal embayments. The spatial distribution of sediments and seagrass cover in the survey area were surveyed using sediment samples, towed video and acoustic backscatter (BS) data collected with a multi-beam echo sounder (MBES). Sediment grain size was determined following standard dry sieving procedures. The MBES BS data were processed using the Centre for Marine Science and Technology (CMST)'s multibeam sonar processing toolbox and the BS strength as a function of incidence angle (known as Angular Response curve, AR) was extracted at the ground truth locations. The mean BS and slope of the oblique angles of the AR curves allow an initial separation of different habitat types, but are significantly correlated. A multivariate statistical approach (Fisher's Linear Discriminant Analysis) was used to derive uncorrelated parameters that were useful for seafloor classification. Additional data will be analysed in the area to refine the existing model, which will further investigate the relationships between BS strength and the density and canopy height of macroalgae and seagrass.*

***Keywords:** multibeam backscatter, angular response, habitat mapping, sediment grain size, seagrass, macroalgae.*

1. INTRODUCTION

Sediment budget studies aim to determine the volume of sand circulating in coastal environments, and are based on the understanding of sediment sources, sinks and transport pathways. A sediment budget study is ongoing at Geraldton (Western Australia) and preliminary results show that the highest *in situ* production of sediment is linked to shallow seagrass communities.

A multi-beam echo sounder (MBES) system was used to produce bathymetry and backscatter (BS) data throughout the study area. The bathymetry data is used to describe the underwater morphology which influences sediment pathways and is partly a result of the local sediment transport. The bathymetry data also identifies topographic features indicative of sediment pathways (i.e. ripples, sand waves, scours) and repeated bathymetric surveys provide information on sediment volume changes, which are useful for sediment budget calculations. The BS data are used to map the benthic habitats, which are closely connected to sediment production and beach stability. The South and Western Australian coast is dominated by shallow seagrass meadows associated with fine sands, and these contribute to supplying sediment to the beaches and trapping sediment moving offshore and circulating in the coastal environment. Macroalgae dominated reef systems, associated with medium/coarse sands, are also common off the Geraldton coast and protect the coastal embayments from swell waves, which also influence sediment dynamics.

Analysis of MBES BS data has been used to carry an acoustic classification of seafloor habitats along the Australian coastal zone [1]. The correlation between sediment grain size and MBES BS has been extensively documented [2, 3] and the utilisation of backscatter angular response (AR) curves for seafloor characterisation is well established [4], however the acoustic response from seagrass meadows is not well understood [5]. The relationship between MBES BS properties and seafloor epi-benthic cover, such as seagrass, and sediment grain size extracted at the ground truth locations is investigated in this paper.

2. METHODS

2.1 Data collection

Geraldton is situated approximately 400 km north of Perth in Western Australia and sediment samples were collected there, along a 1km x 1km spaced grid in November 2009. During the survey, it was found that the sediment/water interface was sufficiently consolidated to impede grab sampling; consequently a steel pipe dredge was used. The pipe dredge sampling operations involved boat drifting, this combined with the positioning system capability neat positioning accuracy ± 20 m for the sediment samples.

A MBES survey was carried out in November 2010 using a Western Australian Department of Transport hydrographic vessel. The survey area covered the embayments north and south of the city of Geraldton, between 2 and 30 m depth. Only part of these data is presented in this study, located in an area of significant complexity, in terms of morphology, habitats and substrates. Data were acquired using a Reson Seabat 8101 MBES system, which operates at 240 kHz and has a swath width 150° across track and 1.5° along track.

A towed video survey followed the MBES survey in December 2010. The video transects were 200 m long and their locations replicated the sediment sample positions. High resolution images were captured from the video footage approximately every 10 m and the positioning system used had an accuracy of ± 15 m.

2.2 Analysis of ground truth data

Salts were removed from the sediment samples, and representative samples of the bulk were isolated using standard procedures. Dried samples were sieved using a mechanical sediment sieve shaker with -1 to 4 ϕ sieve units at 0.5 ϕ intervals based on the Udden-Wentworth grain size scale. GRADISTAT software [6] was used in the calculation of grain size statistics.

Underwater photography was used to assess the relative abundance of epi-benthic cover through visual comparison with a photo guide specifically developed for seagrass dominated habitats [7]. Seagrass, macroalgae and sandy substrates were the main categories identified in the study area. Seagrasses included *Posidonia* sp. and *Halophila* sp.

2.3 MBES backscatter data processing

The BS data were collected using a Reson Seabat 8101 MBES through the snippet option, which collects seafloor BS envelopes for each beam. MBES data were processed using the Centre for Marine Science and Technology (CMST)'s multibeam sonar processing toolbox, which was developed in MATLAB[®] [8]. The CMST's processing toolbox calculates the BS energy from the snippet signals and reduces these values to the width of the transmitted pulse, and removes the time variable gain (TVG) applied by the MBES system. The surface scattering coefficients are calculated by correcting the BS energy for the actual spreading and absorption loss for each beam and normalised for the footprint insonification area, and the dB scale values are referred to as BS intensity throughout this paper. The across-track beam pattern for Reson Seabat 8101 MBESs is known to not be uniform [9] and this has not been measured or corrected for the MBES system used in this study, so the BS data are compared relatively to each other. To produce a map of mean BS intensity the AR was corrected by removing the mean AR from a sliding window of 30 consecutive pings of data, then restoring values to the mean BS at 30° [1, 8].

2.4 Analysis of MBES backscatter data

BS AR curves were constructed for each ground truth station using a search radius of 50m. From these AR curves the mean BS and mean slope were calculated for near-vertical (0° - 15°) and oblique incidence (20° - 60°) angles.

Fisher's Linear Discriminant Analysis (LDA) was used to derive features from the AR curves that were useful for separating the main seafloor habitats: seagrass > 50%, algae > 50%, sand > 50%, and seagrass, algae and sand <50%. A total of 89 cases was used for the analysis.

3. RESULTS

Fig.1 shows a map (1 m grid) of mean BS intensity of the study area, with ground truth stations overlaid on it. The study area is characterised by complex morphology and habitat distribution, with a prominent feature consisting of shallow reefs colonised by macroalgae on a medium/coarse sandy substrate (2-20 m depth). Seagrass meadows are common closer to the shoreline (2-7 m depth), but their distribution is discontinuous and seagrass density variable. *Halophila* sp. was found associated with medium sands, while *Posidonia* sp. is associated with fine sand substrates. The canopy height of *Halophila* sp. is generally <20 cm,

a marked contrast with *Posidonia sp.* that reaches 1 m height. Sandy patches are often adjacent to seagrasses and macroalgae dominated habitats, varying from well sorted fine sands to medium/coarse sandy substrates. A combination of seagrasses and macroalgae was also observed on predominantly medium/coarse sandy substrates.

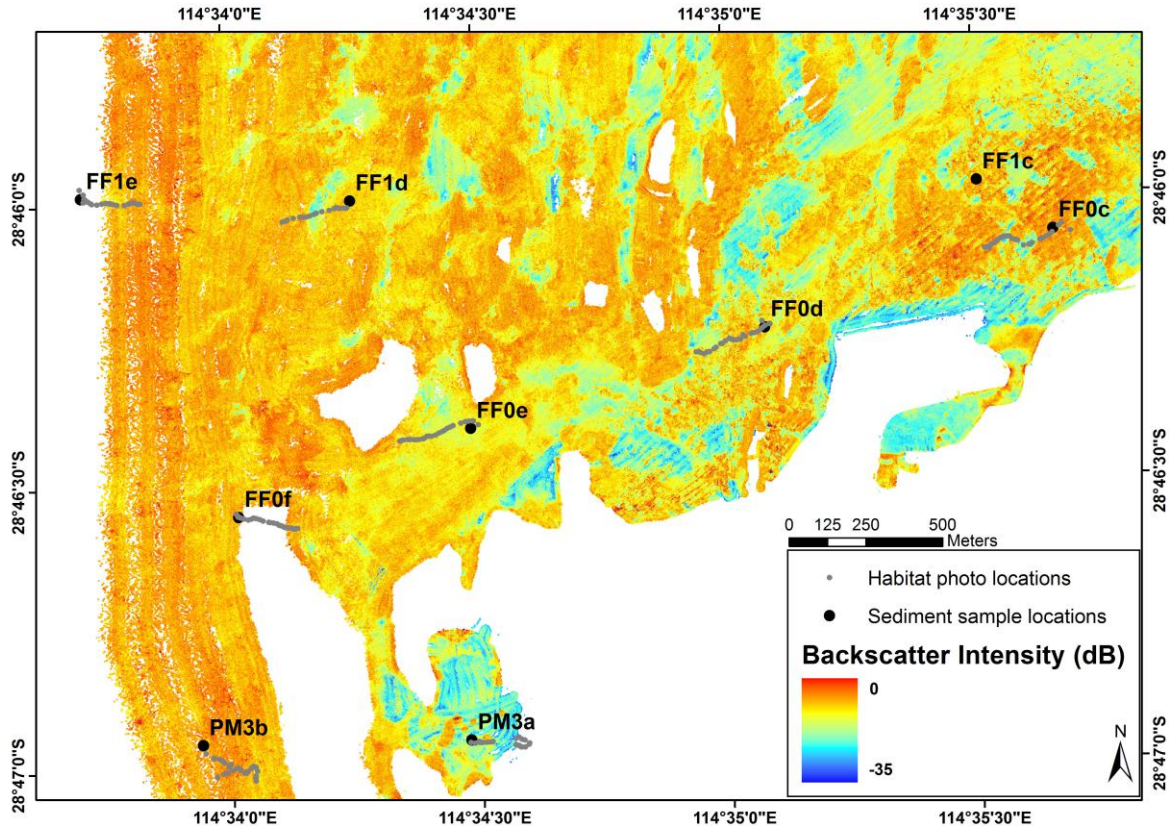


Fig.1: Map of BS intensity and ground truth stations.

The AR curves allowed us to distinguish the seabed types found in the study area (Fig.2): macroalgae >50%, seagrass (*Halophila sp.* and *Posidonia sp.*) >50%, sand >50% differentiated as fine sands and medium/coarse sands, and finally a combination of macroalgae cover <50%, seagrass <50% and sand <50%. Dense macroalgae communities have the highest BS intensity measured, but have a similar AR curve to medium/coarse sandy substrates, *Halophila sp.* communities and mixed seagrass/macroalgae habitats. *Posidonia sp.* meadows on fine sands show a similar AR curve to fine sandy substrates and have the lowest range of BS intensity measured and the highest slope gradient.

Of the different metrics calculated from the AR curves, the most useful for seafloor classification were the mean BS intensity and slope of the oblique incidence. These AR properties can be used to identify the different seafloor types (Fig.3), but these properties were highly correlated ($R = 76\%$). The mean BS intensity and slope of oblique incidence angles of macroalgae dominated habitats and medium/coarse sandy substrates were between -9 and -13 dB, and -0.09 and 0.03 dB/deg., respectively. These parameters from *Posidonia sp.* meadows and fine sandy substrates were more dispersed than macroalgae with a range of values between -13 and -19 dB for the mean BS intensity and between -0.3 and -0.09 dB/deg for the slope of AR at oblique incidence angles. The heterogeneous habitats resulting from a

combination of low seagrass and macroalgae cover and the *Halophila* communities do not show a clear pattern.

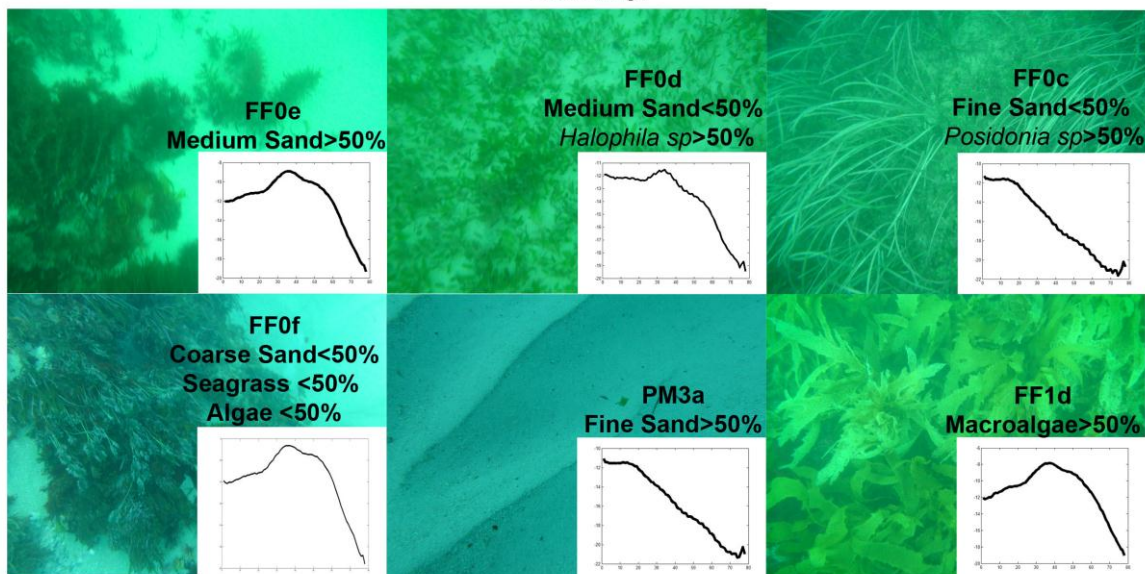
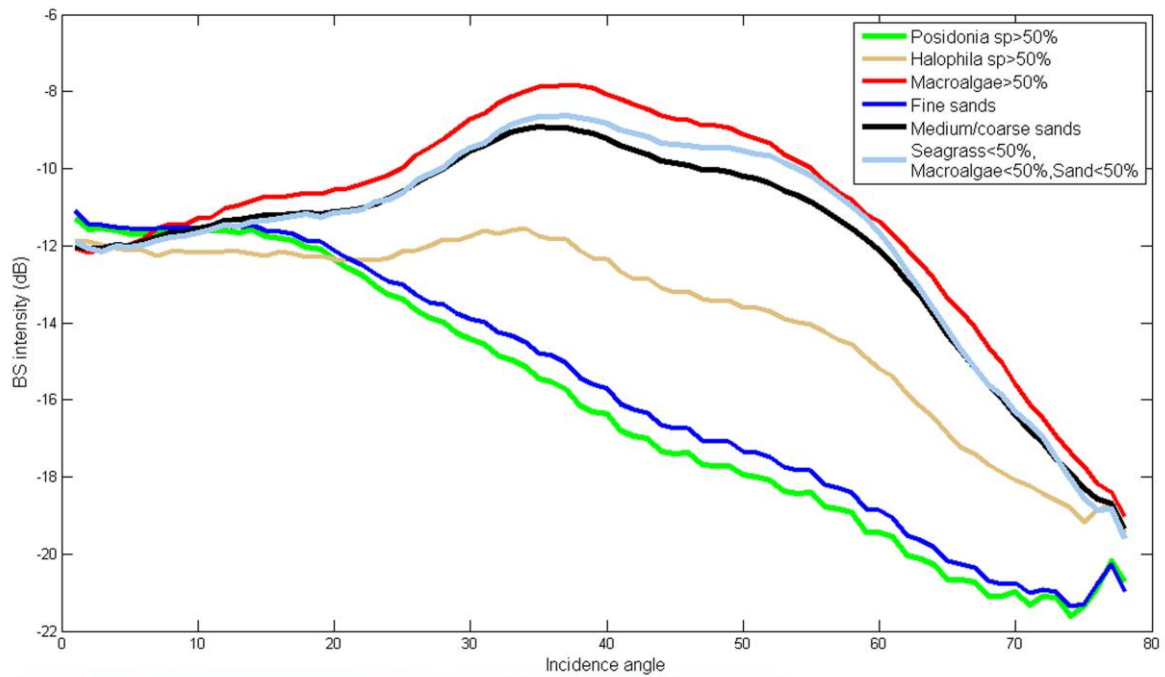


Fig.2: AR curves of the main seabed types found in the study area. Refer to Fig.1 for their location on the BS map.

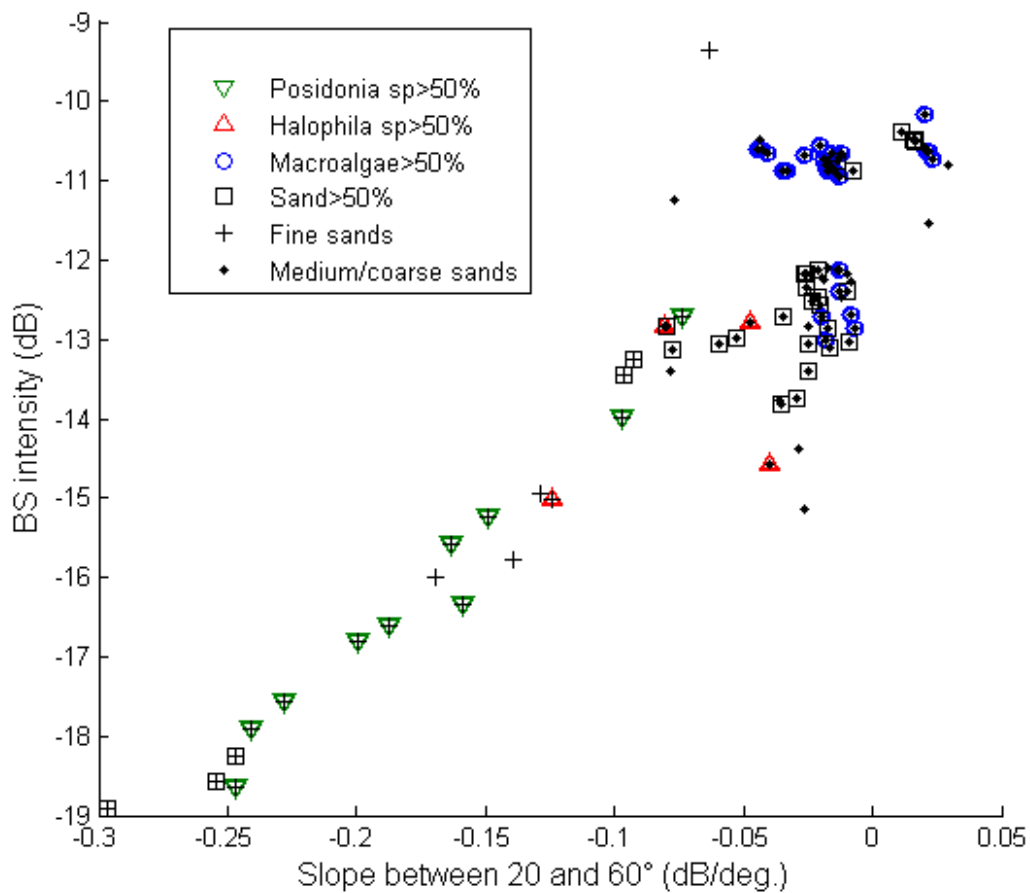


Fig.3: Mean BS intensity versus slope of the oblique incidence angles of the AR. Posidonia meadows and fine sandy substrates are characterised by low BS and AR slopes. Macroalgae communities and medium/coarse sediments have higher BS and slope values.

The main seafloor habitats found throughout the study area were also distinguished through the features derived from Fisher's LDA of the AR curves. Fig. 4 shows the scores of first (Feature 1) and second (Feature 2) linear combinations derived from Fisher's LDA. Feature 1 separates the different habitats identified in this study (as visible in Fig.4 from left to right): seagrass meadows, sandy substrates, mixed seagrass and macroalgae communities surrounded by sandy substrates, and macroalgae dominated communities. Macroalgae and seagrass communities (top of Fig.4) were also distinguished from sandy substrates and mixed seagrass and macroalgae communities (bottom of Fig.4) by Feature 2. The separation between habitats in Fig. 4 is greater than in Fig. 3 and they are also not significantly correlated.

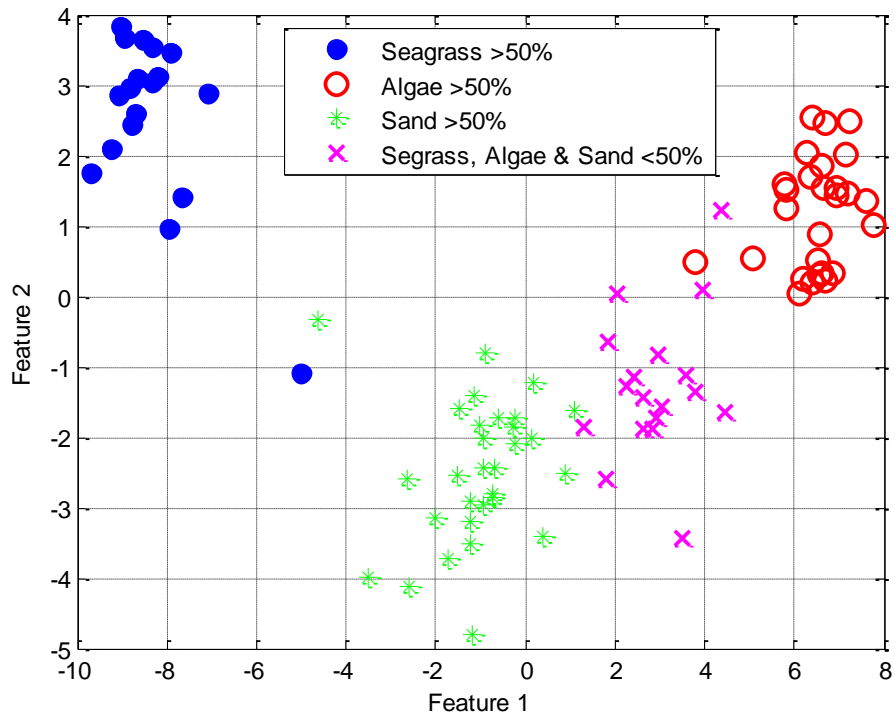


Fig.4: Plot of scores deriving from Fisher's LDA of the BS AR curves. Four seabed types were differentiated: seagrass meadows, sandy substrates, macroalgae communities and mixed seagrass and macroalgae communities.

4. CONCLUSIONS

The results presented here show that BS intensity is influenced by sediment grain size, and extent of the epi-benthic cover on the sea bottom as previously identified by other studies [2, 3, 4, 5]. At the moment, though, it is unclear whether the high BS intensity from macroalgae was due to scattering from the macroalgae or the coarse sediments and hard bottom beneath these communities. Also, further investigation is required to explain the large variation in BS intensity from seagrass communities, in particular, to determine if it is related to the type of seagrass, % of seagrass cover, changes in the sediment beneath the seagrass or a combination of these parameters.

As only part of the available data has been analysed and is presented in this paper, a more detailed and comprehensive analysis will further develop our understanding of this complex relationship between BS and seafloor habitat properties. For instance, canopy height of macroalgae and seagrasses are additional data available for this study, and will hopefully provide further inside about the different acoustic response of different seagrass species.

Although the mean BS intensity and slope of the oblique angles of the AR curves were able to separate different seafloor habitats, they were highly correlated, which is to be expected. Hence, a multivariate statistical approach (Fisher's LDA) was used to derive uncorrelated parameters that were useful for seafloor classification.

ACKNOWLEDGEMENTS

This project is funded by the Department of Transport of Western Australia, the authors are grateful for their support, especially Mr John Mullally for data collection and preliminary processing. The Geraldton Port Authority is also acknowledged for data provision.

REFERENCES

- [1] Siwabessy, P.J.W., Parnum, I.M., Gavrilov, A. and McCauley, R.D., Overview of Coastal Water Habitat Mapping Research For Coastal CRC, Cooperative Research Centre for Coastal Zone, Estuary and Waterway Management, Technical Report 86, Australia, 2006.
- [2] Goff, J.A., Kraft, B.J., Mayer, L.A., Schock, S.G., Sommerfield, C.K., Olson, H.C., Gulick, S.P.S. and Nordfjord, S., Seabed Characterization on the New Jersey Middle and Outer Shelf: Correlatability and Spatial Variability of Seafloor Sediment Properties, *Marine Geology*, 209, pp.147–172, 2004.
- [3] Ferrini, V.L., and Flood, R.D., The Effects of Fine-Scale Surface Roughness and Grain Size on 300 Khz Multibeam BS Intensity in Sandy Marine Sedimentary Environments, *Marine Geology*, 228, 153–172, 2006.
- [4] Hughes Clarke, J.E., Danforth, B.W., and Valentine, P., Aerial Seabed Classification Using BS Angular Response at 95 Khz. In *Shallow Water*, NATO SACLANTCEN, Conference Proceedings Series CP, vol. 45, pp. 243–250, 1997.
- [5] De Falco, G., Tonielli, R., Di Martino, G., Innangi, S., Simeone, S. and Parnum, I. M., Relationships Between Multibeam BS, Sediment Grainsize and Posidonia Oceanica Seagrass Distribution, *Continental Shelf Research*, 30, pp.1941-1950, 2010.
- [6] Blott S.J. and Pye K., Gradistat: a Grain Size Distribution and Statistics Package for the Analysis of Unconsolidated Sediments, *Earth Surface Processes and Landforms*, 26, pp.1237-1248, 2001.
- [7] Short, F.T., McKenzie, L.J., Coles, R.G., and Vidler, K.P., SeagrassNet Manual for Scientific Monitoring of Seagrass Habitat, Queensland Department of Primary Industry, Queensland Fisheries Service, Cairns, pp.56, 2002.
- [8] Parnum, I.M., Benthic Habitat Mapping Using Multibeam Sonar System. PhD Thesis Curtin University of Technology, Department of Imaging and Applied Physics, Centre for Marine Science and Technology, pp. 213, 2007.
- [9] Foote, K.G., Chu, D., Baldwin, K.C., Mayer, L.A., McLeod, A., Hufnagle, L.C., Jr., Jech, J.M., and Michaels, W., Protocols for Calibrating Multibeam Sonar, *The Journal of the Acoustical Society of America*, vol. 114, no. 4, pp. 2307-8, 2003.

APPENDIX 3 – Reports, Publications and Presentations

Reports

Tecchiato, S., Collins, L.B., and Stevens, A. M., 2012. GERALDTON EMBAYMENTS COASTAL SEDIMENT BUDGET STUDY. Applied Sedimentology, Coastal and Marine Geoscience Group Report 2012/01, Curtin University"©, Department of Applied Geology Western Australia School of Mines. Prepared for Department of Transport, Marine House, 1 Essex St, Fremantle, WA 6160.

Tecchiato, S., and Collins, L.B. (Applied Sedimentology and Marine Geoscience Group, Department of Applied Geology Curtin University of Technology, WA). - SEDIMENT MAPPING FOR IDENTIFICATION OF SEDIMENT SOURCES, TRANSPORT PATHWAYS AND SINKS FOR COMPONENTS OF THE BATAVIA COAST, WITH SPECIAL CONSIDERATION OF THE INSHORE WATERS AND COAST BETWEEN THE GREENOUGH RIVER AND BULLER RIVER (Coastal Vulnerability & Risk Assessment Program - Project 2-Stage 2) - Preliminary Report 31/03/2010. PRODUCED FOR: Department of Transport, Marine House, 1 Essex St, Fremantle.

Scientific articles

Tecchiato, S., Collins, L., Stevens, A., Soldati, M. and Pevzner, R. (submitted). An integrated approach to coastal dynamics in temperate Midwestern Australia: Sediment budget of a wave dominated carbonate system. Submitted to *Geomorphology*.

Tecchiato, S., Collins, L., Parnum, I. and Stevens, A. (submitted). The influence of shallow water geomorphology and sedimentary processes on the benthic habitat distribution of a temperate water littoral environment: Geraldton, Midwestern Australia. Submitted to *Marine Geology*.

Tecchiato S., Collins L., and Parnum I., 2013. Application of multi-beam echo-sounder data to studies of sediment dynamics: an example from Geraldton, Midwestern Australia. International Congress on Natural Sciences and Engineering; Taipei, Taiwan, January 2013.

Tecchiato S., Parnum I.M., Collins L. and Grailov A., 2011. Using multibeam echo-sounder to map sediments and seagrass cover in shallow coastal areas. Proceedings of the Fourth International Conference on Underwater Acoustic Measurements: Technologies and Results. Kos Island, Greece, June 2011.

Abstracts

Tecchiato, S., Collins, L., and Stevens, A. (2014). Coastal evolution and sediment dynamics of the Geraldton embayments: implications for coastal management in regional Western Australia. Coast to Coast Conference, Mandurah, Western Australia, October 2014.

Tecchiato S., Parnum I.M., Collins L., 2014. Capability of multibeam backscatter data to discriminate between temperate water habitats and substrates. GeoHab 2014, Lorne, Australia, May 2014.

Tecchiato, S., Collins, L., and Stevens, A. (2012). Semi-quantitative Coastal Sediment Budget of the Geraldton Embayments (Midwestern Australia). 34th International Geological Conference, Brisbane, Australia, August 2012.

Tecchiato, S., and Collins, L., (2012). Relationship between geomorphology, sediments and habitat distribution: sediment transport dynamics in a shallow coastal environment. 34th International Geological Conference, Brisbane, Australia, August 2012.

Presentations

- ✓ 2014 GeoHab – International Conference on Marine Geological and Biological Habitat Mapping
- ✓ 2013 Royal Society of Western Australia Conference - Perth - presenter
- ✓ 2012 International Geological Conference – Brisbane – presenter
- ✓ 2012 Final Project Presentation for the Western Australian Department of Transport – presenter
- ✓ 2011 Progress Presentation for the Western Australian Department of Transport – presenter
- ✓ 2011 Fourth International Conference on Underwater Acoustic Measurements: Technologies and Results - Kos Island, Greece – presenter
- ✓ 2010 Progress Presentation for the Western Australian Department of Transport – presenter